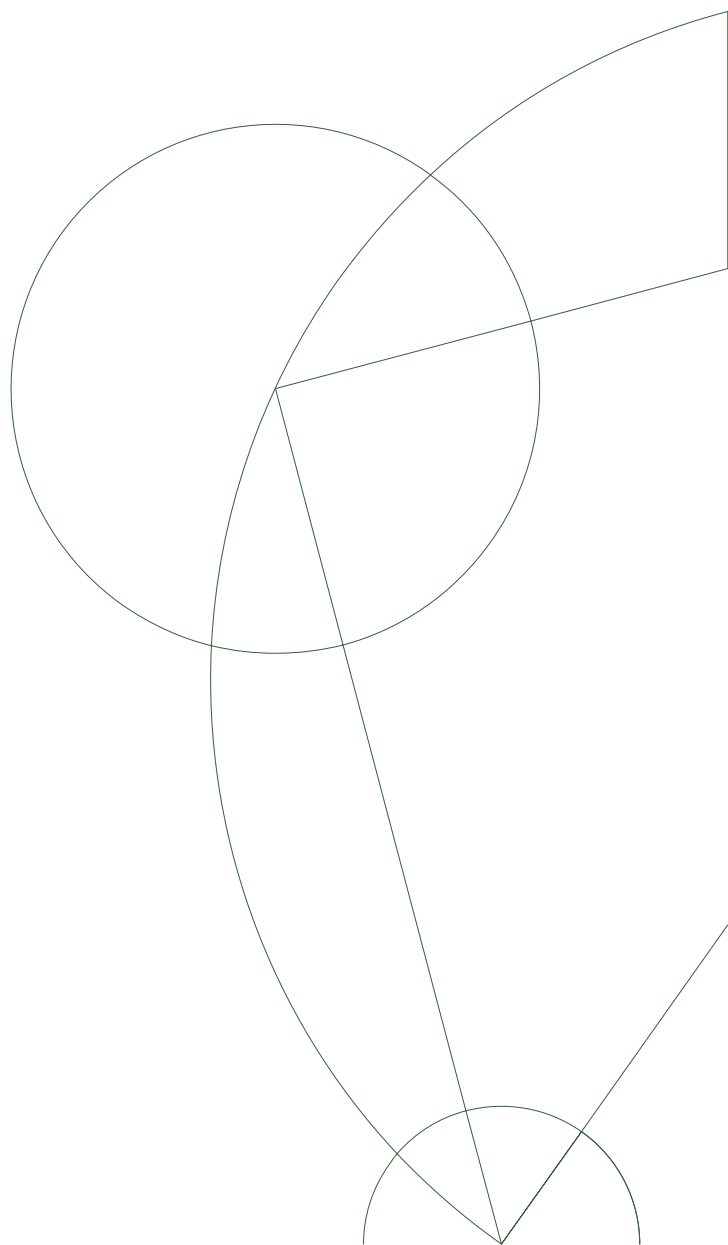




Ph.D. Thesis

Andreas Vigand Pedersen

Effective gravitational theories in string theory
and the AdS/CFT correspondence



Principal supervisor: Niels Anne Jacob Obers

Submitted: February 28, 2014

Abstract

We consider various aspects of effective gravitational theories, including supergravity, within the framework of the blackfold approach. The thesis is naturally split into three parts. In the first part of the thesis, we explore the blackfold approach and explain how it is possible to write down an effective theory for higher dimensional extended black holes in a fluid/elastic perturbative derivative expansion. Moreover, we show that the approach is quite universal and can be extended to various supergravities. Finally, we consider a new generalization of the method, which allows us to treat (SUGRA) probe branes in fluxed dilatonic backgrounds. In the second part, we construct and analyze thermal spinning giant gravitons in IIB/M-theory. The analysis employs the thermal brane probe method based on the blackfold approach. In addition to heating up the solution, and examining the effects from having a non-zero temperature, we also switch on new quantum numbers, namely internal spins along the directions of the wrapping sphere. We examine the effects of this new type of excitation and in particular analyze the physical quantities in various regimes, including that of small temperatures as well as low/high spin. As a byproduct of our analysis, we find a new stationary dipole-charged black hole solution on the $\text{AdS} \times S$ backgrounds of type IIB/M-theory. We finally consider, via a double scaling extremal limit, a novel null-wave zero-temperature giant graviton exhibiting a BPS spectrum. Finally, in the third part of the thesis, we switch focus and consider long-wavelength perturbations of charged black branes. More specifically, we consider hydrodynamic fluctuations of the black p -brane solution of Einstein/Maxwell gravity in $D = p + n + 3$ dimensions. We extract the first order dissipative transport coefficients from our perturbatively corrected solution, including the modified shear and bulk viscosities, and a new transport coefficient associated with charge diffusion. Having obtained the transport coefficients, we consider some of the usual hydrodynamic bounds and show that the shear viscosity to entropy bound is saturated, as expected. We also consider some of the proposed bounds for the bulk viscosity which are found to be violated in certain regimes of the charge. We finally compute the next-to-leading order dispersion relations for the effective fluid. For small values of the charge, the speed of sound is found to be imaginary and the brane is therefore Gregory-Laflamme unstable, as expected. For sufficiently large values of the charge density, the sound mode is found to be stable, however, in this regime the hydrodynamic mode associated with charge diffusion is found to be unstable. The electrically charged black brane is therefore found to be (classically) unstable for all values of the charge in agreement with thermodynamic arguments.

Acknowledgements

I would like to thank a few people who have helped, supported and inspired me during my time as a Ph.D. student at the Niels Bohr Institute under the supervision of Niels Obers.

First and foremost, I would like to give my thanks to Niels for his guidance and encouragements. Thank you, Niels. Secondly, I need to give a thanks to some of the (past and present) Ph.D. students at the institute, Kirstejn, Anne Mette, Agnese, Jay, and Jakob. Especially Jakob, thanks a lot.

I would also like to thank my family from the bottom of my heart. Kathrine, Louise, you have been there always. I love you and I (still) owe you everything. I also need to thank Hanne, Søren, Gnuggi, and Bo.

Finally, a shout-out to all of my friends outside physics; Holle, Jeppe, Trads, Karl, Eirik, Madsen, SBA, Boo, all of DSS, Søgaaard, Troels (who actually is in physics), and all the ones I have forgot. I sincerely believe that you are the best collection of friends a man could find.

Copenhagen, February 28, 2013.

List of Publications

- J. Armas, T. Harmark, N. A. Obers, M. Orselli, and A. V. Pedersen, “Thermal Giant Gravitons,” *JHEP* **1211** (2012) 123, [arXiv:1207.2789](#) [[hep-th](#)]
- J. Armas, N. A. Obers, and A. V. Pedersen, “Null-Wave Giant Gravitons from Thermal Spinning Brane Probes,” *JHEP* **1310** (2013) 109, [arXiv:1306.2633](#) [[hep-th](#)]
- J. Gath and A. V. Pedersen, “Viscous Asymptotically Flat Reissner-Nordström Black Branes,” *Accepted for publication in JHEP* (2013) , [arXiv:1302.5480](#) [[hep-th](#)]

Contents

Introduction	1
Outline of thesis	4
1 The blackfold approach	5
1.1 Introduction	5
1.2 The effective blackfold theory	7
1.2.1 The blackfold expansion	7
1.2.2 The quasi-local worldvolume stress tensor	9
1.2.3 The spacetime blackfold stress tensor	10
1.2.4 The blackfold equations of motion	10
1.3 The effective blackfold fluid	11
1.3.1 The neutral black brane	12
1.3.2 Dissipative corrections	13
1.3.3 Stationary solutions	14
1.3.4 Elastic corrections	16
1.4 The blackfold construction and conserved quantities	17
1.4.1 The blackfold construction	17
1.4.2 Integrated quantities and thermodynamics	18
1.4.3 Odd-sphere blackfolds	21
1.5 Blackfolds in supergravity	21
1.5.1 The blackfold expansion	22
1.5.2 Action principles	23
1.5.3 The effective fluid stress tensor from supergravity	24
1.5.4 Stationary solutions	26
1.5.5 Extremal limits	28
1.5.6 Lower form charged blackfolds	29
1.5.7 Stationary solutions	30
1.6 Blackfolds in background fluxes	31
1.6.1 The extrinsic equation from long-wavelength perturbations	32
1.6.2 Force terms as modified constraint equations	34
1.6.3 Integrating the EOM to an action	36
1.6.4 More general force terms	37
1.7 The blackfold construction in fluxed backgrounds	38

1.7.1	Conserved charges	38
2	Thermal spinning giant gravitons	41
2.1	Introduction	41
2.1.1	Thermal probe branes à la blackfolds	42
2.2	Giant graviton on S^n revisited	44
2.2.1	Setup and action	45
2.2.2	Solution branches and stability	46
2.3	Construction of finite temperature giant graviton on S^n	49
2.3.1	Blackfold action and equation of motion	49
2.3.2	Solution space and thermodynamics	52
2.3.3	The extremal limit	54
2.4	Thermal spinning giant graviton	55
2.4.1	Main features of solution space	55
2.4.2	Low temperature expansion	57
2.4.3	Spinning black hole configuration	60
2.5	The non-spinning giant graviton on $\text{AdS}_5 \times S^5$ - Finite temperature effects	62
2.5.1	The solution space	62
2.5.2	Stability	63
2.6	Null-wave giant graviton	64
2.6.1	Extremal giant graviton solution with null-wave	65
2.6.2	An action for null-wave branes	67
2.7	Thermal giant gravitons on AdS_m	69
2.7.1	Extremal giant gravitons on AdS_m	70
2.7.2	Construction of thermal giant graviton on AdS_m	71
2.7.3	Thermal giant graviton on AdS_5 - finite temperature effects	71
2.7.4	Low temperature expansion	72
2.7.5	Null-wave giant graviton expanded into AdS_m	73
3	Hydrodynamics of charged black branes	75
3.1	Introduction	75
3.2	Reissner-Nordström branes and effective zeroth order fluid	77
3.2.1	Reissner-Nordström black branes	77
3.2.2	Thermodynamics and effective blackfold fluid	78
3.3	The perturbative expansion	78
3.3.1	Setting up the perturbation	79
3.3.2	A digression: Reduction of Einstein-Maxwell theory	81
3.4	First order equations	82
3.4.1	Scalars of $SO(p)$	82
3.4.2	Vectors of $SO(p)$	85
3.4.3	Tensors of $SO(p)$	86
3.4.4	Comment on the homogeneous solution	86
3.4.5	Imposing asymptotically flatness	87

CONTENTS

3.5	Viscous stress tensor and current	88
3.5.1	First order fluid dynamics	88
3.5.2	Computing the effective stress tensor and current	89
3.5.3	Hydrodynamic bounds	90
3.6	Stability and dispersion relations	90
3.6.1	Dispersion relations	91
3.6.2	Thermodynamic stability	94
4	Discussion	95
4.1	Summary	95
4.2	Future directions	97
A	Geometry of embedded worldvolumes	100
A.1	Basic definitions and relations	100
A.1.1	Redshift factors	103
A.2	The blackfold action from the embedding	103
B	The F1-Dp bound state	105
C	Thermal giant gravitons	107
C.1	Thermodynamic blackfold action and Smarr relation	107
C.2	The upper branch, CFT dual and correlation functions	108
C.3	Details on solution space	111
C.3.1	Alternative parameterization of solution space	111
C.3.2	The special case $\Omega = \omega$	113
D	Details for Chapter 3	115
D.1	Reduction	115
D.1.1	Reduction of Einstein-Maxwell theory on an Einstein manifold	115
D.1.2	Reduction of the zeroth order solution	116
D.2	Coefficients of the large r expansions	116
D.3	Thermodynamic coefficients	118
	References	119

Introduction

Since its discovery, almost one hundred years ago, general relativity has been studied in great detail and has been used to probe the large scale structure of the observable universe with great success. Black holes show up as an inseparable part of general relativity as a mathematical consequence of Einstein's field equations. These objects, by now observed in abundance in nature [4], represent a locale of spacetime of extreme (ultimately singular) curvature. As is well-known, many properties of four dimensional black holes have been established throughout the years. In particular, four dimensional black holes are known to be completely determined by their mass, angular momentum, and electric charge [5]. Moreover, upon closer inspection, black holes are found to be essentially thermal in nature; they radiate, they have an entropy and they even have an associated first law of thermodynamics [6; 7]. Although tremendous work has gone into understanding the nature of black holes, they are still profoundly mysterious. Despite the fact that Nature seems to hide singularities behind event horizons, the smooth geometric structure of spacetime must break down in regions where the curvature approaches the Planck length i.e. close to the black hole singularity. Moreover, the thermal properties of black holes and their uniqueness theorems do not seem to be compatible in a quantum setting, information is lost. This is the (in)famous black hole information paradox. Finally, the entropy of a black hole is proportional to the area of its event horizon. Since, in general, the entropy of a system is a measure of the internal degrees of freedom, this is a very weird result. The informational content of a black hole seems to be entirely contained in surface fluctuations of the event horizon.

These issues should all be explained by a satisfying quantum theory of gravity. As is well-known, general relativity is notoriously incompatible with the framework of quantum theory. Instead of directly quantizing classical gravity, general relativity is seen as a low energy effective description of the "true" (quantum) theory of gravity. The modern approach to quantizing gravity is therefore proposing the quantum theory, requiring it to be mathematically consistent and that it contains Einstein's theory in the low energy effective limit. One such proposal is string theory (or more generally M-theory) [8]. Although not verified (directly or indirectly) experimentally, string theory provides a promising framework for unifying gravity and quantum mechanics. String theory correctly reproduces general relativity *viz.* supergravity in the low energy effective description, albeit in higher dimensions. Indeed, higher than four spacetime dimensions seems to be an essential property of quantum gravity. This has sparked a large interest in higher dimensional gravity. Indeed,

understanding the classical regime of any theory is vital for understanding its quantum aspects. Of particular interest to string/M-theory, and their related supergravities, are p -branes which, much like the black hole in four dimensions, show up as soliton-like classical solutions to the supergravity equations of motion [9]. On the other hand, these objects admit a dual description as (non-perturbative) excitations of the quantum theory. For instance, the D-branes of string theory manifest themselves as extended hypersurfaces whose quantum dynamics is described in terms of open strings whose ends are constrained to end on them [10]. The dual description of D-branes in terms of supergravity (closed strings) and gauge theory (open strings), along with the expectation that these two descriptions essentially contain the same physics (heavily aided by powerful theorems in supersymmetry), has led to many fascinating results and insights e.g. the microscopic counting of black hole entropy [11] and the celebrated AdS/CFT correspondence [12–15].

The AdS/CFT correspondence is the best understood manifestation of the holographic principle which (in its original formulation) predicts the equivalence between IIB string theory on $\text{AdS}_5 \times S^5$ and $\mathcal{N} = 4$ Super Yang-Mills, a conformal field theory, defined on the four dimensional projective boundary of AdS_5 . Most studied in the planar limit, the AdS/CFT correspondence has been used to gain new insights into the nature of strongly coupled field theories. Although $\mathcal{N} = 4$ SYM is not a viable theory for any real-world quantum system, for obvious reasons, it has still been used to give qualitative predictions for various strongly coupled real-world systems that are realized in the laboratory. In this way the AdS/CFT correspondence has provided applications for string theory and higher dimensional gravity outside high energy theoretical physics. In particular we mention the predictions for the quark-gluon plasma (AdS/QCD) [16] studied at various colliders and condensed matter systems (AdS/CMT) [17] including superconducting physics [18]. Related to the holographic study of the quark gluon plasma is the hydrodynamical limit of AdS/CFT also known as the fluid/gravity correspondence [19–22]. Here one considers the limit of the dual CFT where it is completely thermalized and have an effective description in terms of hydrodynamics. This hydrodynamic behavior is captured by, through the correspondence, long-wavelength fluctuations of the AdS black brane. Reversing the logic, this allows one to extract the hydrodynamic properties of the dual CFT characterized by a set of transport coefficients providing a holographic explanation for the experimentally observed very low viscosity of the quark-gluon liquid.

In context of the AdS/CFT correspondence, probe F-strings and D-branes, typically related to heavy operators on the gauge theory side, have played an important role for uncovering the nature of the duality. In particular, the intricate interrelation between the “blowing up” behaviour of multiple coincident probes [23; 24] (at large energies) and the non-(linear/Abelian) structure of the DBI action has been studied in great detail. In this context we mention the giant graviton configuration [25–27] (blown up from a point particle probe) as well as the D3/D5 description of the multiple wrapped Wilson loop [28] (blown up from a string probe). The success of relating DBI probes to gauge theory observables has naturally led to the use of probe string/branes in thermal backgrounds, i.e., hot AdS or an AdS black hole background, in order to gain insight into various aspects of thermal strongly coupled theories. Applications include the study of meson spectroscopy

at finite temperature including the melting phase transition of mesons and other types of phase transitions with fundamental matter (see e.g. [29; 30]).

This thesis is centered around the so-called *blackfold approach* and some of its applications. The blackfold approach has been used to construct new approximate black hole solutions with exotic horizon geometries [31–37]. Moreover the approach has been used to map the effective dynamics of black holes to that of fluids and solids [3; 38–47]. Finally, as will be explained in the following chapters, the blackfold approach has provided an alternative framework for treating (thermal) probe branes in string/M-theory [48–53] and in AdS/CFT [1; 2; 54]. The blackfold approach is an effective long-wavelength theory for extended black objects in two-derivative Einstein gravity (including supergravity). The approach builds on the universal principle that when a system exhibits two widely separated scales, the dynamics should simplify and be captured by an effective theory in a perturbative expansion. The situation is well-known. We consider here two examples. *i)* Consider the classical theory of hydrodynamics. Here the, in general extremely complicated, short-wavelength physics of the underlying system can be integrated out when the mean free path of its constituents is much smaller than the scale of which the system is probed. This leaves a long-wavelength fluid dynamical effective theory whose (universal) effective equations are just the conservation equations of energy and momentum. The situation is reminiscent of that found in the fluid/gravity correspondence. Here the fluid dynamic (derivative) expansion on the field theory side applies when the length scale of the fluctuations of the AdS black brane is much larger than the length scale set by the (inverse) temperature of the dual field theory. However, effective descriptions of black holes in terms of hydrodynamics are not expected to be confined to AdS black holes and holographic setups. Indeed, fluid dynamics is the natural generalization of the global thermodynamics for any black hole, including asymptotically flat ones. *ii)* Another relevant example is the effective motion of a “small” black hole. If we consider a black hole propagating in some background that varies on scales much larger than the horizon radius, it is well-known (or at least in accordance with intuition), that the black hole can be given an effective description in terms of a probe point particle whose effective dynamics is nothing but the geodesic equation (and mass conservation) in the given background [55]. In a nutshell: The blackfold approach is the natural synthesis of *i)* and *ii)*.

Outline of thesis

The thesis is naturally split into three parts. A part concerning the development of the blackfold approach along with an analysis of blackfolds in external fields (Chap. 1), a part concerning a concrete application of the effective methods to thermal (spinning) giant gravitons (Chap. 2), and finally a part concerning the hydrodynamics of charged black branes (Chap. 3). Each chapter is structured as follows.

- In chapter 1, we review the blackfold approach and explain how the effective theory can be used to construct new approximate black hole solutions exhibiting non-trivial horizon topologies. Having reviewed the basic ideas, we explain how the effective theory naturally is extended to more general settings including supergravity. Finally, we extend the formalism to blackfolds embedded in dilatonic flux backgrounds.
 - The blackfold review aims to give an original presentation of the blackfold approach developed in the papers [31; 36–38; 40; 44; 46; 56; 57]. Moreover, the chapter contains a subset of results which will be presented in the future publication [58].
- In chapter 2, we apply the blackfold approach to study the giant graviton solution on $\text{AdS}_m \times S^n$ in IIB/M-theory as the background is heated up to finite temperature, using the method of thermal branes originating from the blackfold approach. Moreover, the thermal approach allows us to switch on new quantum numbers, namely internal spins in the directions parallel to the configuration. We start the chapter out by motivating the approach and reviewing the usual DBI giant graviton. We then move on to heating up the configuration and examine the effects from finite temperature and spin. Finally, we consider a novel extremal double scaling limit leading to a zero-temperature null-wave giant graviton, exhibiting a BPS spectrum, which does not have an analogue in terms of the conventional weakly coupled world-volume theory.
 - The results are based on the papers [1; 2].
- In chapter 3, we consider intrinsic long-wavelength fluctuations of charged black branes along the directions of the worldvolume. More specifically, we consider the asymptotically flat Maxwell charged black brane (which we dub the Reissner-Nordström black brane) of general spatial dimension and co-dimension. We analyze and solve the full set of Einstein/Maxwell equations to first order in a derivative expansion by requiring horizon regularity and asymptotically flatness. From the obtained solution, we compute the transport coefficients of the effective blackfold fluid including a new transport coefficient associated with charge diffusion. We then move on to discussing some hydrodynamic bounds and finally we compute the next-to-leading order dispersion relation of the black branes hydro modes and discuss its stability properties.
 - The results are based on the paper [3].
- In chapter 4, we summarize the obtained results and mention some open problems and future directions.

1 | The blackfold approach

1.1 Introduction

In this chapter we introduce the *blackfold approach* [31; 36–38; 40; 44; 46; 56; 57], which has been used to probe the effective dynamics of various black hole solutions (in certain regimes), and to construct a wealth of new (approximate) black hole solutions. According to the well-known no-hair theorem of black hole physics, all (regular), stationary, asymptotically flat solutions to the Einstein-Maxwell (EM) equations in $D = 4$ dimensions fall into the Kerr-Newman family of solutions, and are thereby uniquely determined by their mass M , angular momentum J , and electric charge Q [5]. In particular, the only possible topology of the horizon of a stationary black hole in $D = 4$ is spherical i.e. that of an S^2 . In $D = 4$, the black hole phase structure is therefore very simple, as there is only one phase available. However, in higher spacetime dimensions $D \geq 5$, the phase structure becomes much richer. Already in $D = 5$, the phase structure becomes significantly more complicated. Besides the usual Myers-Perry rotating black hole solution with horizon topology S^3 [59], the asymptotically flat black ring solution (horizon topology $S^1 \times S^2$), was found by Emparan and Reall in [60]. Moreover, [60] found a range of values for the mass and angular momentum for which there exists a rotating Myers-Perry black hole solution, as well as a black ring solution (actually two ring solutions). Later $D = 5$ black ring of EM theory (and more generally of Einstein-Maxwell-Dilaton (EMD) theory) was found in [61]. The uniqueness theorems of four dimensional gravity do therefore not extend to higher dimensions. In general, finding black hole solutions to Einstein gravity in $D \geq 4$ is highly non-trivial task due the tremendous complexity of the equations of motion. Unfortunately, the techniques used in $D = 5$ are not available in $D > 5$, however, approximate methods exist in $D \geq 5$ spacetime dimensions. One method, which will be considered in this thesis, builds on the simple observation that in certain regimes of solution space, higher dimensional black holes exhibit a clear separation of scales. In general in D dimensions a (neutral) black hole has two length scales associated with its geometry determined by its mass M and angular momentum J ,

$$\ell_M \sim (GM)^{\frac{1}{D-3}}, \quad \ell_J \sim J/M. \quad (1.1)$$

For small angular momenta $\ell_J \ll \ell_M$, the physics of the black hole is expected to resemble that of the D dimensional Myers-Perry solution. The regime where the two length scales are of the same parametric order $\ell_J \approx \ell_M$ contains new very non-trivial black objects

e.g. the black ring. This regime involves the full non-linearity of general relativity and is in general very hard to access using analytical methods (however, various classification schemes exist, see e.g. [62] and related works). Finally, we can consider the regime where $\ell_M \ll \ell_J$. In this regime, corresponding to the *ultra-spinning* regime of solution space, the black hole horizon topology exhibits widely separated scales in different directions. This is in accordance with intuition; for very large angular momentum, the “centrifugal” pull, due to rotation, forces the radius of the black ring to become very large (compared to the horizon thickness), and the black ring locally looks like a boosted black string. Similarly, in the ultra-spinning limit, the Myers-Perry black hole “pancakes” along the plane of rotation and locally looks like a boosted black brane [63]. It is worth noticing that, while the ultra-spinning regime can always be reached in $D \geq 4$, it does not exist in $D = 4$. Indeed, in $D = 4$, the Kerr bound requires that $J \leq GM^2$, so $\ell_J \leq \ell_M$. In conclusion, in certain regimes of solution space, complicated black hole solutions exhibit a horizon topology where some directions are much larger than others. In this regime the black hole locally looks like a (boosted) piece of black brane/string. This suggests that, in certain regimes, black hole physics can be understood in terms of an effective long-wavelength theory. This effective long-wavelength theory is the blackfold approach.

The reduction of a physical theory to a simpler effective theory, when the system exhibits two widely separated scales, is well-known in physics. Indeed, the quintessential example of an effective theory is hydrodynamics. Here the, in general extremely complicated, short-wavelength physics of the underlying system can be integrated out when the mean free path of its constituents is much smaller than the scale of which the system is probed. This leaves a long-wavelength fluid dynamical effective theory whose effective equations of motion are nothing but the conservation equations of energy and momentum. Another example is the effective description of the Nielsen-Olesen vortex of the Abelian Higgs model [64]. In general these string-like objects can bend and fluctuate and their full non-linear behavior is extremely complicated. However, when one considers deformations which are much larger than the radius of the vortex, the effective dynamics is well-captured by the Nambu-Goto string action. Another well-known example of an effective theory comes from string theory and the theory of D-branes. In string theory D-branes are introduced as planes where open strings can end. It is well-known that D-branes are not static but dynamical objects in their own right, however, their full non-linear dynamics is again very complicated. If we consider the limit where the deformations of the D-brane (in both worldvolume embedding and fields) occur on length scales that are much larger than the string length ℓ_s , the short-wavelength degrees of freedom can be integrated out to yield the Dirac-Born-Infeld (DBI) effective action for D-branes [65].

Along these lines, we seek to develop an effective gravitational theory of perturbed black branes. Instead of considering various ultra-spinning limits of known black hole solutions, in the blackfold approach we turn the picture around and write down a long-wavelength effective theory which tells us how to bend/perturb black branes. In essence, the blackfold approach therefore tells us how to consistently glue small pieces of boosted black branes together into a global (approximate) solution to a given order a perturbative expansion. In this way, the blackfold approach is very powerful for probing various limits of

certain black holes whose solutions are not known for the entire region of parameter space (i.e. spin, charge, etc.), with the black ring in $D \geq 6$ being the quintessential example. When writing down the effective blackfold theory, we shall rely heavily on the intuition of gluing flat black branes together which in turn is inspired by ideas from the fluid/gravity correspondence [19] and Carter's brane dynamics [66].

Notation: In the following we will use the standard notation used in the literature. The total spacetime dimension is denoted D and we use Greek letters μ, ν, \dots to denote spacetime indices. The background metric is denoted $g_{\mu\nu}$ and the corresponding covariant derivative is denoted ∇_μ .

In general, we use p to denote the spatial dimension of a given blackfold configuration (constructed from p -branes). Moreover, the dimension of the (small) transverse sphere is denoted by $n + 1$. In this way, the co-dimension of the blackfold is $n + 2$. Also note that,

$$D = n + p + 3 . \quad (1.2)$$

The volume of the transverse unit sphere S^{n+1} is denoted $\Omega_{(n+1)}$.

Blackfold indices are denoted by Latin letters a, b, \dots . We will use σ^a to denote the coordinates on the blackfold and the embedding functions are denoted $X^\mu(\sigma^a)$. The collected worldvolume geometry of the blackfold is denoted \mathcal{W}_{p+1} and the spatial part of \mathcal{W}_{p+1} is denoted \mathcal{B}_p , so that $\mathcal{W}_{p+1} \sim \text{time} \times \mathcal{B}_p$. Moreover, we shall reserve R to denote the characteristic extrinsic scale of \mathcal{W}_{p+1} (i.e. characteristic radius of curvature of \mathcal{B}_p). The induced metric on \mathcal{W}_{p+1} inherited from $g_{\mu\nu}$ is denoted γ_{ab} and the corresponding covariant derivative on \mathcal{W}_{p+1} (from γ_{ab}) is denoted by D_a . Finally, we denote the Hodge dual on \mathcal{W}_{p+1} by $\star_{(p+1)}$.

1.2 The effective blackfold theory

In this section we explain the basics of the blackfold idea and argue how the effective dynamics of a generic black brane can be replaced by that of a fluid brane i.e. a localized submanifold with a (fluid) stress tensor on its worldvolume, when the brane exhibits a large separation of scales, $r_0 \ll R$. We also argue that the effective stress tensor T_{ab} is of the quasi-local type and explain how it is computed. The ideas presented in this section were first considered in [56; 57].

1.2.1 The blackfold expansion

We consider a quite general theory of two-derivative Einstein gravity,

$$I = \frac{1}{16\pi G} \int \star \mathcal{R} + I_M . \quad (1.3)$$

Here I_M denotes a generic action which describes potential matter fields of the theory and their coupling to gravity (which could be zero i.e. pure Einstein gravity). The equations of motion (EOMs) corresponding to the action S are

$$\mathcal{G}_{\mu\nu} \equiv \mathcal{R}_{\mu\nu} - \frac{1}{2} g_{\mu\nu} \mathcal{R} = 8\pi G \mathbf{T}_{\mu\nu} , \quad \mathbf{T}_{\mu\nu} = -\frac{2}{\sqrt{-g}} \frac{\delta I_M}{\delta g^{\mu\nu}} , \quad (1.4)$$

where we use boldface $\mathbf{T}_{\mu\nu}$ to denote the gravitational stress in order to distinguish it from the effective blackfold stress tensor T_{ab} introduced below. A large class of asymptotically flat exact black brane solutions to these equations are known for many theories (see e.g. [67]).

In general a black brane solution is characterized by its spatial dimension p , a transverse sphere S^{n+1} (so that the total spacetime dimension D is given by $D = n + p + 3$), and a set of geometric parameters collectively denoted Φ . In general Φ consists of the radius r_0 of the transverse S^n corresponding to the black brane horizon, a boost velocity u^μ of the brane or equivalently the null Killing vector on the horizon, a set of charge parameters (depending on the matter content of the theory), and finally the embedding coordinates X^\perp of the black brane,

$$\Phi = \{r_0, u^\mu, \dots; X^\perp\} . \quad (1.5)$$

Here the ellipsis denotes the presence of possible charge parameters.¹ As explained in the introduction, in the blackfold approach we promote the collective brane parameters Φ to worldvolume fields $\Phi \rightarrow \Phi(\sigma^a)$ write down the effective gravitational theory as a derivative expansion in these fields,

$$\Phi \rightarrow \Phi(\sigma^a) = \{r_0(\sigma^a), u^\mu(\sigma^a), \dots; X^\perp(\sigma^a)\} . \quad (1.6)$$

In order to handle the perturbative expansion, we introduce the notion of effective blackfold currents. Here we will concentrate on the effective stress tensor, but other (matter) currents follow the same principle and will be treated in Sec. 1.5. In the blackfold approach we replace the effective dynamics of the (slightly perturbed) black brane by a set of localized conserved currents sourcing the long-wavelength fields of the (perturbative) gravitational solution. In more detail, we assume that the metric splits up into a short-wavelength component and a long-wavelength component, $g_{\mu\nu}$. The short-wavelength component of the metric lives close to the brane while the long-wavelength component $g_{\mu\nu}$ permeates the entire spacetime. The effective action and associated stress tensor and currents are then obtained by integrating out the short-wavelength degrees of freedom of the black brane. Schematically,

$$I[g_{\mu\nu}, \Phi] \approx \frac{1}{16\pi G} \int \star R + I_{\text{eff}}[g_{\mu\nu}, \Phi] , \quad (1.7)$$

where the effective action $S_{\text{eff}}[g_{\mu\nu}, \Phi]$ comes from the coupling between the short-wavelength component and the long-wavelength component. Due to the wide separation of scales, we assume that the coupling is localized to a *small* neighborhood of brane; the blackfold. We denote the (to leading order infinitely thin) submanifold spanned by the black brane by \mathcal{W}_{p+1} . The interaction can then be written

$$I_{\text{eff}}[g_{\mu\nu}, \Phi] = \int_{\mathcal{W}_{p+1}} \star_{(p+1)} \mathcal{L}_{\text{eff}}[g_{\mu\nu}, \Phi] = \int_{\mathcal{W}_{p+1}} d^{p+1} \sigma \sqrt{-\gamma} \mathcal{L}_{\text{eff}}[g_{\mu\nu}, \Phi(\sigma^a)] , \quad (1.8)$$

¹As reviewed in Sec. 1.5 for the Dp -brane there is one charge parameter Q_p while for more general p -brane bound states there will be additional charge parameters (or more properly currents) corresponding to the distribution of lower-form brane currents dissolved on the worldvolume. In general this also includes the possibility of transverse spin on the S^{n+1} (thus breaking the symmetry in the transverse directions), however, transverse spin will not be considered in this thesis.

Here the geometry on the worldvolume of the blackfold \mathcal{W}_{p+1} is the one that is induced by $g_{\mu\nu}$. Therefore, denoting the embedding functions of \mathcal{W}_{p+1} by $X^\mu(\sigma^a)$, the induced metric γ_{ab} and extrinsic curvature $K_{ab}{}^\rho$ are given by

$$\gamma_{ab} = g_{\mu\nu} \partial_a X^\mu \partial_b X^\nu, \quad K_{ab}{}^\rho = -\partial_a X^\mu \partial_b X^\nu \nabla_\mu \perp_\nu{}^\rho. \quad (1.9)$$

We refer to App. A for details on the induced geometry on \mathcal{W}_{p+1} . We can now associate an effective stress tensor to the worldvolume in the usual manner

$$T_{\text{eff}}^{\mu\nu} = -\frac{2}{\sqrt{-g}} \frac{\delta I_{\text{eff}}}{\delta g_{\mu\nu}}. \quad (1.10)$$

This is in itself not a very useful expression for the blackfold stress tensor. However, the fact that the gravitational coupling is localized allows us to compute the stress tensor using well-known techniques as we will now explain.

1.2.2 The quasi-local worldvolume stress tensor

In the infinitely thin approximation, only directions tangential to \mathcal{W}_{p+1} will play a role and the effective stress tensor (1.10) takes the form

$$T_{\text{eff}}^{ab} = -\frac{2}{\sqrt{-\gamma}} \frac{\delta I_{\text{eff}}}{\delta \gamma_{ab}}. \quad (1.11)$$

We will now argue that the effective stress tensor T_{eff}^{ab} is exactly the quasi-local stress tensor originally introduced by Brown and York [68]. In order to see this we enclose a small neighborhood around a given point on the brane by a timelike boundary hypersurface and identify the effective action S_{eff} with the classical on-shell gravitational action (of that given region). In practice we imagine that we place the (transverse part of the) hypersurface at the sphere S_r^{n+1} of radius r . In order to capture the full effective dynamics, we must take $r \gg r_0$, and eventually let $r \rightarrow \infty$. Moreover, notice that far away from the brane, $r \gg r_0$, the geometry of the boundary hypersurface (in the brane directions) is just that of \mathcal{W}_{p+1} while the metric reduces to that of the background. In this way the induced metric from the gravitational solution on the boundary hypersurface, in the brane directions, is just that induced by the background on the geometry \mathcal{W}_{p+1} , which is exactly how γ_{ab} was defined (cf. Eq. (1.9)). The effective stress tensor is therefore precisely recognized as the Brown-York quasi-local stress tensor, $T_{\text{eff}}^{ab} = T_{\text{(BY)}}^{ab}$. The quasi-local stress tensor is computed according to the usual prescription by integrating over the transverse sphere S_r^{n+1} ,

$$T_{ab}^{(\text{BY})} = \lim_{r \rightarrow \infty} \int_{S_r^{n+1}} \tau_{ab} \simeq \lim_{r \rightarrow \infty} r^{n+1} \tau_{ab}. \quad (1.12)$$

Here τ_{ab} is the combination

$$16\pi G \tau_{ab} = \left(\Theta_{ab} - h_{ab} \Theta \right) - \text{counter terms}. \quad (1.13)$$

where Θ_{ab} is the extrinsic curvature associated to the enclosing surface, h_{ab} is the induced metric, and $\Theta = h_{ab} \Theta^{ab}$. As is well-known, since the extrinsic curvature contains terms that

diverge as $r \rightarrow \infty$, a set of counter terms must be included in order to render τ_{ab} finite [69]. In Minkowski spacetimes these counter terms can be introduced by the standard background subtraction method [38; 57], however, special care must be taken in the case of charged black branes [3; 36] (for a more systematic treatment of counter terms in the blackfold approach see Ref. [70]).

1.2.3 The spacetime blackfold stress tensor

Equivalently, to leading order in the blackfold expansion, the stress tensor T_{ab} can be computed using the usual ADM prescription [71]. The method builds on the principle of equivalent sources and the stress tensor is simply computed by determining the stress-energy distribution that sources (1.4) to linear order (around the background $g_{\mu\nu}$). In essence, the stress tensor (1.11) replaces the (local) effective gravitational dynamics of the (perturbed) brane on scales $r_0 \ll r \ll R$. On scales $\sim R$ the total effective stress tensor (denoted by hat) is thus given by [40]

$$\hat{T}_{\mu\nu}(x) = \int_{\mathcal{W}_{p+1}} d^{p+1}\sigma \sqrt{-\gamma} \left(\frac{T_{\mu\nu}(\sigma) \delta^{(D)}(x - X(\sigma))}{\sqrt{-g}} \right). \quad (1.14)$$

The worldvolume scalar $T_{\mu\nu}$ is tangential to \mathcal{W}_{p+1} and is related to the (local) effective stress tensor (1.11) under the natural identification

$$T^{\mu\nu} = \partial_a X^\mu \partial_b X^\nu T^{ab}, \quad \perp_{\rho\nu} T^{\mu\nu} = 0. \quad (1.15)$$

Notice that the stress tensor (1.14) is manifestly diffeomorphism invariant. As we briefly discuss below, the stress tensor (1.14) is in fact only the *monopole* contribution to the full effective gravitational stress tensor. Dipole (and in general higher multipole) corrections show up at higher order in the small blackfold expansion parameter $\varepsilon = r_0/R$, and will not be relevant for the applications considered in this thesis.

1.2.4 The blackfold equations of motion

Here we discuss the blackfold equations which govern the effective black brane dynamics to leading order in the derivative expansion (1.6). The study of generic brane theories, i.e. theories confined to supporting worldsheets of lower dimension than the background spacetime, was originally carried out by Carter in [66], and many of the considerations of this work carry directly on to the blackfold approach, however, with the important input that the worldvolume black brane effective stress tensor is provided by gravity.

In order to derive the blackfold equations of motion, we rely on the fundamental assumption that the worldvolume effective theory exists and can be consistently coupled to gravity, or equivalently, that spacetime diffeomorphism invariance of the effective theory holds. In the probe approximation, where the black brane does not back-react onto the background spacetime geometry $g_{\mu\nu}$, and in the absence of external background fluxes, this assumption then translates into the condition that the effective blackfold stress tensor (1.14) is covariantly conserved,

$$\nabla_\nu \hat{T}^{\mu\nu} = 0, \quad (1.16)$$

where ∇_ν refers to the background. Notice that when the blackfold carries charge, this equation is supplemented by a set of (charge) current conservation equations, see sec. 1.5. The conservation equation (1.16) (+ potential charge current conservation equations) determines the (leading order) EOMs for the collective worldvolume fields $\Phi(\sigma^a)$ captured by the stress tensor T_{ab} and extrinsic curvature $K_{ab}{}^\rho$. To see this, we project (1.16) onto directions tangential and orthogonal to the worldvolume \mathcal{W}_{p+1} . The conservation equation decompose according to (see Eq. (A.18))

$$\nabla_\nu \hat{T}^{\mu\nu} = \int_{\mathcal{W}_{p+1}} d^{p+1}\sigma \sqrt{-\gamma} \frac{\delta(x - X(\sigma))}{\sqrt{-g}} \left(\partial_b X^\mu \left(D_a T^{ab} \right) + T^{ab} K_{ab}{}^\mu \right) = 0. \quad (1.17)$$

The D spacetime equations (1.16) therefore split into $p+1$ worldvolume equations parallel to \mathcal{W}_{p+1} , and $n+2$ equations orthogonal to \mathcal{W}_{p+1} ,

$$\begin{aligned} D_a T^{ab} &= 0 \quad (\text{intrinsic}), \\ T^{ab} K_{ab}{}^\rho &= 0 \quad (\text{extrinsic}). \end{aligned} \quad (1.18)$$

The first equation is hydrodynamic nature and is simply the statement that the worldvolume effective stress tensor is conserved along the directions of \mathcal{W}_{p+1} . It is referred to as the *intrinsic equation*. The second equation is of elastic nature (see Ref. [41] for an (relativistic) elastostatic interpretation) and can be interpreted as a balancing condition for the blackfold worldvolume in the given background. It is referred to as the *extrinsic equation*. We end this section by noting that the two blackfold equations (1.18) have a clear interpretation: They are the higher dimensional p -brane generalization of the point particle geodesic equation, $u^\mu \partial_\mu m = 0$, $m \dot{u}^\mu = 0$.

1.3 The effective blackfold fluid

In general the monopole stress tensor is of hydrodynamic nature with time evolution described by dissipative fluid dynamics. In the absence of time evolution, the configuration is stationary, and the effective stress tensor should thus be described by a perfect fluid stress tensor. This is indeed the case: Following [42], there is a natural way to see that the effective stress tensor of a stationary blackfold must necessarily be that of a perfect fluid. In the following we assume the configuration to be in thermal equilibrium with the surroundings with temperature T . In general, stationarity requires a high degree of symmetry of the embedding geometry and configuration. The stationary configuration is therefore characterized in terms of the embedding X , the induced geometry γ_{ab} , a (timelike) Killing vector \mathbf{k}^a . The latter statement will be justified from a fluid dynamic perspective below in Sec. 1.3.3. The only natural scalar one can construct from this data is $\mathbf{k} \equiv (-\gamma_{ab} k^a k^b)^{1/2}$.² Therefore, the action must be of the form

$$I[X^\mu] = \int_{\mathcal{W}_{p+1}} \mathcal{L}(\sqrt{-\gamma}, \mathbf{k}, T) = \int_{\mathcal{W}_{p+1}} d^{p+1}\sigma \sqrt{-\gamma} \lambda_0(\mathbf{k}, T). \quad (1.19)$$

²This argument applies for neutral blackfolds along with Maxwell charged ($q = 0$) and top-form charged ($q = p$) blackfolds. When lower form currents ($0 < q < p$) are introduced on the worldvolume, there are additional (spacelike) vectors defining the stationary flow, see Sec. 1.5.6.

We now consider variations of the embedding, $\delta X^\mu = \Phi^a \delta_a X^\mu + \Phi^i n_i^\mu$ where n_i^μ denotes the i th normal vector of \mathcal{W}_{p+1} . Under small variations the induced metric changes with a Lie derivative according to

$$\mathcal{L}\gamma_{ab} = 2D_{(a}\Phi_{b)} - 2K_{ab}{}^i\Phi_i . \quad (1.20)$$

Performing the variation of the action (1.19) wrt. the embedding X^μ , keeping the components \mathbf{k}^a and the temperature T fixed, then yields

$$\delta I = - \int d^{p+1}\sigma \sqrt{-\gamma} \left[D_a \left(T^{ab}\Phi_b \right) - \Phi_b D_a T^{ab} - T^{ab} K_{ab}{}^i \Phi_i \right] \quad (1.21)$$

where T^{ab} is the effective stress tensor (1.11) evaluated using the stationary action (1.19). We now demand the variation to vanish. The first term is a total derivative and in order for the variational problem to be well-posed, we require that $T^{ab}\eta_a|_{\partial\mathcal{W}_{p+1}} = 0$, where η^a denotes the normal vector at the boundary $\partial\mathcal{W}_{p+1}$. After this, the two equations coming from requiring $\delta I = 0$, are recognized as the intrinsic and extrinsic blackfold equations (1.18), respectively. However, we emphasize that the blackfold equations in general also are valid outside the stationary regime.

As advocated above, the action of the form (1.19) directly implies perfect fluid dynamics expected for stationary configurations. To see this, simply notice that $\delta\mathbf{k} = -\mathbf{k}/2 u^a u^b \delta\gamma_{ab}$ with $u^a = k^a/\mathbf{k}$. We then have

$$T^{ab} = - \frac{2}{\sqrt{-\gamma}} \frac{\delta I}{\delta\gamma_{ab}} = -\lambda_0(\mathbf{k}, T)\gamma^{ab} + \lambda'_0(\mathbf{k}, T)\mathbf{k}u^a u^b , \quad (1.22)$$

where $\lambda'_0(\mathbf{k})$ denotes the derivative of $\lambda_0(\mathbf{k})$ wrt. \mathbf{k} . The stress tensor (1.22) is recognized as that of a perfect fluid (fluid velocity u^a , $u_a u^b = -1$),

$$T_{(0)}^{ab} = \varrho u^a u^b + P\Delta^{ab} , \quad \Delta^{ab} = \gamma^{ab} + u^a u^b , \quad (1.23)$$

under the identifications

$$P = -\lambda_0(\mathbf{k}, T) , \quad \varrho = \frac{d(\lambda_0(\mathbf{k}, T)\mathbf{k})}{d\mathbf{k}} , \quad s = \frac{1}{T}\lambda'_0(\mathbf{k}, T)\mathbf{k}^2 . \quad (1.24)$$

The expression for the entropy density s follows from assuming the Gibbs-Duhem relation $\varrho + P = \mathcal{T}s$ and using the fact that the local temperature \mathcal{T} is given by a simple redshift $\mathcal{T} = T/\mathbf{k}$ for stationary flows (see Sec. 1.3.3). Finally, notice that the intrinsic equation $D_a T^{ab} = 0$ is trivially satisfied for the stress tensor (1.22), as expected (by virtue of Killing's equation).

1.3.1 The neutral black brane

Here we compute the effective fluid of the simplest black brane solution, namely that of a neutral boosted (boost velocity u^a , $u_a u^b = -1$) black p -brane of pure Einstein gravity,

$$ds^2 = (\Delta_{ab} - f(r)u_a u_b) d\sigma^a d\sigma^b + f^{-1}(r) dr^2 + r^2 d\Omega_{(n+1)}^2 , \quad a = 0, 1, \dots, p , \quad (1.25)$$

where

$$f(r) = 1 - \left(\frac{r_0}{r}\right)^n \quad \text{and} \quad \Delta^a_b = \delta^a_b + u^a u_b . \quad (1.26)$$

Here Δ_{ab} is the projector onto directions orthogonal to u^a in the brane directions, $d\Omega_{(n+1)}^2$ denotes the metric on the transverse unit $(n+1)$ -sphere, and indices are raised/lowered using the induced (flat) geometry on the brane i.e. with η_{ab} . It is easy to evaluate (1.12) for this particular solution. The stress tensor T_{ab} is found to be that of a perfect fluid with

$$\varrho = \frac{\Omega_{(n+1)}}{16\pi G} (n+1) r_0^n , \quad P = -\frac{1}{n+1} \varrho . \quad (1.27)$$

Notice that the pressure P is negative in accordance with the intuition that gravitation is attractive. Using familiar techniques [72], it is straightforward to compute the temperature \mathcal{T} and entropy density of the black brane,

$$\mathcal{T} = \frac{n}{4\pi r_0} , \quad s = \frac{\Omega_{(n+1)}}{4G} r_0^{n+1} . \quad (1.28)$$

It is easy to verify that the thermodynamic quantities satisfy the usual first law along with the thermodynamic Euler relation

$$d\varrho = \mathcal{T} ds , \quad w \equiv \varrho + P = \mathcal{T} s . \quad (1.29)$$

These two relations are of course nothing but the local density generalizations of the usual black hole thermodynamics.

1.3.2 Dissipative corrections

Perturbations longitudinal to the worldvolume are generically of hydrodynamic nature meaning that *i)* the effective dynamics is captured by a hydrodynamic derivative expansion in the worldvolume fields. *ii)* The effective dynamics is governed by energy-momentum conservation $D_a T^{ab} = 0$ of the (in general dissipative) fluid stress tensor.³

Following the usual procedure of relativistic fluid dynamics [73], to any given order n in the derivative expansion, we decompose a general fluid stress tensor according to

$$T_{(n)}^{ab} = T_{(0)}^{ab} + \Pi_{(n)}^{ab} + \mathcal{O}(D^{n+1}) . \quad (1.30)$$

Here Π_{ab} is the viscous part of the stress tensor and contains derivatives up to order $\mathcal{O}(D^n)$ while $T_{ab}^{(0)}$ denotes the $\mathcal{O}(D^0)$ perfect fluid stress tensor (1.23). To first order in the derivative expansion, the viscous stress tensor is determined by two transport coefficients, and is given by the familiar expression

$$\Pi_{(1)}^{ab} = -2\eta\sigma^{ab} - \zeta\vartheta\Delta^{ab} , \quad \sigma^{ab} = \Delta^{ac} \left(D_{(c} u_{d)} - \frac{\vartheta}{p} \Delta_{cd} \right) \Delta^{db} . \quad (1.31)$$

Here σ^{ab} is the shear tensor, $\vartheta = D_a u^a$ is the fluid expansion.⁴ The coefficients η and ζ are respectively the shear and bulk viscosity transport coefficients. Similarly to second order

³When the brane/fluid is charged these equations are supplemented by one or more charge conservation equations, see Chap. 3.

⁴Notice Π_{ab} is written in the canonical gauge $u_a \Pi^{ab} = 0$ (Landau frame). Also note that for conformal fluids $\Pi^a_a = 0$ and the bulk viscosity ζ must necessarily vanish.

in the derivative expansion the stress tensor is characterized in terms of 10 (independent) transport coefficients [74; 75]. In general, at order n in the derivative expansion, the dynamics of the fluid is then given by energy-momentum conservation of the order $n - 1$ stress tensor,

$$\mathcal{O}(D^n) : \quad D_a T_{(n-1)}^{ab} = 0 \quad \Rightarrow \quad \left. \begin{aligned} \dot{\varrho} + w\vartheta + u_a D_b \Pi_{(n-1)}^{ab} \\ w\dot{u}^a - \gamma^{ab} D_b P + \Delta^a_b D_c \Pi_{(n-1)}^{cd} \end{aligned} \right\} = 0, \quad (1.32)$$

which constitute the fundamental equations of viscous fluid dynamics. To order $n = 2$ these equations are the familiar Euler equations with first order viscous dissipative corrections.

Returning to the specific case of the effective blackfold fluid, in order to measure the transport coefficients one has to do an actual full (bulk) gravity computation. For completeness of the presentation, we here briefly outline the procedure and refer to Chap. 3 for a detailed account. In order to determine the effective stress tensor, and thus the transport coefficients, one solves the full set of non-linear Einstein equations, while imposing regularity at the putative horizon along with asymptotic flatness, in a derivative perturbative expansion in the worldvolume fields and reads off the effective quasi-local stress tensor (1.12) from the full corrected gravitation solution order by order. When going from order n to order $n + 1$ in the derivative expansion, the (fluid) conservation equation $D_a T_{(n)}^{ab} = 0$ shows up as a constraint equation in the full set of Einstein equations. After imposing these constraints, the remaining system of equation can then be solved while imposing the boundary conditions, and the stress tensor $T_{(n+1)}^{ab}$ can be computed. This was done in Ref. [38] for the neutral (extrinsically flat) black brane (1.25) to first order in the derivative expansion. In particular we mention that by computing the speed of sound in the effective viscous fluid of the neutral black brane the authors of [38] were able to identify the unstable sound mode of the effective fluid with the Gregory-Laflamme (GL) instability [76]. We also note that the general features of the instability can be seen already to leading order i.e. at the perfect fluid level [57].

1.3.3 Stationary solutions

Here we write down the general condition for stationary intrinsic fluid flow and examine the implications for the local thermodynamics and extrinsic equation. We therefore search for solutions to

$$D_a \left(\varrho u^a u^b + P \Delta^{ab} \right) = 0, \quad \Pi_{(n)}^{ab} = 0. \quad (1.33)$$

To this end we invoke the general result [77] that in order for the dissipative tensor structures in the stress tensor to vanish (and ditto the divergence of the entropy current), the velocity u^a of the fluid must lie along an isometry of the worldvolume i.e. u^a must be proportional to a timelike Killing vector k^a on \mathcal{W}_{p+1} ,

$$u^a = \mathbf{k}^a / \mathbf{k}, \quad D_{(a} k_{b)} = 0, \quad \mathbf{k}^2 \equiv -|\mathbf{k}|^2 = -\mathbf{k}_a \mathbf{k}^a. \quad (1.34)$$

We note that $u_a u^a = -1$ implies that $\dot{u}^a \equiv u^b D_b u^a = D_a \log \mathbf{k}$. It is easy to show that the relativistic Navier-Stokes equation for a stationary fluid configuration implies [78]

$$\dot{u}_a = -D_a \log \mathcal{T}, \quad q^a = -\kappa \Delta^{ab} (D_b \mathcal{T} + \mathcal{T} \dot{u}_b), \quad (1.35)$$

where q^a is the heat flux vector and $\kappa \geq 0$ is the associated heat conductivity. Hydrodynamical stationarity and thermal equilibrium are therefore seen to be equivalent. In particular stationarity implies for the local temperature \mathcal{T} ,

$$\mathcal{T}(\sigma^a) = T/\mathbf{k} , \quad T = \text{const.} \quad (1.36)$$

Here T is a constant which can be interpreted as the global temperature of the stationary fluid. The local temperature \mathcal{T} is thus obtained by a simple redshift of the global temperature T .⁵

In the following we assume that the isometries of \mathcal{W}_{p+1} are inherited from the background so that \mathbf{k}^a extends to a Killing vector field of the background, \mathbf{k}^μ . Therefore

$$u^\mu = \mathbf{k}^\mu / \mathbf{k} , \quad \nabla_{(\mu} \mathbf{k}_{\nu)} = 0 , \quad \mathbf{k}^2 = -\mathbf{k}_a \mathbf{k}^a = -\mathbf{k}_\mu \mathbf{k}^\mu . \quad (1.37)$$

In this manner the stationary fluid velocity can be extended to the background (at least in a neighborhood of \mathcal{W}_{p+1}). In the case of stationarity, where the stress tensor is that of a perfect fluid, and the fluid velocity u^a is given by (1.37), the extrinsic equation then takes the simple form

$$-PK^\rho = w \perp^\rho{}_\mu \dot{u}^\mu , \quad K^\rho \equiv \gamma^{ab} K_{ab}{}^\rho , \quad (1.38)$$

where we used the identity $K_{ab}{}^\rho v^a v^b = \perp^\rho{}_\mu \dot{v}^\mu$ for any tangent v^a to \mathcal{W}_{p+1} (cf. Eq. (A.16)). We note that the local blackfold enthalpy density $w = \varrho + P$ is always found to be positive (in agreement with the energy conditions). According to the discussion of Sec. 1.2.2, the stationary extrinsic equation (1.38) can be derived from the action⁶

$$I = \int_{\mathcal{W}_{p+1}} d^{p+1} \sigma \sqrt{-\gamma} P . \quad (1.39)$$

For the neutral brane, the Lagrangian (i.e. pressure for fixed \mathbf{k} and T) takes the form $P = \lambda_0(\mathbf{k}, T)$ (using Eqs. (1.27), (1.28), (1.36)),

$$P = \lambda_0(\mathbf{k}, T) = -\frac{\Omega_{(n+1)}}{16\pi G} \left(\frac{n}{4\pi} \frac{\mathbf{k}}{T} \right)^n . \quad (1.40)$$

The fact that the stationary extrinsic equation (1.38) derives from the action (1.39) can also be explicitly checked by varying the pressure P wrt. the embedding, using the explicit form of the local temperature (1.36) and employing the local thermodynamics (see App. A).

⁵Since the notion of energy, and therefore temperature, suffers local redshifts, the relation (1.36) is exactly expected for a fluid in thermal equilibrium. Note that, in general, the redshift factor \mathbf{k} contains contributions from both a relativistic redshift (due to a non-zero spatial velocity of u^μ) and from a gravitational redshift from the background.

⁶By convention, we henceforth define the blackfold action to be minus the effective action (1.19), so that the Lagrangian is $-\lambda_0 = P$. This in turn implies that the effective stress tensor is computed as $T_{ab} = 2/\sqrt{-\gamma} \delta I / \delta \gamma^{ab}$.

1.3.4 Elastic corrections

Here we briefly discuss elastic corrections to the blackfold stress tensor. Firstly, let us say a few words about elastic stability. By considering small perturbations of the extrinsic embedding one can easily study the elastic properties of the effective fluid on \mathcal{W}_{p+1} (we refer to Ref. [57] for the analysis). In general the system is found to be stable under elastic perturbations i.e. small long-wavelength transverse time-dependent fluctuations (this also holds true for the charged blackfold configurations considered in Sec. 1.5). In analogy with the intrinsic sector, it is also possible to go beyond the leading order description of the extrinsic sector. These ideas have been developed in the series of papers [31; 40–43]. In general, the $\text{SO}(n+2)$ symmetry of the transverse sphere can be broken in two ways; by “bending” the brane and by introducing transverse spin (i.e. on the S^{n+1}) on the worldvolume. This introduces stresses in the transverse directions to the brane and is effectively captured by the quasi-local stress tensor computed using the (to next-to-leading order) unbroken transverse S^n (as opposed to the leading order S^{n+1}). Equivalently, this can be seen as a finite thickness effect, since we consider effects from the small (compared to R), yet finite horizon radius r_0 . Finite thickness effects are captured by a multipole expansion of the stress tensor [79],

$$\hat{T}^{\mu\nu}(x) = \int_{\mathcal{W}_{p+1}} d^{p+1}\sigma \sqrt{-\gamma} \left(\left(\frac{B^{\mu\nu} \delta^D(x-X)}{\sqrt{-g}} \right) - \nabla_\rho \left(\frac{B^{\mu\nu\rho} \delta^D(x-X)}{\sqrt{-g}} \right) \right) + \dots \quad (1.41)$$

Here $B_{\mu\nu}$ is the usual monopole stress tensor (notice that the expansion can be shown to be diffeomorphism invariant). In principle higher multipole corrections can be included by considering higher order δ -function derivatives. The dipole correction $B^{\mu\nu\rho}$ to the stress tensor is considered small compared to $B_{\mu\nu}$ and represents fine structure bending (here ignoring spin) corrections to the stress tensor. The elastic corrections are similar in spirit to the corrections reviewed in Sec. 1.3.2, however, note that they are in general non-dissipative in nature (the brane acts like a solid, not a fluid, in its transverse directions). In particular the corrections are computed from a gravity computation using a matched asymptotic expansion (MAE). In the MAE procedure one (crucially) employs the wide separation of scales $r_0 \ll R$. Although technically quite involved, the idea is simple: the Einstein equations are solved in a near horizon coordinate patch, $r \ll R$, (dubbed the near zone) in a $1/R$ expansion and in a coordinate patch far from the horizon $r_0 \ll r$ (the far zone), where the weak field approximation applies. The solution in the far zone then provides the boundary conditions for the near zone solution in the “overlap region” $r_0 \ll r \ll R$ which is, as the name suggests, the overlap between the near and far zones (such an overlap exactly exists due to the wide separation of scales $r_0 \ll R$). In this way, the MAE procedure in principle takes back-reaction into account order by order in the small expansion parameter r_0/R . In the context of blackfolds, these ideas were first employed for the D -dimensional stationary black ring [31] (later generalized to the black ring in AdS [32]) and later generalized to the neutral stationary black brane [44] (to next-to-leading order in the expansion). These works also proved that the perturbed event horizon remains regular. The fine structure dipole corrections can then be read off from

the corrected solution. This beautifully allows one to associate a new elastic response coefficient (the Young modulus) to the black string/brane [40; 44].

1.4 The blackfold construction and conserved quantities

In this section we discuss how the effective blackfold theory is used to construct new (approximate) black hole solutions. In particular, we mention that the blackfold approach correctly reproduces the results, i.e. metric and thermodynamics to leading order, for known exact black solutions in the ultra-spinning limit, discussed in the introduction. Ref. [56] showed that the ultra-spinning “pancaking” limit of the Myers-Perry black hole is reproduced by a certain even-ball blackfold solution with r_0 varying over \mathcal{B}_p and with $r_0 \rightarrow 0$ on $\partial\mathcal{B}_p$ (for a detailed analysis of blackfolds with boundaries, we refer to [57]). Similarly, the ultra-spinning limit of (A)dS rotating Kerr black holes is recovered [32; 33] (in the limit where the length scale associated with the cosmological constant is large compared to r_0). Finally the very thin and long limit, $r_0 \ll R$, of the exact $D = 5$ black ring solution of [60] is reproduced to leading order in the blackfold parameter $r_0/R \ll 1$ [31]. These limits, along with the effective description of the GL instability, serve to provide non-trivial “experimental” tests of the correctness of the blackfold approach.

1.4.1 The blackfold construction

In essence, the blackfold equations (1.18) explain how to consistently glue pieces of flat black branes (with horizon topology $\mathbb{R}^p \times S^{n+1}$) together, to leading order in the effective description. We emphasize that these pieces of (almost) flat brane are small compared to the extrinsic scale R and large compared to the intrinsic scale $r_0 \ll R$. Instead of searching for general solutions to (1.18), we follow here a bottom-up approach and provide the space \mathcal{B}_p on which we wrap the black brane and then search for solutions to (1.18) for the specified geometry. In this way, assuming that solutions exist, the horizon topology of the resulting (approximate) black brane solution becomes⁷

$$\text{Horizon topology} \simeq \text{Topology}(\mathcal{B}_p) \times S^{n+1} . \quad (1.42)$$

In principle \mathcal{B}_p can be dynamical, however, for most applications, we assume stationarity. As explained in the previous section, stationarity requires a high degree of symmetry of the wrapping space \mathcal{B}_p . In the following ξ^a denotes the generator of time translations on \mathcal{W}_{p+1} and $\chi_{(i)}^a$ denotes the complete set of Cartan generators of rotations of \mathcal{W}_{p+1} with closed orbits of periodicity 2π . In this way, the Killing vector describing the stationary fluid flow can be decomposed according to

$$\mathbf{k}^a = \xi^a + \sum_i \Omega_i \chi_{(i)}^a . \quad (1.43)$$

Stationary solutions to the blackfold equations are then obtained by evaluating the action (1.39) on the specified geometry \mathcal{B}_p and requiring the variation to vanish $\delta I = 0$ while

⁷Note that if r_0 is non-zero everywhere (i.e. \mathcal{B}_p compact, $\partial\mathcal{B}_p = \emptyset$), the transverse sphere S^{n+1} is trivially fibered on \mathcal{B}_p and the horizon topology is just $\text{Topology}(\mathcal{B}_p) \times S^{n+1}$.

keeping the angular velocities Ω_i fixed (see also Eq. (1.48) below). We now explain how to compute the global thermodynamics of a given blackfold solution using standard techniques.

1.4.2 Integrated quantities and thermodynamics

As in Sec. 1.3.3, we assume that the Killing directions of the worldvolume \mathcal{W}_{p+1} extend to the background i.e. Eq. (1.37) with $\mathbf{k}^\mu|_{\mathcal{W}_{p+1}} = \mathbf{k}^a \partial_a X^\mu$. Now, for *any* Killing vector k^μ , the contraction between k^μ and the spacetime stress tensor (1.14), $j_k^\mu = \hat{T}^{\mu\nu} k_\nu$, is conserved. This follows directly from the conservation equation (1.16) and Killing's equation. The corresponding conserved spacetime charge $\mathcal{Q}[k]$ is obtained by integrating j_k over a spacelike slice (typically $x^0 = t = \text{const.}$). In this way, we associate a mass, M , and a set of angular momenta, J_i , to the blackfold solution. Inserting the conserved current j_k^μ for respectively, $k = \xi$, $k = \chi_{(i)}$, and using the explicit form of the stress tensor (1.14), we can do the integration over the δ -function to reduce the spacetime integral to an integral over \mathcal{B}_p . All in all,

$$M = \int_{\mathcal{B}_p} dV_{(p)} T^{ab} n_a \xi_b, \quad J_i = - \int_{\mathcal{B}_p} dV_{(p)} T^{ab} n_a \chi_b^{(i)}, \quad (1.44)$$

where we have assumed that the Killing vector ξ is hypersurface orthogonal to \mathcal{B}_p and introduced the unit time-like normal to \mathcal{B}_p by $n^\mu = \xi^\mu|_{\mathcal{W}_{p+1}}/R_0$ (we refer to App. A for the definition of the local geometric quantities R_0 , R_i and V_i). Similarly, we associate a global entropy to the configuration by integrating the entropy density s (1.24) over \mathcal{B}_p . More properly, we define the (perfect fluid) entropy current $j_S^a = s u^a$, and define the global entropy S as

$$S = - \int_{\mathcal{B}_p} dV_{(p)} j_S^a n_a = \int_{\mathcal{B}_p} dV_{(p)} \frac{R_0}{\mathbf{k}} s(\sigma). \quad (1.45)$$

We emphasize that the global temperature T (cf. Eq. (1.36)), the mass and angular momenta (1.44) and the entropy (1.45) represent the (leading order) global thermodynamics of a genuine black brane solution with horizon topology (1.42). Following the arguments presented in Ref. [57], it is possible to argue that the global temperature T and the entropy S are related to the surface gravity κ of the near-horizon geometry and the total horizon area A_H in the expected manner, i.e. as $T = \kappa/2\pi$ and $S = A_H/4\pi$, respectively. Moreover the usual ADM definitions of the conserved charges for the black hole solution only depend on the asymptotic data which is exactly provided by the (fluid) stress tensor T_{ab} .

The expressions (1.44) and (1.45) are valid for any fluid brane and thus for any effective stationary blackfold configuration with stress tensor T_{ab} . Here we record the expressions for the neutral black brane (1.27), (1.28). The mass and angular momenta evaluate to

$$\begin{aligned} M &= \frac{\Omega_{(n+1)}}{16\pi G} \left(\frac{n}{4\pi T} \right)^n \int_{\mathcal{B}_p} dV_{(p)} R_0^{n+1} (1 - V^2)^{\frac{n-2}{2}} (n + 1 - V^2), \\ J_i &= \frac{\Omega_{(n+1)}}{16\pi G} \left(\frac{n}{4\pi T} \right)^n n \Omega_i \int_{\mathcal{B}_p} dV_{(p)} R_0^{n-1} (1 - V^2)^{\frac{n-2}{2}} R_i^2, \end{aligned} \quad (1.46)$$

while the entropy is given by

$$S = \frac{\Omega_{(n+1)}}{4G} \left(\frac{n}{4\pi T} \right)^{n+1} \int_{\mathcal{B}_p} dV_{(p)} R_0^{n+1} (1 - V^2)^{\frac{n}{2}} \quad (1.47)$$

These formulae are only valid for the neutral black brane and receive corrections when the black brane carries charge on its worldvolume. Also, in the charged case, we emphasize that the formulae only apply to backgrounds with no external background fluxes.

Since the quantities M , J_i , Ω_i , S , and T represent the thermodynamics of a black hole solution, they should satisfy the usual first law of black hole mechanics. Indeed, using the general expression (1.44) and (1.45), one can show that [36]

$$I_E = \beta G, \quad \text{with} \quad G = M - \sum_i \Omega_i J_i - TS, \quad I_E = -\beta \int_{\mathcal{B}_p} dV_{(p)} R_0 P. \quad (1.48)$$

Here $iI \rightarrow -I_E$ is the Euclidean blackfold action, obtained by Wick rotating the action (1.39) $t \rightarrow -it_E$, and integrating over the thermal circle of periodicity $\Delta t_E = 1/T \equiv \beta$, while G is the global (Gibbs) free energy of the configuration. Notice that the relation (1.48) holds true for any, in general, off-shell (stationary) configuration. Also notice that,

$$J_i = - \left(\frac{\partial G}{\partial \Omega_i} \right)_{X, T}, \quad S = - \left(\frac{\partial G}{\partial T} \right)_{X, \Omega_i}, \quad (1.49)$$

which can be showed using the general expressions (1.44), (1.45), the action (1.39) along with the form of the Killing vector (1.43). The thermodynamic derivatives (1.49), consistently, justifies G as the Gibbs free energy with the natural variables being the embedding X^μ and the intensive variables Ω_i and T . We can now consider variations in the embedding $X^\mu \rightarrow X^\mu + \delta X^\mu$ while keeping the angular velocities Ω_i and global temperature T fixed. It follows that

$$\delta_X I_E = \beta \left(\delta_X M - \sum_i \Omega_i \delta_X J_i - T \delta_X S \right). \quad (1.50)$$

The variation $\delta_X I_E$ vanishes for any on-shell configuration, and it follows that among stationary solutions,

$$\delta_X I_E = 0 \quad \Leftrightarrow \quad \delta_X M = T \delta_X S + \sum_i \Omega_i \delta_X J_i. \quad (1.51)$$

We therefore conclude that the equilibrium blackfold equations are equivalent to the first law of (black hole) thermodynamics for the configuration.⁸ To make further connection to the thermodynamic nature of the action (1.39), instead of considering variations where the angular velocities are kept fixed, we can consider variations for which we keep the angular momenta J_i fixed. To this end we introduce the Helmholtz free energy F , which is

⁸The first law of black hole mechanics is usually written for variations of the on-shell (in the sense of Einstein equations) extensive thermodynamic variables. Using standard thermodynamic arguments, along with the established relations (1.49), it is easy to show that (1.51) implies $\delta M = T \delta S + \sum_i \Omega_i \delta J_i$ for on-shell (in the sense of blackfold equations) variations.

obtained by a simple Legendre transform of G , $F = M - TS$. It follows that the stationary blackfold equations are equivalent to $(\delta F / \delta X)_{J_i, T} = 0$, i.e., the vanishing of the variation of the Helmholtz free energy for fixed angular momenta J_i and global temperature T . In the thermal probe approach, considered in Chap. 2, this is in many ways the most natural way to write the stationary EOM, since we usually work in an ensemble with fixed temperature (assuming thermal equilibrium with the background) and fixed J_i (by virtue of the gravitational EOMs). Along similar lines, we expect the configuration to obey a Smarr-like relation. Again it is relatively straightforward to show that this is indeed the case. One can show that the following identity holds for the neutral black brane

$$(D - 3)M = (D - 2) \left(\sum_i \Omega_i J_i + TS \right) + \mathcal{T}_{\text{tot}} . \quad (1.52)$$

Here \mathcal{T}_{tot} and is the total tension is given by the worldvolume integral over the local tension $\mathcal{T} = (\gamma_{ab} + n_a n_b) T^{ab}$,

$$\mathcal{T}_{\text{tot}} = - \int_{\mathcal{B}_p} dV_{(p)} R_0 (\gamma_{ab} + n_a n_b) T^{ab} . \quad (1.53)$$

For the neutral black brane the total tension explicitly evaluates to

$$\mathcal{T}_{\text{tot}} = \frac{\Omega_{(n+1)}}{16\pi G} \left(\frac{n}{4\pi T} \right)^n \int_{\mathcal{B}_p} dV_{(p)} R_0^{n+1} (1 - V^2)^{\frac{n-2}{2}} (p - (n+p)V^2) . \quad (1.54)$$

The relation (1.52) is interpreted as the blackfold generalization of the Smarr relation. In asymptotically flat backgrounds the usual black hole Smarr relation must be satisfied [80], and the tension necessarily vanishes $\mathcal{T}_{\text{tot}} = 0$, however, this does not hold true in more general backgrounds [33]. Also note that, as with the thermodynamics and action, the Smarr relation (1.52) also receives contributions when the blackfold carries charge (see Sec. 1.5).

As a final remark, we here discuss how to make connection to the ultra-spinning limits discussed in the introduction. To this end we assume that the length scales along \mathcal{B}_p are of the same order $R_i \sim R$. Moreover we assume that the redshifts are moderate throughout the worldvolume so that \mathbf{k} is parametrically of order 1. Using the thermodynamics of the effective fluid of the neutral brane (1.27), (1.28), it is now straightforward to show that the two length scales ℓ_M and ℓ_J (introduced in Eq. (1.1)) are given by

$$\ell_M \sim (r_0^n R^p)^{\frac{1}{D-3}} , \quad \ell_J \sim R . \quad (1.55)$$

It follows that the expansion parameter of the effective theory $r_0/R \ll 1$ is related to ℓ_M and ℓ_J as

$$\left(\frac{r_0}{R} \right)^n \sim \left(\frac{\ell_M}{\ell_J} \right)^{D-3} . \quad (1.56)$$

In this way, neutral blackfolds are always in the ultra-spinning regime.

1.4.3 Odd-sphere blackfolds

Here we discuss the simplest p -blackfold solution consisting of a product of l rotating *round* odd-spheres, where each sphere rotates with equal angular velocity in all angles. We take

$$\mathcal{B}_p = \prod_{i=1}^l S^{p_i} \quad \text{with} \quad \sum_{i=1}^l p_i = p, \quad (1.57)$$

where $p_i = 2k_i - 1$, $i = 1, \dots, l$.⁹ We note that, since the number of transverse dimensions is given by $n + 2$ and each odd-sphere must have at least one direction orthogonal to \mathcal{B}_p , the number of odd-spheres are limited by $l \leq n + 2$. A particularly simple solution is obtained by taking the embedding so that each p_i -sphere is geometrically round (with corresponding radius R_i) and \mathcal{B}_p is embedded in a flat background (for a similar treatment in AdS, see [33]). This requires that the k_i angular velocities $\Omega_j^{(i)}$, $j = 1, \dots, k_i$, on each separate odd-sphere S^{p_i} are equal, $\Omega_1^{(i)} = \dots = \Omega_{k_i}^{(i)} \equiv \Omega^{(i)}$, $i = 1, \dots, l$ (which can be verified a posteriori). We note that \mathcal{B}_p does not break any of the commuting isometries of the background. In this highly symmetrical case it follows that the velocities introduced in Eq. (A.24) are all independent of the worldvolume coordinates and $V^2 = \sum_{i=1}^l (R_i \Omega^{(i)})^2$, $R_0 = 1$. Now using the action (1.48), and imposing stationary (i.e. Eq. (1.36)) on the local thermodynamics (1.27), (1.28), one finds

$$I_E[R_i] = \frac{\Omega_{(n+1)} \beta^{n+1}}{16\pi G} \left(\frac{n}{4\pi}\right)^n \prod_{j=1}^l \Omega_{(p_j)} R_j^{p_j} \left(1 - \sum_{i=1}^l (R_i \Omega^{(i)})^2\right)^{\frac{n}{2}}. \quad (1.58)$$

Varying the action wrt. the radii R_i , we find the following l equilibrium conditions on the configuration

$$\Omega^{(i)} R_i = \sqrt{\frac{p_i}{n+p}} \quad (\text{no sum over } i). \quad (1.59)$$

Obtaining the global thermodynamics of the solution (1.59) is now straightforward using Eqs. (1.46) and (1.47).

1.5 Blackfolds in supergravity

In this section we develop the effective gravitational theory for branes carrying various types of charges. The effective blackfold theory for branes carrying charge was originally written down in Refs. [36; 37], and we refer to these references for many of the details omitted below.

In addition to the metric, charged branes also source one or more gauge potentials, depending on the specific brane configuration and theory in question. Charged branes arise naturally in various supergravity schemes and low energy effective descriptions of

⁹Even-sphere solutions (and products of even-spheres) are not allowed as blackfold solutions since even-spheres always have fixed point for any rotation i.e. there will always be a direction in which gravitational tension cannot be countered by rotation.

string theory (see e.g. [81]), with the quintessential example being that of the usual Dp -branes of supergravity. In the extremal supersymmetric limit, these branes are associated with the supergravity fields of a (large stack of) Dp -branes, which are charged under the Ramond-Ramond field strength $F_{(p+2)}$ [10]. In the supergravity regime the (stack of) Dp -branes therefore naturally source a Ramond-Ramond field strength $F_{(p+2)}$. In the effective theory, we shall therefore use the terminology that the blackfold, constructed from the supergravity p -brane, carries p -brane charge. In general, the effective worldvolume dynamics of extremal Dp -branes is captured by the DBI action. The effective dynamics of the fundamental string (F1), the NS5 brane of type II string theory as well as the M2 and M5 branes of M-theory is captured by similar effective worldvolume actions [82; 83]. As mentioned above, the gravitational (closed string sector) is appropriate for describing a large stack of Dp -branes. The gravitational (probe blackfold) effective worldvolume theory is therefore appropriate for capturing the effective dynamics of a large stack of perturbed Dp -branes (however, not so large that the branes back-react of the surrounding geometry). Along similar lines, the effective blackfold theory for the gravitational realizations of the above extended objects can be seen as the strong coupling versions of the relevant weakly coupled DBI-like actions. These ideas will be made more clear and employed in Chap. 2.

In addition to p -brane charge, branes can also carry lower form currents on their worldvolume; i.e., the brane sources a $(q+1)$ -form gauge potential $A_{(q+1)}$ with $0 \leq q < p$. The simplest example of such a solution is the singly charged Maxwell charged black brane of Einstein-Maxwell theory (or more generally EMD theory) considered in Chap. 3. Such solutions also arise naturally in the context of string theory where p -branes can carry string charges, or more generally, other types of brane charges “dissolved” on their worldvolume. Some of the most important examples include the F1- Dp , D0- Dp , $D(p-1)$ - $D(p+1)$ bound states which are all related through various dualities [84; 85]. These two-charge solutions carry both p -brane and q -brane charge on their worldvolume, but also more complex bound states exist e.g. the D5-D3-D1 system. We also mention the M2-M5 bound state of eleven dimensional supergravity as an important example [86]. All of these types of multi-charged branes are naturally included in the effective theory, where the effective fluid, living on the blackfold worldvolume, now also carries q -brane charge.

Finally the above described branes can naturally be blackened in the usual way, and thus be taken away from extremality. Again, much like the AdS/CFT correspondence, the effective gravitational dynamics is appropriate for capturing thermal aspects of the strongly coupled regime of the relevant worldvolume theory. When writing down the blackfold theory for charged branes, we will therefore do it for non-extremal black branes, bearing in mind that the extremal limit of these solutions is well-defined [87], and captured by the blackfold approach.

1.5.1 The blackfold expansion

Before considering stationary solutions to the supergravity blackfold EOMs, we will say a few words about regimes of validity. For any brane, we naturally associate a length scale

with the energy (density),

$$r_\varrho = (G\varrho)^{\frac{1}{n}} . \quad (1.60)$$

In the case of the neutral brane, we then simply have $r_\varrho \sim r_0 \sim 1/\mathcal{T}$, and the blackfold derivative expansion makes sense when $r_\varrho \sim r_0 \ll R$, where R denotes the characteristic length scale associated with the fluctuations of the collective variables Φ . This, however, changes when we introduce charge (Q_p) on the worldvolume. The presence of p -charge introduces a new length scale to the problem,

$$r_Q = (GQ_p)^{\frac{1}{n}} , \quad (1.61)$$

which is manifestly independent of the temperature. For the branch connected to the extremal solution, the two length scales r_ϱ and r_Q are parametrically of the same order (with $r_\varrho = r_Q$ at extremality, see next section) and the small parameter governing the blackfold expansion is thus taken to be

$$\frac{r_Q}{R} \sim \frac{r_\varrho}{R} \ll 1 . \quad (1.62)$$

With these considerations, the blackfold expansion goes as explained in Sec. 1.2.

In addition to the usual effective stress tensor $\hat{T}_{\mu\nu}$ (Eq. (1.14)), the p -brane charged blackfold now also carries an effective $(p+1)$ -form current $\hat{J}_{(p+1)}$ sourcing the associated $F_{(p+2)}$ gauge field. In analogy to (1.14), in the monopole approximation, we write

$$\hat{J}_{\mu_0 \dots \mu_p}(x) = \int_{\mathcal{W}_{p+1}} d^{p+1} \sigma \sqrt{-\gamma} \left(\frac{J_{\mu_0 \dots \mu_p} \delta^{(D)}(x - X(\sigma))}{\sqrt{-g}} \right) , \quad (1.63)$$

In the monopole probe approximation, $J_{\mu_0 \dots \mu_p}$ is supplemented by the tangentiality condition $0 = \perp^{\mu\mu_0} J_{\mu_0 \dots \mu_p}$, and it follows that

$$J^{\mu_0 \dots \mu_p} = \partial_{a_0} X^{\mu_0} \dots \partial_{a_p} X^{\mu_p} J^{a_0 \dots a_p} , \quad J_{(p+1)} = \star_{(p+1)} Q_p . \quad (1.64)$$

Here the last equation is understood as a form equation on the worldvolume \mathcal{W}_{p+1} , and

$$Q_p = - \int \star \hat{J} , \quad (1.65)$$

denotes the p -brane charge on the worldvolume. Notice, is with the quasi-local stress tensor (1.12), that the charge Q_p (i.e. the integral (1.65)) is computed in the region $r_0 \ll r \ll R$ (as with the stress tensor, going to next order in the blackfold expansion introduces dipole corrections to the effective current [46; 47]).

1.5.2 Action principles

The charge Q_p is defined as a local quantity in Eq. (1.65), however, it is not difficult to see that Q_p must be conserved along the worldvolume directions of the blackfold. Indeed, gauge invariance of the gauge field sourced by the current implies that the current \hat{J}_{p+1}

must be conserved, $d\star\hat{J} = 0$ (see also Sec. 1.6). This in turn implies that the worldvolume current $J_{a_0\dots a_p}$ is conserved on the worldvolume (see App. A),

$$d\star_{(p+1)} J_{(p+1)} = 0, \quad \text{so} \quad dQ_{p+1} = 0. \quad (1.66)$$

Therefore $\partial_a Q_p = 0$, and we conclude that Q_p is conserved and cannot vary along the worldvolume. Notice that the spacetime conservation equation $d\star\hat{J} = 0$ is purely tangential to \mathcal{W}_{p+1} and has no ‘‘extrinsic’’ equation associated to it. The parameter Q_p is therefore intrinsic to the blackfold and has no fluid dynamic DOFs associated to it. Also notice that, since the charge parameter Q_p , from a microscopic point of view, is basically the number of p -branes of the solution, the conservation of Q_p is quite natural. Although the charge Q_p is not dynamical, it still plays an important role in the formulation of the blackfold thermodynamics. Since the presence of p -brane charge introduces no hydrodynamic DOFs, the effective stationary action (1.19) can only be modified according to $\lambda_0(\mathbf{k}, T) \rightarrow \lambda_0(\mathbf{k}, T, Q_p)$. The effective stress tensor therefore still takes the form of a perfect fluid (1.23), where the charge Q_p now enters as a parameter in the equation of state. Especially, the action is of the form

$$I = \int_{\mathcal{W}_{p+1}} d^{p+1}\sigma\sqrt{-\gamma} P(\mathbf{k}, T, Q_p). \quad (1.67)$$

We also note that Q_p does not appear explicitly in (1.29), in accordance with that Q_p is not a fluid dynamical variable. In order to probe the space of solutions, it will be useful to introduce a local potential Φ along with a global potential Φ_p conjugate to Q_p ,

$$\Phi = \frac{\partial\varrho(s, Q_p)}{\partial Q_p}, \quad \Phi_p = \int_{B_p} dV_{(p)} R_0 \Phi. \quad (1.68)$$

Then, instead of considering P as a function of Q_p , we can shift ensemble and consider it as a function of Φ_p . This is done by a simple Legendre transform of the pressure by introducing the local Gibbs free energy $\mathcal{G}(\mathbf{k}, T, Q_p) = -(P + Q_p\Phi_p)$. It follows that the stationary extrinsic equation can now be obtained from the action

$$I = - \int_{\mathcal{W}_{p+1}} d^{p+1}\sigma\sqrt{-\gamma} \mathcal{G}, \quad (1.69)$$

for variations in the embedding where we keep the temperature, angular velocities, and global potential Φ_p fixed (these should be seen as variations in solution space and not physical variations where Q_p is fixed).

1.5.3 The effective fluid stress tensor from supergravity

Here we write down the boosted (black) p -brane solutions relevant to string and M-theory. Furthermore we compute the effective blackfold fluid of the solutions. In general, p -branes are charged under a $(p+1)$ -form potential. Moreover the branes also source a dilaton. In the following, we consider p -brane solutions to the quite general action in D dimensions [88]

$$I = \frac{1}{16\pi G_D} \int \left[\star R - \frac{1}{2} d\phi \wedge \star d\phi - \frac{1}{2} \sum_{i \in \mathcal{I}} e^{a_i \phi} F_{(i+2)} \wedge \star F_{(i+2)} \right]. \quad (1.70)$$

Here $F_{(i+2)} = dC_{(i+1)}$ is the field strength associated to the gauge potentials $C_{(i+1)}$ (notice that some of the forms can be of the same rank, with nevertheless a different coupling to the dilaton a_i , which distinguishes them) and \mathcal{I} denotes the collective set of gauge potentials in the theory. The action (1.70) captures (the bosonic part of) the supergravity descriptions of IIA, IIB (written in the Einstein frame) and M-theory relevant for describing D/NS-branes and M-branes:¹⁰ The action (1.70) corresponds to IIA (IIB) SUGRA for $D = 10$, $\mathcal{I}_{\text{RR}} = \{0, 2\}$ ($\mathcal{I}_{\text{RR}} = \{1, 3\}$) and $\mathcal{I}_{\text{NS}} = \{1\}$ [89] and eleven-dimensional SUGRA for $D = 11$ and $\mathcal{I}_{\text{M}} = \{2\}$ [90]. As is well-known, branes can both be electrically and magnetically charged under the above potentials. We can unify the description in the standard way by writing the field strengths in the electric ansätze, where now the index i in (1.70) runs over the (allowed) spatial dimension p of the brane. Given a dilaton coupling a , it will be convenient to define an additional parameter N to further unify the description,

$$a^2 = \frac{4}{N} - \frac{2(i+1)(D-i-3)}{D-2}. \quad (1.71)$$

The real parameter N (usually an integer for string/M-theory corresponding to the number of different types of branes in an intersection [91]) is preserved under dimensional reduction [36]. For the D/NS/M-branes of II string theory and M-theory $N = 1$ and $a_{\text{D}p} = (3-p)/2$ for the p -branes while $a^2 = 1$ for the F1 ($a_{\text{F}1} = -1$) and NS5 brane ($a_{\text{NS}5} = 1$). Also notice that the dilaton coupling (1.71) vanishes for $D = 11$, $i = 2, 5$, consistent with the fact that M-theory has no dilaton.

The metric of the boosted black p -brane solution to the generic action (1.70) is given by [9]

$$ds^2 = H^{-\frac{Nn}{D-2}} (\Delta_{ab} - f u_a u_b) d\sigma^a d\sigma^b + H^{\frac{N(p+1)}{D-2}} (f^{-1} dr^2 + r^2 d\Omega_{(n+1)}^2), \quad (1.72)$$

Here $f \equiv f(r)$ and $H \equiv H(r)$ are two harmonic functions given by

$$f(r) = 1 - \left(\frac{r_0}{r}\right)^n, \quad H(r) = 1 + \left(\frac{r_0}{r}\right)^n \sinh^2 \alpha, \quad (1.73)$$

where r_0 is the usual horizon radius and the parameter α parameterizes the charge. The dilaton ϕ and the $(p+1)$ -form gauge potential $C_{(p+1)}$ read

$$e^{2\phi} = H^{a_p N}, \quad C_{(p+1)} = \sqrt{N} \coth \alpha (H^{-1} - 1) dt \wedge dx^1 \wedge \dots \wedge dx^p. \quad (1.74)$$

Obtaining the effective stress tensor and current from the asymptotic form of the above solution is straightforward. The stress tensor and current take the expected perfect fluid form,

$$T_{ab} = \varrho u_a u_b + P \Delta_{ab}, \quad J_{(p+1)} = \star_{(p+1)} Q. \quad (1.75)$$

The energy density ϱ and pressure P are found to be

$$\varrho = \frac{\Omega_{(n+1)}}{16\pi G} r_0^n (n+1 + nN \sinh^2 \alpha), \quad P = -\frac{\Omega_{(n+1)}}{16\pi G} r_0^n (1 + nN \sinh^2 \alpha). \quad (1.76)$$

¹⁰In general the actions also have a Chern-Simons-like term, however, this term does not play a role for obtaining the flat p -brane solutions [81].

Notice that the pressure remains negative for all values of α . The charge Q_p is

$$Q_p = \frac{1}{16\pi G} \int_{S^{n+1}} e^{a_p \phi} \star dC_{(p+1)} = \frac{\Omega_{(n+1)}}{16\pi G} n \sqrt{N} r_0^n \sinh \alpha \cosh \alpha . \quad (1.77)$$

The remaining thermodynamics of the black p -brane is obtained using standard techniques [72] and is found to be

$$\mathcal{T} = \frac{n}{4\pi r_0 (\cosh \alpha)^N} , \quad s = \frac{\Omega_{(n+1)}}{4G} r_0^{n+1} (\cosh \alpha)^N , \quad \Phi = \sqrt{N} \tanh \alpha . \quad (1.78)$$

Here Φ denotes the chemical potential conjugate to the charge Q_p computed as basically the difference between $C_{(p+1)}$ at the horizon and spatial infinity. We note the simple relation for the local Gibbs free energy

$$\mathcal{G} = \varrho - \mathcal{T}s - \Phi Q_p = \frac{\Omega_{(n+1)}}{16\pi G} r_0^n , \quad (1.79)$$

Before concluding this section we should say a few words about hydrodynamic stability in the presence of p -brane charge *vis-à-vis* GL instability. As briefly discussed in Sec. 1.3.2 (which we shall return to in Chap. 3), the onset of the GL instability of the neutral string/brane can be identified with the unstable sound mode of the effective fluid. It is straightforward to repeat the analysis for the charged p -brane (since Q_p has no hydro DOFs associated to it the equations are just modified via the modified equation of state (1.76)). One finds that for branes with $nN > 2$ a stable regime always exists, at least close to extremality. This is in agreement with expectations (see e.g. Ref. [92] and related works).

1.5.4 Stationary solutions

With the remarks of Sec. (1.5.1), most of the consideration of Sec. 1.4 apply directly to p -brane charged supergravity blackfolds with the effective thermodynamics given by Eqs. (1.76), (1.77), (1.78). We note that, as opposed to the stress tensor, the current $J_{(p+1)}$ is Lorentz invariant. This Lorentz invariance manifests itself in the stress tensor. To see this explicitly, simply note that the stress tensor can be written

$$T_{ab} = \mathcal{T}s \left(u_a u_b - \frac{1}{n} \gamma_{ab} \right) - \Phi Q_p \gamma_{ab} . \quad (1.80)$$

Along similar lines, one can easily verify

$$(n+1)P = -(\varrho + n\Phi Q_p) , \quad (1.81)$$

These two expressions show that, as expected, introducing p -charge (\sim tension) on the brane does not break isotropy in the extremal limit $\mathcal{T}s \rightarrow 0$, Q_p fixed (see Sec. 1.5.5). The extrinsic equation (obtained from the action (1.67)) takes the form

$$(\mathcal{T}s + n\Phi Q_p) K^\rho = n\mathcal{T}s \perp_\mu^\rho \dot{u}^\mu , \quad (1.82)$$

This explicitly shows how introducing charge on the worldvolume introduces non-thermal intrinsic tension to the brane.

The global quantities, mass, angular momentum, and entropy are now computed using the general formulae (1.44), (1.45), using the perfect fluid stress tensor with thermodynamics (1.76), (1.77), (1.78). For fixed T and Q_p it is possible to write down expressions similar to (1.46), (1.47), however, solving for the two parameters r_0 and α in terms of T and Q_p in general involves solving a polynomial of degree $nN - 1$ which leads to rather cumbersome (implicit) results. We shall therefore retain the two parameters r_0 and α as a useful parameterization of the thermodynamics. It is easy to verify that the global thermodynamics is still related to the blackfold action as in (1.39), and by a simple shift of ensemble, we arrive at the first law

$$dM = TdS + \sum_i \Omega_i dJ_i + \Phi_p dQ_p, \quad (1.83)$$

where we remember that $dQ_p = 0$ among physical variations. Finally, in analogy to (1.52), one can show the relation

$$(D - 3)M = (D - 2) \left(TS + \sum_i \Omega_i J_i \right) + n\Phi_p Q_p + \mathcal{T}_{\text{tot}}. \quad (1.84)$$

Here \mathcal{T}_{tot} is the total tension and is given in the expression (1.53). As with the neutral black brane, the thermodynamics of the charged brane should also satisfy a Smarr relation. When evaluated on-shell the total tension must therefore vanish.¹¹ Finally notice that current conservation requires the worldvolume \mathcal{W}_{p+1} to be compact. Indeed, if \mathcal{W}_{p+1} had an open boundary Eq. (1.66) would be violated on $\partial\mathcal{B}_p$. In particular, this excludes blackfold solutions of the ball and disc type briefly discussed in Sec. 1.4. Supergravity blackfold solutions are now obtained in the standard way. In particular, the odd-sphere product construction of Sec. 1.4.3 straightforwardly carries on to p -brane charged blackfolds. One obtains the following set of equilibrium conditions,

$$\Omega_i R_i = \sqrt{\frac{p_i(1 + nN \sinh^2 \alpha)}{n + p(1 + nN \sinh^2 \alpha)}}, \quad (1.85)$$

which holds a valid approximation as long as $(GQ_p)^{\frac{1}{n}}/R_i \ll 1$. The brane solution corresponding to (1.85) is in general black but is also a valid solution in the extremal limit as we briefly discuss below. It is straightforward to obtain the global thermodynamics corresponding to (1.85), but the expressions are rather cumbersome and we refer to [37] for explicit expressions. In Figs. 1.1 and 1.2 we have recorded the possible odd-sphere solutions in $D = 10$ type IIA/B supergravity and M-theory, respectively. Notice that it is in principle possible to distort the odd spheres from a round geometry to an ellipsoid geometry leading to more complicated (worldvolume dependent) equilibrium conditions.

¹¹Note that $\mathcal{T}_{\text{tot}} = 0$ only provides one equation and is therefore, in general, not equivalent to the EOMs but rather a consequence of them.

Brane (IIA)	$\mathcal{B}_p = \prod_i S^{p_i}$	$\perp S^{n+1}$	Brane (IIB)	$\mathcal{B}_p = \prod_i S^{p_i}$	$\perp S^{n+1}$
F1	S^1	S^7	F1	S^1	S^7
D2	\mathbb{T}^2	S^6	D1	S^1	S^7
D4	$S^3 \times S^1, \mathbb{T}^4$	S^4	D3	S^3, \mathbb{T}^3	S^5
NS5	$S^5, S^3 \times \mathbb{T}^2$	S^3	NS5	$S^5, S^3 \times \mathbb{T}^2$	S^3
D6	$S^3 \times S^3, S^5 \times S^1$	S^2	D5	$S^5, S^3 \times \mathbb{T}^2$	S^3

Table 1.1: Allowed II odd-sphere solutions in $D = n + p + 3 = 10$ type IIA/B supergravity.

M-brane	$\mathcal{B}_p = \prod_i S^{p_i}$	$\perp S^{n+1}$
M2	\mathbb{T}^2	S^7
M5	$S^5, S^3 \times \mathbb{T}^2, \mathbb{T}^5$	S^4

Table 1.2: Allowed II odd-sphere solutions in $D = 11$ supergravity.

1.5.5 Extremal limits

Here we discuss the extremal limits of the charged blackfolds introduced above. As discussed above, the characteristic length scale for p -branes is set by the total charge Q_p and not by the temperature. This means that the blackfold approximation is valid even in the extremal limit. The extremal limit is obtained in the standard way by letting the horizon radius $r_0 \rightarrow 0$ while keeping the charge Q_p fixed. This in turn implies that $\alpha \rightarrow \infty$ in the extremal limit (here assuming that $Q_p > 0$). Near extremality $\mathcal{T}s/Q_p \ll 1$, the effective stress tensor takes the form,

$$T_{ab} \approx \mathcal{T}s \left(u_a u_b + \left(\frac{N}{2} - \frac{1}{n} \right) \gamma_{ab} \right) - \sqrt{N} Q_p \gamma_{ab} . \quad (1.86)$$

In the extremal limit $\mathcal{T}s \rightarrow 0$, the thermal component vanishes and it follows that

$$P = -\sqrt{N} Q_p . \quad (1.87)$$

Since Q_p is constant on the worldvolume we see that the action (1.67) reduces to that of a Dirac brane i.e. a brane with uniform tension on its worldvolume. The intrinsic fluid dynamics has disappeared and the dynamics is only extrinsic. The absence of compact minimal surfaces in Euclidean space [56] therefore suggests that there are no extremal p -brane blackfold solutions. However, the odd sphere solution (1.85) is clearly a well defined solution, even in the extremal limit. The apparent contradiction is easily resolved and is found in the form of the stress tensor (1.86). Although $\mathcal{T}s \rightarrow 0$ in the extremal limit, the product $\mathcal{T}s u_a u_b$ does not necessarily have to vanish. For the solution (1.85), $\mathbf{k} \rightarrow 0$ and we therefore see that $\mathcal{T}s u_a u_b \rightarrow \mathcal{K} \ell_a \ell_b$ with ℓ^a null and where \mathcal{K} is finite. The odd-sphere solution therefore carries a null-wave on its worldvolume in the extremal limit with momentum density \mathcal{K} which exactly balances out the tension on the brane (null-waves in a

blackfold setting were first considered in Ref. [37]). We refer to Sec. 2.6.2 for a discussion of some of the more general aspects of null-wave blackfolds.

1.5.6 Lower form charged blackfolds

In this section we consider blackfolds carrying lower $(q+1)$ -form currents on their world-volume. The effective fluid (including currents) now derives from p -brane solutions coupled to one or more lower form gauge field $A_{(q+1)}$, $q < p$. In analogy with Eq. (1.63), we write

$$\hat{J}_{\mu_0 \dots \mu_q}(x) = \int_{\mathcal{W}_{p+1}} d^{p+1} \sigma \sqrt{-\gamma} \left(\frac{J_{\mu_0 \dots \mu_q} \delta^{(D)}(x - X(\sigma))}{\sqrt{-g}} \right). \quad (1.88)$$

Assuming gauge invariance of the underlying gravitational theory, it follows that the current $J_{(q+1)}$ is conserved. In the following we let \mathcal{Q}_q denote the q -brane density. By virtue of current conservation one can show that the current $J_{(q+1)}$ is hypersurface-forming. These submanifolds, denoted \mathcal{C}_{q+1} , foliate the worldvolume \mathcal{W}_{p+1} and correspond to the world-sheet/volume of the q -branes carrying the charge \mathcal{Q}_q . Along these lines, we write

$$J_{(q+1)} = \mathcal{Q}_q \star_{(q+1)} 1. \quad (1.89)$$

Here $\star_{(q+1)} 1$ denotes, in somewhat vulgar notation, the unit volume $(q+1)$ -form on \mathcal{C}_{q+1} . In this way, the density \mathcal{Q}_q is constant along \mathcal{C}_{q+1} and can only vary in the directions transverse to \mathcal{C}_{q+1} .

In addition to the usual fluid Killing vector \mathbf{k} , stationary lower-form charged configurations are characterized by q spatial vectors (corresponding to the tangent vectors of \mathcal{C}_{q+1}). The general action therefore takes the form,

$$I[X^\mu] = \int_{\mathcal{W}_{p+1}} d^{p+1} \sigma \sqrt{-\gamma} \lambda_0(\mathbf{k}, T; \ell_1, \dots, \ell_q). \quad (1.90)$$

In analogy with (1.22), we can now compute the stress tensor. Note that, in general, a non-zero temperature breaks Lorentz invariance of the worldvolume. Therefore, in general, $\mathbf{k} \partial_{\mathbf{k}} \lambda_0 \neq \ell_i \partial_{\ell_i} \lambda_0$. However, the current $J_{(q+1)}$ still preserves a $\text{SO}(q)$ symmetry. This implies that $\ell \partial_{\ell} \lambda_0 \equiv \ell_1 \partial_{\ell_1} \lambda_0 = \dots = \ell_q \partial_{\ell_q} \lambda_0$. In the following we let $h_{(q)}^{ab}$ denote the projector onto \mathcal{C}_{q+1} . Now in order to rewrite the stress tensor in terms of thermodynamic variables, we use that, besides the usual relation $T_b^a u^b = -\rho u^a$, we must have $T_b^a w^b = P_{\perp} w^a$ for any w^a orthogonal to \mathcal{C}_{q+1} , $h_{(q)}^{ab} w_b = 0$, and $T_b^a v^b = (P_{\perp} - \Phi_{\mathcal{Q}_q} \mathcal{Q}_q) v^a$ for any (spatial) v^a parallel to \mathcal{C}_{q+1} , $h_{(q)}^{ab} v_b = v^a$, $v_a u^a = 0$. The first condition states that in any direction orthogonal to \mathcal{C}_{q+1} there is a tension due to the (usual) pressure P_{\perp} of the fluid. The latter condition says that in the directions of \mathcal{C}_{q+1} , in addition to the pressure P_{\perp} , there is a pressure component due to the tension $-\Phi_{\mathcal{Q}_q} \mathcal{Q}_q$ (here $\Phi_{\mathcal{Q}_q}$ is the potential conjugate to \mathcal{Q}_q) of the dissolved q -branes. We thus obtain the general form of the stress tensor

$$T^{ab} = P_{\perp} \gamma^{ab} + \mathcal{T} s u^a u^b - \Phi_{\mathcal{Q}_q} \mathcal{Q}_q h_{(q)}^{ab}. \quad (1.91)$$

where we have assumed the underlying thermodynamic relations. The present arguments are easily generalized to fluids carrying more than one lower form current. In the case of a fluid carrying multiple lower form currents, the thermodynamics takes the form

$$\varrho + P_{\perp} = \mathcal{T}s + \sum_{q \neq p} \Phi_{\mathcal{Q}_q} \mathcal{Q}_q, \quad d\varrho = \mathcal{T}ds + \sum_{q \neq p} \Phi_{\mathcal{Q}_q} d\mathcal{Q}_q, \quad (1.92)$$

where the sums run over the lower form q -brane currents excluding $q = p$. The general stress tensor now takes the form

$$T^{ab} = \mathcal{T}su^a u^b - \mathcal{G}\gamma^{ab} - \sum_q \Phi_{\mathcal{Q}_q} \mathcal{Q}_q h_{(q)}^{ab}. \quad (1.93)$$

Here we have unified the expression for the stress tensor (so that the sum runs over all $q \leq p$) and introduced $h_{(p)}^{ab} = \gamma^{ab}$ along with the local Gibbs free energy density given by (here $\mathcal{Q}_p \equiv Q_p$ and $\Phi_{\mathcal{Q}_p} \equiv \Phi$)

$$\mathcal{G} = -(P_{\perp} + \Phi_{\mathcal{Q}_p} \mathcal{Q}_p) = \varrho - \mathcal{T}s - \sum_q \Phi_{\mathcal{Q}_q} \mathcal{Q}_q = \frac{1}{n} \mathcal{T}s. \quad (1.94)$$

Where the last relation holds for all IIA/IIB/11D branes and their toriodal compactifications. Having determined the general form of the stress tensor, it follows that the blackfold Lagrangian is given by the pressure $P_{\perp} = -(\mathcal{G} + \Phi_{\mathcal{Q}_p})$. The extrinsic equation now takes the form

$$\mathcal{T}s \perp^{\rho}_{\mu} \dot{w}^{\mu} = \mathcal{G}K^{\rho} + \perp^{\rho}_{\mu} \left[\sum_q \Phi_{\mathcal{Q}_q} \mathcal{Q}_q K_{(q)}^{\mu} \right] \quad (1.95)$$

where we have defined the mean curvature of the embedding \mathcal{C}_{q+1}

$$K_{(q)}^{\rho} = h_{(q)}^{ab} K_{ab}^{\rho}. \quad (1.96)$$

1.5.7 Stationary solutions

Here we briefly discuss some aspects of stationary solutions carrying lower form charge. According to the above discussion, stationary solutions are obtained by extremizing the action

$$I = \int_{\mathcal{W}_{p+1}} d^{p+1} \sigma \sqrt{-\gamma} P_{\perp}, \quad (1.97)$$

where P_{\perp} denotes the pressure i.e. the scalar multiplying γ_{ab} in (1.93). We note that the action only depends on the orthogonal component of the pressure and thereby none of the pressures induced by the lower form currents. However, we have not discussed how to choose the worldvolume currents $J_{(q+1)}$ for stationary solutions. In general, such an analysis requires writing down all possible hydrodynamic derivative corrections to the effective stress tensor and currents. Such an analysis does currently not exist in the literature, however, an analysis of charged string fluids $q = 1$ can be found in [36]. In Fig. 1.3 we have recorded the possible two charge $q = 0, 1$ bound state odd sphere solutions [37].

IIA	IIB	$\mathcal{B}_p = \prod_i S^{p_i}$	$\perp S^n$
	F1 – D1	S^1	S^7
D0 – D2	F1 – D2	\mathbb{T}^2	S^6
	F1 – D3	S^3, \mathbb{T}^3	S^5
D0 – D4	F1 – D4	$S^3 \times S^1, \mathbb{T}^4$	S^4
	F1 – D5	$S^5, S^3 \times \mathbb{T}^2$	S^3
D0 – D6	F1 – D6	$S^3 \times S^3, S^5 \times S^1$	S^2

Table 1.3: Allowed $q = 0, 1$ bound state \prod odd-sphere solutions in $D = 10$ type IIA/B supergravity.

1.6 Blackfolds in background fluxes

In this section we derive the effective blackfold equations for branes in supergravity backgrounds needed for the analysis presented in Chap. 2. The results of this section will be presented in [58].

When writing down the effective blackfold theory, we assumed that the blackfold was embedded in a pure gravity background (cf. Eq. (1.7)) and the effective EOMs were simply derived from assuming the conservation of the blackfold stress tensor

$$\bar{\nabla}_\mu T^{\mu\nu} = 0 . \quad (1.98)$$

When the blackfold is charged, relevant to various supergravity schemes, this equation is supplemented by a set of blackfold current (essentially intrinsic) conservation equations that derive from the assumption that the effective theory can be consistently coupled to the gauge potentials sourced by the blackfold.

It is now natural to ask how these equations are modified in the presence of non-trivial background (matter) fields. Let us here focus on the p -brane solution (Eqs. (1.72)-(1.74)) relevant to the supergravity cases. In analogy with Eq. (1.7), we write

$$I[g_{\mu\nu}, A_{(p+1)}, \phi, \dots ; \Phi] \simeq I_{\text{SUGRA}} + I_{\text{eff}}[g_{\mu\nu}, A_{(p+1)}, \phi; \Phi] , \quad (1.99)$$

where the ellipsis denote the rest of the supergravity fields in the theory and I_{eff} is the effective coupling between the background and the p -brane (which only involves the fields sourced by the brane i.e. the metric, the $(p+1)$ -form gauge field, and the dilaton). The effective blackfold EOM is therefore expected to be modified according to

$$\bar{\nabla}_\mu T^{\mu\nu} = (\text{Lorentz-like force} + \text{dilaton force}) , \quad (1.100)$$

where the force term is induced by the non-trivial background dilaton and $(p+1)$ -form gauge field. Instead of deriving these force terms from the “test brane” method used in Sec. 1.2.4, i.e., from requiring energy-momentum conservation of the blackfold stress tensor + background (for a review of this method applied to test particles, see e.g. [93; 94]), in this

section we derive the force terms directly from the supergravity EOMs. The derivation will include a review of the derivation of the extrinsic “vacuum” equation originally written down in [44]. Having obtained the effective EOM, we explain how it can be integrated to an action. As mentioned, the focus will be on the p -brane blackfold, however, in Sec. 1.6.4 we will briefly comment on the force terms and modified current conservation equations for bound state supergravity blackfolds (for definiteness we focus on the type II F1-D p case).

1.6.1 The extrinsic equation from long-wavelength perturbations

Following Ref. [44], we here review how the extrinsic equation (1.18) emerges as a constraint equation of the Einstein equations to linear order in a derivative expansion in ∂X_\perp . The main ingredient of this derivation is based on the construction of a set of Fermi normal coordinates adapted to a general submanifold \mathcal{W}_{p+1} (which will play the role of the bended black brane) of general co-dimension $n + 2 = D - p - 1$ and embedded in general flat background.

The adapted coordinates are naturally split up in a $p + 1$ dimensional tangential component σ^a and an $n + 2$ dimensional transverse component y^i defined so that the surface \mathcal{W}_{p+1} corresponds to $y^i = 0$. In general, the first order derivatives of the metric in the directions parallel to \mathcal{W}_{p+1} can be removed by a suitable coordinate transformation. However, the fact that the transverse coordinates are defined so that $y^i = 0$ corresponds to \mathcal{W}_{p+1} implies that the derivatives of the metric in the transverse directions generally cannot be gauged to zero. These, in general non-zero, transverse derivatives $\mathcal{K}_{ab}{}^i$ characterize the shape of the embedding and the leading order surrounding geometry. In the described normal coordinates, the metric takes the following form to leading order

$$ds^2 = (\eta_{ab} - 2\mathcal{K}_{ab}{}^i y_i) d\sigma^a d\sigma^b + \sum_{i=1}^{n+2} dy_i^2 + \mathcal{O}(\partial X_\perp^2). \quad (1.101)$$

Clearly, $K_{ab}{}^i = \Gamma_{ab}^i = \mathcal{K}_{ab}{}^i$, where $K_{ab}{}^i$ is the extrinsic curvature tensor of \mathcal{W}_{p+1} . Note that we use the notation $\partial X_\perp \sim 1/R \sim K_{ab}{}^i$.¹² The small dimensionless parameter controlling the expansion (1.101) is therefore $\sim y/R$, which in practice means discarding all order $\partial X_\perp^2 \sim 1/R^2$ terms. The metric (1.101) is interpreted as the zeroth order (i.e. $\mathcal{O}((r_0/r)^0)$), or background, metric of the bended black brane. When bending the black brane we replace the flat geometry η_{ab} on the brane with the modified bended geometry $\eta_{ab} \rightarrow \eta_{ab} + 2K_{ab}{}^i y_i$ and solve for the metric correction $h_{\mu\nu}$ to linear order in $\partial_\perp X$. For example, bending the boosted neutral black brane (1.25) (as in Ref. [44]) corresponds to perturbatively solving the full set of Einstein equations for the geometry

$$ds^2 = \left(\eta_{ab} - 2K_{ab}{}^i y_i + (1 - f(r)) u_a u_b \right) d\sigma^a d\sigma^b + \frac{dr^2}{f(r)} + r^2 d\Omega_{(n+1)}^2 + h_{\mu\nu}(y^i) dx^\mu dx^\nu + \mathcal{O}((r/R)^2), \quad (1.102)$$

¹²Here X_\perp are used in the sense of Sec. 1.2.1, i.e. $\partial X_\perp = 0$ corresponds to “flat” embedding.

where we have defined $r^2 \equiv y_i y^i$ and where the metric corrections $h_{\mu\nu}$ depend on the parameters r_0 and u^a and is first order in ∂X_\perp . When considering charged black branes we would similarly write down expressions the perturbed “bent” form of the matter fields (plus corrections), however, in the following we shall not be interested in the near-horizon geometry but only consider the overlap region geometry and such (theory dependent) expressions will therefore be omitted. In general, perturbations induced by the extrinsic curvature are coupled. However, in the linearized analysis each transverse direction decouples from each other. We can therefore deal with the deformation in each normal direction separately, and study perturbations where $K_{ab}^{\hat{i}}$ is non-zero along only one distinguished direction $y^{\hat{i}}$.¹³ Under this assumption, we introduce a directional cosine for $y^{\hat{i}}$,

$$y^{\hat{i}} = r \cos \theta . \quad (1.103)$$

In general, the metric perturbation functions $h_{\mu\nu}$ are dipoles of S^{n+1} and therefore decompose according to

$$h_{\mu\nu}(r, \theta) = \cos \theta \hat{h}_{\mu\nu}(r) . \quad (1.104)$$

Similarly the extrinsic curvature deformation is of dipole type $K_{ab}^{\hat{i}} y^{\hat{i}} = r \cos \theta K_{ab}^{\hat{i}}$.

We now consider the metric of the black brane in the overlap region $r_\rho \ll r \ll R$.¹⁴ The asymptotic behaviour of the flat brane metric is provided by the blackfold stress tensor T_{ab} in the usual way and the overlap region metric, including extrinsic curvature, thus takes the form

$$\begin{aligned} ds^2 = & \left(\eta_{ab} - 2K_{ab}^{\hat{i}} r \cos \theta + \frac{16\pi G}{n\Omega_{(n+1)}} \left(T_{ab} - \frac{T}{D-2} \eta_{ab} \right) \frac{1}{r^n} \right) d\sigma^a d\sigma^b \\ & + \left(1 - \frac{16\pi G}{\Omega_{(n+1)}} \frac{1}{D-2} \frac{T}{r^n} \right) dr^2 \left(d\theta^2 + \sin^2 \theta d\Omega_{(n)}^2 \right) \\ & + \cos \theta \hat{h}_{\mu\nu}(r) dx^\mu dx^\nu + \mathcal{O}(\partial X_\perp^2) + \mathcal{O}(T_{ab}^2/r^{2n}) , \end{aligned} \quad (1.105)$$

where $\hat{h}_{\mu\nu}$ is leading order in both T_{ab}/r^n and ∂X_\perp . Having determined the general form of the overlap geometry we can now consider the Einstein equations (1.4) to linearized order (in both r/R and T_{ab}/r^n). In general the gravitational bulk stress tensor $\mathbf{T}_{\mu\nu}$ is quadratic in the monopole matter fields of the brane and thus $\mathbf{T}_{\mu\nu} \sim \mathcal{O}(T_{ab}^2/r^{2n})$. In the overlap zone, the Einstein equations therefore effectively take the form of the vacuum equations, $\mathcal{G}_{\mu\nu} = 0$. A subset of these equations will contain constraint equations of the system (as constraint equations are in general independent of the perturbation functions for all r). In particular, it is possible to show that the following combination does not involve $h_{\mu\nu}$ and is therefore a constraint equation

$$(n+1) \csc \theta \mathcal{G}_{r\theta} - r \sec \theta \mathcal{G}_{rr} = \frac{n+2}{r^n} \frac{8\pi G}{\Omega_{(n+1)}} T^{ab} K_{ab}^{\hat{i}} = 0 . \quad (1.106)$$

¹³An equivalent way to state this: To linear order in $1/R$, we can always perform a $SO(n+2)$ rotation in the transverse directions so that $K_{ab}^{\hat{i}} = K_{ab} \delta_i^{\hat{i}}$. The direction \hat{i} corresponds to the direction in which \mathcal{W}_{p+1} (locally) bends.

¹⁴As explained in Sec. 1.5.1, the characteristic length scale for the p -brane is set by the charge radius r_ρ rather than r_0 . In general the linearized approximation applies when, schematically, $T_{ab}/r^n \ll 1$.

We have therefore obtained the constraint equation $T^{ab}K_{ab}^{\hat{i}} = 0$ for each of the transverse directions and have thus, as promised, arrived at the extrinsic equation (1.18) for a general gravitating brane bend on a submanifold \mathcal{W}_{p+1} . As reviewed in Sec. 1.3.2, intrinsic perturbations are of fluid dynamic nature and of monopole type. The full set of equations therefore split up into a monopole (intrinsic) and a dipole (extrinsic) sector, and it follows that, to linear order in the full derivative expansion, the intrinsic and extrinsic perturbations decouple. In particular, the monopole constraint equations (the intrinsic equations), take the same form as for flat extrinsic geometry $\gamma_{ab} = \eta_{ab}$ and correspond to covariant conservation of the stress tensor T_{ab} and current(s) in the worldvolume directions (see also Chap. 3).

1.6.2 Force terms as modified constraint equations

The arguments presented in the previous section apply to any perturbed brane solution situated in vacuum backgrounds. In this section we explain how the force terms arise as a simple correction to the gravitational constraint equation (1.106). The correction can be seen as a pole-dipole interaction term in the overlap region arising from a derivative expansion of the background fluxes. We focus here on the charged black p -brane. We will therefore analyze the force terms arising from the action (1.70). The bulk stress tensor for the $(p+1)$ -form gauge field and the dilaton reads

$$\begin{aligned} 16\pi G \hat{\mathbf{T}}_{\mu\nu}^{(F)} &= \frac{e^{a_p\phi}}{(p+1)!} \left(F_{\mu}^{\mu_0\dots\mu_p} F_{\nu\mu_0\dots\mu_p} - \frac{1}{2(p+2)} g_{\mu\nu} F_{(p+2)}^2 \right), \\ 16\pi G \hat{\mathbf{T}}_{\mu\nu}^{(\phi)} &= \partial_{\mu}\phi\partial_{\nu}\phi - \frac{1}{2}g_{\mu\nu}(\partial\phi)^2. \end{aligned} \quad (1.107)$$

We now imagine placing the brane in a dilatonic flux background. In the following we let $\phi^{(\text{bg})}$ and $F_{(p+2)}^{(\text{bg})}$ denote the (slowly varying) background dilaton and field strength. The seed solution for the perturbative expansion is the dilatonic p -brane solution (1.72)-(1.74) whose dilaton vanishes at infinity. In order to match with this solution we must therefore ensure that the dilaton vanishes in the overlap zone. To this end we define a shifted dilaton and rescaled field strength,

$$\phi \rightarrow \phi - \phi^{(\text{bg})}, \quad F_{(p+2)} \rightarrow e^{a_p\phi^{(\text{bg})}/2} F_{(p+2)}. \quad (1.108)$$

The solution (1.72)-(1.74) (with the redefined fields) now solves the EOMs corresponding to the action (1.70) to zeroth order in the derivatives of the intrinsic fields, embedding, and background (gauge) fields. We now proceed as in the previous section and perturb the embedding of the brane. As above, the dynamics in the transverse directions decouples to leading order, and we therefore assume that the (transverse part of the) background field strength is only non-zero in the distinguished direction $y^{(i)}$. In principle, $F_{(p+2)}^{(\text{bg})}$ could have legs in two or more transverse directions, however, it is not difficult to realize that such components will not play a role to leading order and only become important to $\mathcal{O}(\partial X_{\perp}^2)$. We therefore expand the slowly varying background field strength according to

$$\begin{aligned} F_{(p+2)}^{(\text{bg})} &= F_{\hat{i}}^{(\text{bg})} dy^{\hat{i}} \wedge \star_{(p+1)} 1 + \mathcal{O}(\partial X_{\perp}^2) \\ &= F_{(\text{bg})}^{\hat{i}} (\cos\theta dr - r \sin\theta d\theta) \wedge \star_{(p+1)} 1 + \mathcal{O}(\partial X_{\perp}^2). \end{aligned} \quad (1.109)$$

Similarly we expand (the derivative of the) background dilaton as

$$d\phi^{(\text{bg})} = \partial_i \phi (\cos \theta dr - r \sin \theta d\theta) + \mathcal{O}(\partial X_\perp^2) . \quad (1.110)$$

In the overlap region, the fully corrected fields then schematically take the form,

$$\begin{aligned} F_{(p+2)} &= F_{(p+2)}^{(\text{M})} (1 + \mathcal{O}(\partial X_\perp)) + F_{(p+2)}^{(\text{bg})} + \mathcal{O}(T_{ab}^2/r^{2n}) , \\ d\phi &= d\phi^{(\text{M})} (1 + \mathcal{O}(\partial X_\perp)) + d\phi^{(\text{bg})} + \mathcal{O}(T_{ab}^2/r^{2n}) , \end{aligned} \quad (1.111)$$

where $F_{(p+2)}^{(\text{M})}$ and $d\phi^{(\text{M})}$ denote the $\mathcal{O}(T_{ab}/r^n)$ monopole (uncorrected) parts sourced by the (unperturbed) brane. They read (cf. Eq. (1.74)),

$$F_{(p+2)}^{(\text{M})} = \frac{16\pi G}{\Omega_{(n+1)}} \frac{Q_p}{r^{n+1}} dr \wedge \star_{(p+1)} 1 , \quad d\phi^{(\text{M})} = -\frac{16\pi G}{\Omega_{(n+1)}} \frac{a_p \Phi Q_p}{2r^{n+1}} dr . \quad (1.112)$$

Here Q_p and Φ is the charge (1.77) and chemical potential (1.78) of the brane, respectively. In the presence of non-trivial background (matter) fields, we therefore see that the bulk stress tensor does not vanish in the overlap zone. However, from (1.111) we see that the overlap stress tensor consists of a simple pole-dipole term and in particular does not involve the metric and matter field corrections. The combination,

$$(n+1) \csc \theta (\mathcal{G}_{r\theta} - 8\pi G \mathbf{T}_{r\theta}) - r \sec \theta (\mathcal{G}_{rr} - 8\pi G \mathbf{T}_{rr}) = 0 , \quad (1.113)$$

is therefore still a constraint equation (with $\mathbf{T}_{\mu\nu} = \mathbf{T}_{\mu\nu}^{(F)} + \mathbf{T}_{\mu\nu}^{(\phi)}$) and takes the modified form

$$\frac{n+2}{r^n} \frac{8\pi G}{\Omega_{(n+1)}} \left(T^{ab} K_{ab}^{\hat{i}} - \mathcal{F}^{\hat{i}} \right) = 0 , \quad (1.114)$$

where $\mathcal{F}^{\hat{i}}$ is the induced force term and is given by the pole-dipole interaction term,

$$\mathcal{F}^{\hat{i}} = \frac{\Omega_{(n+1)}}{n+2} r^n ((n+1) \csc \theta \mathbf{T}_{r\theta} - r \sec \theta \mathbf{T}_{rr}) . \quad (1.115)$$

The force term (1.115) is easily computed from (1.107) and covariantized. Remembering that we redefined the background fields in Eq. (1.108), and introducing

$$J_{(p+1)} = \star_{(p+1)} \mathbf{Q}_p , \quad \mathbf{Q}_p = e^{a_p \phi/2} Q_p , \quad (1.116)$$

we arrive at the following constraint equation

$$T^{ab} K_{ab}^{\rho-} \perp^{\rho\mu} \frac{a_p \Phi Q_p}{2} \partial_\mu \phi = \frac{1}{(p+1)!} \perp^\rho{}_\mu F^{\mu\mu_0 \dots \mu_p} J_{\mu_0 \dots \mu_p} . \quad (1.117)$$

Here $F_{(p+2)}$ and ϕ are the (un-shifted/scaled) background fields and we have dropped the (bg) superscript to ease notation. We emphasize that the quantities appearing in the constraint equation (1.117) are computed in the overlap zone.

1.6.3 Integrating the EOM to an action

We now integrate the EOM (1.117) to an action. To this end consider the combination $T^{ab}K_{ab}{}^\rho$ using the perfect fluid p -blackfold stress tensor (1.75). Usually we require the variation of the charge Q_p to vanish (since it is conserved among physical variations) and relate the derivative of \mathcal{T} to that of P and arrive at the action (1.67) (see App. A). However, in dilatonic backgrounds Q_p is not conserved since the local definition of Q_p depends on the value of the dilaton. Instead we consider variations for which we keep the charge \mathbf{Q}_p in Eq. (1.116) fixed. It follows that

$$T^{ab}K_{ab}{}^\rho = -\perp^{\rho\mu}\partial_\mu P + PK^\rho + \frac{a_p\Phi Q_p}{2}\perp^{\rho\mu}\partial_\mu\phi. \quad (1.118)$$

Using the EOM (1.117), the dilaton terms are therefore seen to cancel out, and it follows that (1.117) can be obtained from the action

$$I = \int_{\mathcal{W}_{p+1}} \left(\star P_\phi + \mathbf{Q}_p \mathbb{P}[A_{(p+1)}] \right), \quad (1.119)$$

for variations in the embedding where we keep the global temperature T and the charge \mathbf{Q}_p fixed. Here $\mathbb{P}[A_{(p+1)}]$ denotes the pullback of the $(p+1)$ -form gauge potential to the worldvolume. Moreover we used the symbol P_ϕ to signify that the blackfold pressure is computed locally i.e. using the rescaled charge Q_p related to \mathbf{Q}_p and the dilaton through (1.116). The condition that \mathbf{Q}_p (rather than Q_p) is taken to be constant might seem a bit *ad hoc*, however, assuming that (1.117) can be derived from an action, the action (1.119) is really the only possibility consistent with gauge invariance which in turn implies that \mathbf{Q}_p is conserved. Ultimately, the conservation equation should follow from considering intrinsic perturbations of the system (like the ones considered in Chap. 3) which will be shown in [58].

Before concluding this section, it is interesting to compare the action (1.119) to the Dp/NS/M-brane worldvolume actions. Assuming that the worldvolume field strengths are turned off, note that these actions take the universal form in the Einstein frame

$$I_p = -T_p \int_{\mathcal{W}_{p+1}} d^{p+1}\sigma e^{-a_p\phi/2} \sqrt{-\gamma_{(E)}} \pm T_p \int_{\mathcal{W}_{p+1}} \mathbb{P}[A_{(p+1)}]. \quad (1.120)$$

Here $+$ stands for branes and the $-$ stands for antibranes, $\gamma_{(E)}$ is the pullback of the metric onto the worldvolume using the Einstein frame metric, and T_p is the tension of the object in question (the dilaton of course vanishes for M -branes). We now consider the blackfold action (1.119) in the extremal limit. In the extremal limit,

$$P_\phi = -|Q_p| = -e^{-a_p\phi/2}|\mathbf{Q}_p|. \quad (1.121)$$

In the extremal limit, under the above assumptions, we therefore find perfect agreement between the (supergravity) p -brane blackfold actions and the corresponding single brane worldvolume actions under the identification¹⁵

$$\mathbf{Q}_p \sim T_p. \quad (1.122)$$

¹⁵The constant of proportionality is naturally identified with the (large) number of branes sourcing the p -brane blackfold.

We postpone a more full discussion of the relation between blackfolds and the DBI-like actions to Chap. 2.

1.6.4 More general force terms

In this section we briefly comment on the force terms arising for more general bound state blackfolds reviewed in Sec. 1.5.6. For definiteness we consider here the F1-D p bound state system and refer to [58] for a complete analysis. For the convenience of the reader, we have recorded the F1-D p bound state solution along with its effective blackfold fluid and currents in App. B. This solution will play the role of the seed solution in the perturbative expansion. Repeating the steps of the above analysis, now including a non-zero background fields $H_{(3)}$ and $F_{(p+2)}$, we recover the expected Lorentz-like couplings. However, since the F1-D p system also sources a non-trivial $C_{(p-1)}$ gauge potential, in general there will also be a non-trivial coupling to a non-zero background $F_{(p)}$ field strength. All in all, we arrive at the following extrinsic equation (assuming here that the background dilaton vanishes),

$$T^{ab}K_{ab}{}^{\rho} = \perp^{\rho}{}_{\mu} \mathcal{F}_{(F1)}^{\mu} + \perp^{\rho}{}_{\mu} \mathcal{F}_{(Dp)}^{\mu} + \perp^{\rho}{}_{\mu} \mathcal{F}_{(F1-Dp)} \quad (1.123)$$

where $\mathcal{F}_{(F1)}$ and $\mathcal{F}_{(Dp)}$ are the usual Lorentz couplings

$$\mathcal{F}_{(Dp)}^{\mu} = \frac{1}{(p+1)} F^{\mu\mu_0\dots\mu_p} J_{\mu_0\dots\mu_p}, \quad \mathcal{F}_{(F1)}^{\mu} = \frac{1}{2!} H^{\mu\nu\lambda} j_{\nu\lambda} \quad (1.124)$$

However, the coupling $\mathcal{F}_{(F1-Dp)}$ is new and is given by the non-trivial cross-term

$$\mathcal{F}_{(F1-Dp)} = \frac{1}{(p-1)!} F^{\mu\mu_0\dots\mu_{p-2}} \tilde{j}_{\mu_0\dots\mu_{p-2}} \quad \text{with} \quad \tilde{j}_{(p-1)} = \star_{(p+1)} j_{(2)} \quad (1.125)$$

It is straightforward to include a dilaton. The dilaton force term (non-trivially) decomposes according to

$$\mathcal{F}_{\text{dilaton}} = \frac{1}{2} (a_{F1} \Phi_{F1} Q_{F1} + a_{Dp} \Phi_{Dp} Q_{Dp}) \perp^{\rho\mu} \partial_{\mu} \phi, \quad (1.126)$$

with $a_{F1} = -1$. Notice that in dilatonic backgrounds the cross coupling $\mathcal{F}_{(F1-Dp)}$ also receives a non-trivial dilaton factor. To complete the discussion, we also need to comment on the effective equations governing the currents, J , j , \tilde{j} . It is straightforward to write down an effective action giving rise to the force terms (1.123) by simply coupling the currents J , j , \tilde{j} to the background fields in the usual manner. By requiring that the effective worldvolume action is gauge invariant under the gauge symmetries of the underlying supergravity, we obtain a set of modified conservation equations for the currents (basically as “force terms” in the conservation equations). The exact form of these equations depends on the type of bound state in question and the general expressions will be presented [58] (see also the recent paper [53] where the effective equations are written down for the M2-M5 system). Equivalently, these equations derive directly from the hydro sector where they basically show up as modified constraint equations coming from the Chern-Simons term of the relevant supergravity.

1.7 The blackfold construction in fluxed backgrounds

In this section we extend the blackfold construction of Sec. 1.4 to blackfolds embedded in flux backgrounds. Most of the considerations carry directly on to the more general case but with some important remarks.

In general, the blackfold Killing vector \mathbf{k}^a pushes forward to a Killing vector of the background i.e., (Ω_i constant)

$$\mathbf{k}^\mu = \xi + \sum_i \Omega_i \chi_{(i)}^\mu, \quad (1.127)$$

where ξ corresponds to the canonically normalized generator of time translations and the χ_1, \dots denote the set of spatial (rotational) isometries of the background (see also App. A). However, with regard to stationarity there is an important further distinction to be made, depending on whether:

- I The vectors χ_1, \dots are also worldvolume Killing vectors.
- II One of the vectors χ_1, \dots , say $\chi_1 \equiv \chi$,¹⁶ is perpendicular to the worldvolume and hence not a worldvolume Killing vector.

In the first case the blackfold world-volume does not break the isometries ξ, χ_1, \dots of the background. The resulting solutions are the standard stationary blackfolds considered in Sec. 1.4. In the second case, which is the one relevant for the analysis of Chap. 2, the blackfold worldvolume only preserves a particular combination of the isometries ξ, χ and should therefore be viewed as a “boosted stationary” solution rotating along the $U(1)$ generated by χ . We will refer to this below as quasi-stationary, since we still have that, seen from the worldvolume, the blackfold configuration is independent of time. As a result, the conserved quantities associated to ξ and χ are of a different nature. In particular, the conserved quantity generated by ξ should be thought of as the total energy E (so not the rest mass of the object) and the quantity generated by χ as the *transverse* momentum J corresponding to the rotational boost. Finally the conserved quantities generated by the rest of the χ_i 's are the usual intrinsic worldvolume spins along the directions of \mathcal{W}_{p+1} .

1.7.1 Conserved charges

We now write down the expressions for the conserved charges corresponding to the asymptotic generators ξ and χ for quasi-stationary blackfolds in flux backgrounds. For simplicity we here focus on the non-dilatonic case. As we have seen, the effective gravitational dynamics is modified according to

$$\nabla_\mu \hat{T}^{\mu\nu} = \frac{1}{(p+1)!} F^{\mu\mu_0 \dots \mu_p} \hat{J}_{\mu\mu_0 \dots \mu_p} \quad (1.128)$$

¹⁶For simplicity we here only consider the case where one of the χ_i 's is perpendicular to \mathcal{W}_{p+1} , however, there could in principle be more than one. Moreover we will also restrict ourselves to static backgrounds. Also note that χ is necessarily Killing. Indeed, if χ was not Killing the worldvolume would be accelerating and would therefore emit gravitational radiation and would thus not be stationary.

It is now straightforward to obtain the modified conserved quantities from this equation, assuming that the background field $F_{(p+2)}$ respects the symmetries of the background.

For any Killing vector field k of the background we have by assumption that the Lie derivative along k of the $(p+2)$ -form $F = F_{(p+2)}$ is zero $\mathcal{L}_k F = 0$. Since $dF = 0$, we find that $0 = dF = \iota_k dF + d(\iota_k F) = d(\iota_k F)$ where ι denotes the usual interior product. Moreover, since k is a symmetry of the background and F , we can pick a gauge in which $\mathcal{L}_k A = 0$. By virtue of Cartan's identity, we therefore see that $0 = \mathcal{L}_k A = \iota_k F + d(\iota_k A)$, thus $\iota_k F = -d(\iota_k A)$. In this gauge the $(p+1)$ -form $\iota_k F$ therefore has the p -form potential $\iota_k A$. Using this, we can now show that the current

$$j_k^\mu = \left(\hat{T}_p^{\mu\nu} + \frac{1}{p!} A^\nu{}_{\rho_1 \dots \rho_p} \hat{J}^{\mu\rho_1 \dots \rho_p} \right) k_\nu, \quad (1.129)$$

is conserved $\nabla_\mu j_k^\mu = 0$. Indeed, using the EOM (1.128), we see that

$$\begin{aligned} p! \nabla_\mu (\hat{T}^{\mu\nu} k_\nu) &= \frac{1}{p+1} k^\nu F_{\nu\rho_1 \dots \rho_{p+1}} \hat{J}^{\rho_1 \dots \rho_{p+1}} = -\frac{1}{p+1} \nabla_{[\rho_1} (\iota_k A)_{\rho_2 \dots \rho_{p+1}]} \hat{J}^{\rho_1 \dots \rho_{p+1}} \\ &= -\nabla_{\rho_1} (\iota_k A)_{\rho_2 \dots \rho_{p+1}} \hat{J}^{\rho_1 \dots \rho_{p+1}} = -\nabla_\mu (A_{\nu\rho_1 \dots \rho_p} \hat{J}^{\mu\rho_1 \dots \rho_p} k^\nu). \end{aligned} \quad (1.130)$$

The current (1.129) therefore gives rise to a conserved charge. Using the form of the monopole stress tensor (1.14) and current (1.63), we can now do the δ -function integrals as in Sec. 1.4 to reduce to integrals over \mathcal{B}_p and obtain the following expression for the conserved charge¹⁷

$$\mathcal{Q}[k] = \int_{\mathcal{B}_p} dV_{(p)} \gamma_\perp^{-1} [T^{\mu\nu} + \mathcal{V}^{\mu\nu}] n_\mu k_\nu \Big|_{x^i = X^i}. \quad (1.131)$$

Here we have defined

$$\mathcal{V}^{\mu\nu} \equiv \frac{1}{p!} A^\nu{}_{\mu_1 \dots \mu_{p-1}} J^{\mu\mu_1 \dots \mu_{p-1}}, \quad \gamma_\perp \equiv \sqrt{\frac{g_{tt}}{\gamma_{\tau\tau}}}. \quad (1.132)$$

The quantity γ_\perp is recognized as a Lorentz contraction factor which must be included since the spatial part of the worldvolume \mathcal{B}_p can suffer Lorentz contractions due to transverse boosts ($\sim \gamma_{\tau\tau}$) and/or gravitational redshifts ($\sim g_{tt}$). Now, we use the result (1.131) to write down the conserved charges corresponding to the background Killing vectors ξ and χ ,

$$E = \int_{\mathcal{B}_p} dV_{(p)} \gamma_\perp^{-1} [T^{\mu\nu} + \mathcal{V}^{\mu\nu}] n_\mu \xi_\nu, \quad J = - \int_{\mathcal{B}_p} dV_{(p)} \gamma_\perp^{-1} [T^{\mu\nu} + \mathcal{V}^{\mu\nu}] n_\mu \chi_\nu. \quad (1.133)$$

The expressions correspond to the E and angular momentum J of the quasi-stationary blackfold moving with constant velocity in a fluxed background along an isometric direction and generalize the standard blackfold expressions discussed in Sec. 1.4. In order to obtain the expressions for the intrinsic spin \mathcal{S}_i , we just replace $\chi \rightarrow \chi_i$ in the expression for J (typically $\mathcal{V}^{\mu\nu}$ vanishes in the χ_i direction and the expression for \mathcal{S}_i will just reduce to the

¹⁷Note that under the assumptions the metric determinants factorize according to $\sqrt{-g} = \sqrt{-g_{tt}} \sqrt{g_{\text{spatial}}}$ and $\sqrt{-\gamma} d^{p+1}\sigma = \sqrt{-\gamma_{\tau\tau}} d\tau dV_{(p)}$.

one recorded in (1.44)). Finally the total entropy is obtained in the usual manner and is given by

$$S = \int_{\mathcal{B}_p} dV_{(p)} \gamma_{\perp}^{-1} u^{\mu} n_{\mu} . \quad (1.134)$$

2 | Thermal spinning giant gravitons

2.1 Introduction

In this chapter we apply the blackfold formalism reviewed in Chap. 1 to certain thermal spinning probe branes in string/M-theory. More specifically, we apply the effective approach to the giant graviton configurations originally considered in [25–27]. The analysis presented here was originally carried out in the two papers [1; 2].

The archetypal giant graviton configuration is that of a D3-brane wrapping a three-sphere with center of mass moving along the equator of the five-sphere in the $\text{AdS}_5 \times S^5$ background. The configuration corresponds to a blown up version of the usual point particle-like Kaluza-Klein graviton (hence its name). The dynamics of the giant graviton is captured by the DBI action coupled to the usual background (self-dual) five-form field strength $F_{(5)}$. In the dual gauge theory description, in the context of the AdS/CFT correspondance [12–15], the giant graviton moving along an S^1 inside the S^5 with angular momentum J is dual to a gauge theory multi-trace operator \mathcal{O}_{gg} with R-charge J and conformal dimension $\Delta = J$. Similarly M-theory giant gravitons exist on $\text{AdS}_4 \times S^7$ and $\text{AdS}_7 \times S^4$ (with similar relevance for the respective dual CFTs) with the M2 giant graviton wrapping a two-sphere in the S^4 and the M5 giant graviton wrapping a five-sphere in the S^7 , respectively. Finally all the described giant graviton configurations have a “dual” version carrying the same quantum numbers (but with no upper bound on the angular momentum), still rotating on the (equator of the) sphere part of $\text{AdS} \times S$, but instead expanded into the AdS part of the background geometry [26; 27].

As will be explained below, the blackfold approach allows us to thermalize probe brane configurations in general backgrounds. Using these ideas, we will construct a thermal spinning version of the giant graviton configurations relevant to IIB/M-theory which we shall henceforth dub the *thermal (spinning) giant graviton*. Heating up the $\text{AdS} \times S$ background with the IIB/M-theory giant graviton in it, then corresponds to a thermal state that results from the ensemble of operators that are fluctuations around \mathcal{O}_{gg} . Thus, in the context of AdS/CFT, having a description of the thermal giant graviton will provide insight into the strong coupling behaviour of the gauge theory side at finite temperature.

2.1.1 Thermal probe branes à la blackfolds

When considering the bending of (locally) supersymmetric brane configurations, most of the work has been done by considering the worldvolume theory of a single probe brane in a given background. The physics of probe branes is conventionally examined using the weakly coupled description in terms of the D-brane (Abelian DBI) or M-brane worldvolume theories or, in the case of F-string probes, the Nambu-Goto action. However, as a consequence of open/closed string duality,¹ the weakly coupled (microscopic) worldvolume picture has a complementary description on the strongly coupled (macroscopic) bulk spacetime side. Indeed, for supersymmetric configurations one can typically find an exact interpolation between the two sides, which has been the heart of, for example, microscopic counting of black hole entropy [11] and the AdS/CFT correspondence. When interpolating from the weakly coupled regime to the strongly coupled regime, one therefore expects that the corresponding brane profiles can be obtained from a supergravity perspective by considering the back-reaction of many branes on top of each other. In order to determine the corresponding brane profiles on the supergravity side, one would have to impose an appropriate ansätze, incorporating the symmetries of the problem and solve, the resulting supergravity equations of motion. A well-known example of this, relevant to the present work, is the relation between giant gravitons and the LLM geometries due to Lin, Lunin and Maldacena [95]. More generally, this type of open/closed duality has been shown to extend beyond the AdS/CFT decoupling limit. For example, in Ref. [96] shapes of brane intersections were studied from the supergravity perspective and found to be in perfect agreement with those found from the DBI action, with the BIon solution [23; 96] being the most simple example. In general, “bending” branes on the supergravity side, i.e., finding non-trivial geometries from the supergravity EOMs, is a highly non-trivial (generally unsolvable) task. Already for the case of the highly (super)symmetric LLM geometries, the amount of computations going into finding the actual solutions is quite impressive. From this point of view, perturbative methods for tackling the complexity of the highly non-linear supergravity EOMs would be very useful. In this context, the effective blackfold theory provides an excellent perturbative framework for addressing these problems. To leading order, the effective theory takes the form of a worldvolume theory similar in nature to the DBI worldvolume action (and its M/NS cousins) and the full exact supergravity solution can then in principle be perturbatively reconstructed order by order through the matched asymptotic expansion procedure outlined in Sec. 1.3.4 (and generalized to include matter fields). However, already at the level of the effective worldvolume (probe) theory, a great deal of information about the physics of the system can be extracted.

In addition, in the effective gravitational theory, the brane probe under consideration can be blackened and thus be brought into thermal equilibrium with a background of finite temperature. The blackfold approach therefore naturally provides us with a tool for describing the physics of thermal probe branes. In particular, the blackfold approach naturally takes into account that the degrees of freedom living on the brane themselves get

¹We use this terminology here in the loose sense to denote the duality between the worldvolume and spacetime/bulk descriptions.

thermalized (which is evident from the near-extremal form of the stress tensor recorded in Eq. (1.86)). This has revealed a number of new qualitative and quantitative effects, as compared to the conventional method for treating probe branes in finite temperature backgrounds (see [48] for a brief review and references). These ideas were first employed in Refs. [48; 49] where the BIon solution of [23; 96] was identified and thermalized in the blackfold approach. In addition to thermalizing the phases available at zero temperature, the thermal analysis also revealed the existence of new phases not visible in the extremal limit. Although the effective worldvolume theories of the (DBI) BIon and the thermal BIon of [48] are similar in spirit, and produce essentially equivalent results in the extremal limit (in accordance with the discussion in previous paragraph), we emphasize that the physics of the two systems is very different: The conventional (DBI) BIon consists of a single D3-brane with the worldvolume gauge field turned on, while the (thermal) BIon of [48] is described by the effective blackfold theory of a (black) D3-F1 brane bound state geometry. Along these lines, the M-theory M2-M5 version of the BIon system was analyzed in the blackfold approach in Refs. [50; 51], including a spinning M2-M5 ring intersection [52].² The ideas presented here are naturally applied to (thermal) F-string/brane probes in context of the AdS/CFT correspondence. The first application of the blackfold formalism in an AdS/CFT setting was carried out in [54] where the effective theory was used to analyze the thermalized gravity dual of the rectangular Wilson loop using a black F-string probe ending on the boundary of $\text{AdS}_5(\times S^5)$.

Along these lines, we here construct a thermal spinning version of the giant graviton. Notice that the possibility of adding internal spin (i.e. in the brane directions) is a new feature of the thermal giant graviton that is not present in the case of the standard extremal (supersymmetric) giant gravitons. The reason is that at zero temperature the worldvolume stress tensor of the giant graviton is locally Lorentz invariant, as can be seen directly from the D/M-brane actions (for zero worldvolume gauge fields). This means that the internal spin of the giant graviton is not visible in the extremal limit. However, turning on a temperature breaks the local Lorentz invariance of the worldvolume stress tensor and thus makes internal spin an important effect to consider. Moreover, we find that it is possible to perform a non-trivial double scaling extremal limit, giving rise to a novel null-wavegiant graviton with BPS spectrum.

Notation and regimes of validity: We will follow that notation and basic setup of [26]. As explained in the introduction, we focus on the conformal cases, namely we consider D3-branes in $D = 10$ IIB supergravity and M2- and M5 branes in $D = 11$ supergravity in the backgrounds of the form $\text{AdS}_m \times S^n$ with,

$$(m, n) = \{(5, 5); (4, 7); (7, 4)\} , \quad (2.1)$$

along with the appropriate gauge potentials. Note that n and m are related by $n = (3m - 5)/(m - 3)$, but for ease of notation, we keep the two symbols separately below. The geometries, along with the corresponding gauge potentials, compromise maximally

²Recently these ideas were extended to supersymmetric long-wavelength perturbations in the blackfold framework in Ref. [53] providing new intriguing insights into the ‘‘SUGRA/DBI correspondence’’.

supersymmetric solutions to the corresponding supergravity. The four-form field strength, corresponding to the three-form M-theory potential, is proportional to the four dimensional component of $\text{AdS}_m \times S^n$. The IIB self-dual five-form field strength naturally splits up in a component proportional to the volume-form on the AdS_5 part and the S^5 part of the geometry, respectively. Finally, the radius of curvature for AdS_m is denoted \tilde{L} while that for the S^n is denoted L . For the cases under consideration, they are related as

$$\tilde{L} = \frac{m-3}{2}L. \quad (2.2)$$

Before ending this paragraph, we will say a few words about the validity of the blackfold approach for our specific physical setup (we postpone the details to Sec. 2.3.2). In order for the blackfold probe approximation to hold we require

$$1 \ll N_{\text{D3}} \ll N \ll \lambda N_{\text{D3}}, \quad 1 \ll N_{\text{M5}}^2 \ll N, \quad 1 \ll N_{\text{M2}} \ll N^2. \quad (2.3)$$

where N is the (large positive integer) units of n -form flux through the sphere S^n and λ is the 't Hooft coupling (for the $n = m = 5$ case). We note that the last two M-theory conditions can be rewritten as $\lambda_M \ll 1$ and $\lambda_M \gg 1$ respectively, in terms of the 't Hooft-like coupling $\lambda_M = N_{\text{M5}}^2/N_{\text{M2}}$ that was identified in Ref. [51] in the context of the self-dual string soliton of the M5-brane theory. Here we use the fact that for the M5-brane case our N is the parameter of the M2-brane theory and for the M2-brane case N is the parameter of the M5-brane theory. Another important remark about the validity of the analysis is related to the Hawking-Page temperature $T_{\text{HP}} \sim 1/L$, above which the AdS black hole background will become dominant over the hot AdS space-time background [97] considered in this work. We find that for the bounds (2.3) (again we postpone the details to Sec. 2.3.2),

$$T_{\text{HP}} \ll T_{\text{max}}, \quad (2.4)$$

where T_{max} is the maximal temperature allowed for the blackfold giant graviton solution. We thus see that in the regime where the probe blackfold approximation is valid, the maximum temperature of the solution is far above the Hawking-Page temperature. As a consequence this maximum temperature is not physical in the sense that before reaching it one should change the background to the AdS black hole, and hence our solution is most relevant for small temperatures.

2.2 Giant graviton on S^n revisited

In this section we review the giant graviton configuration in IIB string/M-theory on $\text{AdS}_m \times S^n$ (using the conventions explained in the introduction). For definiteness, we focus on the case in which the giant graviton is expanded in the S^n , and correspondingly also the construction of the (spinning) thermal giant graviton in Sec. 2.3 will be confined to this case. The case in which the giant graviton is expanded on the AdS_m and its thermal version is considered separately in Sec. 2.7.

The review will serve to set our notation and properly define the configurations that will be heated up and spun using the thermal blackfold method. At the same time we highlight that, beyond the usual 1/2 BPS solution, there is a stable branch of giant gravitons that has not received much attention in the literature. Some unnoticed properties of this branch is discussed in Sec. C.2 of App. C.

2.2.1 Setup and action

As explained in the introduction, we consider IIB string/M-theory on $\text{AdS}_m \times S^n$ with n -form flux

$$F_{(n)} = (n-1)\text{Vol}_{(n)}/L, \quad (2.5)$$

where $\text{Vol}_{(n)}$ is the unit volume form on the S^n and L denotes the radius of the S^n and is related to the anti de-Sitter radius through (2.2). For the S^n , we take the parametrization

$$d\Omega_{(n)}^2 = L^2 \left[d\theta^2 + \cos^2 \theta d\phi^2 + \sin^2 \theta d\Omega_{(n-2)}^2 \right], \quad (2.6)$$

where $d\Omega_{(n-2)}$ denotes the line element on S^{n-2} (with coordinates $\chi_1, \dots, \chi_{n-2}$). In these particular coordinates, the $(n-1)$ -form gauge potential associated to the flux (2.5) takes the form

$$A_{(n-1)} = (L \sin \theta)^{n-1} d\phi \wedge \text{Vol}_{(n-2)} = r^{n-1} d\phi \wedge \text{Vol}_{(n-2)}, \quad (2.7)$$

where $r \equiv L \sin \theta$ denotes the radius of the S^{n-2} . The giant graviton is obtained by considering a (rotating) D/M($n-2$)-brane that wraps an S^{n-2} the S^n inside the $\text{AdS}_m \times S^n$. Denoting the worldvolume coordinates on the brane probe as $\{\sigma^0 \equiv \tau, \sigma^1, \dots, \sigma^{n-2}\}$, its embedding into the background is taken to be

$$t = \tau, \quad \phi = \beta_n \Omega \tau, \quad \chi^1 = \sigma^1, \dots, \chi^{n-2} = \sigma^{n-2}, \quad \theta = \arcsin(r/L) = \text{const.}, \quad (2.8)$$

where the D/M($n-2$)-brane sits at the origin of the AdS_m space (as a point). The parameter β_n is simply a sign which takes the specific values $\beta_4 = \beta_5 = 1$, $\beta_7 = -1$.³ The size of the giant graviton configuration is thus $r = L \sin \theta$ and it rotates with angular velocity $\beta_n \Omega$ on the S^n , satisfying the geometric bound $\Omega^2(L^2 - r^2) \leq 1$. The resulting induced metric on the probe brane worldvolume is easily computed,

$$\gamma_{ab} d\sigma^a d\sigma^b = -\mathbf{k}^2 d\tau^2 + r^2 d\Omega_{(n-2)}^2, \quad (2.9)$$

where $a = \tau, 1, \dots, n-2$ runs over the worldvolume directions and

$$\mathbf{k} \equiv |k^a| = \sqrt{1 - \Omega^2(L^2 - r^2)}, \quad (2.10)$$

is the norm of the rotational Killing vector satisfying $0 \leq \mathbf{k} \leq 1$.

With this setup, the giant graviton is found by solving the EOM of the brane DBI action I_{DBI} in this background. We have

$$I_{\text{DBI}} = \int d\tau L_{\text{DBI}}, \quad L_{\text{DBI}} = \int_{S^{n-2}} \mathcal{L} = -T_{(n-2)} \int_{S^{n-2}} (\sqrt{-\gamma} - A_{\tau\sigma_1 \dots \sigma_{n-2}}), \quad (2.11)$$

³The choice of sign β_n is introduced for convenience to simplify the formulae below, treating the D3, M2 and M5-branes uniformly. Alternatively, one can take a plus sign for all cases, and reverse the sign of the M5-brane charge, turning it into an anti-M5-brane.

where γ is the determinant of the induced metric (2.9), $A_{\sigma_0\sigma_1\dots\sigma_{n-2}}$ is the pullback of the $(n-1)$ -form gauge potential onto the worldvolume, and $T_{(n-2)}$ is the $(n-2)$ -brane tension. Using the embedding (2.8), this gives

$$L_{\text{DBI}} = -T_{(n-2)}\Omega_{(n-2)}r^{n-2}(\mathbf{k} - r\Omega) . \quad (2.12)$$

The angular momentum and Hamiltonian are then computed as

$$\begin{aligned} J &= \int_{S^{n-2}} \frac{\partial \mathcal{L}}{\partial \Omega} = T_{(n-2)}\Omega_{(n-2)}r^{n-2} \left(\frac{\Omega(L^2 - r^2)}{\mathbf{k}} + r \right) , \\ H &= J\Omega - \int_{S^{n-2}} \mathcal{L} = \frac{T_{(n-2)}\Omega_{(n-2)}r^{n-2}}{\mathbf{k}} . \end{aligned} \quad (2.13)$$

We finally note that the overall factor in all these expressions involves the product $\Omega_{(n-2)}T_{(n-2)}$ which can be re-written in terms of the background variables as

$$\Omega_{(n-2)}T_{(n-2)} = \frac{N}{L^{n-1}} , \quad (2.14)$$

where L is the radius and N is the (large) integer denoting the (quantized) background flux through S^n .

2.2.2 Solution branches and stability

Varying the Lagrangian (2.12) with respect to the radial coordinate r we obtain the EOM

$$n - 2 - (n - 2)L^2\Omega^2 + (n - 1) \left(r\Omega - \sqrt{1 - \Omega^2(L^2 - r^2)} \right) = 0 . \quad (2.15)$$

This equation has two branches of solutions⁴

$$\Omega_- = \frac{1}{L} , \quad \Omega_+ = \frac{n - 2}{\sqrt{(n - 2)^2L^2 - (n - 1)(n - 2)r^2}} , \quad (2.16)$$

which we will dub the lower and upper brach, respectively. Notice that for the upper branch we have that $1 \leq \Omega L \leq n - 2$. It is interesting to note that a maximal size giant graviton ($r = L$) exists in both branches with either $\hat{\Omega}_- = L^{-1}$ or $\hat{\Omega}_+ = (n - 2)L^{-1}$. Moreover, it is also worth noticing that both branches connect to the point-particle case, in the limit $r \rightarrow 0$.

To elucidate these branches and connect to a more physical parameterization, we use (2.13) to compute the on-shell angular momentum and energy. We introduce a rescaled (dimensionless) angular momentum and energy according to $\mathbf{J} = J/N$ and $\mathbf{E} = (L/N)E$ along with the dimensionless ratio $\hat{r} = r/L$. We then find on the lower solution branch

$$\mathbf{J}_- = \mathbf{E}_- = \hat{r}^{n-3} . \quad (2.17)$$

while for the upper branch, we have

$$\mathbf{J}_+ = \hat{r}^{n-3}(n - 2 - (n - 3)\hat{r}^2) , \quad \mathbf{E}_+ = \hat{r}^{n-3}\sqrt{(n - 2)^2 - (n - 1)(n - 3)\hat{r}^2} . \quad (2.18)$$

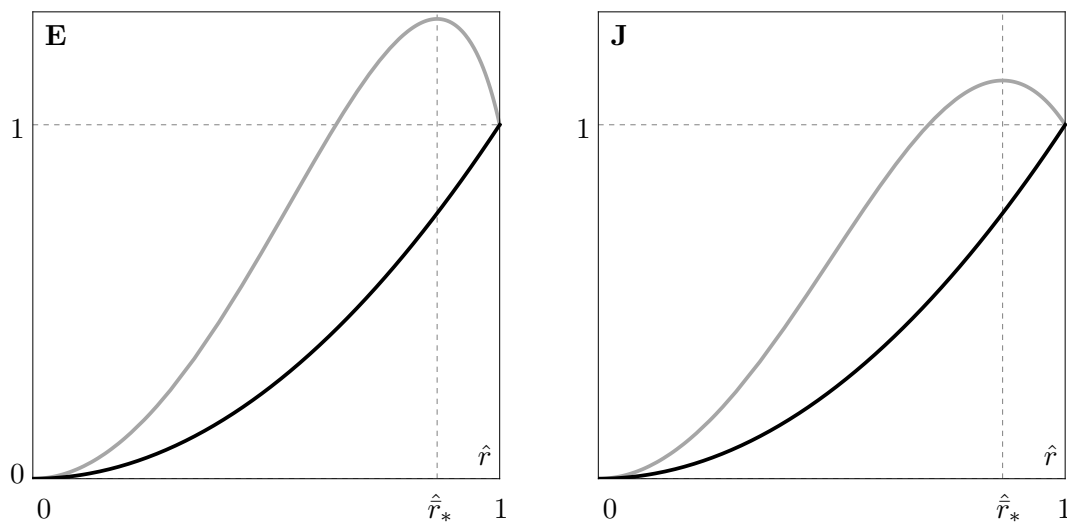


Figure 2.1: $\mathbf{E} = (L/N)E$ (left) and $\mathbf{J} \equiv J/N$ (right) versus $\hat{r} \equiv r/L$ for the lower (black) and upper (grey) solution branches of the extremal giant graviton, respectively.

For clarity, we have depicted these results in the plot of Fig. 2.1.

One observes that the angular momentum is confined to the range $0 \leq \mathbf{J} \leq 2\hat{r}_*^{n-1}$, where

$$\hat{r}_* = \sqrt{\frac{n-2}{n-1}}. \quad (2.19)$$

We see that for each value in the (full) range of angular momentum there are two possible solutions, with different values of \hat{r} . Comparing the two corresponding values of the energy for each of these two values of \hat{r} (given \mathbf{J}), one finds that the one with highest \hat{r} minimizes the energy. To see this more clearly, we exhibit \mathbf{E} versus \mathbf{J} in the left plot of Fig. 2.2. Hence we expect that the stable branch of solutions consists of the entire lower branch (for $0 \leq \mathbf{J} \leq 1$ and $0 \leq \hat{r} \leq 1$) together with the part of the upper branch that has $1 \leq \mathbf{J} \leq 2\hat{r}_*^{n-1}$ and $\hat{r}_* \leq \hat{r} \leq 1$. Conversely, the part of the upper branch spanned by $0 \leq \mathbf{J} \leq 2\hat{r}_*^{n-1}$ and $0 \leq \hat{r} \leq \hat{r}_*$ will be for given \mathbf{J} a local maximum of the energy. More properly, this result on the dynamical stability can be derived by computing the off-shell Hamiltonian from (2.13)

$$H = T_{(n-2)}\Omega_{(n-2)} \sqrt{r^{2(n-2)} + \frac{(J - r^{n+1})^2}{L^2 - r^2}} \quad (2.20)$$

Varying this with respect to \hat{r} for constant \mathbf{J} gives, as expected, the extrema $\Omega = \bar{\Omega}_{\pm}$ found before. To see which part of the branches are stable we vary H once more with respect to \hat{r} at constant \mathbf{J} , and demand positivity, so that we are at a minimum. The result is that the lower branch $\Omega = \bar{\Omega}_-$ is stable for all values of \hat{r} ($0 \leq \hat{r} \leq 1$) and the upper branch $\Omega = \bar{\Omega}_+$ is stable for $r_* \leq \hat{r} \leq 1$. This is in accord with the arguments of the

⁴The limit $r = 0$ of these solutions describes the point-particle limit of the giant graviton, where one should be careful in taking the limit $r \rightarrow 0$ such as to obtain sensible conserved charges [26].

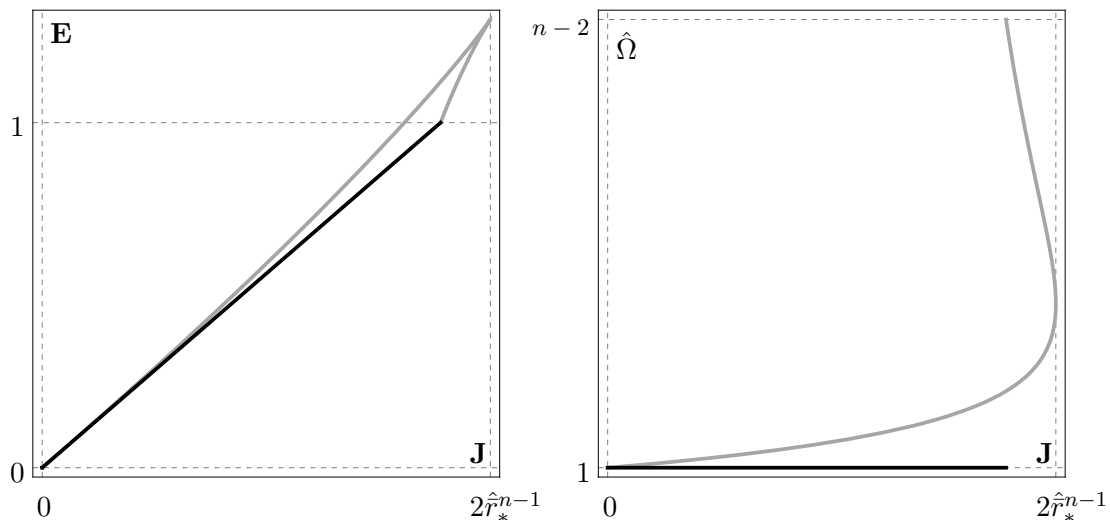


Figure 2.2: $\mathbf{E} = (L/N)E$ (left) and $\hat{\Omega}$ (right) versus \mathbf{J} for the two solution branches.

previous paragraph (see also App. A of [1] where the same conclusion is obtained from a more detailed stability analysis that includes time derivatives of the radial coordinate). Finally, we note that the point $\hat{r} = r_*$ where the upper branch becomes unstable can also be seen as a turning point in a plot of Ω as a function of J (see right plot of Fig. 2.2).

The main motivation of the review above and the various plots that are presented is that they will be instructive to illustrate the new features that appear when constructing and analyzing the thermal giant gravitons in Secs. 2.4 and 2.5.

Having established which solutions are stable, we will now discuss their physical relevance. First we note that they are distinguished by the angular momentum \mathbf{J} . In terms of \hat{r} they coexist when $\hat{r}_* \leq \hat{r} \leq 1$, but from (2.17), (2.18) we easily see that the energy on the lower branch is lower than that of the upper branch, for a given \hat{r} in that range, except when $\hat{r} = 1$ where they have the same energy. The lower branch is the usual 1/2 BPS branch extensively considered in the literature, and from (2.18) we immediately recognize the BPS condition $E_- = J_-/L$. The other stable solution which is part of the upper branch was noted in [26] (see in particular Figs. 1 and 2 of that reference), but has otherwise largely been ignored. First of all this branch is not connected to the point particle case as a stable configuration since local stability requires $\hat{r}_* \leq \hat{r} \leq 1$. Furthermore, while it is a local minimum of the energy it is not a global one, so it is a metastable configuration and has $E_+ \geq J_+/L$ where the bound is saturated for $\hat{r} = 1$. This thus raises the question whether this configuration indeed preserves 1/2 of the supersymmetries. By repeating the steps of Sec. 3 of [26], it is possible to verify that this is indeed the case. The main point here is that the Ω -dependent terms in this computation vanish at $\hat{r} = 1$. So we see that at $\hat{r} = 1$ we can have either $\bar{\Omega}_- = 1/L$ or $\bar{\Omega}_+ = (n-2)/L$, both satisfying the same BPS bound and both being supersymmetric. In particular, we cannot distinguish these

configurations according to their energy.⁵ In the first case the center of mass is rotating at the speed of light while in the second the center of mass is rotating at a superluminal velocity. However this should not be an argument for discarding the latter solution since the center of mass being a geometrical construction can be moving with superluminal velocities as long as every point on the brane is subluminal. The existence of these two BPS configurations at $\hat{r} = 1$, arising from two distinct solution branches raises the question of what the dual CFT interpretation is of the one connected to the non-BPS branch, and we briefly comment on this in Sec. C.2 of App. C.

2.3 Construction of finite temperature giant graviton on S^n

In this section we discuss the setup that we employ to obtain thermal spinning giant gravitons. Beyond the setup and the resulting blackfold equation of motion, this section presents the corresponding thermal spinning giant gravitons solutions, the regime of validity and the extremal limit.

2.3.1 Blackfold action and equation of motion

As explained in the introduction, we aim to study giant graviton solutions of type II string theory and M-theory as the $\text{AdS}_m \times S^n$ background is heated up to finite temperature, treating the giant gravitons as probes of these backgrounds, but heating them up to the same (finite) temperature. This is done by going to the supergravity regime and replacing the thermal probe branes by an effective description in terms of their stress tensor and charge current.

The probe brane setup and internal spin

Our first input to set up the problem is the stress tensor and charge current of the black $(n-2)$ -brane probes. To leading order in the blackfold approximation the stress tensor is that of an $(n-1)$ -dimensional perfect fluid tensor $T_{ab} = (\varrho + P)u_a u_b + P\gamma_{ab}$ where $\sigma^a = \tau, \sigma^1, \dots, \sigma^{n-2}$ label the worldvolume coordinates, u_a is the $(n-1)$ -velocity and γ_{ab} the induced metric on the brane. Furthermore, the energy, pressure, entropy density and local temperature are given by (reviewed in Sec. 1.5.3)

$$\varrho = \mathcal{T}s - P, \quad P = -\mathcal{G} (1 + (m-1) \sinh^2 \alpha), \quad \mathcal{T}s = (m-1)\mathcal{G}, \quad \mathcal{T} = \frac{m-1}{4\pi r_0 \cosh \alpha}, \quad (2.21)$$

where \mathcal{G} denotes the Gibbs free energy recorded in Eq. (1.79),

$$\mathcal{G} \equiv \frac{\Omega_{(m)}}{16\pi G} r_0^{m-1}, \quad (2.22)$$

with $\Omega_{(m)}$ the volume of the unit transverse m -sphere. The parameters of the black $(n-2)$ -brane stress tensor and thermodynamics are thus r_0 , α and the co-dimension of the brane $m+1$. Note that we can replace Newton's constant G in terms of the tension

⁵They also satisfy the zero temperature limit of a general Smarr relation that is derived in App. C.1.

$T_{(n-2)} = ((2\pi)^{n-2} l_p^{n-1})^{-1}$ of the $(n-2)$ -brane using the relation (2.14).⁶ The black $(n-2)$ -brane furthermore has the $(n-1)$ -form charge current $J_{(n-1)} = \star_{(n-1)} Q_{(n-2)}$, where $Q_{(n-2)}$ is the charge

$$Q_{(n-2)} = (m-1)\mathcal{G} \sinh \alpha \cosh \alpha = N_{(n-2)} T_{(n-2)} , \quad (2.23)$$

and $N_{(n-2)}$ the number of probe black $(n-2)$ -branes. Again note that current conservation on the worldvolume implies that $N_{(n-2)}$ is constant.

In order to describe the thermal version of the giant graviton we use the same geometrical setup as in Sec. 2.2. In particular, the giant graviton spatial worldvolume is spanned by an S^{n-2} and it moves around the $S^1 \subset S^n$ described by the coordinate ϕ with angular velocity $\dot{\phi} \equiv \beta_n \Omega$. The size r of the giant graviton and the distance to the equator of the S^n is described by the θ coordinate, $r \equiv L \sin \theta$. As mentioned above, in addition to heating up the giant graviton configuration, we seek to examine the effects of intrinsic spin. To incorporate this, we introduce a set of directional cosines on the spatial part of the induced metric of the worldvolume

$$d\Omega_{(n-2)}^2 = \sum_i d\mu_i^2 + \sum_j \mu_j^2 d\phi_j^2 , \quad \sum_i \mu_i^2 = 1 , \quad (2.24)$$

where the sum over i runs from 1 to $\lfloor n/2 \rfloor$, while the sum over j runs from 1 to $\lfloor (n-1)/2 \rfloor$. We will now consider the following fluid velocity

$$\mathbf{k} u^a \partial_a = \mathbf{k}^a \partial_a = \partial_\tau + \omega \sum_{i=1} \partial_{\phi_i} , \quad \mathbf{k}^2 \equiv -\gamma_{ab} \mathbf{k}^a \mathbf{k}^b , \quad (2.25)$$

where $\omega = 0$ corresponds to the fluid being at rest $u^a \partial_a \sim \partial_\tau$. We thus take the maximally symmetric situation with equal angular velocities in each of the Cartan directions of the S^{n-2} , and, for reasons explained below we will assume that n is odd. We then have the norms

$$\mathbf{k}^2 = |k_{\text{w.v.}}|^2 - \mathcal{W}^2 , \quad \mathcal{W} \equiv \omega r \quad |k_{\text{w.v.}}|^2 \equiv |\partial_\tau|^2 = 1 - (\Omega L)^2 + \mathcal{V}^2 \quad \mathcal{V} \equiv \Omega r . \quad (2.26)$$

Note that for n even the first expression above would depend on one of the direction cosines $\mu_{n/2}$, leading to a Killing vector with a norm that is angular dependent. In analogy with the neutral blackfold solutions reviewed in Sec. 1.4.3, this will lead to an inconsistency in the EOM. We can therefore only consistently switch on internal spin for the D3 and M5-brane, where the branes wrap odd-spheres. The results below still hold for the M2-brane provided one sets the internal angular velocity ω to zero.

Thermal giant graviton equation of motion

We will now derive the EOM for the thermal spinning giant graviton. We derive the EOM from the worldvolume action found in Eq. (1.119). The (non-dilatonic) action takes the form

$$I = \int_{\mathbb{R} \times S^{(n-2)}} \{ \star P + Q_{(n-2)} \mathbb{P} [A_{(n-1)}] \} , \quad (2.27)$$

⁶Note that for this one uses $16\pi G = (2\pi)^{m+n-3} l_p^{m+n-2}$, where we recall that for the IIB string theory case $l_p^8 = g_s^2 l_s^8$.

where \mathbb{R} denotes time, $\mathbb{P}[A_{(n-1)}]$ is the pull-back of the background gauge field $A_{(n-1)}$ (2.7) to the worldvolume, and $Q_{(n-2)} = N_{(n-2)}T_{(n-2)}$ is the total charge of the giant graviton (cf. (2.23)). We also remark that since the $(n-2)$ -brane is expanded on the $(n-2)$ -sphere the local temperature has a redshift as compared to the global temperature T of the background space-time that we are probing, i.e. $\mathcal{T} = T/\mathbf{k}$ (see also Sec. 1.3.3).

Using the embedding given above, and employing the $\text{SO}(n-1)$ symmetry of the configuration, the action takes the form

$$\beta I_E = -\Omega_{(n-2)} r^{n-2} (|k_{\text{w.v.}}|P + r\Omega Q_{(n-2)}) , \quad (2.28)$$

where we have gone to Euclidean space and the factor $\beta = 1/T$ results from the integration over Euclidean time. The EOM is obtained by varying the action keeping fixed the global temperature T , angular velocities Ω , ω , and the charge $Q_{(n-2)}$. Using the definitions in (2.26) and the identity $\delta_r \log P = -(\mathcal{T}s/P)\delta_r \log \mathbf{k}$, we find after some algebra the EOM in the form

$$(n-2)(\mathbf{k}^2 + \mathcal{W}^2) + \mathcal{V}^2 + \frac{\mathbf{k}^2 + \mathcal{W}^2}{\mathbf{k}^2} \mathcal{R}_1 (\mathcal{W}^2 - \mathcal{V}^2) + (n-1)\mathcal{V}\sqrt{\mathbf{k}^2 + \mathcal{W}^2} \mathcal{R}_2 = 0 , \quad (2.29)$$

where we have introduced the two dimensionless ratios

$$\mathcal{R}_1 \equiv \frac{\mathcal{T}s}{P} = \frac{1-m}{1+(m-1)\sinh^2 \alpha} , \quad \text{and} \quad \mathcal{R}_2 \equiv \frac{Q_{(n-2)}}{P} = \frac{(1-m)\sinh \alpha \cosh \alpha}{1+(m-1)\sinh^2 \alpha} . \quad (2.30)$$

Conserved quantities

Given a solution of the EOM (2.29), the configuration has a number of conserved quantities. For use below, we present the (off-shell) expressions of these conserved quantities, which follow from the general results for blackfolds in flux backgrounds, derived in Sec. 1.7.1. Upon direct evaluation, these are found to be

$$E = \frac{\Omega_{(n-2)} r^{n-2}}{|k_{\text{w.v.}}| \mathbf{k}^2} [\varrho |k_{\text{w.v.}}|^2 + P (|k_{\text{w.v.}}|^2 - \mathbf{k}^2)] , \quad S = \frac{1}{T} (m-1) \Omega_{(n-2)} \mathcal{G} |k_{\text{w.v.}}| r^{n-2} ,$$

$$J = E \Omega \rho^2 + Q_{(n-2)} \Omega_{(n-2)} r^{n-1} , \quad \mathcal{S} = \frac{\Omega_{(n-2)} \mathcal{G} \omega r^n |k_{\text{w.v.}}|}{\mathbf{k}^2} . \quad (2.31)$$

Here E is the energy, S the entropy, J the angular momentum along the $S^1 \subset S^n$, and

$$\mathcal{S}_i = \frac{2}{n-1} \mathcal{S} , \quad i = 1, \dots, (n-1)/2 , \quad (2.32)$$

are the intrinsic angular momenta on S^{n-2} . Here and in the following we have also introduced $\rho \equiv \sqrt{L^2 - r^2}$ and we remind the reader that ϱ , P , \mathcal{G} are defined in (2.21), (2.22). In App. C.1 we check that the Euclidean action in (2.28) satisfies $\beta I_E = E - TS - \Omega J - \omega \mathcal{S}$ along with a Smarr relation. The equation of motion is therefore equivalent to requiring the first law of thermodynamics for the specific configuration as expected.

2.3.2 Solution space and thermodynamics

We now describe the solution space of the EOM (2.29). We work in the ensemble with given temperature T , fixed charge (number of $(n-2)$ -branes) $Q_{(n-2)}$ and intrinsic spin \mathcal{S} . We now explain how the norm of the fluid killing vector \mathbf{k} can be used to (formally) parameterize the solution space. For a given $\mathbf{k}, \mathcal{R}_1, \mathcal{R}_2$ and \mathcal{W} we can solve the EOM (2.29) for \mathcal{V} since it is a simple quadratic equation,

$$\mathcal{V}_{\pm}(\mathbf{k}, \mathcal{W}) = \frac{1}{2} \frac{(n-1)\mathcal{R}_2\sqrt{\mathbf{k}^2 + \mathcal{W}^2} \mp \sqrt{\mathcal{D}_{\mathcal{W}}^{(n)}}}{(\mathcal{R}_1 - 1)\mathbf{k}^2 + \mathcal{R}_1\mathcal{W}^2} \mathbf{k}^2, \quad (2.33)$$

with

$$\mathcal{D}_{\mathcal{W}}^{(n)} = (\mathbf{k}^2 + \mathcal{W}^2) \left[4 \left(n - 2 + \frac{\mathcal{R}_1}{\mathbf{k}^2} \mathcal{W}^2 \right) \left(\mathcal{R}_1 - 1 + \frac{\mathcal{R}_1}{\mathbf{k}^2} \mathcal{W}^2 \right) + (n-1)^2 \mathcal{R}_2^2 \right]. \quad (2.34)$$

In analogy to the DBI giant graviton, we will refer to the two solution branches as the lower ($-$) and upper ($+$) branch respectively. At the end of this section, we show that for zero intrinsic spin and zero temperature the lower branch reduces to the standard $\frac{1}{2}$ -BPS giant graviton. Similarly the upper branch reduces to the upper brach of the DBI analysis (2.16). Using (2.26) we can now find the expression for respectively $\hat{r} \equiv r/L$, $\hat{\Omega} \equiv \Omega L$ and $\hat{\omega} \equiv \omega L$. One finds

$$\hat{r}(\mathbf{k}, \mathcal{W}) = \frac{\mathcal{V}}{\sqrt{1 + \mathcal{V}^2 - \mathcal{W}^2 - \mathbf{k}^2}}, \quad \hat{\Omega}(\mathbf{k}, \mathcal{W}) = \frac{\mathcal{V}}{\hat{r}}, \quad \hat{\omega}(\mathbf{k}, \mathcal{W}) = \frac{\mathcal{W}}{\hat{r}}, \quad (2.35)$$

where $\mathcal{V}(\mathbf{k}, \mathcal{W})$ is given by (2.33). Now for a given value of \mathbf{k} we can (explicitly) work out the values of $\mathcal{R}_1 \equiv \mathcal{R}_1(\mathbf{k})$ and $\mathcal{R}_2(\mathbf{k})$ and (implicitly) the value of $\mathcal{W} \equiv \mathcal{W}(\mathbf{k})$ by the requirement that $Q_{(n-2)}, T$ and \mathcal{S} are kept fixed. This will be explained in the following.

First of all, we can determine the value of \mathcal{R}_1 and \mathcal{R}_2 (see (2.30)) for a given \mathbf{k} . To this end, we introduce the parameter $\phi \equiv 1/\cosh^2 \alpha$. The charge quantization condition (2.23) can then be rewritten as

$$\phi^{m-2} - \phi^{m-3} + \frac{(m-3)^{m-3}}{(m-2)^{m-2}} \sin^2 \delta = 0, \quad \sin \delta = \left(\frac{\hat{T}}{\mathbf{k}} \right)^{m-1}, \quad (2.36)$$

with

$$\hat{T} \equiv \frac{T}{T_{\text{stat}}}, \quad T_{\text{stat}}^{m-1} = \frac{1}{Q_{(n-2)} G} \frac{(m-1)^m \Omega_{(m)}}{4(4\pi)^m} \sqrt{\frac{(m-3)^{m-3}}{(m-2)^{m-2}}}. \quad (2.37)$$

The equation (2.36) is a polynomial of degree $m-2$ whose solution we will denote by $\phi(\mathbf{k})$ (for simplicity of notation we suppress the \hat{T} dependence in all expressions below). For $m=4$ (M5-brane on S^7), it becomes a simple quadratic equation with solution

$$(m, n) = (4, 7): \quad \phi(\mathbf{k}) = \sin^2 \left(\frac{\delta(\mathbf{k})}{2} \right). \quad (2.38)$$

In the case of $m=5$ (D3-brane on S^5), the equation is a cubic equation with solution

$$(m, n) = (5, 5): \quad \phi(\mathbf{k}) = \frac{2}{3} \frac{\sin(\delta(\mathbf{k}))}{\sqrt{3} \cos(\delta(\mathbf{k})/3) - \sin(\delta(\mathbf{k})/3)}. \quad (2.39)$$

We will analyse various properties of the D3-brane finite temperature non-spinning giant graviton in Sec. 2.5 using this equation. Finally, we note that it is not possible to write down an analytical expression for $m = 7$ (M2-brane on S^4), however, $\phi(\mathbf{k})$ can in principle easily be obtained numerically.

The second parameter \mathcal{W} is determined by the (fixed) intrinsic spin \mathcal{S} . Rewriting \mathcal{S} is straightforward using the expression in (2.31). We have

$$\mathcal{S}(\mathbf{k}, \mathcal{W}) = LQ_{(n-2)}\Omega_{(n-2)} \frac{\phi(\mathbf{k})\mathcal{W}\sqrt{\mathbf{k}^2 + \mathcal{W}^2}}{\mathbf{k}^2\sqrt{1 - \phi(\mathbf{k})}} \hat{r}(\mathbf{k}, \mathcal{W})^{n-1}, \quad (2.40)$$

where we recall that \hat{r} is given in (2.35). This equation does not in general have an analytical solution but it is a simple algebraic equation in one variable \mathcal{W} and its solution is again easy to obtain numerically. We denote the solution by $\mathcal{W}(\mathbf{k})$. The equations (2.33)-(2.37) and (2.40) formally parameterize the solution in terms of \mathbf{k} for given \hat{T} , $Q_{(n-2)}$ and \mathcal{S} .

Range of \mathbf{k}

Finally, we need to address the range of \mathbf{k} . First of all we note that \mathbf{k} necessarily lies in the range $\hat{T} \leq \mathbf{k} \leq 1$, where the lower bound follows from (2.37) and the upper bound from the geometric relation $r \leq L$. However, this is only a necessary condition and the form of the solution, notably positivity of the discriminant in (2.34), leads to further restrictions. In particular, for the non-spinning giant graviton ($\mathcal{S} = 0$) this leads to the restricted range $\tilde{T} \equiv T/T_{\max} \leq \mathbf{k} \leq 1$. Here T_{\max} is the maximum temperature that the solution can have in that case (see App. C.3.1), and we note that $\hat{T} < \tilde{T}$ because $T_{\text{stat}} > T_{\max}$. More generally, as soon as we turn on spin one finds that the range of possible \mathbf{k} values becomes more intricate but can be computed in principle for given \hat{T} , \mathcal{S} .

As an illustration we give some details on the range of \mathbf{k} in App. C.3.1, while we also refer the reader to Sec. 2.4, where we will plot the solution branches at maximal size $r = L$ for a representative value of \hat{T} . This indicates that \mathbf{k} goes from 1 (low spin regime) to \hat{T} (for which the maximum spin is obtained) and a small interval of \mathbf{k} 's which is excluded by the EOM. As a consequence, we see that each of the lower and upper branches, branch up further into two branches, a low spin and high spin branch.

Physical quantities

Given a spinning giant graviton solution, we can write down the on-shell physical quantities using the expressions in (2.31). We define a rescaled dimensionless energy, entropy, and angular momenta by

$$\mathbf{E} \equiv \frac{EL}{NN_{(n-2)}}, \quad \mathbf{S} \equiv \frac{ST_{\text{stat}}}{NN_{(n-2)}}, \quad \mathbf{J} \equiv \frac{J}{NN_{(n-2)}}, \quad \mathcal{S} \equiv \frac{\mathcal{S}}{NN_{(n-2)}}, \quad (2.41)$$

and use the dimensionless ratios $\hat{r} \equiv r/L$, $\hat{\rho} \equiv \rho/L$. Notice that \mathbf{J} (respectively \mathcal{S}) is the ratio between orbital (respectively internal) angular momentum and the orbital angular momentum of the maximal size giant graviton at $r = L$. We then record the expressions

of \mathbf{E} , \mathbf{S} , \mathbf{J} and \mathcal{S} in terms of \mathbf{k} , \mathcal{W} , $\phi(\mathbf{k})$ and $\hat{r}(\mathbf{k}, \mathcal{W})$

$$\begin{aligned} \mathbf{E} &= \frac{1}{\sqrt{(\mathbf{k}^2 + \mathcal{W}^2)(1 - \phi)}} \left(1 + \frac{\phi}{\mathbf{k}^2} \mathcal{W}^2 + \frac{\phi}{m-1} \right) \hat{r}^{n-2}, & \mathbf{S} &= \frac{\phi}{\hat{T}} \sqrt{\frac{\mathbf{k}^2 + \mathcal{W}^2}{1 - \phi}} \hat{r}^{n-2}, \\ \mathbf{J} &= \mathbf{E} \hat{\rho} \sqrt{1 - \mathcal{W}^2 - \mathbf{k}^2} + \hat{r}^{n-1}, & \mathcal{S} &= \frac{\phi \mathcal{W} \sqrt{\mathbf{k}^2 + \mathcal{W}^2}}{\mathbf{k}^2 \sqrt{1 - \phi}} \hat{r}^{n-1}. \end{aligned} \quad (2.42)$$

The expression for \mathcal{S} suggests that maximum intrinsic spin is attained for $\mathbf{k} = \hat{T}$, which is confirmed by the analysis in the next section.

Validity of the probe approximation

We now address the validity of the (leading order) blackfold approach in which the $(n-2)$ -brane is treated in the probe approximation. For the probe approximation to be valid for our supergravity black $(n-2)$ -brane probe we must require the transverse length scale r_s of the probe to satisfy the conditions that r_s is much smaller than any of the scales r_{int} , r_{ext} and L , where r_{int} and r_{ext} are the length scales associated with the intrinsic and extrinsic curvature of the embedding of the brane, respectively, and L is the length scale of the $\text{AdS}_m \times S^n$ background. A detailed analysis leads to the (sufficient) requirement (2.3).⁷ We now examine how these bounds relate to the Hawking-Page temperature $T_{\text{HP}} \sim 1/L$, above which the AdS black hole background will become dominant over the hot AdS space-time background. Using the results for the maximal temperature collected in App. C.3.1 we have first of all in the case of zero intrinsic spin that

$$T_{\text{max}} \sim N^{\frac{1}{n-1}}, \quad T_{\text{HP}} \sim N^{\frac{1}{(n-2)}}. \quad (2.43)$$

Using (2.3), we thus see that in the regime where the probe blackfold approximation is valid, the maximum temperature of the solution is far above the Hawking-Page temperature, $T_{\text{HP}} \ll T_{\text{max}}$. We also remark that when the intrinsic spin is turned on the maximum temperature decreases.

2.3.3 The extremal limit

To make contact with the standard zero-temperature giant graviton reviewed in Sec. 2.2 we consider here the extremal limit of the above solution. This is obtained by letting $\phi \rightarrow 0$ so $\mathcal{R}_1 \rightarrow 0$ and $\mathcal{R}_2 \rightarrow -1$. Since $\mathcal{S} = 0$ for all \mathcal{W} , we expect \mathcal{W} to drop out of the problem.⁸ Indeed, we should not be able to see intrinsic rotation in the extremal limit, due to Lorentz invariance of the worldvolume stress tensor. In further detail, we obtain from the solution (2.33) by setting $\mathcal{R}_1 = 0$ and $\mathcal{R}_2 = -1$ that

$$\mathcal{V}_- = |k_{\text{w.v.}}|, \quad \mathcal{V}_+ = (n+1)\mathcal{V}_-, \quad (2.44)$$

⁷We note that the upper bounds $N_{(n-2)} \ll N^{\frac{m-1}{n-1}}$ follow from setting $r = L$ in the necessary requirement $N_{(n-2)} \ll N^{\frac{m-1}{n-1}} (r/L)^{m-1}$ (see also [1]).

⁸Another extremal limit, involving a double scaling, will be considered in Sec. 2.6.

which are manifestly independent of \mathcal{W} . Using (2.35), we then obtain the lower and upper branch, respectively

$$\hat{\Omega}_- = 1, \quad \hat{\Omega}_+ = \frac{n-2}{\sqrt{(n-2)^2 - (n-1)(n-2)\hat{r}^2}}, \quad (2.45)$$

which coincides with the angular velocities from the DBI analysis (2.16) (here denoted with a bar to distinguish them from their thermal counterparts). Using the equations (2.42) we can now compute the energy and angular momentum associated with the extremal solution. We find

$$\bar{\mathbf{J}}_- = \bar{\mathbf{E}}_- = \hat{r}^{n-3}. \quad (2.46)$$

while for the upper branch, we have

$$\bar{\mathbf{J}}_+ = \hat{r}^{n-3}(n-2 - (n-3)\hat{r}^2), \quad \bar{\mathbf{E}}_+ = \hat{r}^{n-3}\sqrt{(n-2)^2 - (n-1)(n-3)\hat{r}^2}. \quad (2.47)$$

Reintroducing the units using Eq. 2.41, we thus recover the extremal results for the energy (2.17) and angular velocity (2.18) up to a factor $N_{(n-2)}$ alluding the fact that in the blackfold analysis we consider a (large) stack of $N_{(n-2)}$ branes (as opposed to the DBI analysis where we consider only a single brane).

2.4 Thermal spinning giant graviton

In this section we examine the physics of the thermal and internally spinning version of the giant graviton configuration consisting of an $(n-2)$ -brane wrapped on an $(n-2)$ -sphere moving on the n -sphere of $\text{AdS}_m \times S^n$. We will start by elucidating some of the main features of the solution space obtained from the EOM (2.29).

2.4.1 Main features of solution space

As explained in the introduction, from the point of view of the dual field theory, the most interesting giant graviton configuration is the one close to maximal size, $r \simeq L$. In this section we examine the configuration space at $r = L$ when turning on temperature and intrinsic spin. We mention that in principle it is possible to numerically do a similar analysis for any $r > 0$, however, this is not particularly illuminating and such an analysis has thus been omitted. We expect the general features of the results below to hold for any r .

At $r = L$ the Killing vector \mathbf{k} only depends on $\mathcal{W} = \hat{\omega}$. Substituting the expression for \mathcal{W} in terms of \mathbf{k} into (2.33), we obtain the solution for $\mathcal{V}_\pm = \hat{\Omega}_\pm$ parameterized in terms of $\mathbf{k} = (1 - \hat{\omega}^2)^{1/2}$ at maximal size. In Fig. 2.3 the angular velocity Ω is plotted as a function of \mathbf{k} for both branches for the D3- and M5-brane, respectively. Here we describe the main features of the solutions.

As can be seen from the plot, there is a small range of values of \mathbf{k} which admits no solutions to the EOM. Therefore each branch splits up into a low spin branch and a high spin branch⁹. At low spin the angular velocity Ω_\pm and thermodynamics get small quadratic

⁹This effect can also be deduced by looking at the behavior of the quantity $\mathcal{D}_\mathcal{W}$ in (2.34), see App. C.3.

spin corrections. This is simply because the conserved quantities depend quadratically on the spin parameter \mathcal{W} except the intrinsic angular momentum which only depends linearly on \mathcal{W} to lowest order. However, these corrections will be sub-leading to the thermal corrections from the non-zero temperature of the background (see Sec. 2.4.2 below).

In the high spin regime the situation is very different and the solution space is dominated by the effects of internal spin. As already pointed out in Sec. 2.3.2, the maximal value for the intrinsic angular momentum is attained as $\mathbf{k} \rightarrow \hat{T}$. This can also be seen from the plots in Fig. 2.3. As \mathbf{k} approaches \hat{T} , we see that the angular velocity Ω_- crosses zero and becomes negative. In order to examine the solution space near maximal spin we expand around maximal spin $\mathbf{k} = \hat{T}(1 + \delta^2)$, $\delta \ll 1$. It is straightforward to solve the charge quantization equation (2.36) to leading order in δ . Notice that for $\mathbf{k} = \hat{T}$, we have

$$\phi(\hat{T}) = \frac{m-3}{m-2}. \quad (2.48)$$

It is now straightforward to compute the thermodynamics for small δ . For the D3 giant graviton we find to leading order in \hat{T}

$$\mathbf{E} = \frac{2}{\sqrt{3}\hat{T}^2} \left(1 - \frac{4\sqrt{2}}{\sqrt{3}}\delta + \mathcal{O}(\delta^2) \right), \quad \mathbf{S} = \frac{1}{2\sqrt{3}\hat{T}^2} \left(1 - \frac{4\sqrt{2}}{\sqrt{3}}\delta + \mathcal{O}(\delta^2) \right). \quad (2.49)$$

Similarly we find for the M5-brane configuration

$$\mathbf{E} = \frac{1}{\sqrt{2}\hat{T}^2} \left(1 - \frac{3\sqrt{3}}{\sqrt{2}}\delta + \mathcal{O}(\delta^2) \right), \quad \mathbf{S} = \frac{1}{3\sqrt{2}\hat{T}^2} \left(1 - \frac{3\sqrt{3}}{\sqrt{2}}\delta + \mathcal{O}(\delta^2) \right). \quad (2.50)$$

Note that to leading order $\hat{T}\mathbf{S}$ is of order $\mathcal{O}(\hat{T}^0)$. To leading order, the free energy is therefore equal to the energy. The above relations can be used to eliminate the small

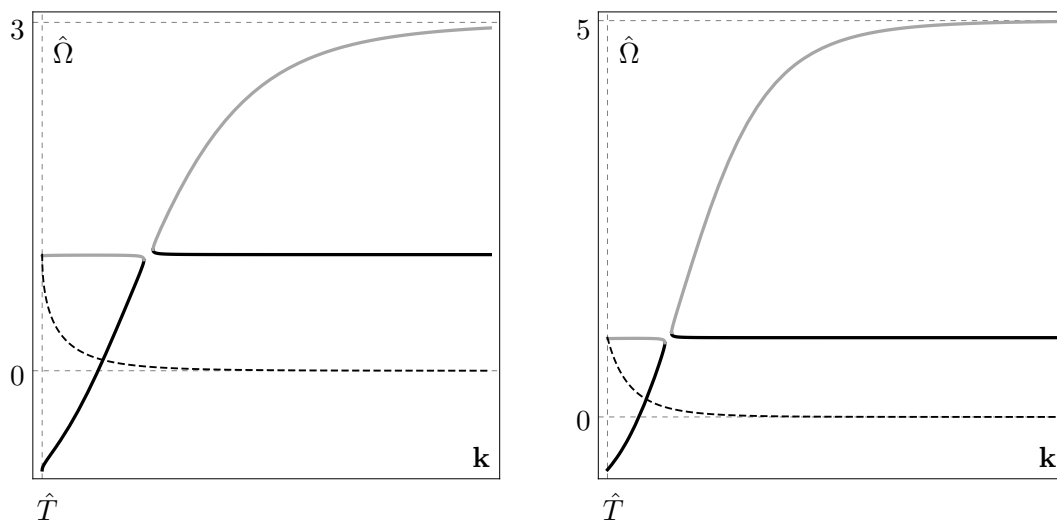


Figure 2.3: The angular velocities $\hat{\Omega}_-$ (black), $\hat{\Omega}_+$ (grey), and relative intrinsic angular momentum $\mathcal{S}/\mathcal{S}_{\max}$ (dashed) plotted as a function of \mathbf{k} for the D3 (left) and M5 (right) thermal giant graviton configurations. The plots are drawn for $\hat{T} = 0.2$ and have been cut off at $\mathbf{k} = 0.6$ to enhance features.

expansion parameter δ and write the energy in terms of the intrinsic angular momentum in the high spin limit. For the D3 giant graviton, we find to leading order in $\Delta\mathcal{S} \equiv \mathcal{S}_{\max} - \mathcal{S}$,

$$E = \frac{1}{L} \left(\frac{2\sqrt{2}}{3 \cdot 3^{1/4} \pi^2} \frac{\sqrt{N^3 N_{D3}}}{(LT)^2} - 4\Delta\mathcal{S} \right), \quad S_{\max} = \frac{1}{3 \cdot 3^{1/4} \sqrt{2} \pi^2} \frac{\sqrt{N^3 N_{D3}}}{(LT)^2}. \quad (2.51)$$

where we have re-introduced the physical units using (2.14) and (2.37). Similarly, we find for the M5-brane

$$E = \frac{1}{L} \left(\frac{9}{8\sqrt{2} \pi^2} \frac{(N^4 N_{M5})^{1/3}}{(LT)^2} - 3\Delta\mathcal{S} \right), \quad S_{\max} = \frac{3}{8\sqrt{2} \pi^2} \frac{(N^4 N_{M5})^{1/3}}{(LT)^2}. \quad (2.52)$$

As is clear from the expressions above, the maximally spinning giant graviton configurations are very heavy objects compared to their non-spinning counterparts.¹⁰

2.4.2 Low temperature expansion

In this section we give an approximate solution to the giant graviton EOMs in terms of the radial coordinate r in a low temperature expansion and without intrinsic spin. Moreover, we briefly examine the low spin and the maximal spin case for a given r in a low temperature expansion, respectively.

The low temperature limit with no intrinsic spin: In order to work out the low temperature expansion we take $T \rightarrow 0$, or equivalently $\phi \rightarrow 0$ while keeping \mathbf{k} finite. First, since $\phi \ll 1$, we can immediately solve the charge conservation equation (2.36). Indeed, in this limit the ϕ^{m-2} term can be dropped and the solution to (2.36) is given by

$$\phi = C_m \left(\frac{\hat{T}}{\mathbf{k}} \right)^{\gamma_m}, \quad (2.53)$$

where

$$\gamma_m = \frac{2(m-1)}{m-3} \quad \text{and} \quad C_m = (m-3)(m-2)^{\frac{2-m}{m-3}}. \quad (2.54)$$

Notice that for the values of n and m under consideration, we have $\gamma_m = \gamma_{D-n} = n-1$. In the limit with no intrinsic spin, we therefore find the following solution for ϕ

$$\phi = \phi_0 \mathbf{k}^{1-n}, \quad \phi_0 \equiv \phi|_{r=L} = f_n \hat{T}^{n-1}, \quad (2.55)$$

where we have defined $f_n \equiv C_{D-n}$ and

$$f_4 = \frac{4}{5 \cdot 5^{1/4}}, \quad f_5 = \frac{2}{3\sqrt{3}}, \quad f_7 = \frac{1}{4}. \quad (2.56)$$

Notice that the limit $\phi \ll 1$ requires that $\mathbf{k} \gg \hat{T}$ which is equivalent to $\hat{r} \gg \hat{T}$. We now proceed and expand around the extremal solution (2.45). It is straightforward to expand

¹⁰We note that the energy in (2.51) is proportional to $N^2(N_{D3}/N)^{1/2}$, while (2.52) is proportional to $N^{3/2}\lambda_M^{1/6}$ in terms of the 't Hooft like coupling λ_M defined below (2.3).

\mathcal{V}_\pm with $\mathcal{W} = 0$ in terms of ϕ . One finds¹¹

$$\mathcal{V}_- = \mathbf{k} + \mathcal{O}(\phi^2), \quad \mathcal{V}_+ = (n-2)(1-\phi)\mathbf{k} + \mathcal{O}(\phi^2). \quad (2.57)$$

It is seen that for the physically relevant values of n and m , \mathcal{V}_- gets no first order correction as was also seen in the D3-brane case. Now using $\mathbf{k}^2 = 1 - \hat{\Omega}^2 \hat{r}^2$ and $\mathcal{V} = \hat{r}\hat{\Omega}$, we can solve for $\hat{\Omega}$

$$\hat{\Omega}_- \simeq \hat{\bar{\Omega}}_- + \mathcal{O}(\phi^2), \quad \hat{\Omega}_+ \simeq \hat{\bar{\Omega}}_+ \left(1 - \left(\frac{\hat{\bar{\Omega}}_+ \hat{r}}{n-2} \right)^2 \phi \right) + \mathcal{O}(\phi^2). \quad (2.58)$$

where the expressions for the angular velocities $\hat{\bar{\Omega}}_\pm$ at extremality were recorded in Eq. (2.45).

Using Eqs. (2.42) it is now possible to compute the on-shell quantities for the lower and upper branch, respectively. For the lower branch, we find

$$\begin{aligned} \mathbf{E}_- &\simeq \bar{\mathbf{E}}_- + \frac{n-2}{n-1} \frac{\phi_0}{\hat{r}^2}, \quad \mathbf{J}_- \simeq \bar{\mathbf{J}}_- + \frac{n-2}{n-1} \left(\frac{\hat{\rho}}{\hat{r}} \right)^2 \phi_0, \\ \hat{T}\mathbf{S}_- &\simeq \phi_0, \quad \mathbf{F}_- \simeq \bar{\mathbf{E}}_- - \left(\hat{r}^2 - \frac{n-2}{n-1} \right) \frac{\phi_0}{\hat{r}^2}. \end{aligned} \quad (2.59)$$

where $\bar{\mathbf{E}}_-$ and $\bar{\mathbf{J}}_-$ were written down in equations (2.46) and (2.47), and $\mathbf{F} = \mathbf{E} - \hat{T}\mathbf{S}$ is the normalized (Helmholtz) free energy of the system. Similarly for the upper branch we find

$$\begin{aligned} \mathbf{E}_+ &\simeq \bar{\mathbf{E}}_+ + \frac{n-2}{n-1} \left(\frac{n-2}{\hat{\bar{\Omega}}_+} \right)^{n-2} \left(n-1 - \frac{n-2}{\hat{r}^2} \right) \phi_0, \quad \mathbf{J}_+ \simeq \bar{\mathbf{J}}_+ - \frac{n-2}{n-1} \left(\frac{n-2}{\hat{\bar{\Omega}}_+} \right)^{n-1} \left(\frac{\hat{\rho}}{\hat{r}} \right)^2 \phi_0, \\ \hat{T}\mathbf{S}_+ &\simeq \left(\frac{n-2}{\hat{\bar{\Omega}}_+} \right)^{n-2} \phi_0, \quad \mathbf{F}_+ \simeq \bar{\mathbf{E}}_+ + \frac{n-2}{n-1} \left(\frac{n-2}{\hat{\bar{\Omega}}_+} \right)^{n-2} \left(\frac{(n-1)(n-3)}{n-2} - \frac{n-2}{\hat{r}^2} \right) \phi_0, \end{aligned} \quad (2.60)$$

with $\bar{\mathbf{E}}_+$ and $\bar{\mathbf{J}}_+$ given in equations (2.46) and (2.47). If needed, it is easy to reintroduce the dimensions and write the expression in terms of the physical quantities. Simply use that

$$\frac{\phi_0 N N_{M2}}{(LT)^3} = \frac{\sqrt{2} 2^5 \pi^3}{3^3} N_{M2}^{3/2}, \quad \frac{\phi_0 N N_{D3}}{(LT)^4} = \pi^4 N_{D3}^2, \quad \frac{\phi_0 N N_{M5}}{(LT)^6} = \frac{2^7 \pi^6}{3^6} N_{M5}^3. \quad (2.61)$$

We now express the free energy $F = E - TS$ on the lower branch in terms of the angular momentum. We find

$$\begin{aligned} F_{M2} &= \frac{J}{L} - \frac{\sqrt{2} 2^5 \pi^3}{3^4} N_{M2}^{3/2} L^2 T^3 + \mathcal{O}(T^6), \\ F_{D3} &= \frac{J}{L} - \frac{\pi^4}{4} N_{D3}^2 L^3 T^4 + \mathcal{O}(T^8), \\ F_{M5} &= \frac{J}{L} - \frac{2^6 \pi^6}{3^7} N_{M5}^3 L^5 T^6 + \mathcal{O}(T^{12}). \end{aligned} \quad (2.62)$$

¹¹Note that the expressions and manipulations pertaining to this section only apply to the physical values of n and m .

We observe that, to leading order, the difference $F - J/L$ is proportional to the free energy of the field theories living on the giant graviton branes [98]. In this connection, we note that it is non-trivial that the J -dependence has cancelled out in this difference. It is straightforward to write down similar expressions for the upper branch, however, the resulting expressions involve complicated functions of the angular momentum multiplying the thermal corrections, so we omit them here.

Finally, we compute the ratio J/E for the lower branch. We find

$$\begin{aligned}\frac{J_{M2}}{E_{M2}} &= L - \frac{\sqrt{2} 2^6 \pi^3 L}{3^4 J} N_{M2}^{3/2} (LT)^3, \\ \frac{J_{D3}}{E_{D3}} &= L - \frac{3\pi^4 L}{4J} N_{D3}^2 (LT)^4, \\ \frac{J_{M5}}{E_{M5}} &= L - \frac{5 \cdot 2^6 \pi^6 L}{3^7 J} N_{M5}^3 (LT)^6.\end{aligned}\tag{2.63}$$

The first term is recognized as the usual Kaluza-Klein contribution [25] while the second term is due to thermal effects from the thermal excitations of the $(n-1)$ -dimensional field theories living on the giant graviton worldvolume.

Stability issues: We now turn our attention to stability. To this aim we consider the localized giant graviton to be in thermodynamical equilibrium with the background at temperature $T = \hat{T} T_{\text{stat}}$. Moreover, since the total angular momentum J is conserved, the relevant variables for describing the thermodynamic ensemble are the size of the giant graviton r , the temperature T , the angular momentum J and the (conserved) total charge $Q = T_{(n-2)} N_{(n-2)}$. The stable solutions to the blackfold EOMs are then characterized by the paths in configuration space for which the Helmholtz free energy $F = E - TS$ is minimized for T , J and Q held fixed. In other words, the stable solutions are determined by the requirements

$$F_{(1)} \equiv \left. \frac{\partial F}{\partial r} \right|_{T,J,Q} = 0 \quad \text{and} \quad F_{(2)} \equiv \left. \frac{\partial^2 F}{\partial r^2} \right|_{T,J,Q} > 0\tag{2.64}$$

The first of these equations is equivalent to the EOM (2.29). The formulae (2.42) for the conserved quantities allows us to obtain the free energy of a (in general off-shell) given thermodynamical configuration. Therefore, having described the solution space for low temperatures essentially means that we have solved the first derivative $\mathbf{F}_{(1)} = 0$ of the off-shell free energy $F = E - TS$ for $\hat{T} \ll 1$, $\hat{T} \ll \hat{r}$ to leading order in \hat{T} . To analyze stability, we therefore now compute the second derivative $\mathbf{F}_{(2)}$ for both branches around the on-shell configurations. We find to leading order in ϕ_0

$$\mathbf{F}_{(2)}^- \simeq \frac{(n-3)^2 \hat{r}^{n-3}}{2\hat{\rho}^2} \left(1 - \frac{(n-2)(n^2 + 4 - 3n - (n-1)(n-3)\hat{r}^2)}{(n-1)(n-3)\hat{r}^{n-1}} \phi_0 \right),\tag{2.65}$$

and

$$\mathbf{F}_{(2)}^+ \simeq \frac{(n-3)^2 \hat{\Omega}_+ \hat{r}^{n-3}}{2(n-2)\hat{\rho}^2} \left((n-1)r^2 - (n-2) - \delta_n(r)\phi_0 \right),\tag{2.66}$$

where the expression for the function $\delta_n(r)$ is easily worked out but is rather cumbersome and has thus been omitted. Solving for $\mathbf{F}_{(2)} = 0$ determines where a solution goes from stable to unstable. Since the low temperature expansion is only valid for $r \gg \hat{T}L$, we see that the entire part of the lower branch captured by the low temperature expansion remains stable. However, the value of r for which the upper branch becomes unstable is pushed up when we turn on a temperature. Indeed, solving $\mathbf{F}_{(2)}^+ = 0$, we find that the upper branch becomes unstable at

$$r_* \simeq \bar{r}_* \left(1 + \frac{f_n}{2} \frac{\sqrt{(n-1)^{n-1}}}{n-3} \hat{T}^{n-1} \right), \quad (2.67)$$

where the \bar{r}_* denotes the extremal radial value for onset of instability recorded in (2.19). Note also that as a consistency check, the same value of r_* is obtained by finding the maximum of \mathbf{J}_+ in the low-temperature expansion, i.e. $\partial \mathbf{J}_+ / \partial r|_{r=r_*} = 0 + \mathcal{O}(\hat{T}^8)$.

The low temperature limit with low intrinsic spin: Since $\mathcal{S} \sim \phi$ (cf. Eqs. (2.42)), for a given temperature \hat{T} , the scale set for \mathcal{S} is given by ϕ_0 . Let us therefore define $\mathcal{S} = s \phi_0$. In this way the low spin regime is when $s \ll 1$. In this regime we have $\mathcal{W} \sim s \ll 1$ and $\mathbf{k} \simeq |k_{\text{w.v.}}|$. If we further take the low temperature limit, we find to leading order

$$\hat{\omega}_- = s, \quad \hat{\omega}_+ = \left(\frac{\hat{\Omega}_+}{n-2} \right)^n s. \quad (2.68)$$

In the low temperature regime, the effects of internal spin are first visible to order $\mathcal{O}(\phi_0^2)$. The expression for the conserved quantities (2.59) and (2.60) are therefore not changed to leading order.

Low temperature and maximal spin case: For a given $\hat{T} \ll 1$, maximal spin is attained for $\mathbf{k} = \hat{T}$. Indeed, the lowest possible value for \mathbf{k} is \hat{T} (cf. the discussion in Sec. 2.3.2). In the low temperature limit, the middle term in the extrinsic equation (2.36) dominates and therefore $\mathcal{V} \simeq \mathcal{W}$. We therefore conclude

$$\hat{\omega} \simeq \pm \hat{\Omega}_\pm = 1 + \mathcal{O}(\hat{T}^2). \quad (2.69)$$

In the high spin limit we therefore see that the upper and lower branch are on completely the same footing. The upper branch is rotating in the positive direction while the lower branch rotates in the negative direction around the S^1 . As the intrinsic spin is decreased, the two angular velocities increase so that $\hat{\Omega}_+$ goes from 1 to $\hat{\Omega}_+$ (+ thermal corrections) and $\hat{\Omega}_-$ goes from -1 to 1 (+ thermal corrections). This behavior can also be seen on the plot in Fig. 2.3. It is easy to work out the maximal spin thermodynamics for any $r \gg \hat{T}$. One finds the same results as in Sec. 2.4.1 scaled with suitable powers of \hat{r} .

2.4.3 Spinning black hole configuration

Very much as in flat backgrounds, the extrinsic equation allows for stationary $\Omega = 0$ odd-sphere solutions [37] (i.e. configurations with only intrinsic spin and $(m, n) =$

$\{(5, 5), (4, 7)\}$). In order to make connection with Ref. [37] and related works (see also Sec. 1.5.2), instead of working in the usual ensemble where we keep T , r and $N_{(n-2)}$ fixed and determine the one parameter space of solutions parameterized by internal spin \mathcal{S} , in this section we keep the size of the giant graviton r , the temperature T and the global dipole potential¹²

$$\Phi_{(n-2)} = \Omega_{(n-2)} r^{n-2} \tanh \alpha , \quad (2.70)$$

fixed. This amounts to simply taking

$$\alpha_\Phi = \operatorname{arctanh} \left(\frac{\Phi_{(n-2)} r^{2-n}}{\Omega_{(n-2)}} \right) . \quad (2.71)$$

As we now go along the one parameter family of solutions parameterized by the internal spin \mathcal{S} at fixed r and T , the dipole potential $\Phi_{(n-2)}$ will be constant but the charge $Q_{(n-2)} = T_{(n-2)} N_{(n-2)}$ will vary. For $\Omega = 0$, the extrinsic equation (2.29) takes the simple form

$$(n-2) (1 - \omega_r^2 r^2) = -\mathcal{R}_1(\alpha_\Phi) \omega_r^2 r^2 , \quad (2.72)$$

with the solution

$$\omega_r = \frac{1}{r} \sqrt{\frac{n-2}{n-2 - \mathcal{R}_1(\alpha_\Phi)}} , \quad (2.73)$$

for the internal angular velocity. The balancing condition (2.73) is the same as the one obtained for flat backgrounds [37]. This was expected since the coupling to the background n -form flux is proportional to Ω combined with the fact that the extrinsic EOM is a local equation. We emphasize that the solution (2.73) represent a stationary *bona fide* three-parameter¹³ black hole solution on $\text{AdS}_m \times S^n$. Using the formulas (2.31) (by substituting $\mathbf{k} = 1 - \omega_R^2 R^2$ with α fixed), it is possible to obtain the expressions for the black hole mass and thermodynamics in a straightforward manner. However, note that although the balancing condition (2.73) is equivalent to the balancing equation for odd-sphere solutions in flat backgrounds, the thermodynamics is not the same due to the non-trivial (global) background geometry. In particular the curvature of the S^n will introduce a tension term in the Smarr relation [1]. Also note that the angular momentum J of these configurations is not vanishing (as it would trivially be in flat backgrounds) due to the presence of the background flux.

If we want to determine the stationary $\Omega = 0$ solutions for a given charge $Q_{(n-2)}$ (i.e. switch back to the canonical ensemble), in addition to Eq. (2.73) we must also impose (2.36). This gives an implicit equation for ω_r which is neither captured by the high spin regime nor the usual low temperature regime. However, it is easy to see that a solution exists by continuity (which can also be seen on the plot in Fig. 2.3) and obtaining the solution is straightforward numerically.

¹²Notice that the expression only holds for $\Omega = 0$, see [37].

¹³Described by parameters (r, r_0, α) or through a set of transformations (captured by Eqs. (2.21),(2.70)) the physical parameters $(r, T, \Phi_{(n-2)})$.

2.5 The non-spinning giant graviton on $\text{AdS}_5 \times S^5$ - Finite temperature effects

Here we describe the details of the solution space of the non-spinning ($\mathcal{S} = 0$) $\text{AdS}_5 \times S^5$ thermal giant graviton expanded into the S^5 following [1].

2.5.1 The solution space

As explained in Sec. 2.3.2 and App. C.3.1, in the non-spinning case \mathbf{k} is confined to region 1 in the range

$$\tilde{T} \leq \mathbf{k} \leq 1, \quad (2.74)$$

with $\tilde{T} \equiv T/T_{\text{max}}$ where the maximum temperature $T_{\text{max}} < T_{\text{stat}}$ is given by

$$T_{\text{max}} = \left(\frac{8\sqrt{5}}{27\pi^2} \frac{T_{\text{D3}}}{N_{\text{D3}}} \right)^{\frac{1}{4}}, \quad \tilde{T}^4 = \frac{3\sqrt{3}}{2\sqrt{5}} \hat{T}^4. \quad (2.75)$$

The solution $(r_{\pm}(\mathbf{k}); \Omega_{\pm}(\mathbf{k}))$ to the D3 giant graviton EOM takes the form

$$\hat{\Omega}_{\pm}(\mathbf{k}) = \sqrt{\frac{8\mathbf{k}^2(1 + \Delta_{\pm}) + 1 - 8\Delta_{\pm}}{1 - 8\Delta_{\pm}}}, \quad \hat{r}(\mathbf{k}) = \frac{3\mathbf{k}}{\sqrt{1 - 8\Delta_{\pm}} \Omega_{\pm}(\mathbf{k})}, \quad (2.76)$$

where $\Delta_{\pm} \equiv \Delta_{\pm}(\phi(\mathbf{k}))$ is defined in (C.23) (with $\omega = 0$) and where $\phi = \phi(\mathbf{k})$ is a function of \mathbf{k} through the charge quantization equation (2.39). Using the expressions in Eqs. (2.42) with $\mathcal{W} = 0$ and $\mathbf{k} = |k_{\text{w.v.}}|$, we can compute the (off-shell) thermodynamics of the configuration. The parameterization (2.76) now lets us compute the on-shell thermodynamics for the non-spinning thermal giant graviton on the S^5 of $\text{AdS}_5 \times S^5$. In Fig. 2.4 we have depicted (\hat{r}, \mathbf{F}) as well as (\hat{r}, \mathbf{J}) for various values of \hat{T} (similar plot for the rest of the thermodynamics variables and the angular velocity Ω can be made but have been omitted here). Note that the corresponding plots for the energy in the extremal case were given in Fig. 2.1. We now describe some of the salient features of the solution space. At the upper bound in (2.74), we have $r = L$ and $\hat{\Omega}_{-} \geq 1$ and $\hat{\Omega}_{+} \leq 3$ where the equal sign applies at extremality. Furthermore, we observe that the values of r are restricted to $0 \leq r_{\text{min}} \leq r \leq L$, and r_{min} approaches L as the maximum temperature is approached. The minimal size thermal giant graviton r_{min} lies on the lower branch (the black curve in Fig. 2.4), which curves back to meet the upper branch (the grey curve) in the point corresponding to the lower bound $\mathbf{k} = \tilde{T}$.¹⁴

That the minimal size of the giant graviton is greater than zero is an important consequence of the finite-temperature physics of the giant graviton. For the extremal giant graviton the two branches meet in the singular solution $r = 0$ which in turn corresponds to the graviton particle with same angular momentum. What we see at finite temperature is that: a) there is a minimal possible size r_{min} of the giant graviton and b) unlike in the extremal case, it is possible to move in the solution space from one branch to another

¹⁴Note that $r_{-}(\mathbf{k}) \rightarrow r_{+}(\mathbf{k})$ for $\mathbf{k} \rightarrow \tilde{T}$ since $\phi(\mathbf{k}) \rightarrow 4/9$ so $\mathcal{D}(\phi(\mathbf{k})) \rightarrow 0$ for $\mathbf{k} \rightarrow \tilde{T}$ (cf. (C.24)).

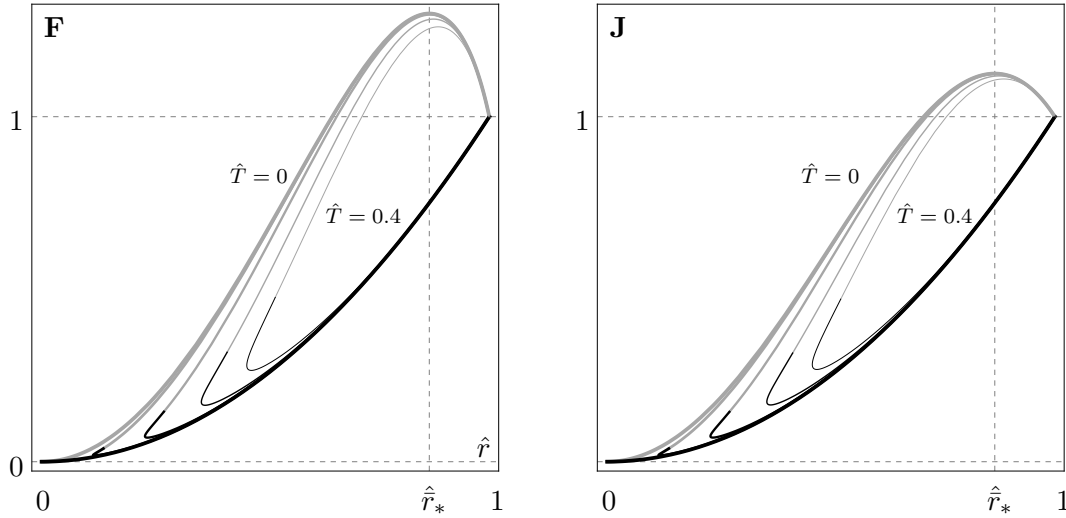


Figure 2.4: \mathbf{F} versus \hat{r} (left plot) and versus \mathbf{J} (right plot) for the two solution branches of thermal giant gravitons.

since the meeting point of the two branches at \tilde{r} is not a singular solution. Note that the fact that the thermal giant graviton attains a minimal possible size has an analogue in the thermal BIon as well as in the thermal Wilson line cases studied in [48; 49; 54].

2.5.2 Stability

To address the stability we turn our attention to the on-shell free energy plotted in the Fig. 2.4. Just as in the extremal case where the maximal (minimal) energy E is obtained for maximal (minimal) angular momentum J we see that in the thermal case the maximal (minimal) free energy F is obtained for maximal (minimal) angular momentum. This can be seen by doing a (F, J) plot, however, the plot looks very similar to 2.2 for the entire range of temperatures and has thus been omitted. Comparison of the free energies then shows that the lower branch is expected to be stable for $r_{J_{\min}} \leq r \leq L$ (with $\mathbf{J}_{\min} \leq \mathbf{J} \leq 1$) and the upper branch for $r_{J_{\max}} \leq r \leq 1$ (with $1 \leq \mathbf{J} \leq \mathbf{J}_{\max}$). This is entirely in parallel with the stability properties of the extremal giant graviton (see Sec. 2.2.2), the difference being that as a consequence of the finite temperature, a part of the lower branch has become unstable and there is a minimum angular momentum. Note that it follows that the minimum size *stable* thermal giant graviton is thus $r_{J_{\min}}$, which is greater than r_{\min} (for which the solution is unstable). We also see that the point where the branches meet in \tilde{r} is always in the unstable region. On the other hand, the branches also meet in $r = L$, but for different values of Ω . The fact that J_{\min} and J_{\max} denote the onset of instability in the lower and upper branch respectively is further corroborated by looking at the turning points in a $(\mathbf{J}, \hat{\Omega})$ plot, which is shown in Fig. 2.5. We see that these boundaries of stability occur precisely at the turning points where $dJ/d\Omega = 0$, in accord with expectations based on the Poincaré turning point method (see e.g. [99] and references therein).

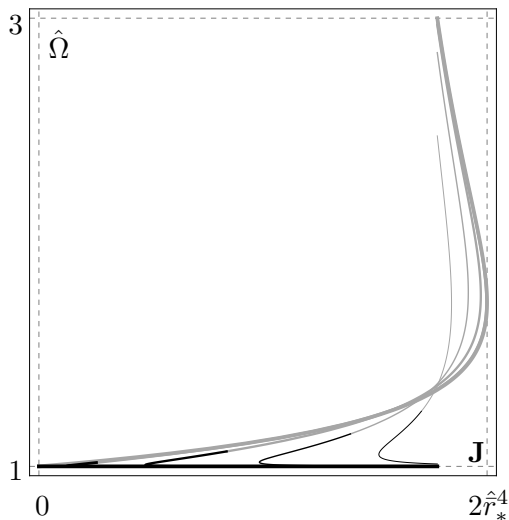


Figure 2.5: $\hat{\Omega}$ versus \mathbf{J} for the two solution branches of thermal giant gravitons.

Maximal and minimal angular momentum

We also derive the low temperature limit expression for the maximal and minimal value of the angular momentum, found on the upper and lower branch respectively. The largest value of \mathbf{J} is exactly attained on the upper branch where it goes from stable to unstable. So $\mathbf{J}_{\max} = \mathbf{J}_+(r_*)$. Using this, we find

$$\mathbf{J}_{\max} = \frac{9}{8} - \frac{\sqrt{3}}{2} \hat{T}^4 + \mathcal{O}(\hat{T}^8) \quad (2.77)$$

The minimal value of \mathbf{J} is attained close to $r = 0$. This means that an analytical expression for \mathbf{J}_{\min} is not obtainable from the low temperature expansion (as it is only valid for $\hat{r} \gg \hat{T}$). However, we expect the following behavior for small \hat{T}

$$\mathbf{J}_{\min} \sim \hat{T}^\beta \quad (2.78)$$

It is then possible to do a fit of the numerically obtained values for J_{\min} . Doing this one finds that $\beta \approx 1.89$.

2.6 Null-wave giant graviton

In this section we examine a specific solution of Eq. (2.33), consisting of a zero temperature excitation of the usual extremal giant graviton obtained by taking a particular limit for which the fluid velocity becomes null.¹⁵ Motivated by this configuration we then write down an action for null-wave branes and show that the result obtained from varying this action and approaching zero temperature in a non-trivial way leads to the same solution. Finally, as an application of this action we obtain the ‘dual’ version of this configuration expanded into AdS_m .

¹⁵A similar null-wave on the M2-M5 brane intersection was considered in Ref. [52] using blackfold methods.

2.6.1 Extremal giant graviton solution with null-wave

Here we show that the thermal giant graviton solution obtained in Secs. 2.3 and 2.4 admits a zero-temperature limit which can be regarded as a null-wave excitation of the extremal giant graviton presented in Sec. 2.3.3. This null-wave limit consists in approaching extremality by sending $\phi \rightarrow 0$ such that

$$\phi \mathbf{k}^{-1} = \mathbf{P} \mathbf{k} \quad , \quad \mathbf{k} \rightarrow 0 \quad , \quad (2.79)$$

while keeping $\mathbf{P} \geq 0$ and the charge $Q_{(n-2)}$ constant. Note that this zero-temperature limit is consistent with (2.36). In this particular double scaling limit, the EOM (2.29) takes the form

$$(n-2)\mathcal{W}^2 + \mathcal{V}^2 - \mathcal{W}^2 \mathbf{P} (\mathcal{W}^2 - \mathcal{V}^2) - (n-1)\mathcal{V}\mathcal{W} = 0 \quad , \quad (2.80)$$

with the corresponding solutions

$$\mathcal{V}_{\pm} = \left(\frac{n-1 \pm |n-3-2\mathbf{P}\mathcal{W}^2|}{2(1+\mathbf{P}\mathcal{W}^2)} \right) \mathcal{W} \quad . \quad (2.81)$$

Note that the solution to (2.81) can also be obtained by taking the appropriate limit (2.79) in the general solution (2.33). As in the extremal case of Sec. 2.3.3, this results in two branches of solutions

$$\hat{\Omega}_- = \hat{\omega} \quad , \quad \hat{\Omega}_+ = \left(\frac{n-1}{1+\mathbf{P}\mathcal{W}^2} - 1 \right) \hat{\omega} \quad . \quad (2.82)$$

The off-shell ‘‘thermo’’-dynamic properties associated with these configurations are obtained from Eqs. (2.31) together with (2.79) and take the following form:

$$\mathbf{E} = \left(\frac{1 + \mathbf{P}\hat{\omega}^2\hat{r}^2}{\hat{\omega}} \right) \hat{r}^{n-3} \quad , \quad \mathbf{J} = \mathbf{E} \hat{\rho} \sqrt{1 - \hat{\omega}^2\hat{r}^2} + \hat{r}^{n-1} \quad , \quad \mathcal{S}_i = \left(\frac{2\mathbf{P}\hat{\omega}^2}{n-1} \right) \hat{r}^{n+1} \quad . \quad (2.83)$$

Contrary to the usual 1/2-BPS case presented in Sec. 2.3.3, we see that the null-wave giant graviton carries spin along the Cartan directions of the worldvolume, which vanishes when the momentum density \mathbf{P} vanishes. Also note that $\hat{T}\mathbf{S} = 0$ for the null-wave configuration. The null-wave excitation of the extremal giant graviton therefore excites $(n-1)/2$ new quantum numbers of equal magnitude. We will now analyze the thermodynamic properties and stability of both branches (2.82) and compare the results with the extremal giant graviton.

Lower branch: For the branch of solutions $\hat{\Omega}_-$, the requirement that $\mathbf{k} = 0$ implies that $\hat{\Omega}_- = \hat{\omega} = 1$. In fact, this means that not only the center of mass is moving at the speed of light but also all points in the expanded brane. This was not possible for the extremal graviton solution of Sec. 2.3.3 as there all brane points are required to move along a timelike Killing vector field. In this case, using Eq. (2.83), the on-shell thermodynamic quantities take the form

$$\mathbf{E} = \bar{\mathbf{E}}_- + \frac{\mathcal{S}}{\hat{r}^2} \quad , \quad \mathbf{J} = \bar{\mathbf{J}}_- + \left(\frac{\hat{\rho}}{\hat{r}} \right)^2 \mathcal{S} \quad , \quad (2.84)$$

where $\bar{\mathbf{E}}_- = \bar{\mathbf{J}}_-$ denote the energy and angular momentum of the lower branch extremal giant graviton given in Sec. 2.3.3 and \mathcal{S} denotes the sum of all the spins, i.e.,

$$\mathcal{S} = \sum_i \mathcal{S}_i = \mathbf{P} \hat{r}^{n+1} . \quad (2.85)$$

These relations are of particular interest as they indeed show that this configuration can be seen as a zero-temperature excitation of the lower branch of the extremal giant graviton. In Fig. 2.6 we have plotted E versus \hat{r} and the angular momentum \mathbf{J} on the lower branch. Furthermore, from (2.84) we obtain the relation

$$\mathbf{E} = \mathbf{J} + \mathcal{S} . \quad (2.86)$$

This relation is interesting in its own right as it shows, in the case of $\text{AdS}_5 \times S^5$, that we are dealing with a configuration that exhibits a 1/8-BPS spectrum since it satisfies the expected BPS bound

$$\text{D3: } \mathbf{E} = \mathbf{J} + \mathcal{S}_1 + \mathcal{S}_2 . \quad (2.87)$$

Similarly, in the case of $\text{AdS}_4 \times S^7$ the configuration exhibits a 1/16-BPS spectrum

$$\text{M5: } \mathbf{E} = \mathbf{J} + \mathcal{S}_1 + \mathcal{S}_2 + \mathcal{S}_3 . \quad (2.88)$$

Notice that if the giant graviton has maximal size, $\hat{r} = 1$, the BPS relation (2.86) simplifies to $\mathbf{E} = \mathbf{J} + \mathbf{P}$.

Upper branch and comparison between branches: For the upper branch solution Ω_+ , one can also solve the constraint $\mathbf{k} = 0$. The resulting expression is a cubic equation in ω whose solution can easily be obtained, but is rather complicated, and will not be presented here. Nevertheless, in the limit in which \mathbf{P} vanishes the constraint $\mathbf{k} = 0$ yields the value $\hat{\omega} = \hat{\Omega}_+ / (n-2)$, which when inserted into (2.83) gives rise to the thermodynamic properties of the upper branch of the extremal giant graviton as given in Sec. 2.3.3. The upper branch solution in (2.82) exhibits a generically non-BPS spectrum for all values of \mathbf{P} . This is clear when looking at Fig. 2.6. Also note that for all \mathbf{P} the two branches meet at $\hat{r} = 1$ and therefore the charges \mathbf{E} and \mathbf{J} are equal at maximum size. The plots for the upper branch are obtained by solving the constraint $\mathbf{k} = 0$ for the upper branch and obtaining $\hat{r}(\mathbf{P})$. The bound on \hat{r} , i.e., $0 < \hat{r} \leq 1$ implies the bound $1/3 \leq \hat{\omega} \leq 1$ on $\hat{\omega}$. These bounds in turn imply that at maximality the total spin \mathcal{S} is equal for both branches. In contrast with the thermal spinning case analyzed in Sec. 2.4 the spin of these null-wave giant graviton configurations is not bounded from above and from Eqs. (2.84) neither is the energy nor the orbital angular momentum

Stability: To study the stability of the solution branches (2.82) we employ the method used in Sec. 2.4.2 which consists in considering the thermodynamic ensemble parametrized by the size r , the conserved orbital angular momentum \mathbf{J} , the conserved spins \mathcal{S}_i , and the

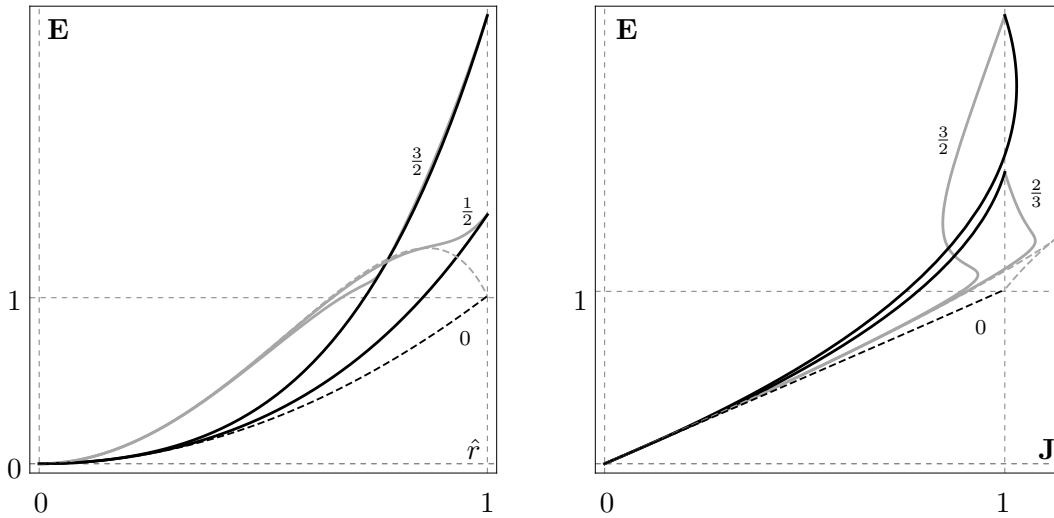


Figure 2.6: The energy \mathbf{E} versus \hat{r} (left) and \mathbf{J} (right) for the upper (grey) and lower (black) branch of the null-wave excited giant graviton on $\text{AdS}_5 \times S^5$ with the respective values of P indicated. The dashed curves correspond to the extremal giant graviton with no null-wave, $P = 0$.

conserved total charge $Q_{(n-2)}$, and looking for the configurations that minimize the energy \mathbf{E} . A small off-shell perturbation along r of the angular velocity ω and the momentum density P , with \mathbf{J} , \mathcal{S}_i and $Q_{(n-2)}$ held fixed, allows us to determine the second derivative of \mathbf{E} with respect to r . For the lower branch this takes the simple form

$$\mathbf{E}_{(2)}^- = \frac{(n-3-2P\hat{r}^2)^2}{2\hat{\rho}^2(1+P\hat{r}^2)} \hat{r}^{n-3}. \quad (2.89)$$

In the case $P = 0$ we recover the second variation of the energy for the lower branch extremal giant graviton found in (2.65) (with $\phi_0 = 0$). Since $P \geq 0$, we have that $\mathbf{E}_{(2)}^- > 0$ for the entire range of r . This means that the lower branch of the null-wave giant graviton is stable for all $0 \leq r \leq 1$ as expected for BPS configurations. A similar analysis can be performed for the upper branch. By expanding out the extremal ($P = 0$) solution one shows that as the null-wave spin is increased from 0, the threshold value r_* increases (from \hat{r}_* at $P = 0$). Essentially, as one increases the spin, the range of stability of the upper branch is decreased.

2.6.2 An action for null-wave branes

In this section we obtain an action for null-wave branes by taking an appropriate limit of the action (2.27). We begin by stressing that the extremal limit of (2.27) that yields the DBI action multiplied by a factor of $N_{(n-2)}$ is obtained by sending $r_0 \rightarrow 0$ and $\alpha \rightarrow \infty$ such that the total charge $Q_{(n-2)}$ is held constant. Equivalently, using the parameter ϕ introduced in Sec. 2.3.2, the same limit is obtained by sending $\phi \rightarrow 0$. However, we are interested in near-extremal situations for which ϕ is taken to be small but non-zero. In these cases, the fluid pressure approaches $P \rightarrow -Q_{(n-2)}(1 - \phi/(n-1))$. Using now the low

temperature expansion obtained in Eqs. (2.53)-(2.54) as $\phi \rightarrow 0$, the action (2.27) reduces to¹⁶

$$I = -Q_{(n-2)} \int_{\mathcal{W}_{n-1}} d^{n-1} \sigma \sqrt{-\gamma} \left[1 - \frac{f_n}{n-1} \left(\frac{\hat{T}}{\mathbf{k}} \right)^{n-1} \right] + \int_{\mathcal{W}_{n-1}} \mathbb{P}[A_{(n-1)}] . \quad (2.90)$$

In the case for which the temperature is taken to zero, the action (2.90) reduces to $N_{(n-2)}$ times the DBI action plus the Wess-Zumino contribution. When the temperature is non-zero, it accounts for near-extremal excitations of ground state configurations. Noting that by definition $\mathbf{k} = |-\gamma_{ab} \mathbf{k}^a \mathbf{k}^b|^{\frac{1}{2}}$, the worldvolume stress tensor of the excited state can be obtained from (2.90) in the usual way and takes the form (cf. Eq. (1.86))

$$T^{ab} = Q_{(n-2)} f_n \left(\frac{\hat{T}}{\mathbf{k}} \right)^{n-1} \left(u^a u^b + \frac{1}{n-1} \gamma^{ab} \right) - Q_{(n-2)} \gamma^{ab} . \quad (2.91)$$

From the form of the worldvolume stress tensor it is clear that as $\hat{T} \rightarrow 0$ we obtain the known result for Dirac branes at zero temperature.

As noted in Sec. 1.5.5, the expression (2.91) suggests the existence of a scaling limit as $\hat{T} \rightarrow 0$ different from the usual extremal limit. This is obtained by sending $\hat{T} \rightarrow 0$ while the fluid velocity approaches the speed of light $\mathbf{k} \rightarrow 0$ such that

$$\sqrt{f_n} (\hat{T}/\mathbf{k})^{\frac{n-1}{2}} u^a \rightarrow \sqrt{\mathbf{P}} l^a , \quad (2.92)$$

for constant \mathbf{P} . Here we have introduced a null-vector l^a satisfying $l^a l_a = 0$. In this case, the worldvolume stress tensor of the excitation is given by

$$T^{ab} = \mathcal{K} l^a l^b - Q_{(n-2)} \gamma^{ab} , \quad (2.93)$$

where we have introduced the momentum density \mathcal{K} via the relation $\mathcal{K} = Q_{(n-2)} \mathbf{P}$.¹⁷ The worldvolume stress tensor (2.93) is that of a null-wave: a zero-temperature excitation of the Dirac brane worldvolume stress tensor carrying a conserved momentum current along a null-vector l^a . When the momentum density \mathcal{K} vanishes, one obtains the result for Dirac branes. For the case of non-zero \mathcal{K} , the near-extremal action (2.90) can be exchanged by a simpler one for which the variational principle holds the momentum density \mathcal{K} constant instead of the temperature T ,¹⁸

$$I = -Q_{(n-2)} \int_{\mathcal{W}_{n-1}} d^{n-1} \sigma \sqrt{-\gamma} \left(1 + \frac{1}{2} \mathbf{P} \mathbf{k}^2 \right) + \int_{\mathcal{W}_{n-1}} \mathbb{P}[A_{(n-1)}] . \quad (2.94)$$

¹⁶We have written the action (2.90) adapted to the background space-time and configurations studied here but we stress that this action is easily generalized for any other background and for the large class of branes studied in [37].

¹⁷The worldvolume stress tensor (2.93) can also be obtained by taking the equivalent limit $r_0 \rightarrow 0$ and $\mathbf{k} \rightarrow 0$ such that $(\Omega_{(n+1)} n r_0^n)^{\frac{1}{2}} \mathbf{k}^a = (16\pi G \mathcal{K})^{\frac{1}{2}} \mathbf{k} l^a$ [37].

¹⁸Note that the variational principle also holds the charge $Q_{(n-2)}$ constant since $D_a Q_{(n-2)} = 0$ and hence \mathbf{P} is also held constant. Further, in order to write (2.94) we have used the fact that the variation of $\delta\phi$ is given by $\delta\phi = -(1/\gamma_m) \phi \delta \log \mathbf{k}$. Furthermore, the action (2.94) is general for all p -branes studied in [37] and for any background space-time if one simply replaces n by $p+2$.

The worldvolume stress tensor (2.93) then follows from (2.94) by first obtaining it for general \mathbf{k} and afterwards taking the limit $\mathbf{k} \rightarrow 0$. The EOM that follow by varying (2.94) take the usual form

$$D_a T^{ab} = 0 \quad , \quad T^{ab} K_{ab}{}^\mu = \frac{1}{(n-1)!} \perp^\mu{}_\nu F^{\nu\rho_1\dots\rho_{n-1}} J_{\rho_1\dots\rho_{n-1}} \quad , \quad (2.95)$$

where T_{ab} now is the null-wave stress tensor. Note that the first equation in (2.95) is trivially satisfied as a consequence of stationarity [42] and the only non-trivial dynamics are encoded in the second equation of (2.95). When introducing (2.93) into (2.95) leads to Eq. (2.80) for the particular embedding geometry of the giant graviton.

Conserved momentum current and spin

The EOM (2.95) that arise by varying the action (2.94) express conservation of the worldvolume stress tensor (2.93) along worldvolume directions and balance of mechanical forces along transverse directions to the worldvolume. However, the first equation in (2.95) now splits into two equations

$$l^b D_b l^a = 0 \quad , \quad D_a (\mathcal{K} l^a) = 0 \quad . \quad (2.96)$$

The first equation above requires the null vector l^a to generate geodesics along the worldvolume while the second equation expresses the conservation of the momentum current. The momentum current can be integrated in order to obtain a conserved momentum charge associated with the near-extremal configuration. However this charge is not independent and is related to the existence of angular momenta along worldvolume directions (spin) of the configuration. Indeed, for the configurations presented in the previous sections, the spin along the worldvolume Killing vector field χ_i can be evaluated using the expression

$$\mathcal{S}_i = \mathcal{K} \int_{\mathcal{B}_{n-2}} d^{n-2} \sigma \sqrt{-\gamma} l_a \chi_i^a \quad , \quad (2.97)$$

where \mathcal{B}_{n-2} is the spatial part of the worldvolume. If the momentum density \mathcal{K} vanishes, the configuration carries no spin. Using (2.97) results in the value for the spin written in (2.83). The energy and angular momentum along transverse directions to the worldvolume can be evaluated using the formulae given in [1] together with the worldvolume stress tensor (2.93).

2.7 Thermal giant gravitons on AdS_m

Here we obtain the ‘dual’ version of the giant graviton configuration of Sec. 2.6.1, namely that of $N_{(m-2)}$ M/D($m-2$)-branes expanded into the S^{m-2} sphere of the AdS_m part of $\text{AdS}_m \times S^n$ (but still moving on the S^1 inside the S^n). For simplicity we will consider the non-spinning configuration and only consider intrinsic spin in the last section where we examine the null-wave limit. We will start by briefly reviewing the corresponding DBI solution originally considered in [26; 27]

2.7.1 Extremal giant gravitons on AdS_m

We parameterize the AdS_m metric according to

$$ds^2 = -f^2 dt^2 + f^{-2} dy^2 + y^2 d\Omega_{(m-2)}^2, \quad f(y) = \frac{1}{\tilde{L}} \sqrt{\tilde{L}^2 + y^2}, \quad (2.98)$$

where \tilde{L} is related to L through (2.2) and the metric on the $(m-2)$ -sphere is parametrized by coordinates $\alpha^1, \dots, \alpha^{m-2}$. In these coordinates the background gauge field with support on the $S^{(m-2)}$ takes the form

$$A_{(m-1)} = -\frac{y^{m-1}}{\tilde{L}} dt \wedge \text{Vol}_{(m-2)}. \quad (2.99)$$

The dual giant graviton configuration now spans the surface $y = r$ while moving on the equator of the S^n (as a point) with constant angular velocity Ω . In detail, we use the embedding

$$y = r, \quad t = \tau, \quad \phi = \beta_n \Omega \tau, \quad \alpha^1 = \sigma^1, \dots, \alpha^{m-2} = \sigma^{m-2}. \quad (2.100)$$

The induced metric on the worldvolume takes the same form as the in (2.9), but now with

$$\mathbf{k} = \sqrt{R_0^2 - \Omega^2 L^2}, \quad (2.101)$$

where the (gravitational) redshift factor R_0 is given by $R_0 = f(r)$. Notice that \mathbf{k} is not bounded from above as was case of the giant graviton expanded in S^n . The DBI Lagrangian now takes the form¹⁹

$$\mathcal{L} = \Omega_{(m-2)} T_{(m-2)} r^{m-2} \left(-\mathbf{k} + \frac{r}{\tilde{L}} \right). \quad (2.102)$$

It is now straightforward to derive the resulting EOM and conserved quantities. Just as for the giant graviton expanded into the S^n , we find two branches of solutions for the giant graviton on AdS_m ,

$$\Omega_- = \frac{1}{L}, \quad \Omega_+ = \frac{1}{L} \frac{\sqrt{(m-2)^2 \tilde{L}^2 + (m-1)(m-3)r^2}}{(m-2)\tilde{L}}, \quad (2.103)$$

using the relation (2.2) between L and \tilde{L} . We notice that the upper branch Ω_+ is unbounded since the size of the giant graviton r is unbounded (which is not true for its S^n counterpart). It is now possible to compute the energy E and angular momentum J . In particular on the lower branch the configuration carries the same quantum numbers as its S^n cousin,

$$\bar{\mathbf{E}}_- = \bar{\mathbf{J}}_- = r^{m-3}. \quad (2.104)$$

Moreover, analysis of the stability properties of the two branches à la Sec. 2.2.2 shows that the lower branch is stable while the now the entire upper branch is unstable. Finally it can be shown that the lower branch is 1/2 BPS (in accordance with (2.104)) and that the entire upper branch is not BPS.

¹⁹Notice that in accord with [26] we here consider the anti-brane i.e. the sign on the term coming from the WZ term has been reversed.

2.7.2 Construction of thermal giant graviton on AdS_m

Here we consider the non-spinning thermal version of the giant graviton on AdS_m. The technology developed for the canonical giant graviton of Sec. 2.3 carries directly on to the AdS giant graviton, with the only differences being the geometrical setup and the introduction of the non-trivial redshift factor R_0 . The action (1.119) yields the following Euclidean action for the configuration

$$\beta I_E = -\Omega_{(m-2)} r^{m-2} \left(\mathbf{k}P + \frac{rQ_{(m-2)}}{\tilde{L}} \right), \quad (2.105)$$

where we again note that $Q_{(m-2)}$ denotes the anti-brane charge. Notice that the thermodynamics now is that of a black $(m-2)$ -brane of co-dimension $n-1$. The thermodynamics is therefore simply obtained by substituting $m \rightarrow n$ in the expressions (2.21), (2.22), (2.23). Moreover the charge quantization condition for the $(m-2)$ -branes can be written in the form (2.36), again with the substitution $m \rightarrow n$. Varying the action (2.105) wrt. the size of the configuration r , we obtain the following EOM

$$(m-2)\tilde{L}^2 \mathbf{k}^2 + r^2(1 - \mathcal{R}_1) + (m-1)\tilde{L}kr\mathcal{R}_2 = 0 \quad (2.106)$$

We briefly examine the solution space for the thermal D3 giant graviton on AdS₅ in the next section. In Sec. 2.7.4 we compute the solution and associated thermodynamics in the low temperature limit for general (m, n) .

Using Eqs. (2.42) we can now compute the (in general off-shell) expressions for the energy E , angular momentum J , and entropy of the configuration. We obtain

$$J = \frac{\Omega \Omega_{(m-2)} r^{m-2} \varrho}{\mathbf{k}}, \quad E = \frac{R_0^2 J}{\Omega} - \frac{\Omega_{(m-2)} Q_{(m-2)} r^{m-1}}{\tilde{L}}, \quad S = \frac{1}{T} (n-1) \Omega_{(m-2)} s \mathbf{k} r^{m-2}. \quad (2.107)$$

In parallel with (2.41), we define $\hat{r} \equiv r/\tilde{L}$, $\hat{\Omega} = L\Omega$, and the dimensionless rescaled variables

$$\mathbf{J} = \frac{J}{N_{(m-2)} T_{(m-2)} \tilde{L}^{m-2} L}, \quad \mathbf{E} = \frac{E}{N_{(m-2)} T_{(m-2)} \tilde{L}^{m-2}}, \quad \mathbf{S} = \frac{T_{\text{stat}} S}{N_{(m-2)} T_{(m-2)} \tilde{L}^{m-2}}. \quad (2.108)$$

In terms of these variables, the thermodynamics takes the form

$$\mathbf{J} = \frac{\hat{\Omega}}{\mathbf{k} \sqrt{1-\phi}} \left(1 + \frac{\phi}{m-1} \right) \hat{r}^{m-2}, \quad \mathbf{E} = \frac{1 + \hat{r}^2}{\hat{\Omega}} \mathbf{J} - \hat{r}^{m-1}, \quad \hat{T} \mathbf{S} = \frac{\phi \mathbf{k}}{\sqrt{1-\phi}} \hat{r}^{m-2}. \quad (2.109)$$

2.7.3 Thermal giant graviton on AdS₅ - finite temperature effects

Analogously to the S^5 case examined in Sec. 2.5, we find from (2.106) (note that now $L = \tilde{L}$)

$$\hat{r}_{\pm}(\mathbf{k}) = \frac{3\mathbf{k}}{\sqrt{1-8\Delta_{\pm}}}, \quad (2.110)$$

where Ω_{\pm} takes the same form as for the S^5 case given by Eq. (2.76). We note that, as opposed to the non-spinning configuration expanded on S^5 whose maximal temperature

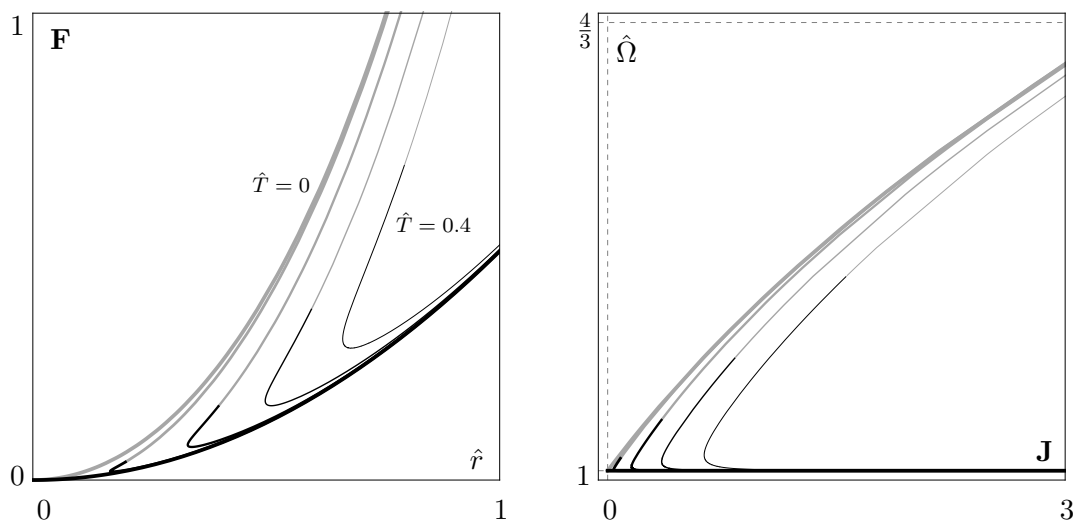


Figure 2.7: Left: The free energy \mathbf{F} versus $\hat{r} \equiv r/\tilde{L}$ for the lower (black) and upper (grey) solution branches of the extremal giant graviton on AdS_5 , respectively. Right: The angular velocity versus the angular momentum \mathbf{J} for the two solution branches.

is given by T_{max} , the maximal temperature of the giant graviton configuration on AdS_m is simply T_{stat} . Using the obtained parametrization of the solution space, we obtain the on-shell thermodynamics of the configuration. In the left plot of Fig. 2.7 we have plotted the rescaled free energy \mathbf{F} as a function of \hat{r} . As with the giant graviton on S^n , we see that there is a minimal size of the thermal configuration. However, as already noted, there is no upper bound on the radius of the configuration. Moreover, in the right plot of Fig. 2.7, we have plotted the angular velocity Ω versus the angular momentum \mathbf{J} . We see that as in the S^5 case, the angular momentum of the thermal giant graviton on AdS_5 is bounded from below by a non-zero value. However, as with the size r , there is no upper bound on \mathbf{J} . In accordance with the arguments presented in 2.5, we see that when turning on temperature, the lowermost part of the lower branch becomes unstable (at the turning point) while the entire upper branch stays unstable at finite temperature.

2.7.4 Low temperature expansion

Here we work out the low temperature solution to the extrinsic equation on the lower branch, which is the most interesting as the entire upper branch is unstable. In the low temperature limit, the solution to the charge quantization equation is given by

$$\phi = \phi_0 \mathbf{k}^{m-1}, \quad \phi_0 = f_m \hat{T}^{m-1}, \quad (2.111)$$

where f_m is given in Eq. (2.56). As for the giant graviton on S^n , we find that the angular velocity on the lower branch is unchanged to leading order,

$$\Omega_- = 1 + \mathcal{O}(\phi_0^2). \quad (2.112)$$

Also we see that the expansion is valid as long as $\hat{T} \ll r$. We can now compute the low temperature thermodynamics. We find

$$\begin{aligned} \mathbf{E}_- &\simeq \bar{\mathbf{E}}_- + \frac{m-2}{m-1} \left(\frac{1+\hat{r}^2}{\hat{r}^2} \right) \phi_0, & \mathbf{J} &\simeq \bar{\mathbf{J}}_- + \frac{m-2}{m-1} \frac{\phi_0}{\hat{r}^2}, \\ \hat{T}\mathbf{S}_- &\simeq \phi_0, & \mathbf{F}_- &\simeq \bar{\mathbf{E}}_- + \left(\frac{m-2-\hat{r}^2}{m-1} \right) \frac{\phi_0}{\hat{r}^2}. \end{aligned} \quad (2.113)$$

We therefore obtain the following relation between \mathbf{F} and \mathbf{J} on the lower branch

$$\mathbf{F} = \mathbf{J} - \frac{\phi_0}{m-1}. \quad (2.114)$$

This is the same relation as was found on the lower branch of the giant graviton on S^n (with the substitution $m \rightarrow n$). Correspondingly we find the same relations (2.62) on the lower branch of the giant graviton on AdS_m . Also the relations (2.63) are found to hold in the AdS case. It is therefore interesting to note that the leading order thermal correction to the free energy as a function of J and the ratio J/E takes the same form on the lower branches of the thermal giant graviton on S^n and AdS_m , respectively.

2.7.5 Null-wave giant graviton expanded into AdS_m

The null-wave action (2.94) takes the simple form

$$\beta I_E = Q_{(n-2)} \Omega_{(m-2)} r^{m-2} \left[|k_{\text{w.v.}}| \left(1 + \frac{1}{2} \mathbf{P} \mathbf{k}^2 \right) - \frac{r}{\tilde{L}} \right]. \quad (2.115)$$

Explicit variation and taking the limit $\mathbf{k} \rightarrow 0$ leads to the EOM

$$(m-2)\mathcal{W}^2 \tilde{L}^2 + r^2 + \mathcal{W}^2 \mathbf{P} (1 - \omega^2 \tilde{L}^2) r^2 - (m-1)\mathcal{W} \tilde{L} r = 0. \quad (2.116)$$

This equation admits two branches of solutions as its ‘dual’ version in Sec. 2.6.1. However, the upper branch of solutions is less interesting as it is never BPS. This is in fact the same feature observed for the upper branch of the usual $\frac{1}{2}$ -BPS giant graviton [1]. Our focus will be on the lower branch of solutions which takes the simple form of

$$\hat{\Omega}_- = 1, \quad \hat{\omega} = 1, \quad (2.117)$$

where we have rescaled ω such that $\hat{\omega} = \omega \tilde{L}$.

Thermodynamic properties and stability: Using the formulae for thermodynamic quantities Eq. (2.97) for the spin of the configuration we obtain the following off-shell expressions

$$\mathbf{E} = \frac{1}{\hat{\omega}} R_0^2 (1 + \mathbf{P} \hat{\omega}^2 \hat{r}^2) \hat{r}^{m-3} - \hat{r}^{m-1}, \quad \hat{T}\mathbf{S} = 0, \quad (2.118)$$

$$\mathbf{J} = \frac{1}{\hat{\omega}} \sqrt{1 + \hat{r}^2 (1 - \hat{\omega}^2)} (1 + \mathbf{P} \hat{\omega}^2 \hat{r}^2) \hat{r}^{m-3}, \quad \mathcal{S}_i = \frac{2}{n-1} \mathbf{P} \hat{\omega}^2 \hat{r}^{m+1}. \quad (2.119)$$

For the specific solution (2.117) one can find the relations

$$\mathbf{E} = \bar{\mathbf{E}}_- + \left(\frac{1 + \hat{r}^2}{r^2} \right) \mathbf{S} \quad , \quad \bar{\mathbf{J}} = \mathbf{J}_- + \frac{\mathbf{S}}{\hat{r}^2} \quad , \quad (2.120)$$

implying the BPS bound $\mathbf{E} = \mathbf{J} + \mathbf{S}$, where \mathbf{S} is the sum over all the $(n - 1)/2$ spins. As the spin is increased both the energy and angular momentum increase for fixed \hat{r} . The stability properties can be analyzed using the method outlined in Sec. 2.6.1. In this case we find for the second variation of the energy on the lower branch

$$\mathbf{E}_{(2)}^- = \frac{1}{2} \frac{(m - 3 - 2\mathbf{P}\hat{r}^2)^2}{(1 + \hat{r}^2)(1 + \mathbf{P}\hat{r}^2)} \hat{r}^{m-3} \quad . \quad (2.121)$$

Therefore we see that these configurations are always stable for any value of r as expected for BPS configurations.

3 | Hydrodynamics of charged black branes

3.1 Introduction

In this chapter we examine hydrodynamic fluctuations of asymptotically flat charged black branes in the blackfold approach. The analysis was first presented in the paper [3] and provides a non-trivial generalization of Ref. [38] to charged branes. In detail, we consider long-wavelength fluctuations around the black brane solution of Einstein-Maxwell gravity (which we shall dub the Reissner-Nordström black brane) following the ideas outlined in Sec. 1.3.2. We solve the full set of Einstein/Maxwell equations to first order in the hydro derivative expansion and compute the first order dissipative corrections to the effective stress tensor and charge current. This provides the charge generalizations of the shear and bulk viscosities along with a charge diffusion transport coefficient not present in the neutral case. Although expected on physical grounds, the analysis proves that the hydrodynamic effective blackfold description extends to the charged regime. In particular, we show that the perturbed event horizon stays regular and that the solution is completely determined once the boundary conditions (horizon regularity and asymptotic flatness) are imposed (after a suitable gauge fixing).

As explained in Sec. 1.3.2, the Gregory-Laflamme (GL) instability [100; 101] of the neutral black string/brane is identified with the unstable sound mode of the effective blackfold fluid. The instability is already seen to leading order in the effective description i.e. at the perfect fluid level [57] where leading order dispersion relation yields an imaginary speed of sound. By computing the first order derivative corrections to the neutral black brane solution, and subsequently extracting the first order transport coefficients of the effective fluid, Ref. [38] was able to obtain refinement of the dispersion relation of the GL instability which showed remarkable agreement with numerical data. In addition, the agreement was found to be improving with the number of transverse dimensions (suggesting that gravity simplifies in the $D \rightarrow \infty$ limit, see also [102; 103]). Carrying out a similar exercise for the charged black brane is interesting for many reasons. First, charged branes play an important role in string theory and supergravity and methods for studying their stability properties (other than numerical) are interesting for obvious reasons. Secondly, it is also interesting to investigate the relation between dynamical stability and thermodynamical stability. Thermodynamic arguments show that the Reissner-Nordström black

brane is expected to be unstable for all values of the charge density. Indeed, by computing the specific heat and isothermal permittivity one can show that the requirement of thermodynamical stability, i.e., that both these quantities are positive (see e.g. [104]), puts complementary conditions on the charge density on the brane. This effect is not visible from the leading order (perfect fluid) dynamical analysis, but can be explained from the next-to-leading order hydrodynamical expansion.

In many ways, studying intrinsic fluctuations of branes in the blackfold approach is similar in spirit to the well-known hydrodynamical regime of AdS/CFT (the fluid/gravity correspondence) [19]. We also mention that the AdS/CFT fluid/gravity computation analogous to the one presented here (i.e. hydro fluctuations of the AdS₅ Reissner-Nordström black brane¹ of co-dimension 1) was carried out in the papers [105–108]. However, we emphasize that the computation presented here deals with asymptotically flat black branes of general spatial dimension and co-dimension. Recently a connection between the fluid/gravity correspondence and the blackfold approach has appeared (the so-called “AdS/Ricci-flat correspondence”) [39; 109]. This was done by constructing a map from asymptotically AdS_{d+1} solutions compactified on \mathbb{T}^{d-p-1} to Ricci-flat solutions by replacing the torus with an $(n+1)$ -sphere and subsequently performing an analytical continuation $d \rightarrow -n$ (while also performing an appropriate Weyl rescaling of the involved geometries). This allowed the authors of [39; 109] to extract the second order (blackfold) transport coefficients from the known second order AdS_{d+1} results [20]. Crucially, one has to know the analytical dependence of the involved dimensions in order to perform the analytical continuation and for the map to work. In this connection, we should also mention the work [70] where the hydrodynamics of the D3 brane was studied. This was done by studying the hydrodynamics on a cutoff surface parallel to the brane. Placing the cutoff surface near infinity then reproduces the blackfold approach while moving the cutoff surface near the AdS₅ × S⁵ throat correctly interpolates to the fluid/gravity correspondence. However, the possible connection between [70] (if any) and the AdS/Ricci-flat correspondence is currently poorly understood. Seen in this light, this provides another motivation for our analysis as it could potentially provide important insights as to how to generalize the AdS/Ricci-flat correspondence to more general settings including matter fields.

Notation: We use μ, ν to label the $D = p + n + 3$ spacetime directions. Moreover, we denote the $p + 1$ worldvolume directions of the brane in Schwarzschild coordinates by $x^a = (t, x^i)$ and in Eddington-Finkelstein coordinates by $\sigma^a = (v, \sigma^i)$ with $a = 0 \dots p$ and $i = 1, \dots, p$. The co-dimension of the brane is $n + 2$. For simplicity of the presentation we restrict ourselves to the cases where $n > 1$ due to a slightly different behavior at infinity for the $n = 1$ solution. However, treating the special case of $n = 1$ should be straightforward using similar considerations as for the neutral case.

¹possibly with a Chern-Simons term.

3.2 Reissner-Nordström branes and effective zeroth order fluid

In this section we review the generalized Gibbons-Maeda solution for $q = 0$ which was found in [36]. The generalized Gibbons-Maeda solution describes a black p -brane with horizon topology $\mathbb{R}^p \times S^{n+1}$ which has electric q -charge diluted on its worldvolume. The solution was obtained from the Gibbons-Maeda solution [110] through an elaborate double uplifting procedure. The general solution is given in terms of a metric, a dilaton and a $(q+1)$ -form gauge field under which (the q -charge diluted on the) black p -brane is charged. A particularly nice property of the generalized Gibbons-Maeda solution is that the dilaton coupling a can be treated as a free parameter. This especially means that we are free to set $a = 0$. This is of course not possible for the well-known supergravity solutions such as the D0-D p system. Moreover, we will restrict ourselves to the $q = 0$ case (Maxwell charge).

3.2.1 Reissner-Nordström black branes

As explained above, we consider branes of Einstein-Maxwell theory. The action is

$$S = \frac{1}{16\pi G} \int d^D x \sqrt{-g} \left[R - \frac{1}{4} F_{\mu\nu} F^{\mu\nu} \right], \quad (3.1)$$

where $F_{\mu\nu}$ is the field strength of the Maxwell gauge field A_μ , $F = dA$. We now present the boosted Reissner-Nordström black brane solution. The solution is characterized by p flat spatial directions x^i , a time direction t , a radial direction r along with the usual transverse sphere S^{n+1} , and finally a uniform boost u^a . The metric is given by

$$ds^2 = h^B \left((\Delta_{ab} - h^{-N} f u_a u_b) dx^a dx^b + f^{-1} dr^2 + r^2 d\Omega_{(n+1)}^2 \right), \quad (3.2)$$

where $\Delta^a_b \equiv \delta^a_b + u^a u_b$ is the usual orthogonal projector defined by the boost u^a . The two harmonic functions $f \equiv f(r)$ and $h \equiv h(r)$ are given by

$$f(r) = 1 - \left(\frac{r_0}{r} \right)^n, \quad h(r) = 1 + \left(\frac{r_0}{r} \right)^n \gamma_0. \quad (3.3)$$

The two parameters r_0 and γ_0 are related to the thermal and electrostatic energy of the solution (see below). The parameter $B \equiv B(p, n)$ is given by²

$$B = \frac{2}{n+p}. \quad (3.4)$$

Finally the gauge field A is given by

$$A = \frac{\sqrt{N}}{h} \left(\frac{r_0}{r} \right)^n \sqrt{\gamma_0(\gamma_0 + 1)} u_a dx^a, \quad (3.5)$$

where $N = B + 2$ corresponds to the parameter recorded in Eq. (1.71) with $a = 0$ and $i = 0$. Notice that here N does not take integer values. In the next section we review the thermodynamics and effective blackfold description of this solution.

²The full generalized Gibbons-Maeda solution has an additional parameter A . However, for the non-dilatonic Reissner-Nordström solution one has $A = 2$.

3.2.2 Thermodynamics and effective blackfold fluid

The blackfold theory of branes supporting lower form q charge was reviewed in Sec. 1.5.6. Here we consider an effective fluid carrying $q = 0$ charge. The general stress tensor is given by Eq. (1.93) and it follows that the stress tensor of the system under consideration takes the form

$$T_{(0)}^{ab} = \mathcal{T} s \left(u^a u^b - \frac{1}{n} \gamma^{ab} \right) + \Phi \mathcal{Q} u^a u^b, \quad (3.6)$$

where γ_{ab} is the induced metric on the blackfold and where we have used the relation $\mathcal{G} = \mathcal{T} s/n$ (which can easily be verified). For our purposes (flat extrinsic geometry), we have $\gamma_{ab} = \eta_{ab}$. The above thermodynamic quantities \mathcal{T} , s , \mathcal{Q} , and Φ are parameterized in terms of a charge parameter γ_0 and the horizon thickness r_0 :

$$\begin{aligned} \mathcal{T} &= \frac{n}{4\pi r_0 \sqrt{(1+\gamma_0)^N}}, & s &= \frac{\Omega_{(n+1)}}{4G} r_0^{n+1} \sqrt{(1+\gamma_0)^N}, \\ \mathcal{Q} &= \frac{\Omega_{(n+1)}}{16\pi G} n \sqrt{N} r_0^n \sqrt{\gamma_0(1+\gamma_0)}, & \Phi &= \sqrt{\frac{N\gamma_0}{1+\gamma_0}}. \end{aligned} \quad (3.7)$$

Since $r_0^n \sim \mathcal{T} s$, r_0 gives us a measure of the thermal energy (density) of the given solution. In a similar manner γ_0 is identified with the thermodynamic ratio,

$$\gamma_0 = \frac{1}{N} \frac{\Phi \mathcal{Q}}{\mathcal{T} s}, \quad (3.8)$$

and γ_0 therefore measures the electrostatic energy relative to the thermal energy of the black brane. It is straightforward to indentify the energy density and pressure of the brane,

$$\varrho = \frac{\Omega_{(n+1)}}{16\pi G} r_0^n (n+1 + nN\gamma_0), \quad P = -\frac{\Omega_{(n+1)}}{16\pi G} r_0^n, \quad w = \frac{n\Omega_{(n+1)}}{16\pi G} r_0^n (1 + N\gamma_0), \quad (3.9)$$

where $w = \varrho + P$ denotes the local enthalpy. Finally the $q = 0$ current supported by the p -brane is given by

$$J_{(0)}^a = \mathcal{Q} u^a. \quad (3.10)$$

To leading order, the intrinsic blackfold equations take the form of the worldvolume conservation equations $\nabla_a T_{(0)}^{ab} = 0$ and $\nabla_a J_{(0)}^a = 0$. For flat extrinsic geometry $\gamma_{ab} = \eta_{ab}$, they evaluate to the equations

$$\dot{\varrho} = -w\vartheta, \quad \dot{i}^a = -w^{-1} \Delta^{ab} \partial_b P, \quad \dot{\mathcal{Q}} = -\mathcal{Q}\vartheta, \quad (3.11)$$

where $\vartheta \equiv \partial_a u^a$ is the expansion of u^a and a dot denotes the directional derivative along u^a . The (first order) equations will be important in the perturbative analysis. As expected, they will show up as constraint equations when solving the Einstein-Maxwell system perturbatively.

3.3 The perturbative expansion

As explained in the introduction, we aim to solve the Einstein-Maxwell system in a derivative expansion around the solution given in Sec. 3.2. In this section we define the appropriate coordinates to handle this problem and explain how the perturbations are classified according to their transformation properties under $\text{SO}(p)$.

3.3.1 Setting up the perturbation

Before perturbing the brane, we first need to cast the metric (3.2) into Eddington-Finkelstein-like (EF) form. The reason is two-fold. First, it is essential for the computation that we can ensure regularity at the horizon and since the Schwarzschild description breaks down at the horizon, it is clearly more useful to use EF coordinates. Secondly, since a gravitational disturbance moves along null-lines, in order to control the perturbation, we want the lines of constant worldvolume coordinates to be radial null-curves i.e. $g_{rr} = 0$. This is exactly the defining property of EF coordinates. For a general boost u^a , we define the EF coordinates σ^a by

$$\sigma^a = x^a + u^a r_\star, \quad r_\star(r) = r + \int_r^\infty \left(\frac{f - h^{N/2}}{f} \right) dr. \quad (3.12)$$

Here r_\star is chosen such that $r'_\star = h^{N/2}/f$ and $r_\star \rightarrow r$ for large r . The first condition ensures that $g_{rr} = 0$ while the latter is chosen such that the EF coordinates reduce to ordinary radial Schwarzschild light cone coordinates for large r . Notice that it is possible to write down a closed form expression for r_\star in terms of the hypergeometric Appell function F_1

$$r_\star(r) = r F_1 \left(-\frac{1}{n}; -\frac{N}{2}, 1; 1 - \frac{1}{n}; 1 - h, 1 - f \right) \approx r \left(1 - \frac{1}{n-1} \frac{r_0^n}{r^n} \left(1 + \frac{N\gamma_0}{2} \right) \right), \quad (3.13)$$

where the last equality applies for large r and is valid up to $\mathcal{O}(\frac{1}{r^{2n-1}})$. It is nice to note that the hypergeometric Appell function F_1 reduces to the ordinary hypergeometric function ${}_2F_1$ in the neutral limit $\gamma_0 \rightarrow 0$. Indeed

$$\lim_{\gamma_0 \rightarrow 0} r_\star(r) = r_\star(r) \Big|_{\gamma_0=0} \equiv r + \int_r^\infty \left(\frac{f-1}{f} \right) dr = r {}_2F_1 \left(1; -\frac{1}{n}; 1 - \frac{1}{n}; 1 - f \right), \quad (3.14)$$

which is the r_\star used in [38]. With this definition of r_\star we will limit our analysis to the case for which $n \geq 2$. In EF coordinates, the metric (3.2) takes the form

$$ds_{(0)}^2 = h^B \left((\Delta_{ab} - h^{-N} f) u_a u_b d\sigma^a d\sigma^b - 2h^{-N/2} u_a d\sigma^a dr + r^2 d\Omega_{(n+1)}^2 \right). \quad (3.15)$$

Here the subscript indicates that the metric solves the Einstein-Maxwell equations to zeroth order in the derivatives. Notice that in these coordinates the gauge field will acquire a non-zero A_r component. However, we shall work in a gauge where this component is zero. We therefore take

$$A^{(0)} = \frac{\sqrt{N}}{h} \left(\frac{r_0}{r} \right)^n \sqrt{\gamma_0(\gamma_0 + 1)} u_a d\sigma^a, \quad \text{and in particular } A_r^{(0)} = 0, \quad (3.16)$$

Having determined the EF form of the metric and gauge field, we are now ready to set up the perturbative expansion.

In accordance with the general blackfold philosophy outlined in Sec. 1.2.1, we promote the parameters u^a, r_0 and γ_0 to *slowly* varying worldvolume fields:

$$u^a \rightarrow u^a(\sigma^a), \quad r_0 \rightarrow r_0(\sigma^a), \quad \gamma_0 \rightarrow \gamma_0(\sigma^a). \quad (3.17)$$

By slowly varying we mean that the derivatives of the worldvolume fields are sufficiently small. In order to quantify this, we introduce a set of re-scaled coordinates $\sigma_\varepsilon^a = \varepsilon\sigma^a$, $\varepsilon \ll 1$, and consider the worldvolume fields to be functions of σ_ε^a . In this way each derivative will produce a factor of ε . Moreover, two derivatives will be suppressed by a factor of ε compared to one derivative and so on. Effectively what we are doing is to consider arbitrary varying worldvolume fields (no restrictions on the size of derivatives) and “stretching” them by a factor of $1/\varepsilon \gg 1$. In this way we will only consider slowly varying fields and the derivative expansion is controlled by the parameter ε .³ The fields can now be expanded around a given point \mathcal{P}

$$\begin{aligned} u^a(\sigma) &= u^a|_{\mathcal{P}} + \varepsilon\sigma^b\partial_b u^a|_{\mathcal{P}} + \mathcal{O}(\varepsilon^2), & r_0(\sigma) &= r_0|_{\mathcal{P}} + \varepsilon\sigma^a\partial_a r_0|_{\mathcal{P}} + \mathcal{O}(\varepsilon^2), \\ \gamma_0(\sigma) &= \gamma_0|_{\mathcal{P}} + \varepsilon\sigma^a\partial_a\gamma_0|_{\mathcal{P}} + \mathcal{O}(\varepsilon^2). \end{aligned} \quad (3.18)$$

We now seek derivative corrections to the metric and gauge field denoted by respectively $ds_{(1)}^2$ and $A_{(1)}$, so that

$$ds^2 = ds_{(0)}^2 + \varepsilon ds_{(1)}^2 + \mathcal{O}(\varepsilon^2) \quad \text{and} \quad A = A_{(0)} + \varepsilon A_{(1)} + \mathcal{O}(\varepsilon^2), \quad (3.19)$$

solves the equations of motion to order ε . By a suitable choice of coordinates, we can take the point \mathcal{P} to lie at the origin $\sigma^a = (0, \mathbf{0})$. Moreover, we can choose coordinates so that $u^v|_{(0,0)} = 1$, $u^i|_{(0,0)} = 0$, $i = 1, \dots, p$ (the rest frame of the boost in the origin)⁴. In these particular coordinates, the 0th order metric $ds_{(0)}^2$ takes the form

$$\begin{aligned} ds_{(0)}^2 &= h^B \left[-2h^{-\frac{N}{2}} dvdr - \left(\frac{f}{h^N} \right) dv^2 + \sum_{i=1}^p (d\sigma^i)^2 + r^2 d\Omega_{(n+1)}^2 \right] \\ &+ \varepsilon h^B \left[\frac{1}{h^N} \frac{r_0^n}{r^n} \left(\frac{n}{r_0} \left(1 + \frac{2f}{h} \gamma_0 \right) \sigma^a \partial_a r_0 + \frac{2f}{h} \sigma^a \partial_a \gamma_0 \right) dv^2 \right. \\ &+ \frac{B}{h} \frac{r_0^n}{r^n} \left(\frac{n\gamma_0}{r_0} \sigma^a \partial_a r_0 + \sigma^a \partial_a \gamma_0 \right) \left(\sum_{i=1}^p (d\sigma^i)^2 + r^2 d\Omega_{(n+1)}^2 \right) \\ &+ 2 \left(\frac{f}{h^N} - 1 \right) \sigma^a \partial_a u_i dv d\sigma^i - \frac{2}{h^{N/2}} \sigma^a \partial_a u_i d\sigma^i dr \\ &\left. + \frac{B-2}{h^{N/2+1}} \frac{r_0^n}{r^n} \left(\frac{n\gamma_0}{r_0} \sigma^a \partial_a r_0 + \sigma^a \partial_a \gamma_0 \right) dvdr \right], \end{aligned} \quad (3.20)$$

where we have denoted $r_0|_{(0,0)} \equiv r_0$ and $\gamma_0|_{(0,0)} \equiv \gamma_0$. Clearly the system has a large amount of gauge freedom. Following the discussion of the definition of r_* , we want the r coordinate to maintain its geometrical interpretation. We therefore choose

$$g_{rr}^{(1)} = 0, \quad (3.21)$$

and we moreover take

$$g_{\Omega\Omega}^{(1)} = 0 \quad \text{and} \quad A_r^{(1)} = 0. \quad (3.22)$$

³In the end of the computation, we of course set $\varepsilon = 1$ and keep in mind that the expressions only hold as a derivative expansion i.e. for sufficiently slowly varying configurations.

⁴In these coordinates $u^v = 1 + \mathcal{O}(\varepsilon^2)$.

The background $g_{(0)}$ exhibits a residual $\text{SO}(p)$ invariance. We can use this to split the system up into sectors of $\text{SO}(p)$. The scalar sector contains 4 scalars, $A_v^{(1)}$, $g_{vr}^{(1)}$, $g_{vv}^{(1)}$ and $\text{Tr}g_{ij}^{(1)}$. The vector sector contains 3 vectors $A_i^{(1)}$, $g_{vi}^{(1)}$ and $g_{ri}^{(1)}$. Finally, the tensor sector contains 1 tensor $\bar{g}_{ij}^{(1)} \equiv g_{ij}^{(1)} - \frac{1}{p}(\text{Tr}g_{kl}^{(1)})\delta_{ij}$ (the traceless part of $g_{ij}^{(1)}$). We parameterize the three $\text{SO}(p)$ sectors according to

$$\begin{aligned} \text{Scalar: } A_v^{(1)} &= -\sqrt{N\gamma_0(1+\gamma_0)} \frac{r_0^n}{r^n} h^{-1} a_v, \quad g_{vr}^{(1)} = h^{B-N/2} f_{vr}, \\ g_{vv}^{(1)} &= h^{-1} f_{vv}, \quad \text{Tr} g_{ij}^{(1)} = h^B \text{Tr} f_{ij}, \\ \text{Vector: } A_i^{(1)} &= -\sqrt{N\gamma_0(1+\gamma_0)} a_i, \quad g_{vi}^{(1)} = h^B f_{vi}, \quad g_{ri}^{(1)} = h^{B-N/2} f_{ri}, \\ \text{Tensor: } \bar{g}_{ij}^{(1)} &= h^B \bar{f}_{ij}, \end{aligned} \quad (3.23)$$

where $\bar{f}_{ij} \equiv f_{ij} - \frac{1}{p}(\text{Tr}f_{kl})\delta_{ij}$. The parameterization is chosen in such a way that the resulting EOMs only contain derivatives of f_{ab} and a_a and will thus be directly integrable.

3.3.2 A digression: Reduction of Einstein-Maxwell theory

Here we explain how it is possible to treat general n and p by integrating out the transverse non-fluid dynamic directions.

In order to work out the full set of solutions and find the general form of the stress tensor and current, it is enough to consider fluid dynamic fluctuations in $1+d$ ($2 \leq d < p$) directions of the brane. In particular, it is enough to consider $d=2$. Indeed, since the background is $\text{SO}(p)$ invariant, the correction $ds_{(1)}^2$ will consist of $\text{SO}(p)$ invariant tensor structures. The same holds for the effective blackfold stress tensor and current. In order to identify these tensor structures, it is enough to consider fluctuations in only $1+d$ directions (time + d flat spatial directions) of the brane. Considering only fluctuations in $1+d$ brane dimensions, the metric is of the form (reduction of the p -brane with $n+2$ transverse dimensions)

$$ds^2 = ds_{(f)}^2 + e^{2\psi(\sigma_f)} d\Omega_{(n+1)}^2 + e^{2\phi(\sigma_f)} \sum_{i=d+1}^p (d\sigma^i)^2, \quad (3.24)$$

with the one-form gauge field of the form $A_\mu = A_a(\sigma_f)$. Here the subscript f means 'fluid' since the $d+2$ -dimensional base space with the metric $ds_{(f)}^2$ will contain the fluid dynamical degrees of freedom in our computations. Integrating out the S^{n+1} and \mathbb{T}^{p-d} (see appendix D.1), the EOMs of the system take the form

$$\begin{aligned} R_{ab}^{(f)} &= \mathcal{F}_{ab} + (n+1)(\nabla_a \psi \nabla_b \psi + \nabla_a \nabla_b \psi) + (p-d)(\nabla_a \phi \nabla_b \phi + \nabla_a \nabla_b \phi), \\ \square \psi + [(p-d)\nabla_b \phi + (n+1)\nabla_b \psi] \nabla^b \psi &= n e^{-2\psi} + \kappa, \\ \square \phi + [(p-d)\nabla_b \phi + (n+1)\nabla_b \psi] \nabla^b \phi &= \kappa, \\ \nabla_a F^{ab} &= j^b, \end{aligned} \quad (3.25)$$

where the tensor \mathcal{F}_{ab} , vector j^a , and scalar κ are given by

$$\mathcal{F}_b^a = \frac{1}{2} F^{ac} F_{bc} - \kappa \delta_b^a, \quad j^a = F^{ab} ((n+1)\nabla_b \psi + (p-d)\nabla_b \phi), \quad \kappa = \frac{F_{ab} F^{ab}}{4(p+n+1)}. \quad (3.26)$$

Working with these effective EOMs allows us to treat a general number of transverse and brane dimensions.

3.4 First order equations

In order to compute the effective stress tensor and current and thereby extract the transport coefficients, we need the large r asymptotics of the perturbation functions which are decomposed and parametrized according to Eq. (3.23). We denote the first order Einstein and Maxwell equations by

$$\begin{aligned} R_{\mu\nu} - \frac{1}{2}F_{\mu\rho}F_{\nu}{}^{\rho} + \frac{1}{4(n+p+1)}F_{\rho\sigma}F^{\rho\sigma}g_{\mu\nu} &\equiv \varepsilon\mathcal{E}_{\mu\nu} + \mathcal{O}(\varepsilon^2) = 0, \\ \nabla_{\rho}F^{\rho}{}_{\mu} &\equiv \varepsilon\mathcal{M}_{\mu} + \mathcal{O}(\varepsilon^2) = 0. \end{aligned} \quad (3.27)$$

In this section we will find the solution to each $SO(p)$ sector in turn and explain how the regularity on the horizon is ensured.

3.4.1 Scalars of $SO(p)$

The scalar sector consists of seven independent equations which correspond to the vanishing of the components: $\mathcal{E}_{vv}, \mathcal{E}_{rv}, \mathcal{E}_{rr}, \text{Tr}\mathcal{E}_{ij}, \mathcal{E}_{\Omega\Omega}, \mathcal{M}_v, \mathcal{M}_r$.⁵

Constraint equations: There are two constraint equations; $\mathcal{E}_v^r = 0$ and $\mathcal{M}_r = 0$. The two equations are solved consistently by

$$(n+1+pB\gamma_0)\partial_v r_0 = -r_0(1-B\gamma_0)\partial_i u^i, \quad (3.28)$$

and

$$(n+1+pB\gamma_0)\partial_v \gamma_0 = -2\gamma_0(1+\gamma_0)\partial_i u^i. \quad (3.29)$$

The first equation corresponds to conservation of energy while the second equation can be interpreted as current conservation. These are equivalent to the scalar conservation equations given by (3.11) in the rest frame.

We now proceed to solve for the first order correction to the scalar part of the metric and gauge field under the assumption that the fluid configuration satisfy the above constraints. Imposing the constraint equations will make \mathcal{E}_{rv} and \mathcal{E}_{vv} linear related and one is therefore left with five equations with four unknowns.

Dynamical equations: The coupled system constituted by the dynamical equations is quite intractable. One approach to obtaining the solution to the system is to decouple the trace function $\text{Tr}f_{ij}$. Once $\text{Tr}f_{ij}$ is known, it turns out, as will be presented below, all the other functions can be obtained while ensuring that they are regular on the horizon.

It is possible to obtain a 3rd order ODE for $\text{Tr}f_{ij}$ by decoupling it through a number of steps. One way is to use \mathcal{E}_{rr} to eliminate f'_{rv} and then take linear combinations of the

⁵In the reduction scheme outlined in Sec. 3.3.2 we have $\mathcal{E}_{\Omega\Omega} = \mathcal{E}_{\psi}$, where \mathcal{E}_{ψ} is the EOM for ψ given in (3.25). Similarly, we have $\text{Tr}\mathcal{E}_{ij} = \text{Tr}\mathcal{E}_{ij}^{(f)} - (p-d)h^B\mathcal{E}_{\phi}$, where \mathcal{E}_{ϕ} is the EOM for ϕ .

remaining equations. The resulting combinations can then be used to eliminate f'_{vv} and f''_{vv} such that one is left with two equations in terms of a_v and $\text{Tr}f_{ij}$ which can then be decoupled by standard means. The resulting equation is schematically of the form

$$H_3^{(n,p)}(r) [\text{Tr}f_{ij}]'''(r) + H_2^{(n,p)}(r) [\text{Tr}f_{ij}]''(r) + H_1^{(n,p)}(r) [\text{Tr}f_{ij}]'(r) = S_{\text{Tr}}(r), \quad (3.30)$$

where H_1, H_2 and H_3 do not depend on the sources (worldvolume derivatives) and the source term S_{Tr} only depends on the scalar $\partial_i u^i$. The expressions for these functions are however very long and have therefore been omitted. After some work, one finds that the equation is solved by

$$\text{Tr}f_{ij}(r) = c_{\text{Tr}}^{(1)} + \gamma_0 c_{\text{Tr}}^{(2)} G(r) - 2(\partial_i u^i) \text{Tr}f_{ij}^{(s)}(r), \quad (3.31)$$

where the terms containing the two integration constants $c_{\text{Tr}}^{(1)}$ and $c_{\text{Tr}}^{(2)}$ correspond to the homogeneous solution. The entire family of homogeneous solutions to Eq. (3.30) of course has an additional one-parameter freedom which has been absorbed in the particular solution $\text{Tr}f_{ij}^{(s)}(r)$ and been used to ensure horizon regularity⁶. The function G is given by

$$G(r) = p \frac{r_0^n}{r^n} \left(2 + pB \frac{r_0^n}{r^n} \gamma_0 \right)^{-1}. \quad (3.32)$$

The particular solution which is regular on the horizon is given by

$$\text{Tr}f_{ij}^{(s)}(r) = -\frac{r_0}{n} (1 + \gamma_0)^{\frac{N}{2}} \alpha \gamma_0 G(r) + \left(r_* - \frac{r_0}{n} (1 + \gamma_0)^{\frac{N}{2}} \log f(r) \right) (1 - \beta \gamma_0 G(r)), \quad (3.33)$$

with the coefficients

$$\alpha = 2B \left[\frac{2(n+1) + pB\gamma_0}{(n+1 + pB\gamma_0)^2} \right] \quad \text{and} \quad \beta = B \left[\frac{n+2 + pB\gamma_0}{n+1 + pB\gamma_0} \right]. \quad (3.34)$$

With $\text{Tr}f_{ij}$ given, the equation $\mathcal{E}_{rr} = 0$ will provide the derivative of f_{rv} ,

$$f'_{rv}(r) = \frac{r}{\left(2(n+1) + pB \frac{r_0^n}{r^n} \gamma_0 \right) h(r)^{\frac{B}{2}}} \frac{d}{dr} \left[h(r)^{\frac{N}{2}} [\text{Tr}f_{ij}]'(r) \right]. \quad (3.35)$$

Since the equation is a 1st order ODE, the regularity of the horizon is ensured by $\text{Tr}f_{ij}$. Note that it is possible to perform integration by parts and use that the derivative of r_* takes a simpler form. One can thereafter obtain an analytical expression for the resulting integral. This expression is however rather long and does not add much to the question we are addressing for which we are in principle only interested in the large r behavior given by

$$f_{rv}(r) \approx c_{rv} - \gamma_0 c_{\text{Tr}}^{(2)} \frac{G(r)h(r)}{\left(2 + pB \frac{r_0^n}{r^n} \gamma_0 \right)} + (\partial_i u^i) \sum_{k=1}^{\infty} \frac{r_0^{nk}}{r^{nk}} \left[\alpha_{rv}^{(k)} r + \beta_{rv}^{(k)} r_0 \right]. \quad (3.36)$$

The first two terms constitute the homogeneous solution and the particular solution is given in terms of the coefficients $\alpha_{rv}^{(k)}$ and $\beta_{rv}^{(k)}$ which depend on n, p , and γ_0 . The first set of coefficients are given in appendix D.2.

⁶Note that Eq. (3.30) has been derived under the assumption that $\partial_i u^i \neq 0$. This especially means that when there are no sources the one-parameter freedom disappears in accordance with (3.31).

Using the expression for f'_{rv} in terms of $\text{Tr}f_{ij}$, the Maxwell equation $\mathcal{M}_v = 0$ becomes a 2nd order ODE for the gauge field perturbation,

$$\frac{d}{dr} \left[\frac{1}{r^{n-1}} a'_v(r) \right] = \frac{nr^2}{\left(2(n+1) + pB \frac{r_0^n}{r^n} \gamma_0\right)} \frac{d}{dr} \left[\frac{1}{r^{n+1}} [\text{Tr}f_{ij}]'(r) \right]. \quad (3.37)$$

This equation is solved by a double integration. The inner integral is manifestly regular at the horizon, one can therefore work directly with the asymptotic behavior of the right-hand side before performing the integrations. The large r behavior of the perturbation function is thus found to be

$$a_v(r) \approx c_v^{(1)} r^n + c_v^{(2)} + \frac{1}{2} \gamma_0 c_{\text{Tr}}^{(2)} G(r) + (\partial_i u^i) \left[-\frac{n}{n-1} r + \sum_{k=1}^{\infty} \frac{r_0^{nk}}{r^{nk}} \left[\alpha_v^{(k)} r + \beta_v^{(k)} r_0 \right] \right], \quad (3.38)$$

where the first three terms constitute the homogeneous solution and the particular solution is given in terms of the coefficients $\alpha_v^{(k)}$ and $\beta_v^{(k)}$ depending on n, p , and γ_0 . The first set of coefficients are given in appendix D.2.

The last perturbation function f_{vv} can be obtained from $\mathcal{E}_{vv} = 0$. Using the expression for f'_{rv} in terms of $\text{Tr}f_{ij}$ the equation is schematically of the form

$$\frac{d}{dr} \left[r^{n+1} f'_{vv}(r) \right] = G_1 [\text{Tr}f_{ij}(r)] + G_2 [a_v(r)] + S_{ii}(r), \quad (3.39)$$

where G_1, G_2 are non-trivial differential operators and the source S_{ii} depends on $\partial_i u^i$. Again, the full expressions have been omitted and we only provide the large r behavior,

$$f_{vv}(r) \approx f_{vv}^{(h)}(r) + (\partial_i u^i) \sum_{k=1}^{\infty} \frac{r_0^{nk}}{r^{nk}} \left[\alpha_{vv}^{(k)} r + \beta_{vv}^{(k)} r_0 \right], \quad (3.40)$$

with the homogeneous part given by

$$f_{vv}^{(h)}(r) = c_{vv}^{(1)} + \frac{c_{vv}^{(2)}}{r^n} + \frac{r_0^n}{r^n} \frac{\gamma_0}{h(r)} \left[2(1 + \gamma_0) \frac{r_0^n}{r^n} (c_v^{(2)} - c_v^{(1)} r_0^n \gamma_0) - \frac{G(r)}{2} \left(1 + 2\gamma_0 - \frac{r_0^n}{r^n} \gamma_0 \right) c_{\text{Tr}}^{(2)} \right]. \quad (3.41)$$

The solution is ensured to be regular at the horizon. The coefficients $\alpha_{vv}^{(k)}$ and $\beta_{vv}^{(k)}$ depend on n, p , and γ_0 . The first set of coefficients are listed in appendix D.2.

Finally, one must ensure that the equations coming from $\text{Tr}\mathcal{E}_{ii}$ and the angular directions ($\mathcal{E}_{\Omega\Omega} = 0$) are satisfied. This will impose the following relations between the integration constants,

$$c_{vv}^{(1)} = -2c_{rv}, \quad (3.42)$$

$$c_{vv}^{(2)} = -\frac{r_0^n}{4} \left((n+p)c_{\text{Tr}}^{(2)} + 8(1 + \gamma_0)(c_v^{(2)} - c_v^{(1)} r_0^n \gamma_0) \right). \quad (3.43)$$

This completes the analysis of the scalar sector. The remaining undetermined integration constants are thus: $c_{\text{Tr}}^{(1)}, c_{\text{Tr}}^{(2)}, c_{rv}, c_v^{(1)}, c_v^{(2)}$ for which c_{rv} and $c_{\text{Tr}}^{(1)}$ will be fixed by requiring the spacetime to be asymptotically flat while the rest constitute the freedom of the homogeneous solution. Note that the above functions reproduce the neutral case as $\gamma_0(\sigma^a) \rightarrow 0$.

3.4.2 Vectors of $SO(p)$

The vector sector consists of $3p$ independent equations which correspond to the vanishing of the components: \mathcal{E}_{ri} , \mathcal{E}_{vi} and \mathcal{M}_i .

Constraint equations: The constraint equations are given by the Einstein equations $\mathcal{E}^r{}_i = 0$ and are solved by

$$\partial_i r_0 = r_0(1 + N\gamma_0)\partial_v u_i, \quad (3.44)$$

which are equivalent to conservation of stress-momentum. These are part of the conservation equations given by (3.11) in the rest frame. Similar to above we now proceed solving for the first order corrections to the metric and gauge field under the assumption that the fluid profile satisfy the above constraint (3.44).

Dynamical equations: The remaining equations consist of p pairs consisting of one Einstein equation $\mathcal{E}_{vi} = 0$ and one Maxwell equation $\mathcal{M}_i = 0$. The structure of these equations is the same as in the scalar sector. The Einstein equation $\mathcal{E}_{vi} = 0$ is schematically of the form,

$$L_3^{(n,p)}(r)f_{vi}''(r) + L_2^{(n,p)}(r)f_{vi}'(r) + L_1^{(n,p)}(r)a_i'(r) = S_{vi}(r), \quad (3.45)$$

while the Maxwell equation $\mathcal{M}_i = 0$ is,

$$M_3^{(n,p)}(r)a_i''(r) + M_2^{(n,p)}(r)a_i'(r) + M_1^{(n,p)}(r)f_{vi}'(r) = S_i(r). \quad (3.46)$$

Again the functions L_k and M_k , $k = 1, \dots, 3$ have been omitted.

To decouple the system we differentiate \mathcal{E}_{vi} once and eliminate all $a_i(r)$ terms in \mathcal{M}_i . Doing so, one obtains a 3rd order ODE for $f_{vi}(r)$ which can be written on the form,

$$\frac{d}{dr} \left[\frac{r^{n+1}f(r)}{h^N} \left(1 - c_1 \frac{r_0^n}{r^n} \right)^2 \frac{d}{dr} \left[\frac{r^{n+1}h^{N+1}}{\left(1 - c_1 \frac{r_0^n}{r^n} \right)} f_{vi}'(r) \right] \right] = S_{vi}(r), \quad (3.47)$$

with

$$c_1 = \frac{N-1}{1+N\gamma_0}\gamma_0. \quad (3.48)$$

It is possible to perform the first two integrations analytically and ensure regularity at the horizon. The first integration is straightforward while the second involves several non-trivial functions. The large r behavior of the f_{vi} function is found to be

$$f_{vi}(r) \approx c_{vi}^{(1)} - \left(1 - \frac{f(r)}{h(r)^N} \right) c_{vi}^{(2)} - (\partial_v u_i)r + \sum_{k=1}^{\infty} \frac{r_0^{nk}}{r^{nk}} \left[\alpha_{vi}^{(k)} r + \beta_{vi}^{(k)} r_0 \right], \quad (3.49)$$

where the first two terms constitute the homogeneous solution. The first set of coefficients $\alpha_{vi}^{(k)}$ and $\beta_{vi}^{(k)}$ are given in appendix D.2. Notice that the sum vanishes in the neutral limit.

Once the solution of f_{vi} is given we can use \mathcal{E}_{vi} to determine a_i ,

$$a_i(r) \approx c_i^{(1)} + \frac{r_0^n}{r^n} \frac{1}{h(r)} c_{vi}^{(2)} + \sum_{k=1}^{\infty} \frac{r_0^{nk}}{r^{nk}} \left[\alpha_i^{(k)} r + \beta_i^{(k)} r_0 \right], \quad (3.50)$$

where the first two terms correspond to the homogeneous solution. The first set of coefficients $\alpha_i^{(k)}$ and $\beta_i^{(k)}$ are given in appendix D.2.

The remaining undetermined integration constants are thus: $c_i^{(1)}$, $c_{vi}^{(1)}$, and $c_{vi}^{(2)}$. The constant $c_{vi}^{(2)}$ corresponds to an infinitesimal shift in the boost velocities along the spatial directions of the brane while $c_i^{(1)}$ is equivalent to an infinitesimal gauge transformation. The last constant $c_{vi}^{(1)}$ will be determined by imposing asymptotically flatness at infinity.

3.4.3 Tensors of $SO(p)$

There are no constraint equations in the tensor sector and $p(p+1)/2 - 1$ dynamical equations given by

$$\mathcal{E}_{ij} - \frac{\delta_{ij}}{p} \text{Tr}(\mathcal{E}_{ij}) = 0. \quad (3.51)$$

This gives an equation for each component of the traceless symmetric perturbation functions \bar{f}_{ij} ,

$$\frac{d}{dr} \left[r^{n+1} f(r) \bar{f}'_{ij}(r) \right] = -\sigma_{ij} r^n \left(2(n+1) + pB \frac{r_0^n}{r^n} \gamma_0 \right) h(r)^{\frac{B}{2}}, \quad (3.52)$$

where

$$\sigma_{ij} = \partial_{(i} u_{j)} - \frac{1}{p} \delta_{ij} \partial_k u^k. \quad (3.53)$$

The solution is given by,

$$\bar{f}_{ij}(r) = \bar{c}_{ij} - 2\sigma_{ij} \left(r_* - \frac{r_0}{n} (1 + \gamma_0)^{\frac{N}{2}} \log f(r) \right), \quad (3.54)$$

where horizon regularity has been imposed and the constant \bar{c}_{ij} is symmetric and traceless and will be determined by imposing asymptotically flatness.

3.4.4 Comment on the homogeneous solution

We have now obtained the solution to the Einstein-Maxwell equations for any first order fluid profile which fulfill the constraint equations. These have been provided in large r expansions and are ensured to have the right behavior at the horizon for any of the remaining integration constants. One remark that is worth mentioning is that f_{ri} did not appear in the analysis above and corresponds to a gauge freedom. This gauge freedom does not play a role for $n \geq 2$, but is expected to play a role for $n = 1$ to ensure asymptotically flatness.

We now want to provide some insight into the meaning of the remaining integration constants. One can separate the constants into two categories; the subset that are fixed by asymptotically flatness and the subset that corresponds to the ε -freedom of the parameters in the zeroth order fields. The latter corresponds exactly to the remaining freedom of the homogeneous solution. In the above the homogeneous part of the fields are given exact.

One finds that the homogeneous part of the scalar sector corresponds to shifts in $r_0 \rightarrow r_0 + \varepsilon \delta r_0$, $\gamma_0 \rightarrow \gamma_0 + \varepsilon \delta \gamma_0$, and the gauge freedom $a_v \rightarrow a_v + \varepsilon \delta a_v$ of the zeroth order metric given by Eq. (3.2). Indeed, performing the above shifts and redefining the r coordinate,

$$r \rightarrow r \left(1 - \varepsilon \gamma_0 \frac{r_0^n}{r^n} \frac{n \delta \log r_0 + \delta \log \gamma_0}{n + p h(r)} \right), \quad (3.55)$$

such that the angular directions does not receive first order contributions in accordance with the gauge choice (3.22), one can relate the integration constants to the two shifts and gauge transformation by,

$$\begin{aligned} c_{\text{Tr}}^{(2)} &= 2B (n \delta \log r_0 + \delta \log \gamma_0), \\ c_v^{(2)} &= -n \delta \log r_0 - \frac{1 + 2\gamma_0}{2(1 + \gamma_0)} \delta \log \gamma_0 - \frac{\gamma_0}{\sqrt{N \gamma_0 (1 + \gamma_0)}} \delta a_v, \\ c_v^{(1)} &= -\frac{\delta a_v}{r_0^n \sqrt{N \gamma_0 (1 + \gamma_0)}}. \end{aligned} \quad (3.56)$$

For the vector sector one finds that the homogeneous part corresponds to the shift of $u_i \rightarrow u_i + \varepsilon \delta u_i$ and the gauge transformation $a_i \rightarrow a_i + \varepsilon \delta a_i$. The first transformation corresponds to global shifts in the boost velocities. In the same r -coordinate, one has

$$\begin{aligned} c_{vi}^{(2)} &= \delta u_i, \\ c_i^{(1)} &= -\frac{\delta a_i}{\sqrt{N \gamma_0 (1 + \gamma_0)}}. \end{aligned} \quad (3.57)$$

This accounts for all the ε -freedom in the full solution.

3.4.5 Imposing asymptotically flatness

We now turn to imposing the boundary condition at infinity, namely requiring the solution to be asymptotically flat. To impose this we must first change coordinates back to the Schwarzschild-like form. Moreover, we need the fields expressed in Schwarzschild coordinates for obtaining the effective stress tensor and current. In order to change coordinates, we use the inverse transformation of the one stated in Eq. (3.12). The transformation can be worked out iteratively order by order. To first order the transformation from EF-like coordinates to Schwarzschild-like coordinates for a general $r_0(\sigma^a)$ and $\gamma_0(\sigma^a)$ is given by,

$$\begin{aligned} v &= t + r_\star + \varepsilon \left[(t + r_\star) (\partial_{r_0} r_\star \partial_t r_0 + \partial_{\gamma_0} r_\star \partial_t \gamma_0) + x^i (\partial_{r_0} r_\star \partial_i r_0 + \partial_{\gamma_0} r_\star \partial_i \gamma_0) \right] + \mathcal{O}(\varepsilon^2), \\ \sigma^i &= x^i + \varepsilon \left[(t + r_\star) \partial_t u^i + \sigma^j \partial_j u^i \right] r_\star + \mathcal{O}(\varepsilon^2). \end{aligned} \quad (3.58)$$

It is now possible to transform all the fields to Schwarzschild coordinates and impose asymptotically flatness. This leads to

$$c_{rv} = 0, \quad c_{vi}^{(1)} = 0, \quad c_{\text{Tr}}^{(1)} = 0, \quad \bar{c}_{ij} = 0. \quad (3.59)$$

We now have the complete first order solution for the black brane metric and Maxwell gauge field that solves the Einstein-Maxwell equations.

3.5 Viscous stress tensor and current

In this section we will compute the effective stress tensor and current of the first order solution obtained above. Before doing this, we shall briefly discuss the general form of the first order derivative corrections to the stress tensor and current.

3.5.1 First order fluid dynamics

We write the stress tensor and the current as

$$T^{ab} = T_{(0)}^{ab} + \Pi_{(1)}^{ab} + \mathcal{O}(\partial^2), \quad J^a = J_{(0)}^a + \Upsilon_{(1)}^a + \mathcal{O}(\partial^2), \quad (3.60)$$

where the perfect fluid terms were written down for our specific fluid in Sec. 3.2.2. The tensors $\Pi_{(1)}^{ab}$ and $\Upsilon_{(1)}^{ab}$ are the first order dissipative derivative corrections to the perfect fluid stress tensor and current, respectively. The specific form of $\Pi_{(1)}^{ab}$ and $\Upsilon_{(1)}^{ab}$ are encoded in the first order correcting solution obtained in the previous section. To first order in the derivative corrections, the presence of charge introduces no new terms in the dissipative part of the stress tensor. The most general form of $\Pi_{(1)}^{ab}$ is therefore given by Eq. (1.31) and is completely characterized in terms of the shear and bulk viscosities which are associated with the scalar and tensor fluctuations, respectively. However, note that although the overall form of $\Pi_{(1)}^{ab}$ is the same as in the neutral case, the transport coefficients are now expected to depend on both the temperature and the charge i.e. on both r_0 and γ_0 . Also note that the viscosities η and ζ are required to be positive in order to ensure entropy creation in the fluid [111].

Using similar reasoning leading to the first order dissipative stress tensor, it is possible to show that the most general form of $\Upsilon_{(1)}^a$ (in the Landau frame) is given by⁷

$$\Upsilon_{(1)}^a = -\mathfrak{D} \left(\frac{\mathcal{Q}\mathcal{T}}{w} \right)^2 \Delta^{ab} \partial_b \left(\frac{\Phi}{\mathcal{T}} \right). \quad (3.61)$$

Here \mathfrak{D} is the charge diffusion constant which is associated with the vector fluctuations. Indeed, it is possible to derive that with $\mathfrak{D} > 0$, the term (3.61) is the only term which can be constructed from the fields and that is consistent with the 2nd law of thermodynamics [111]. Plugging in the values of Φ and \mathcal{T} in terms of r_0 and γ_0 and using the vector constraint Eq. (3.44), we find that (in the rest frame)

$$\Upsilon_{(1)}^v = 0, \quad \Upsilon_{(1)}^i \sim \gamma_0(1 + \gamma_0) \partial_v u^i + \frac{1}{2} \partial_i \gamma_0. \quad (3.62)$$

Since the derivatives appear in a very specific combination in this expression, this in fact provides us with a non-trivial check of the blackfold fluid description.

⁷It is possible to include a parity violating term as was found in [105]. However, since we have no Chern-Simons term in the theory such a term is not relevant.

3.5.2 Computing the effective stress tensor and current

Having determined the (large r asymptotics) of the first order corrected black brane solution, the effective stress tensor can now be extracted. This is done by computing the quasi-local stress tensor (1.13) for the specific setup. Following the prescription outlined in Sec. 1.2.2, we find

$$\begin{aligned}
T_{tt} &= \frac{\Omega_{(n+1)}}{16\pi G} (n+1 + nN(\gamma_0 + \varepsilon(\delta\gamma_0 + x^a\partial_a\gamma_0))) (r_0 + \varepsilon(\delta r_0 + x^a\partial_a r_0))^n, \\
T_{ij} &= -\frac{\Omega_{(n+1)}}{16\pi G} \left(\delta_{ij} (r_0 + \varepsilon(\delta r_0 + x^a\partial_a r_0))^n \right. \\
&\quad \left. + \varepsilon r_0^{n+1} (1 + \gamma_0)^{\frac{N}{2}} \left[2 \left(\partial_{(i} u_{j)} - \frac{1}{p} \delta_{ij} \partial_k u^k \right) + \frac{2}{p} \frac{(n+p+1)(n+1)}{(n+1+pB\gamma_0)^2} \delta_{ij} \partial_k u^k \right] \right), \\
T_{tj} &= -\frac{\Omega_{(n+1)}}{16\pi G} r_0^n n (1 + N\gamma_0) \varepsilon (\delta u_j + x^a \partial_a u_j),
\end{aligned} \tag{3.63}$$

where the expressions are valid to order $\mathcal{O}(\varepsilon)$.

In a similar manner the current is obtained from large r asymptotics of the gauge fields. Ensuring that the Lorenz gauge condition $\nabla^\mu A_\mu = 0$ is satisfied, the current is obtained using

$$J_a = \lim_{r \rightarrow \infty} \frac{n\Omega_{(n+1)}}{16\pi G} r^n A_a. \tag{3.64}$$

One finds

$$\begin{aligned}
J_t &= -\frac{\Omega_{(n+1)}}{16\pi G} n\sqrt{N} (r_0 + \varepsilon(\delta r_0 + x^a\partial_a r_0))^n \sqrt{\gamma_0(1+\gamma_0) + \varepsilon(\delta\gamma_0 + x^a\partial_a\gamma_0)(1+2\gamma_0)}, \\
J_i &= \frac{\Omega_{(n+1)}}{16\pi G} n\sqrt{N} r_0^n \sqrt{\gamma_0(1+\gamma_0)} \left(\varepsilon (\delta u_j + x^a \partial_a u_j) - \varepsilon r_0 \frac{\gamma_0(1+\gamma_0)\partial_v u_i + \frac{1}{2}\partial_i\gamma_0}{n(1+N\gamma_0)\gamma_0(1+\gamma_0)^{\frac{B}{2}+1}} \right).
\end{aligned} \tag{3.65}$$

Again these expressions are valid to $\mathcal{O}(\varepsilon)$. It is now possible to read off the transport coefficients. Before doing this, we require that the Landau frame renormalization conditions $\Pi_{(1)}^{tt} = \Pi_{(1)}^{ti} = 0$ and $\Upsilon_{(1)}^t = 0$ are satisfied. Equivalently we require the shifts δr_0 and $\delta\gamma_0$ of the zeroth order solution to vanish. Notice that the stress tensor and current do not depend on the gauge transformation δa_a as they should of course not do. Also recall that the shifts were related to the integrations constants by (3.56).

Setting $\delta r_0 = \delta\gamma_0 = 0$, the shear and bulk viscosities are determined using the form given by Eq. (1.31),

$$\eta = \frac{\Omega_{(n+1)}}{16\pi G} r_0^{n+1} (1 + \gamma_0)^{\frac{N}{2}}, \quad \zeta = \frac{2}{p} \frac{(n+p+1)(n+1)}{(n+1+pB\gamma_0)^2}. \tag{3.66}$$

The second term of J_i is seen to have the right proportionality according to (3.62) and hence using the form of Eq. (3.61) the diffusion constant can be determined,

$$\mathfrak{D} = \frac{\Omega_{(n+1)}}{4G} \frac{1 + \gamma_0}{nN\gamma_0} r_0^{n+2}. \tag{3.67}$$

Notice that all the transport coefficients are found to be positive which is expected for a consistent effective fluid dynamic theory. We have now obtained the first order derivative corrections to the effective stress tensor and current.

3.5.3 Hydrodynamic bounds

We will now check the result of the shear viscosity against the expectation that the transport coefficient should satisfy the well-know bound

$$\frac{\eta}{s} \geq \frac{1}{4\pi}. \quad (3.68)$$

Using Eqs. (3.7) and (3.66), the system is indeed seen to saturate the bound. This agrees with the expectation for any two-derivative gravity theory [22; 112].

In addition, it is worth to investigate the bulk to shear viscosity ratio proposed by Ref. [113],

$$\frac{\zeta}{\eta} \geq 2 \left(\frac{1}{p} - c_s^2 \right) \quad (3.69)$$

where c_s is the speed of sound computed below in Sec. 3.6. Although one should keep in mind that the proposal of this bound relies heavily on holographic considerations, we find when using the value given by Eq. (3.76) for the Reissner-Nordström brane, that the bound is satisfied in the range

$$0 \leq \gamma_0 \leq -\frac{n+1 - \sqrt{1+n(n+p+2)}}{pB}, \quad (3.70)$$

while for large values of γ_0 the bound is found to be violated. If we instead of c_s in (3.69) use the proposed quantity [114; 115]

$$c_{\mathcal{Q}}^2 \equiv \left(\frac{\partial P}{\partial \varrho} \right)_{\mathcal{Q}} = -\frac{1}{1+n} \left[\frac{1+2\gamma_0}{1 + \frac{pB}{n+1}\gamma_0} \right], \quad (3.71)$$

computed for fixed charge density \mathcal{Q} , we find that the bound will always be violated (except for the neutral case where $c_{\mathcal{Q}} = c_s$). In this regard, one might question the validity of the stability analysis for the case of a black brane charged under a top-form gauge field examined in Ref. [37]. Here the dispersion relations were written down using the assumption that the ζ/η bound proposed by [113] is saturated.

3.6 Stability and dispersion relations

In Ref. [57] the Gregory-Laflamme instability was successfully identified with the unstable sound mode of the neutral black brane. This analysis was further refined in [38] and considered for branes charged under top-form gauge fields in [37]. In this section we address the issue of stability and dispersion of long-wavelength perturbations of the Reissner-Nordström black brane. Moreover, we comment on the connection to thermodynamic (in)stability.

3.6.1 Dispersion relations

It is straightforward to show that the first order fluid (conservation) equations take the form

$$\begin{aligned} \dot{\rho} &= -(w - \zeta\vartheta)\vartheta - 2\eta\sigma_{ab}\sigma^{ab}, & \dot{u}^a &= -\frac{\Delta^{ab}\partial_b(P - \zeta\vartheta) - 2\eta\Delta^a_b\partial_c\sigma^{bc}}{w - \zeta\vartheta}, \\ \dot{\mathcal{Q}} &= -\mathcal{Q}\vartheta + \mathfrak{D}\left(\frac{\mathcal{Q}\mathcal{T}}{w}\right)^2 \left(\vartheta u^b + \dot{u}^b + \Delta^{ab}\partial_a\right)\partial_b\left(\frac{\Phi}{\mathcal{T}}\right), \end{aligned} \quad (3.72)$$

where the transport coefficients and the factor associated to \mathfrak{D} are coefficients in the derivative expansion and should be treated as constants. In order to find the speed of sound and dispersion relations, we consider *small* long-wavelength perturbations of the fluid

$$\Phi \rightarrow \Phi + \delta\Phi e^{i(\omega t + k_j x^j)}, \quad \mathcal{T} \rightarrow \mathcal{T} + \delta\mathcal{T} e^{i(\omega t + k_j x^j)}, \quad u^a = (1, 0, \dots) \rightarrow (1, \delta u^i e^{i(\omega t + k_j x^j)}). \quad (3.73)$$

The charge density \mathcal{Q} , energy density ρ , and pressure P are perturbed according to

$$\mathcal{Q} \rightarrow \mathcal{Q} + \delta\mathcal{Q} e^{i(\omega t + k_j x^j)}, \quad \rho \rightarrow \rho + \delta\rho e^{i(\omega t + k_j x^j)}, \quad P \rightarrow P + \delta P e^{i(\omega t + k_j x^j)}, \quad (3.74)$$

where the amplitudes can be expressed in terms of thermodynamic derivatives that depend on the specific equation of state. Note that $\delta p = \mathcal{Q}\delta\Phi + s\delta\mathcal{T}$ as a consequence of the Gibbs-Duhem relation. Plugging the expressions into the first order fluid equations (3.72) and linearizing in the amplitudes, we obtain the $p + 2$ equations

$$\begin{aligned} i\omega \left(\left(\frac{\partial\rho}{\partial\Phi} \right)_{\mathcal{T}} \delta\Phi + \left(\frac{\partial\rho}{\partial\mathcal{T}} \right)_{\Phi} \delta\mathcal{T} \right) + i\omega k_i \delta u^i &= 0, \\ i\omega\omega\delta u^j + ik^j (\mathcal{Q}\delta\Phi + s\delta\mathcal{T}) + k^j \left(\eta \left(1 - \frac{2}{p} \right) + \zeta \right) k_i \delta u^i + \eta k^2 \delta u^j &= 0, \\ i\omega \left(\left(\frac{\partial\mathcal{Q}}{\partial\Phi} \right)_{\mathcal{T}} \delta\Phi + \left(\frac{\partial\mathcal{Q}}{\partial\mathcal{T}} \right)_{\Phi} \delta\mathcal{T} \right) + i\mathcal{Q}k_i \delta u^i + \mathfrak{D}\mathcal{T}\frac{\mathcal{Q}^2}{w^2} \left(\delta\Phi - \frac{\Phi}{\mathcal{T}}\delta\mathcal{T} \right) k^2 &= 0. \end{aligned} \quad (3.75)$$

We stress that the thermodynamic derivatives are not dynamical and do only depend on the equation of state of the fluid in question. In our case they can be computed from (3.7) and (3.9). In order to find the ω that solves this system for a given wave vector k^i , we set the determinant of the system of linear equations in the amplitudes to zero. To linear order in k^i (i.e. at the perfect fluid level) the dispersion relation gives the speed of sound $c_s = \omega/k$. Using the equation of state (3.9) and solving the system to linear order, one finds

$$c_s^2 = \left(\frac{\partial P}{\partial\rho} \right)_{\frac{s}{\mathcal{Q}}} = -\frac{1 - B\gamma_0}{1 + N\gamma_0} (n + 1 + pB\gamma_0)^{-1}. \quad (3.76)$$

As was found with the $p = q$ branes of supergravity [37], the speed of sound only depends on the charge parameter γ_0 . For zero charge $\gamma_0 = 0$ we recover the neutral result $c_s^2 = -1/(n + 1)$. Since a negative speed of sound squared signifies an unstable sound mode, the neutral brane is unstable under long-wavelength perturbations. Indeed, this instability is

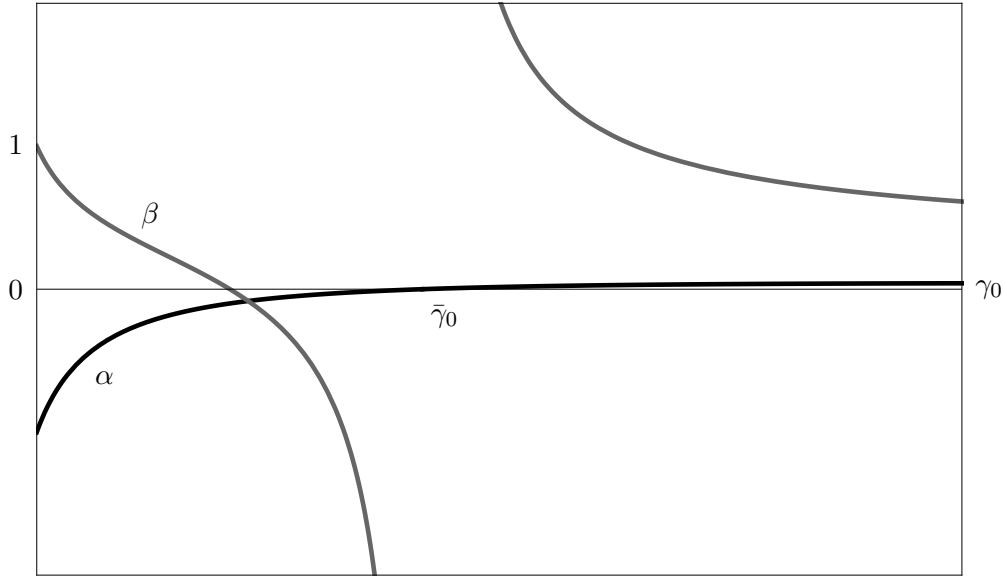


Figure 3.1: The qualitative behavior of the sound mode $\omega = c_s(\gamma_0)k + a(\gamma_0)ik^2 + \mathcal{O}(k^3)$ given by Eq. (3.79) as a function of γ_0 . The linear term (speed of sound) is parametrized according to $c_s^2(\gamma_0) = |c_s^2(0)|\alpha(\gamma_0)$ while the quadratic term (sound mode attenuation) is parametrized as $a(\gamma_0) = |a(0)|\beta(\gamma_0)$. Note that the linear and quadratic term become positive when the charge density passes the threshold $\bar{\gamma}_0$ indicated by the vertical dashed line.

exactly identified with the GL instability [38]. However, as we increase γ_0 the speed of sound squared becomes less and less negative and for

$$\gamma_0 > \bar{\gamma}_0 = \frac{D-3}{2}, \quad (3.77)$$

the $q = 0$ brane becomes stable under long-wavelength perturbations to leading order. Notice that the condition (3.77) can be satisfied for any non-zero charge density if the black brane temperature is low enough. Indeed, stability is obtained for $\mathcal{T} \sim (G\mathcal{Q})^{-1/n}$ (where the exact numerical factor depends on the number of transverse and brane dimensions).

In order to check stability to next to leading order, we now work out the dispersion relation for the fluid to quadratic order in k . We solve the system of equations to $\mathcal{O}(k^2)$. Solving for the longitudinal modes, we find the equation

$$\omega - c_s^2 \frac{k^2}{\omega} - i \frac{k^2}{w} \left(2 \left(1 - \frac{1}{p} \right) \eta + \zeta \right) - \frac{ik^2}{w} \mathfrak{D} \left(\mathcal{R}_1 \left(\frac{k}{\omega} \right)^2 + \frac{\mathcal{R}_2}{w} \right) + \mathcal{O}(k^3) = 0, \quad (3.78)$$

where the coefficients \mathcal{R}_1 , \mathcal{R}_2 , and \mathcal{R} (introduced below) are given in appendix D.3. Solving for the sound mode(s), we find the dispersion relation

$$\omega(k) = \pm c_s k + \frac{ik^2}{w} \left(\left(1 - \frac{1}{p} \right) \eta + \frac{\zeta}{2} \right) + ik^2 \mathcal{R} \mathfrak{D}. \quad (3.79)$$

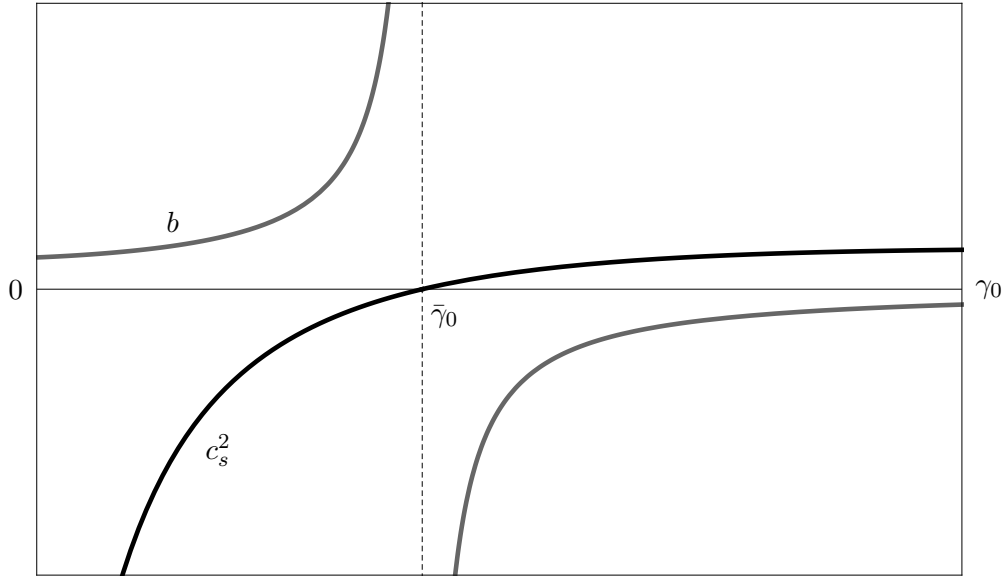


Figure 3.2: The qualitative behavior of the charge diffusion mode $\omega = ibk^2$ as a function of the charge parameter γ_0 , where b is given in Eq. (3.80). When b is positive c_s^2 is negative and vice versa. The critical point $\bar{\gamma}_0$ is indicated by the dashed line.

For a general fluid both the first order term (c_s) and the second order term must be positive in order for it to be dynamically stable. In this case, the above equation describes dampening of the (long-wavelength) sound waves in the fluid. Fig. 3.1 shows the general behavior of c_s and the (second order) attenuation term in (3.79). We see that above the threshold $\bar{\gamma}_0$, the speed of sound squared and sound mode attenuation are both positive. The sound mode is therefore stable to second order. In addition to the sound mode we have a longitudinal diffusion mode given by

$$\omega(k) = -\frac{i\mathcal{D}\mathcal{R}_1}{c_s^2 w} k^2 = i \frac{(1 + \gamma_0)^{1-N}}{4\pi\mathcal{T}(1 - B\gamma_0)} k^2. \quad (3.80)$$

We see that in general this mode is stable if and only if $\mathcal{R}_1/c_s^2 < 0$. In our case this amounts to the condition $\gamma_0 < \bar{\gamma}_0$ i.e. the opposite of the condition (3.77) as shown in Fig. 3.2. The conditions on γ_0 for dynamical stability are found to be complementary; when the sound mode is stable the charge diffusion mode is unstable and vice versa. The Reissner-Nordström brane thus seems to suffer from a GL instability for all values of the charge parameter γ_0 .

Finally, we also have a shear mode which takes the form

$$\omega(k) = \frac{i\eta}{w} k^2. \quad (3.81)$$

The fluctuations of the shear mode are very simple, they are transverse displacement of effective fluid with no variations in the charge and energy densities. Notice that this mode is always stable. It would be interesting for comparison to perform a numerical analysis

of the long-wavelength perturbations in the current setting as was done in the case of the neutral brane, where excellent agreement was found.

3.6.2 Thermodynamic stability

The conditions for thermodynamic stability of the Reissner-Nordström black brane are computed in the grand canonical ensemble since charge is allowed to redistribute itself in the directions of the brane. Using the thermodynamic quantities in Eqs. (3.7) and (3.9), one finds the specific heat capacity C and the (inverse) isothermal permittivity c to be,

$$\begin{aligned} C &= \left(\frac{\partial \rho}{\partial \mathcal{T}} \right)_{\mathcal{Q}} = \left(\frac{n+1 + (2-n(N-2))\gamma_0}{(nN-2)\gamma_0 - 1} \right) s, \\ c &= \left(\frac{\partial \Phi}{\partial \mathcal{Q}} \right)_{\mathcal{T}} = \left(\frac{1}{(\gamma_0+1)(1-(nN-2)\gamma_0)} \right) \frac{1}{s\mathcal{T}}. \end{aligned} \tag{3.82}$$

Thermodynamical stability is obtained if the two quantities are positive. However, these two conditions are complementary and can never be satisfied. This is also what was found for the class of smeared Dp -branes considered in e.g. [104]. Indeed, this complementary behavior is analogous to what was found for the dynamical analysis. However, the critical value of γ_0 where the quantities switch sign is not coinciding for the two analyses. It would be interesting to further investigate how the instability predicted by the dynamic analysis and the thermodynamic computation are related thus making a more precise connection to the correlated stability conjecture in the charged case [104].

4 | Discussion

4.1 Summary

We here summarize some of the main results obtained in this thesis.

Chapter 1: In Chap. 1 we developed an effective long-wavelength theory for extended black objects in various gravity schemes including supergravity (the blackfold approach). The theory was naturally formulated in terms of a fluid/elastic derivative expansions in the collective parameters parameterizing the black brane in question. The dynamics in the directions parallel to the worldvolume was seen to take the form of a dissipative relativistic fluid dynamics while the dynamics in the transverse directions were found to be essentially of elastic nature. Already to leading order (i.e. at the probe level), the blackfold equations contain a great deal of physics and it was explained how the effective theory can be used to construct new approximate black hole solutions and to understand the effective behaviour of black holes *vis-à-vis* instabilities. It was also explained how the theory is naturally formulated in a thermodynamical language which is interpreted as the leading order thermodynamics of the underlying *bona fide* black hole solution.

It was seen how the effective blackfold theory naturally can be coupled to matter fields giving rise to additional conserved effective currents. This allowed us to treat black branes in various supergravity schemes. We also argued that the effective theory in the supergravity regime is not inherently “black” (due to charge) and allows for perturbing extremal branes. In the extremal limit, the effective theory was seen basically to be a purely elastic theory with the important exception of the null-wave configurations. In a supergravity setting, the effective theory also naturally allows for an effective description of various bound states modeled in terms of anisotropic fluids carrying lower dimensional currents representing the dissolved brane charges.

Finally we considered the extension of the blackfold approach to more general flux backgrounds including dilatonic backgrounds. This involved a more rigorous derivation of the extrinsic equation directly from the Einstein equations (a similar analysis for the intrinsic perturbations is presented in Chap. 3). We saw how the force terms naturally appear as modified pole-dipole constraints in the overlap region. Additionally, for the supergravity p -brane, we managed to write down an action for the effective equation of motion, which was seen to have exactly the same form as its single brane counterpart (up to a constant). We also briefly discussed more general force terms for bound state

geometries. Finally, we have derived more general expressions for the conserved global quantities in background fluxes which will be relevant for the analysis presented in the next chapter.

Chapter 2: In Chap. 2, we constructed and analyzed the thermal spinning giant graviton configuration in both type II string theory and M-theory, using the blackfold approach for (thermal) probe branes. We found various new effects from having a non-zero temperature which can be attributed to the thermal excitations of the strongly coupled worldvolume theory living on the expanded brane (in the sense explained in Sec. 2.1). In particular, we found that the thermal giant graviton has a minimal possible value for the angular momentum and correspondingly also a minimal finite radius for the wrapping sphere.

In addition, we saw that the non-zero solution naturally allows for turning on new quantum numbers *viz.* intrinsic spins. Indeed, these spins are not visible in the usual extremal analysis since the worldvolume stress tensor is Lorentz invariant at zero-temperature. In the extremal limit internal spin along the directions of the worldvolume is therefore a gauge degree of freedom and hence “invisible”. The results of the present work show that by thermalizing giant gravitons (in the supergravity regime), we find interesting finite temperature objects in supergravity, exhibiting a variety of new qualitative and quantitative effects. We emphasize that the thermal spinning giant gravitons we have constructed, consisting of the background together with the thermal probe brane placed in it, are *bona fide* solutions of the supergravity equations of motion, to leading order in the blackfold expansion. This is even true for high temperatures (i.e. also above the Hawking-Page temperature) as long as $T \leq T_{\max}$ and provided that we are in the regime of validity in which the black brane can be treated as a probe (see Sec. 2.3.2). However, it would be interesting to see what happens to our solutions when heated up beyond the Hawking-Page temperature by repeating the analysis for the corresponding AdS black hole backgrounds. In this respect we also remind the reader that we, by including internal spins, found a new *stationary* black hole solutions with horizon topology $S^m \times S^{n-2}$ in $\text{AdS}_m \times S^n$ type II/M-theory backgrounds for $(m, n) = (5, 5)$ and $(4, 7)$. It would be interesting to examine these further, and perhaps construct the full solution numerically.

Finally, it was explained how the effects from intrinsic spin survive in a certain extremal limit. This was seen by considering a null-wave double scaling limit, where the temperature is taken to zero, while the fluid velocity is taken to approach the speed of light in a well-defined manner. In this way, the thermal excitations survive, even in the extremal limit. We analyzed the properties of the null-wave giant gravitons and showed that these configurations in particular exhibit a BPS spectrum. We emphasize that the objects do not have a weakly coupled counterpart, as the non-spinning configurations do, despite the fact that they exist at zero-temperature.

Chapter 3: In Chap. 3, we investigated the nature of the hydrodynamic effective theory that governs the intrinsic long wavelength fluctuations of the Reissner-Nordström black brane. Our analysis has extended the established cases of the interrelation between gravity and fluid dynamics. Although the analysis of Sec. 3.4 is quite technical, the problem at hand provides the purest example of a black brane carrying charge. With the extraction of the effective stress tensor and current, our analysis has provided the generalizations of the known neutral shear and bulk viscosities. We find that the shear viscosity receives the expected modification such that $\eta/s = 1/4\pi$. Note that the entropy has the form as given in Eq. (3.7) for the entire family of generalized Gibbons-Maeda black branes, we therefore expect the result for η given by (3.66) to hold in general. In particular, this includes the case of the D3 brane. The bulk viscosity was found to be non-zero positive for all values of the charge as expected since the effective fluid is not conformal. The ζ/η bound proposed by Ref. [113] was found to be violated for certain values of the charge parameter, while it was demonstrated to violate the bound proposed in [114] in the entire range of non-zero γ_0 , thus providing a counter-example. Finally, we computed the charge diffusion constant \mathfrak{D} of the Reissner-Nordström black brane. We note that, as with the shear viscosity η , the value of \mathfrak{D} given in (3.67) only depends on N which could be an indication that the result will hold for more general cases where e.g. the black brane is charged under higher form gauge fields.

Finally, the speed of sound was found to be imaginary for small charge densities, but becomes real for sufficiently large charge parameter $\gamma_0 > (D-3)/2$. For large charge density it therefore seems that the Reissner-Nordström black brane is GL stable under long wavelength perturbations. However, including the first order corrections to the dispersion relations, one finds that the hydrodynamic mode, associated with charge diffusion, is unstable above the threshold value of γ_0 . The Reissner-Nordström black brane is therefore GL unstable for all charge densities, although it is worth noting that the brane is “less” unstable above the threshold, in the sense that the instability is a next-to-leading order effect. This complementary behavior of the instability is also reflected in the thermodynamic stability analysis where the specific heat capacity and isothermal permittivity show a similar behavior.

4.2 Future directions

We have already discussed some open issues and computational generalizations in the main text. We here discuss some future directions which we hope to address in the near future.

Blackfolds

- **Entropy current:** There is a natural way to associate an entropy current with a perturbed event horizon [116]. This was recently considered in a blackfold setting in [109] (using the map briefly discussed in Sec. 3.1). It would be interesting to consider the charged generalization of the entropy current i.e. compute the entropy current for the perturbed solution presented in Chap. 3. Since the analytic form

of the dissipatively corrected entropy current is predicted from fluid dynamics, this would provide a consistency check of the transport coefficients obtained in Chap. 3.

- **q -form hydrodynamics:** A natural future direction of the work presented in Chap. 3 is the generalization to black branes charged under higher form gauge fields including a non-zero dilaton. In particular this would include the p -brane solutions of supergravity. This is work in progress and will appear in [117]. In this regard it would also be interesting to consider more general theories containing a Chern-Simons term which is expected to lead to non-trivial parity violating hydrodynamics as in [105; 106]. This would include developing the hydrodynamic theory for fluids carrying q -form currents not currently existing in the literature which might also find applications in more pure fluid/gravity setups.
- **Bending the D3-brane:** Another outstanding open problem is the bending of the D3-brane. This computation would involve performing the matched asymptotic expansion procedure for the D3-brane now (non-trivially) including the self-dual five-form field strength. While interesting in its own right, this computation would allow one to extract new elastic response coefficients including the five-form piezoelectric moduli. Even more interestingly this could lead to new insights in AdS/CFT by considering the near horizon limit of the bent D3-brane where the transverse sphere would now be deformed. It is currently not clear what deforming the S^5 means on the gauge theory side and whether it is possible to give the response coefficients a dual interpretation.
- **Generalizing the AdS/Ricci-flat map:** As mentioned, our results for the charged brane presented in Chap. 3 provide a natural starting ground for generalizing the map between the blackfold approach and the hydrodynamic regime of AdS/CFT [39; 109] to more general settings where matter fields are included.

The DBI/SUGRA correspondence

- **Couplings to lower form currents:** In Sec. 1.6.3, we showed that the action governing the p -brane blackfold is essentially the same as the single brane DBI action (in the extremal limit). As is well-known, the DBI action allows for couplings to lower form gauge potentials through a set of WZ terms. In this context, it would be very interesting to find out what sense these couplings map to the blackfold/supergravity regime and how they map. As briefly discussed in Sec. 1.6.4, the effective blackfold description naturally accommodates for such couplings through a set of dual currents. At all fits nicely; turning on the worldvolume DBI field strength turns on the lower form couplings. On the other hand, on the supergravity side, turning on the worldvolume gauge field effectively corresponds to considering an F1- Dp bound state which in turn induces couplings (force terms) on the blackfold side.
- **Comparing to known SUGRA solutions:** An important next step in the giant graviton analysis presented in Chap. 2 would be to consider the case in which we

have many giant gravitons moving along the S^1 of S^n and taking the limit in which they are smeared along this circle. This would reveal the the difference between the smeared and non-smeared phases at finite temperature, and elucidate the connections with for example the superstar [118], bubbling AdS solutions [95] and bubbling AdS black holes [119]. A related outstanding question is to examine the connection between our null-wave giant gravitons (which have $SO(m-1) \times U(1)$ isometry with $m = 5$ for D3 and $m = 4$ for M5) and the lower supersymmetric bubbling geometries that have been considered in the literature (see e.g. Refs. [120–123]). In this connection, considering thermal versions of giant gravitons with less supersymmetry [124] is expected to be relevant as well.

- **Null-wave probe branes:** Related to the above, we note that the null-wave giant gravitons do not have a counterpart in the usual weakly coupled worldvolume theory description. It would very be interesting to reconsider this by studying the thermal DBI (recently considered in [125]) theory and exploring an appropriate limit. This would also be worthwhile in view of finding a precise dual description of the null-wave giant gravitons. More generally, via the AdS/CFT correspondence our thermal spinning giant graviton solutions are expected to correspond to a thermal state in the dual gauge theory. It would be very interesting to find a description of this thermal state in the gauge theory and compare its properties to those of the thermal giant graviton, in particular the free energies found in Eq. (2.62) in the low temperature limit and the accompanying low/high spin results.

A | Geometry of embedded worldvolumes

In this appendix we introduce the differential geometry needed for describing embedded worldvolumes and discuss some aspects of the associated variational calculus. For the reader interested in a more detailed account (including some derivations omitted below), we refer to [66].

A.1 Basic definitions and relations

We consider the worldvolume \mathcal{W}_{p+1} embedded in a background with metric $g_{\mu\nu}$ and covariant derivative ∇_μ (spacetime coordinates are denoted by Greek letters). The induced geometry from the background on the worldvolume \mathcal{W}_{p+1} is given by

$$\gamma_{ab} = g_{\mu\nu} \partial_a X^\mu \partial_b X^\nu . \quad (\text{A.1})$$

Here $X^\mu \equiv X^\mu(\sigma)$ denotes the embedding of \mathcal{W}_{p+1} and σ^a denotes worldvolume coordinates (worldvolume indices are denoted by Latin letters). The first fundamental form of \mathcal{W}_{p+1} is defined by

$$h^{\mu\nu} = \gamma^{ab} \partial_a X^\mu \partial_b X^\nu . \quad (\text{A.2})$$

The tensor $h^{\mu\nu}$ acts as a projector onto \mathcal{W}_{p+1} i.e. $\partial_a X^\nu h^\mu{}_\nu = \partial_a X^\mu$, $h^\mu{}_\nu h^\nu{}_\rho = h^\mu{}_\rho$. Similarly we define the orthogonal projector,

$$\perp^\mu{}_\nu = \delta^\mu{}_\nu - h^\mu{}_\nu . \quad (\text{A.3})$$

Using the embedding functions X^μ , worldvolume tensors are converted into spacetime tensors and vice versa in the usual way

$$\mathcal{A}_{a_1 a_2 \dots}{}^{b_1 b_2 \dots} = \partial_{a_1} X^{\mu_1} \partial_{a_2} X^{\mu_2} \dots \partial^{b_1} X_{\nu_1} \partial^{b_2} X_{\nu_2} \dots \mathcal{A}_{\mu_1 \mu_2 \dots}{}^{\nu_1 \nu_2 \dots} , \quad (\text{A.4})$$

where $\partial^a X_\nu \equiv \gamma^{ab} h_{\nu\rho} \partial_b X^\rho$. The map (A.4) defines a bijection between worldvolume tensors and spacetime tensors tangential to \mathcal{W}_{p+1} . Non-tangential tensors have extra structure in the transverse directions and are usually related to finite thickness effects of the worldvolume, not relevant for this work (with the extrinsic curvature tensor $K_{\mu\nu}{}^\rho$, introduced below, being an important exception).

In general, a spacetime tensor \hat{A} localized to \mathcal{W}_{p+1} can be written

$$\hat{A}_{\mu_1\mu_2\dots}^{\nu_1\nu_2\dots}(x) = \int_{\mathcal{W}_{p+1}} d^{p+1}\sigma \sqrt{-\gamma} \left(\frac{\mathcal{A}_{\mu_1\mu_2\dots}^{\nu_1\nu_2\dots}(\sigma) \delta^{(D)}(x - X(\sigma))}{\sqrt{-g}} \right). \quad (\text{A.5})$$

Here $\mathcal{A}_{\mu_1\mu_2\dots}^{\nu_1\nu_2\dots}(\sigma)$ is a worldvolume scalar carrying spacetime indices. Covariant differentiation of tensors on \mathcal{W}_{p+1} is only defined along the directions parallel to \mathcal{W}_{p+1} , we therefore define the tangential projection of ∇_μ onto \mathcal{W}_{p+1} ,

$$\bar{\nabla}_\mu = h_\mu^\nu \nabla_\nu. \quad (\text{A.6})$$

Assuming that $\mathcal{A}_{\mu_1\mu_2\dots}^{\nu_1\nu_2\dots}$ is tangential, it therefore holds (ignoring boundary terms)

$$\nabla_\mu \hat{A}_{\mu_1\mu_2\dots}^{\nu_1\nu_2\dots} = \int_{\mathcal{W}_{p+1}} d^{p+1}\sigma \sqrt{-\gamma} \left(\frac{(\bar{\nabla}_\mu \mathcal{A}_{\mu_1\mu_2\dots}^{\nu_1\nu_2\dots}) \delta^{(D)}(x - X(\sigma))}{\sqrt{-g}} \right), \quad (\text{A.7})$$

Note that the parallel projection of $\bar{\nabla}_\mu \mathcal{A}_{\mu_1\mu_2\dots}^{\nu_1\nu_2\dots}$ is related to $D_a \mathcal{A}_{a_1 a_2 \dots}^{b_1 b_2 \dots}$ as in (A.4), where D_a denotes the covariant derivative induced by γ_{ab} . In particular, we have the following relation between the divergences

$$h^{\nu_1}_{\mu_1} \dots \bar{\nabla}_\rho \mathcal{A}^{\rho \mu_1 \dots} = \partial_{a_1} X^{\nu_1} \dots D_c \mathcal{A}^{c a_1 \dots}. \quad (\text{A.8})$$

It is important to note that even if the tensor $\mathcal{A}_{\mu_1\mu_2\dots}^{\nu_1\nu_2\dots}$ is parallel, the derivative $\bar{\nabla}_\mu \mathcal{A}_{\mu_1\mu_2\dots}^{\nu_1\nu_2\dots}$ in general has an orthogonal component. To tackle this, we introduce the extrinsic curvature tensor. Using the tangential derivative $\bar{\nabla}_\mu$, we define the extrinsic curvature of the embedding as

$$K_{\mu\nu}{}^\rho \equiv h_\mu^\sigma \bar{\nabla}_\nu h_\sigma^\rho = -h_\mu^\sigma \bar{\nabla}_\nu \perp_\sigma{}^\rho. \quad (\text{A.9})$$

By definition, the extrinsic curvature is tangential in its two lower indices and orthogonal in its upper index. Moreover, it can be shown that $K_{\mu\nu}{}^\rho$ is symmetric in its tangential indices,

$$K_{[\mu\nu]}{}^\rho = 0. \quad (\text{A.10})$$

The extrinsic curvature tensor $K_{\mu\nu}{}^\rho$ is the generalization of the usual second fundamental form $\Theta_{\mu\nu}$ of hypersurfaces to submanifolds of co-dimension $k \leq 1$. It is not difficult to show that

$$K_{\mu\nu}{}^\rho = \Theta_{\mu\nu}^{(i)} n_{(i)}^\rho, \quad (\text{A.11})$$

where $n_{(i)}$, $i = 1, \dots, k$ are normal to \mathcal{W}_{p+1} and $\Theta_{\mu\nu}^{(i)}$ denotes the usual second fundamental form computed in the usual way with the i th normal, i.e. $\Theta_{\mu\nu}^{(i)} = \frac{1}{2} \mathcal{L}_{n_{(i)}} \perp_{\mu\nu}$. Since $K_{\mu\nu}{}^\rho$ is tangential in its lower indices we will usually convert it into a mixed tensor $K_{ab}{}^\rho$ carrying both worldvolume indices and a (orthogonal) spacetime index,

$$K_{ab}{}^\rho = \partial_a X^\mu \partial_b X^\nu K_{\mu\nu}{}^\rho = -\partial_a X^\mu \partial_b X^\nu \nabla_\mu \perp_\nu{}^\rho. \quad (\text{A.12})$$

Notice that $K_{\mu\nu}{}^\rho = \partial^a X_\mu \partial^b X_\nu K_{ab}{}^\rho$ by virtue of the tangential properties of $K_{\mu\nu}{}^\rho$. The extrinsic curvature tensor can be seen as the generalization of the usual acceleration of a

worldline to a worldvolume of general co-dimension. This can also be seen explicitly from the expression

$$K_{ab}{}^\rho = D_a \partial_b X^\rho + \Gamma_{\mu\nu}^\rho \partial_a X^\mu \partial_b X^\nu, \quad (\text{A.13})$$

which can be shown after some work. The expression (A.13) provides a useful formula for computing the extrinsic curvature given an embedding X^μ . For a worldline parameterized by τ , then $K_{\tau\tau}{}^\rho = a^\rho = u^\mu \nabla_\mu (dX^\rho/d\tau)$. In analogy to the extrinsic curvature scalar of hypersurfaces, we define the extrinsic curvature vector for general embedded submanifolds by

$$K^\rho = h^{\mu\nu} K_{\mu\nu}{}^\rho = \gamma^{ab} K_{ab}{}^\rho, \quad (\text{A.14})$$

which is normal to \mathcal{W}_{p+1} , i.e. for any tangent t^μ to \mathcal{W}_{p+1} , $t_\rho K^\rho = 0$. Finally it can be shown that for any two tangents s^μ, t^μ , the relation

$$s^\mu t^\nu K_{\mu\nu}{}^\rho = \perp^\rho{}_\mu s^\sigma \nabla_\sigma t^\mu = \perp^\rho{}_\mu t^\sigma \nabla_\sigma s^\mu, \quad (\text{A.15})$$

holds as an identity. Especially for $s^\mu = t^\mu$, we then have

$$t^\mu t^\nu K_{\mu\nu}{}^\rho = \perp^\rho{}_\mu \dot{t}^\mu, \quad (\text{A.16})$$

with $\dot{t}^\mu \equiv t^\nu \nabla_\nu t^\mu$.

Having defined the extrinsic curvature and established some of its properties, we now look at divergences of tangential tensors. Assuming that $\mathcal{A}^{\mu\mu_1\dots}$ is tangential, we see this implies (using (A.9)),

$$\begin{aligned} \bar{\nabla}_\mu \mathcal{A}^{\mu\mu_1\dots} &= \bar{\nabla}_\mu (\mathcal{A}^{\mu\nu\dots} h_\nu{}^{\mu_1}) = \mathcal{A}^{\mu\nu\dots} \bar{\nabla}_\mu h_\nu{}^{\mu_1} + h_\nu{}^{\mu_1} \bar{\nabla}_\mu \mathcal{A}^{\mu\nu\dots} \\ &= \mathcal{A}^{\mu\nu\dots} h_\nu{}^\sigma \bar{\nabla}_\mu h_\sigma{}^{\mu_1} + h_\nu{}^{\mu_1} \bar{\nabla}_\mu \mathcal{A}^{\mu\nu\dots} \\ &= \mathcal{A}^{\mu\nu\dots} K_{\mu\nu}{}^{\mu_1} + h_\nu{}^{\mu_1} \bar{\nabla}_\mu \mathcal{A}^{\mu\nu\dots} \end{aligned} \quad (\text{A.17})$$

This implies for the stress tensor (using (A.8))

$$\bar{\nabla}_\mu T^{\mu\rho} = T^{\mu\nu} K_{\mu\nu}{}^\rho + \partial_b X^\rho D_a T^{ab}. \quad (\text{A.18})$$

If instead J is an n -form, we find (by virtue of the symmetry properties of $K_{\mu\nu}{}^\rho$),

$$h^{\mu_1}{}_{\nu_1} h^{\mu_2}{}_{\nu_2} \dots \bar{\nabla}_\mu J^{\mu\nu_1\nu_2\dots} = \partial_{a_1} X^{\mu_1} \partial_{a_2} X^{\mu_2} \dots D_a J^{a a_1 a_2 \dots} \quad (\text{A.19})$$

This means that $\hat{J}_{\mu\mu_1\dots}$ is a conserved current, $\nabla_\mu \hat{J}^{\mu\mu_1\dots} = 0$ if and only if $J_{aa_1\dots}$ is conserved on the worldvolume $D_a J^{aa_1\dots} = 0$. In particular, as opposed to the stress tensor, current conservation $\nabla_\mu \hat{J}^{\mu\mu_1\dots} = 0$ has no ‘‘extrinsic’’ equation associated to it.

Finally we will briefly discuss some aspects of variational calculus for embedded submanifolds. We refer to App. A of [57] for a more detailed account. We consider a quite general action of the type

$$I = \int_{\mathcal{W}_{p+1}} d^{p+1}\sigma \sqrt{-\gamma} f(\sigma^a), \quad (\text{A.20})$$

where f is some worldvolume function. The action is therefore a simple generalization of the usual Dirac action for minimal surfaces. We now seek to determine the equation

of motion corresponding to (A.20). We therefore consider a variation in the embedding $X^\mu \rightarrow X^\mu + \delta X^\mu$. Under such a variation the action changes with a Lie derivative according to

$$\delta_X I = \mathcal{L}_{\delta X}(\sqrt{-\gamma} f) = \sqrt{-\gamma} (-K^\rho f + \perp^{\rho\mu} \partial_\mu f) \delta X_\rho . \quad (\text{A.21})$$

Requiring the variation of the action to vanish $\delta I = 0$, we therefore obtain the following equation of motion (since δX^μ is arbitrary),

$$K^\rho = \perp^{\rho\mu} \partial_\mu \log f . \quad (\text{A.22})$$

An equation of the type (A.22) can be obtained from the action (A.20).

A.1.1 Redshift factors

In order for a solution to be stationary the fluid velocity u^a must lie along an isometric direction of \mathcal{W}_{p+1} (see Sec. 1.3.3). Since the geometry on \mathcal{W}_{p+1} is induced by the background, this implies that u^a pushes forward to a Killing vector \mathbf{k}^μ of the background. Let ξ denote the generator of asymptotic time translations of the background and let ξ_i denote a set of spatial Killing vectors. We can then write

$$\mathbf{k}^\mu = \xi^\mu + \sum_i \Omega_i \chi_{(i)}^\mu . \quad (\text{A.23})$$

A few comments are in order. If i corresponds to a compact direction of \mathcal{W}_{p+1} , the vector χ_i necessarily corresponds to a Cartan generator of rotations of the background. In the following we assume that all the vectors χ_i correspond to Cartan generators with orbits of periodicity 2π since we can obtain the usual generators of translations by taking the corresponding blackfold radius $\rightarrow \infty$. Also note that \mathbf{k}^μ could contain a component orthogonal to \mathcal{W}_{p+1} coming from the embedding (which is relevant for blackfolds in background fluxes). We refer to Sec. 1.7 for a discussion of this special case.

With these considerations, we introduce

$$R_0 \equiv \sqrt{-\xi^2} \Big|_{\mathcal{W}_{p+1}} , \quad R_i \equiv \sqrt{\chi_{(i)}^2} \Big|_{\mathcal{W}_{p+1}} , \quad V_{(i)} \equiv \frac{\Omega_{(i)} R_{(i)}}{R_0} . \quad (\text{A.24})$$

Here R_0 is a redshift factor between \mathcal{W}_{p+1} and infinity, R_i are the proper radii of the orbits generated by $\xi_{(i)}$ and v_i is the i th velocity component as measured from infinity. Note that in general R_0 and R_i depend on the worldvolume coordinates σ . With these definitions we then have

$$\mathbf{k} = R_0 \sqrt{1 - V^2} , \quad V^2 = \sum_i V_{(i)}^2 . \quad (\text{A.25})$$

A.2 The blackfold action from the embedding

We now explain how to derive the extrinsic equation (1.38) from an action principle. Using $w = \varrho + P = \mathcal{T} s$, the extrinsic equation takes the form

$$-PK^\rho = \perp^\rho{}_\mu s \mathcal{T} \dot{u}^\mu . \quad (\text{A.26})$$

The fact that the local temperature is dictated by the Killing vector \mathbf{k}^a in (1.36) and that \mathbf{k}^a extends to a background Killing vector \mathbf{k}^μ means that the local (worldvolume) thermodynamic fields extend to the entire background, at least in a neighborhood of the actual solution, for constant global temperature T and charge Q_p . We then have

$$s\mathcal{T}\dot{u}_\mu = -s\partial_\mu\mathcal{T} = -\partial_\mu P, \quad (\text{A.27})$$

among stationary solutions. This means that the extrinsic equation for stationary solutions can be written (remember that P is in general negative)

$$K^\mu = \perp^{\mu\nu} \partial_\nu \log(-P). \quad (\text{A.28})$$

This equation can be obtained by extremizing the following action (cf. Eq. (A.22))

$$I = \int_{\mathcal{W}_{p+1}} d^{p+1}\sigma \sqrt{-\gamma} P, \quad (\text{A.29})$$

for variations of the blackfold embedding among stationary fluid configurations on the worldvolume with fixed (global) temperature T and charge Q_p . Instead of considering the ensemble where we keep the charge Q_p constant, we can consider the ensemble where we keep the global potential Φ_p constant (cf. (1.68)). To this end, we note that we can rewrite the extrinsic equation (A.26) in terms of the Gibbs free energy \mathcal{G} as

$$(\mathcal{G} + \Phi Q_p) K^\rho = \perp^{\rho\mu} (\partial_\mu \mathcal{G} + Q_p \partial_\mu \Phi). \quad (\text{A.30})$$

We now consider variations for which the global potential Φ_p is kept fixed. According to Eq. A.21, among such variations, it holds

$$\Phi K^\rho = \perp^{\rho\mu} \partial_\mu \Phi. \quad (\text{A.31})$$

In this way, the extrinsic equation takes the form

$$\mathcal{G} K^\rho = \perp^{\rho\mu} \partial_\mu \mathcal{G}. \quad (\text{A.32})$$

This equation can now be obtained by extremizing the action

$$I = - \int_{\mathcal{W}_{p+1}} d^{p+1}\sigma \sqrt{-\gamma} \mathcal{G}. \quad (\text{A.33})$$

B | The F1-D p bound state

The F1-D p blackfold is described by a D p -brane charged fluid carrying a F-sting current on its worldvolume. The F1-D p bound state geometry is given by [84; 126] (here written in the string frame)

$$\begin{aligned} ds^2 = & D^{-1/2} H^{-1/2} (-f dt^2 + dx_1^2) + D^{1/2} H^{-1/2} \sum_{i=2}^p dx_i^2 \\ & + D^{-1/2} H^{1/2} \left(f^{-1} dr^2 + r^2 d\Omega_{(n+1)}^2 \right) , \end{aligned} \quad (\text{B.1})$$

with $n = 7 - p$ and with corresponding NSNS and RR gauge potentials

$$\begin{aligned} B_{01} = \sin \theta (H^{-1} - 1) \coth \alpha , \quad A_{2\dots p} = \tan \theta (H^{-1} D - 1) , \\ A_{0\dots p} = \cos \theta (H^{-1} - 1) \coth \alpha , \end{aligned} \quad (\text{B.2})$$

and dilaton

$$e^{2\phi} = D^{\frac{p-5}{2}} H^{\frac{3-p}{2}} \quad (\text{B.3})$$

The functions f and H are the usual blackening and charge functions recorded in Eqs. (1.73), while the function D is given by

$$D^{-1} = \cos^2 \theta + \sin^2 \theta H^{-1} . \quad (\text{B.4})$$

The effective blackfold fluid was computed in [37]. The local energy density ϱ , temperature \mathcal{T} and entropy s given by

$$\varrho = \frac{\Omega_{(n+1)}}{16\pi G} r_0^n (1 + \cosh^2 \alpha) , \quad \mathcal{T} = \frac{n}{4\pi r_0 \cosh \alpha} , \quad s = \frac{\Omega_{(n+1)}}{4G} r_0^{n+1} \cosh \alpha . \quad (\text{B.5})$$

The charge densities and associated chemical potentials read

$$\begin{aligned} Q_{Dp} = \frac{\Omega_{(n+1)}}{16\pi G} n r_0^n \cos \theta \cosh \alpha \sinh \alpha , \quad \Phi_{Dp} = \cos \theta \tanh \alpha , \\ Q_{F1} = \frac{\Omega_{(n+1)}}{16\pi G} n r_0^n \sin \theta \cosh \alpha \sinh \alpha , \quad \Phi_{F1} = \sin \theta \tanh \alpha \end{aligned} \quad (\text{B.6})$$

It is straightforward to perform a $\text{SO}(1, p)$ rotation to the solution (B.1)-(B.3). In particular the NSNS and RR potentials read

$$\begin{aligned} B_{(2)} = \sin \theta (H^{-1} - 1) \coth \alpha \hat{V}_{(2)} , \quad A_{(p-1)} = \tan \theta (H^{-1} D - 1) \star_{(p+1)} \hat{V}_{(2)} , \\ A_{(p+1)} = \cos \theta (H^{-1} - 1) \coth \alpha \star_{(p+1)} 1 , \end{aligned} \quad (\text{B.7})$$

Here $\hat{V}_{(2)}$ denotes the volume-form on the worldsheets spanned by the F1, $C_{(2)}$, and can be decomposed according to

$$\hat{V}_{(2)} = u \wedge v , \quad (\text{B.8})$$

for two vectors $u^2 = -1, v^2 = 1, u \cdot v = 0$.¹ The projector onto $C_{(2)}$ is then given by

$$h_{(2)}^{ab} = -u^a u^b + v^a v^b . \quad (\text{B.9})$$

The effective currents now take the form recorded in the expressions (1.75), (1.89) while the effective stress tensor is given by (1.93).

¹denoted $\star_{(2)}1$ in Sec. 1.5.6.

C | Thermal giant gravitons

C.1 Thermodynamic blackfold action and Smarr relation

In this appendix we show that the action (2.28) is equivalent to the thermodynamic action. To this end we first rewrite (2.28)

$$I = \Delta t \int_{\mathcal{B}_p} dV_{(p)} [\mathcal{L}_{(\text{bf})} + \mathcal{L}_{(\text{em})}] \quad (\text{C.1})$$

where from now on the subscripts "bf" and "em" refer to the blackfold and external field respectively. For simplicity we will in the following we assume that $\omega = 0$. In (C.1) we have factored out the integration over the (Killing) time t . This produces a redshift factor which must be included in the Lagrangian densities, e.g. $\mathcal{L}_{(\text{bf})} = \gamma_{\perp}^{-1} R_0 P$ where γ_{\perp} is defined in (1.132). From the conserved quantities derived in (1.133) we also introduce the Hamiltonian and angular momentum densities

$$\begin{aligned} \mathcal{H} &= \mathcal{H}_{(\text{bf})} + \mathcal{H}_{(\text{em})} = \gamma_{\perp}^{-1} \left(T_{(\text{bf})}^{\mu\nu} + \mathcal{V}_{(\text{em})}^{\mu\nu} \right) n_{\mu} \xi_{\nu} , \\ \mathcal{J} &= \mathcal{J}_{(\text{bf})} + \mathcal{J}_{(\text{em})} = \gamma_{\perp}^{-1} \left(T_{(\text{bf})}^{\mu\nu} + \mathcal{V}_{(\text{em})}^{\mu\nu} \right) n_{\mu} \chi_{\nu} \end{aligned} \quad (\text{C.2})$$

where $T_{(\text{bf})}^{\mu\nu}$ is the blackfold stress tensor which encapsulates the gravitational and electromagnetic self-energy/momentum and $\mathcal{V}_{(\text{em})}^{\mu\nu}$ (see (1.132)) is associated with the coupling of the charge current to the external electromagnetic field. Notice that the electromagnetic contributions only depend on the embedding degrees of freedom of the blackfold and not on the effective blackfold fluid degrees of freedom.

Now, for the blackfold degrees of freedom we have the relation (cf. [37])

$$\mathcal{H}_{(\text{bf})} + \gamma_{\perp}^{-1} u^{\mu} n_{\mu} T s = \Omega \mathcal{J}_{(\text{bf})} - \mathcal{L}_{(\text{bf})} \quad (\text{C.3})$$

This is the blackfold generalization of the usual relation $H = \dot{\theta} J - L$ in Hamiltonian mechanics between Hamiltonian and Lagrangian, but now with an extra term contributing to the energy due to the fact that the blackfold has internal thermal degrees of freedom living on it. However, since the external electromagnetic field does not couple to the thermal degrees of freedom living on the blackfold, one has for the electromagnetic part that

$$\mathcal{H}_{(\text{em})} = \Omega \mathcal{J}_{(\text{em})} - \mathcal{L}_{(\text{em})} \quad (\text{C.4})$$

We now use (C.3), (C.4) in (C.1) along with the expression (1.45) for the total entropy S of the blackfold. If we also rotate to Euclidean time so that $\Delta t \rightarrow \Delta\tau = \beta = 1/T$, we then find that the Euclidean action is given by

$$I_E = E - \Omega J - TS \quad (\text{C.5})$$

Smarr relation

Finally, we derive the Smarr formula for blackfolds in external fields. We use the perfect fluid stress tensor $T_{\mu\nu} = (\varrho + P)u_\mu u_\nu + Ph_{\mu\nu}$ and the local thermodynamic relations for charged p -branes in $D = n + p + 3$ dimensions

$$\varrho + P = \mathcal{T}s, \quad \varrho = -(n+1)P - n\Phi_p Q_p \quad (\text{C.6})$$

First, we note that the Smarr relation found previously for blackfolds based on charged p -branes (with zero external field) is easily generalized to the case where ξ^μ is not orthogonal to the world-volume \mathcal{B}_p . One finds

$$(D-3)E_{(\text{bf})} - (D-2)(\Omega J_{(\text{bf})} + TS) - n\Phi_H Q_p = \mathcal{T}_{(\text{bf})}^{(\text{tot})} \quad (\text{C.7})$$

where

$$\Phi_H = \int_{\mathcal{B}_p} dV_{(p)} \gamma_\perp^{-1} R_0 \Phi_p \quad (\text{C.8})$$

$$\mathcal{T}_{(\text{bf})}^{(\text{tot})} = - \int_{\mathcal{B}_p} dV_{(p)} \left(\gamma_\perp^{-1} R_0 T + \gamma_\perp^{-1} T_{(\text{bf})}^{\mu\nu} \xi_\mu n_\nu \right), \quad T \equiv \gamma_{ab} T^{ab} \quad (\text{C.9})$$

We then add to both sides of (C.7) the term $(D-3)E_{(\text{em})} - (D-2)\Omega J_{(\text{em})}$, yielding the generalized Smarr relation

$$(D-3)E - (D-2)(\Omega J + TS) - n\Phi_H Q_p = \mathcal{T}_{\text{tot}} \quad (\text{C.10})$$

where

$$\mathcal{T}_{\text{tot}} = - \int_{\mathcal{B}_p} dV_{(p)} \left(\gamma_\perp^{-1} R_0 T + \gamma_\perp^{-1} \left(T_{(\text{bf})}^{\mu\nu} + \mathcal{V}_{(\text{em})}^{\mu\nu} \right) \xi_\mu n_\nu + (D-2)\mathcal{L}_{(\text{em})} \right) \quad (\text{C.11})$$

Note that, as expected, the total tension gets modified by the presence of the external field.

C.2 The upper branch, CFT dual and correlation functions

The CFT dual operator of a single point-like graviton is a chiral primary of the form

$$\mathcal{O} = \text{Tr} Z^J \quad (\text{C.12})$$

with J the angular momentum on the S^5 and Z a complex scalar field. Standard computations have shown that their two- and three point functions match exactly on both gauge and string theory sides provided J is small.

If $J \gg N/\sqrt{\lambda}$ the correct description is in terms of a giant graviton. The dual gauge theory operator \mathcal{O}_{gg} of the giant graviton is no longer given by (C.12) and arguments based on symmetry (which only really apply close to $r = L$, see [127]) imply that it must be replaced by a Schur polynomial operator of the form

$$\mathcal{O}_{\text{gg}} \sim \chi_R(Z) = \frac{1}{J!} \sum_{\sigma \in S_J} \chi_{R_J}(\sigma) Z_{i_1}^{i\sigma(1)} \dots Z_{i_J}^{i\sigma(J)} \quad (\text{C.13})$$

where Z is a complex matrix, R_n denotes an irreducible representation of $U(N)$ described in terms of a Young tableau with J boxes.

As explained above, there is another (upper) branch of giant gravitons which is 1/2 BPS at $r = L$ in the large J limit with the same quantum numbers as the lower branch. We speculate that there exists another 1/2 BPS Schur polynomial operator in the CFT at $J = N$ that is distinct from the Schur polynomial relevant to the usual (lower) BPS branch and which is dual to the upper branch of giant gravitons at $r = L$. We present indications of this below.

Two-point correlation functions

As an explicit check of the statement above, we now compute the two-point function for the CFT operator dual to the $r = L$ point on the upper branch, showing that it has the same properties as the $r = L$ solution of the lower branch. It is easiest to do the computation simultaneously for both branches. Our method is based on the general prescription, reviewed in [128], for computing two-point correlation functions for massive (or light) particles moving in a background spacetime.

The giant graviton is a brane, not a particle, however as seen from the AdS_5 part it is a point-particle with a certain mass [129]. This can be seen by introducing motion in the AdS_5 part, i.e. introducing the dependence $x^\mu(\tau)$, $\mu = 0 \dots 4$ on the coordinates of AdS_5 with metric $G_{\mu\nu}$. Following [129] one can then show that the DBI action can equivalently be written as

$$I_{\text{DBI}} = \frac{1}{2} \int d\tau \left(\frac{G_{\mu\nu} \dot{x}^\mu \dot{x}^\nu}{e} + \frac{\Omega^2(L^2 - r^2)}{e} - m^2 e + m^2 r \Omega \right) \quad (\text{C.14})$$

where we have defined $m = Nr^3/L^4$ and e is an einbein which acts as a Lagrangian multiplier. Using (2.13) we can eliminate Ω in favor of J and arrive at the action

$$I = \frac{1}{2} \int d\tau \left(\frac{G_{\mu\nu} \dot{x}^\mu \dot{x}^\nu}{e} + e M^2 \right) \quad (\text{C.15})$$

where we have defined

$$M = \sqrt{\frac{J^2 - L^2 m^2}{L^2 - r^2}} \quad (\text{C.16})$$

However, to arrive at the interpretation that from the AdS_5 perspective the giant graviton is a massive point particle moving along a timeline geodesic, one should take into account that J must be conserved along any path. Hence, one should consider the Routhian \mathcal{R}

which is obtained by doing a Legendre transformation in the cyclic coordinates. In this case it coincides with the Hamiltonian, and hence we find

$$\mathcal{R} = H = \Omega J - L = -\frac{1}{2} \left(\frac{G_{\mu\nu} \dot{x}^\mu \dot{x}^\nu}{e} - eE^2 \right) \quad (\text{C.17})$$

where E is the on-shell energy (2.17), (2.18) for each of the branches. So we find that from the AdS₅ perspective the giant graviton is a point particle with mass E . Following [128], we can now compute the two-point function using the Routhian

$$G(0, \epsilon; x, \epsilon) = e^{-\mathcal{R}} \sim \left(\frac{|x|}{\epsilon} \right)^{-2E_{\pm}} \quad (\text{C.18})$$

showing for both branches equality of the anomalous dimension and the energy. We thus conclude that the anomalous dimension of the operator is equal to the energy for both branches, thus giving strong indication of being in both cases a Schur polynomial at the $r = L$ point.

It is important to note that the correct result is reproduced here using the Routhian, and not the action, as was also advocated in [130]. Indeed, evaluating the quantity M in (C.16) for each of the solution branches found in subsection 2.2.2 one finds¹

$$M_- = NL^3 \hat{r}^2 = E_- , \quad M_+ = NL^3 \hat{r}^2 \sqrt{9 - 4\hat{r}^2} \neq E_+ \quad (\text{C.19})$$

as compared to the energies given in Eqs. (2.17), (2.18).

Three-point correlation functions

To gain further insight into the nature of the new state at $r = L$ one may consider the three-point correlation function between one point particle and two giant gravitons. For the lower branch this analysis was performed in [131]. The procedure consists in analyzing the supergravity modes which describe fluctuations in the Euclidean D-brane action of the metric and 4-form potential, which are dual to chiral primary operators with R-charges in the $\mathcal{N} = 4$ SYM theory. The resulting three-point function structure constant for the maximal size 1/2-BPS giant graviton was found to be zero in agreement with the gauge theory side. Following the same steps for the upper branch $r = L$ state gives zero as well, since one can check that in that case the result is independent of Ω . This provides further confirmation that the gauge theory description of the upper branch $r = L$ state is a Schur polynomial. It would be very interesting to calculate this three-point function more generally for the entire (non-BPS) upper branch, but this is beyond the scope of the present work. A naive application of the ideas mentioned above does not give sensible results, so perhaps one should use the Routhian rather than the action and/or introduce an appropriate cutoff to regularize the divergent integrals.

¹In Ref. [131] the action was used to compute the two-point function, but since this computation was for the lower (1/2-BPS) branch, for which the terms conspire to give $M_- = E_-$, this still gives the correct result.

C.3 Details on solution space

In this appendix we give further details on the solution space presented in Secs. 2.3-2.4 and establish the relation between the results presented in this thesis and those obtained in [1].

C.3.1 Alternative parameterization of solution space

Here we reparameterize the equations of motion and solution space of Sec. 2.3 such that the connection with the solution space of the non-spinning thermal giant graviton found in [1] is more apparent. To this aim, we define a new parameter ω such that

$$\omega = \frac{\omega^2 r^2}{\mathbf{k}^2} . \quad (\text{C.20})$$

Using this newly defined parameter, the equation of motion (2.29) can be rewritten as

$$(n - 2 + \mathcal{R}_1 \omega) |k_{\text{w.v.}}|^2 + \Omega^2 r^2 (1 - \mathcal{R}_1(\omega + 1)) + (n - 1) \Omega r |k_{\text{w.v.}}| \mathcal{R}_2 = 0 , \quad (\text{C.21})$$

where $\mathcal{R}_1 \equiv \mathcal{R}_1(\phi)$ and $\mathcal{R}_2 \equiv \mathcal{R}_2(\phi)$ are given by Eq. (2.30). For clarity of presentation we focus on the case $n = 5$. In this situation Eq. (C.21) admits the following family of solutions

$$\Omega_{\pm} = \frac{|3 + \omega \mathcal{R}_1|}{\sqrt{(3 + \omega \mathcal{R}_1)^2 L^2 - 8(1 + \Delta_{\pm}(\phi, \omega)) r^2}} , \quad (\text{C.22})$$

where we have defined

$$\Delta_{\pm}(\phi, \omega) = -\frac{1}{8} \left(3\mathcal{R}_1 + 8\mathcal{R}_2^2 \pm 4\mathcal{R}_2 \sqrt{\mathcal{D}(\phi, \omega)} + \omega \mathcal{R}_1 (\mathcal{R}_1 - 4) \right) + \frac{1}{2} , \quad (\text{C.23})$$

with

$$\mathcal{D}(\phi, \omega) = -3(1 - \mathcal{R}_1) + 4\mathcal{R}_2^2 + \omega \mathcal{R}_1 (2 + \mathcal{R}_1(\omega + 1)) . \quad (\text{C.24})$$

Indeed, setting $\omega = 0$ in Eq. (C.22) yields the form of Ω_{\pm} obtained in [1] for thermal giant gravitons expanded into the S^5 part of $\text{AdS}_5 \times S^5$. A necessary condition for the solution (C.22) to exist is $\mathcal{D}(\phi, \omega) \geq 0$. In Fig. C.1 we exhibit the dependence of $\mathcal{D}(\phi, \omega) \geq 0$ on α within the range $0 \leq \omega \leq 1$.

From Fig. C.1 we see that there are two regions of possible spinning giant graviton configurations (here and below we parameterize the charge in terms of $\alpha = \text{arccosh}(1/\sqrt{\phi})$). The black dashed line depicts the case $\omega = 0$ obtained in [1] for which there is only one region of possible solutions. As the spin is increased the solution space is composed of a blue region (Region 1) and of a red region (Region 2). It is possible to determine analytically the ranges of α defining both regions by solving $\mathcal{D}(\alpha, \omega) = 0$. This leads to the ranges

$$\begin{aligned} \text{Region 1: } & \left(\frac{9}{4} + \omega \right) \leq \cosh^2 \alpha < \infty , \quad \omega \geq 0 \\ \text{Region 2: } & 1 \leq \cosh^2 \alpha \leq \left(\frac{1}{4} + \omega \right) , \quad \omega > \frac{3}{4} . \end{aligned} \quad (\text{C.25})$$

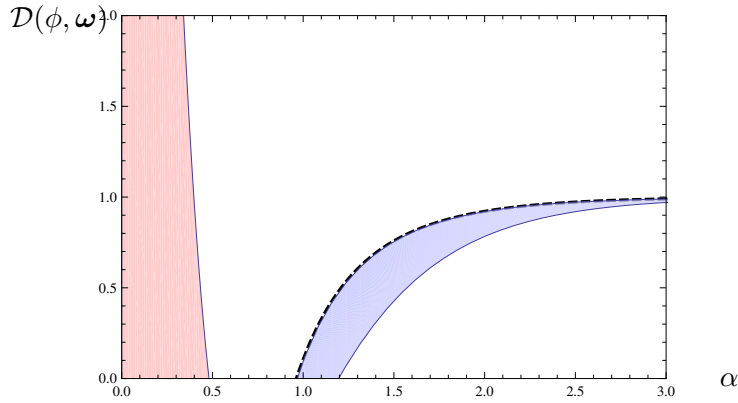


Figure C.1: $\mathcal{D}(\phi, \omega)$ as a function of $\alpha = \operatorname{arccosh}(1/\sqrt{\phi})$ for $0 \leq \omega \leq 1$ and $n = 5$. The dashed black line represents the case $\omega = 0$. The vertical axis was restricted to the interval $0 \leq \mathcal{D}(\phi, \omega) \leq 2$ while the horizontal axis was restricted to $0 \leq \alpha \leq 3$.

From (C.25) we see that Region 1 exists for all values of ω while Region 2 only appears after the spin parameter ω is increased beyond the value $\omega = 3/4$. At the lower bound of Region 1 and at the upper bound of Region 2 the two branches of solutions Ω_{\pm} meet each other. Note that Region 2 can be decomposed into a thermodynamically stable and unstable part. The unstable part lies within the range $1 \leq \cosh^2 \alpha \leq 3/2$ as it has negative heat capacity [48]. For generic (m, n) we obtain similar bounds as in (C.25), in particular for the non-spinning case, these are $5/3 \leq \cosh^2 \alpha < \infty$ for the M5-giant graviton and $10/3 \leq \cosh^2 \alpha < \infty$ for the M2-giant graviton.

Range of \mathbf{k}

The ranges (C.25) together with charge conservation (2.23) allow to determine the bounds on \mathbf{k} mentioned in Sec. 2.3.2. Focusing on $n = 5$ and on the lower bound of Region 1 we obtain the bound for \mathbf{k}

$$\text{Region 1: } \hat{T} \frac{(9 + 4\omega)^{\frac{3}{8}}}{2^{\frac{1}{4}}(3\sqrt{3})^{\frac{1}{4}}(5 + 4\omega)^{\frac{1}{8}}} \leq \mathbf{k} \leq 1 \quad . \quad (\text{C.26})$$

In the case $\omega = 0$ this agrees with the result found for non-spinning giant gravitons in [1]. For Region 2, the upper bound in (C.25) allows us to write the bound on the thermodynamically stable part as

$$\text{Region 2 stable: } \hat{T} \leq \mathbf{k} \leq \hat{T} \frac{(1 + 4\omega)^{\frac{3}{8}}}{2^{\frac{1}{4}}(3\sqrt{3})^{\frac{1}{4}}(4\omega - 3)^{\frac{1}{8}}} \quad , \quad (\text{C.27})$$

while for the unstable part it is instead allowed in the entire interval

$$\text{Region 2 unstable: } \hat{T} \leq \mathbf{k} \leq 1 \quad . \quad (\text{C.28})$$

For the bounds on \mathbf{k} for the stable part of both regions we observe that there is a gap in the allowed values of \mathbf{k} for which there does not exist a giant graviton configuration. This is the gap observed in Sec. 2.4 for the maximal size giant graviton. The same features are observed for the other values of (m, n) .

Maximum temperature

The solution space does not admit configurations at any temperature T . As already seen for the non-spinning giant graviton in [1] there exists a maximum temperature beyond which giant graviton configurations cease to exist. This bound is obtained from the charge conservation equation (2.23) which can be recast into the form

$$\mathbf{k}^{m-1} = \frac{Q_{(n-2)}G}{\Omega_{(m)}} \frac{4(4\pi)^m \mathcal{R}_1(\alpha) \cosh^{m-1} \alpha}{(m-1)^m \mathcal{R}_2(\alpha)} T^{m-1} , \quad (\text{C.29})$$

where the ratios \mathcal{R}_1 and \mathcal{R}_2 are defined in (2.30). The maximum temperature that the giant graviton can attain in the thermodynamically stable region is obtained from (C.29) when $\cosh \tilde{\alpha}$ takes the value that gives rise to the lower bound of Region 1 in (C.25). Generically, we can define the maximum temperature as

$$T_{\max}^{m-1} = \left[\frac{Q_{(n-2)}G}{\Omega_{(m)}} \frac{4(4\pi)^m \mathcal{R}_1(\alpha) \cosh^{m-1} \alpha}{(m-1)^m \mathcal{R}_2(\alpha)} \right]^{-1} \Big|_{\alpha=\tilde{\alpha}} . \quad (\text{C.30})$$

For the case of the spinning giant graviton on $\text{AdS}_5 \times S^5$ this results in

$$T_{\max} = T_{\text{static}} \left(\frac{6\sqrt{3}\sqrt{5+4\omega}}{(9+4\omega)^{\frac{3}{2}}} \right)^{\frac{1}{4}} . \quad (\text{C.31})$$

From the above expression we see that as the spin parameter ω increases, the maximum temperature that the giant graviton can attain decreases. This is again a generic feature for any (m, n) .

C.3.2 The special case $\Omega = \omega$

Here we analyze the case for which $\Omega = \omega$. This is a peculiar case as it corresponds to a branch of solutions for which there is no continuous limit that connects it with the thermal non-spinning giant graviton of [1] but it still admits a limit in which it connects to the usual $\frac{1}{2}$ -BPS giant graviton. In this situation the spin orbit interaction term in (2.29) vanishes and the equation of motion can be written as

$$(n-2)(1 - \Omega^2(L^2 - r^2)) + \Omega^2 r^2 + (n-1)\Omega r \sqrt{1 - \Omega^2(L^2 - r^2)} \mathcal{R}_2 = 0 . \quad (\text{C.32})$$

For clarity of presentation we focus on the case $n = 5$ but we note that the above equation admits a solution for any n . For $n = 5$ the solution takes the form

$$\Omega_{\pm} = \frac{3}{\sqrt{9L^2 - 8(1 + \Delta_{\pm}(\alpha))r^2}} , \quad (\text{C.33})$$

where

$$\Delta_{\pm}(\alpha) = -\frac{1}{2} \left(2\mathcal{R}_2^2(\alpha) \pm \mathcal{R}_2(\alpha) \sqrt{\mathcal{D}(\alpha)} \right) + \frac{1}{2} , \quad \mathcal{D}(\alpha) = 4\mathcal{R}_2^2(\alpha) - 3 . \quad (\text{C.34})$$

We see that (C.33) allows for two branches of solutions. However, one must remember that the condition $\mathbf{k}^2 = 1 - \Omega_{\pm}^2 L^2 \geq 0$ must be imposed, implying $\Omega_{\pm} \leq L^{-1}$. A straightforward

check tells us that the upper branch solution always violates this requirement (except in the strict limit $\alpha \rightarrow \infty$). Hence we conclude that for the case $\Omega = \omega$ only the lower branch of solutions exists. Imposing the same requirement on the fluid velocity \mathbf{k} for the lower branch leads to the allowed range for α in solution space

$$\frac{9}{8} \leq \cosh^2 \alpha < \infty . \quad (\text{C.35})$$

This range implies that there is a thermodynamically stable region and an unstable region which ranges from $9/8 \leq \cosh^2 \alpha \leq 3/2$. This furthermore means that this branch of solutions does not admit a neutral limit (as one cannot approach $\alpha = 1$), i.e., they must be always charged and supported by the background gauge field. Moreover, the range (C.35) implies that in both stable and unstable regions, the fluid velocity must satisfy the bound $\hat{T} \leq \mathbf{k} \leq 1$. Another interesting feature of this branch of solutions is that both ends of the interval (C.35) correspond to zero-temperature limits. The limit $\alpha \rightarrow \infty$ corresponds to either the usual extremal limit of Sec. 2.3.3 or the null-wave limit of Sec 2.6. The limit $\alpha \rightarrow 9/8$, using the fact that $\Delta_-(9/8) = -1$, implies $\Omega_- = L^{-1}$ and hence that $\mathbf{k} \rightarrow 0$. Therefore, by charge conservation (C.29) we see that for the charge $Q_{(n-2)}$ to remain constant we must have $T \rightarrow 0$. This is another type of null-wave giant graviton configuration but not a regular one since in this limit the thickness r_0 remains finite and hence all thermodynamic quantities presented in Sec. 2.3 diverge except for the product TS which remains finite. Further, in this limit the configuration satisfies the relation $\mathbf{F} = \mathbf{E} - \hat{T}\mathbf{S} = \mathbf{J} + \mathcal{S}$, which is the BPS relation found in Sec. 2.6.

D | Details for Chapter 3

D.1 Reduction

In the first part of this appendix we will show how the equation of motions for the general case of a reduction of an Einstein-Maxwell theory on an Einstein manifold can be obtained. In the second part we will provide the example of applying the procedure for $d = 2$ on the zeroth order solution.

D.1.1 Reduction of Einstein-Maxwell theory on an Einstein manifold

We consider Einstein-Maxwell theory on a D -dimensional space of the form

$$ds^2 = g_{\mu\nu} dx^\mu dx^\nu = ds_{(b)}^2 + e^{2\psi(x_b)} ds_{(E)}^2. \quad (\text{D.1})$$

Here $ds_{(b)}^2$ denotes the metric of the base manifold $\mathcal{M}_{(b)}$, $x_{(b)}^i$ denotes the coordinates on $\mathcal{M}_{(b)}$, ψ is a function on $\mathcal{M}_{(b)}$ and $ds_{(E)}^2$ is the metric of an Einstein manifold $\mathcal{M}_{(E)}$ with coordinates $x_{(E)}^A$. Since $\mathcal{M}_{(E)}$ is an Einstein manifold, we have

$$d_E R^{(E)} = R_E g^{(E)}, \quad (\text{D.2})$$

where d_E , $g^{(E)}$, $R^{(E)}$ and R_E are respectively the dimension, the metric, the Ricci tensor and (constant) curvature scalar of $\mathcal{M}_{(E)}$. Moreover we consider a gauge field (minimally coupled to gravity) A_μ which only depends on $x_{(b)}^i$ and only takes values along the base manifold $\mathcal{M}_{(b)}$. Schematically

$$A_\mu(x) = A_i(x_b). \quad (\text{D.3})$$

The action S of the system is given by

$$S = S_g + S_{\text{EM}}, \quad S_g = \int d^D x \sqrt{|g|} R, \quad S_{\text{EM}} = \int d^D x \sqrt{|g|} \left[-\frac{1}{4} F_{\mu\nu} F^{\mu\nu} \right], \quad (\text{D.4})$$

where R denotes the Ricci scalar of the full metric $g_{\mu\nu}$. We can now perform a reduction and integrate out $\mathcal{M}_{(E)}$, one finds

$$\begin{aligned} S_g &\sim \int_{\mathcal{M}_b} d^{d_b} x_b \sqrt{|g_b|} e^{d_E \psi(x_b)} \left\{ R_b + R_E e^{-2\psi(x)} - d_E (d_E - 1) (\nabla \psi)^2 \right\}, \\ S_{\text{EM}} &\sim - \int_{\mathcal{M}_b} d^{d_b} x_b \sqrt{|g_b|} e^{d_E \psi(x_b)} F_{ij} F^{ij}. \end{aligned} \quad (\text{D.5})$$

Having worked out the reduced action, it is easy to work out the equations of motion. As usual, the resulting system is EM theory on \mathcal{M}_b coupled to a dynamical scalar field and a current. The EOMs are

$$\begin{aligned} R_{ij}^{(b)} &= \frac{1}{4} \left(2F_i{}^k F_{jk} - \frac{1}{D-2} g_{ij}^{(b)} F_{mn} F^{mn} \right) + d_E (\nabla_a \psi \nabla_b \psi + \nabla_a \nabla_b \psi), \\ \square \psi + d_E (\nabla \psi)^2 - \frac{F_{mn} F^{mn}}{4(D-2)} &= \frac{R_E e^{-2\psi}}{d_E}, \\ \nabla_i F^{ij} &= d_E F^{kl} \nabla_l \psi. \end{aligned} \quad (\text{D.6})$$

D.1.2 Reduction of the zeroth order solution

In this section we demonstrate how the reduction works for the 0th order solution with (fluid) dynamics in two spatial directions (in other words, an ordinary boost in the (σ_1, σ_2) direction). Now the base space is composed of the three fluid brane directions (one time σ^0 and two spatial directions, (σ^1, σ^2) along with the radial direction r). The metric has the form

$$ds^2 = h^B \left[\left(\eta_{ab} + \left(1 - \frac{f}{h^N} \right) u_a u_b \right) d\sigma^a d\sigma^b + \frac{dr^2}{f} + r^2 d\Omega_{(n+1)}^2 + \sum_{i=3}^p \left(dx_{\parallel}^i \right)^2 \right], \quad (\text{D.7})$$

with $a, b = 0, 1, 2$ and where x_{\parallel}^i , $i = 3, \dots, p$ are the $p-2$ static brane directions. We now integrate out the transverse sphere and the $p-2$ brane directions. The functions ψ and ϕ are given by

$$\phi(r) = \psi(r) + 2 \log r = B \log h(r). \quad (\text{D.8})$$

It is now straightforward to compute κ , j^μ and \mathcal{F}_ν^μ . Here x^μ denotes coordinates of the four dimensional base space $x^\mu = (\sigma^0, \sigma^1, \sigma^2, r)$. One finds

$$\begin{aligned} \kappa &= -\frac{Bn^2}{2} \left(\frac{r_0}{r} \right)^{2n} \frac{\gamma_0 (1 + \gamma_0)}{r^2 h^N(r)}, \\ j^\mu \partial_\mu &= \frac{n^2}{2B} \left(\frac{r_0}{r} \right)^{2n} \frac{\sqrt{N\gamma_0(1+\gamma_0)}}{h^{N-1}(r)} \left(1 + \frac{2}{B} + \frac{p}{n} h(r) + 2 \left(\frac{r_0}{r} \right)^n \gamma_0 \right) u^a \partial_{\sigma_a}, \\ \mathcal{F}_\nu^\mu \partial_\mu \otimes dx^\nu &= \frac{N\kappa}{B} \left(u^a u_b + \left(1 - \frac{2}{N} \delta_b^a \right) \right) \partial_{\sigma_a} \otimes d\sigma^b - \frac{2\kappa}{B} \partial_r \otimes dr. \end{aligned} \quad (\text{D.9})$$

It is now possible to show that, as expected, the reduced system obeys the EOMs with these effective sources. The above sources get derivative corrections in the perturbative expansion.

D.2 Coefficients of the large r expansions

In this section, we list the first set of large r expansion coefficients of the metric and gauge field given in section 3.4.

Scalar sector

Below is listed the first set of coefficients for the large r expansions of f_{rv} ,

$$\alpha_{rv}^{(1)} = -\frac{n((n+p)^2 + (n+p)(2(p+1) + n(p+2))\gamma_0 + 2p(p+2)\gamma_0^2)}{(n-1)(n+p)^2((n+1) + pB\gamma_0)}. \quad (\text{D.10})$$

Below is listed the first set of coefficients for the large r expansions of a_v ,

$$\alpha_v^{(1)} = \frac{n((2n+1)(n+p)^2 + (n+p)(1 + n(2n+3)(p+1))\gamma_0 + 2p(1-p + 2n(p+1)\gamma_0^2)}{(n-1)(2n-1)(n+p)^2((n+1) + pB\gamma_0)},$$

$$\beta_v^{(1)} = \frac{(1+\gamma_0)^{\frac{N}{2}}}{n} \left[1 - p\gamma_0 B \left[\frac{2(n+1) + pB\gamma_0}{((n+1) + pB\gamma_0)^2} \right] \right]. \quad (\text{D.11})$$

Below is listed the first set of coefficients for the large r expansions of f_{vv} ,

$$\alpha_{vv}^{(1)} = \frac{1}{(n-1)} \left(n(1 + 2\gamma_0) + \frac{4\gamma_0(n+p(1+\gamma_0))}{(n+p)^2((n+1) + pB\gamma_0)} \right), \quad (\text{D.12})$$

$$\beta_{vv}^{(1)} = -(1+\gamma_0)^{\frac{N}{2}} \frac{2(n+1)}{n(n+1 + pB\gamma_0)^2}.$$

Vector sector

Below is listed the first set of coefficients for the large r expansions of f_{vi} ,

$$\alpha_{vi}^{(1)} = (\partial_v \beta_i) \gamma_0 \left[-\frac{(n+p+1)(p+n(n+p+1)(1+2\gamma_0))}{(n-1)(n+p)^2} \right] + (\partial_i \gamma_0) \left[-\frac{n+p+1}{(n-1)(n+p)} \right],$$

$$\alpha_{vi}^{(2)} = \frac{n+p+1}{2(n-1)(2n-1)(n+p)^3} \left[\left(2(n+p)(n(n+p) + (4n^2 + n - 1 - 2p + 4np)\gamma_0) \right) (\partial_i \gamma_0) \right. \\ \left. \left(\gamma_0(4n(n+p)^2 + (n+p)(-1 - 2p + n(-3 + 2p + 4n(4 + 3n + 3p)))\gamma_0) \right. \right. \\ \left. \left. + 4n(1+n+p)(-1+n+4n^2 - 2p + 4np)\gamma_0^2 \right) (\partial_v \beta_i) \right],$$

$$\beta_{vi}^{(1)} = 0,$$

$$\beta_{vi}^{(2)} = -\frac{N}{4n} \left(\frac{2\gamma_0(1+\gamma_0)(\partial_v u_i) + (\partial_i \gamma_0)}{(1+\gamma_0)^{\frac{B}{2}}(1+N\gamma_0)} \right). \quad (\text{D.13})$$

Below is listed the first set of coefficients for the large r expansions of b_i ,

$$\alpha_i^{(1)} = \frac{1}{2(n-1)} \left[\left(\frac{2(n+p+2n(n+p+1)\gamma_0)}{n+p} \right) (\partial_v \beta_i) + \left(\frac{1+2\gamma_0}{\gamma_0(1+\gamma_0)} \right) (\partial_i \gamma_0) \right]. \quad (\text{D.14})$$

$$\beta_i^{(1)} = \beta_{vi}^{(2)} \left[\frac{n+p}{(n+p+1)\gamma_0(1+\gamma_0)} \right]$$

D.3 Thermodynamic coefficients

In this appendix we list a number of thermodynamic coefficients related to the analysis of section 3.6. The two coefficients \mathcal{R}_1 and \mathcal{R}_2 are given by

$$\begin{aligned}\mathcal{R}_1 &= \mathcal{Q}^2 \left[\left(\frac{\partial \mathcal{Q}}{\partial \mathcal{T}} \right)_\Phi \left(\frac{\partial \rho}{\partial \Phi} \right)_\mathcal{T} - \left(\frac{\partial \mathcal{Q}}{\partial \Phi} \right)_\mathcal{T} \left(\frac{\partial \rho}{\partial \mathcal{T}} \right)_\Phi \right]^{-1}, \\ \mathcal{R}_2 &= -\mathcal{R}_1 \left[\mathcal{T} \left(\frac{\partial \rho}{\partial \mathcal{T}} \right)_\Phi + \Phi \left(\frac{\partial \rho}{\partial \Phi} \right)_\mathcal{T} \right].\end{aligned}\quad (\text{D.15})$$

Writing out the speed of sound given in equation (3.76) it takes the form

$$c_s^2 = \frac{\mathcal{R}_1}{\mathcal{Q}^2 w} \left[w \left(\mathcal{Q} \left(\frac{\partial \mathcal{Q}}{\partial \mathcal{T}} \right)_\Phi - s \left(\frac{\partial \mathcal{Q}}{\partial \Phi} \right)_\mathcal{T} \right) - \mathcal{Q} \left(\mathcal{Q} \left(\frac{\partial \rho}{\partial \mathcal{T}} \right)_\Phi - s \left(\frac{\partial \rho}{\partial \Phi} \right)_\mathcal{T} \right) \right]. \quad (\text{D.16})$$

Finally the coefficient associated to the dispersion relation of the sound mode is given by

$$\mathcal{R} = -\frac{1}{2} \frac{\mathcal{R}_1^2}{\mathcal{Q}^2 w^3 c_s^2} \left(\mathcal{Q} \left(\frac{\partial \rho}{\partial \mathcal{T}} \right)_\Phi - s \left(\frac{\partial \rho}{\partial \Phi} \right)_\mathcal{T} \right) \left(\mathcal{Q} \frac{\mathcal{R}_2}{\mathcal{R}_1} + w \left(\left(\frac{\partial \mathcal{Q}}{\partial \Phi} \right)_\Phi \Phi + \left(\frac{\partial \mathcal{Q}}{\partial \mathcal{T}} \right)_\mathcal{T} \right) \right). \quad (\text{D.17})$$

For the Reissner-Nordström solution we have

$$\begin{aligned}\frac{\mathcal{R}_1}{\mathcal{T}} &= \frac{N\gamma_0}{n+1+pB\gamma_0}, & \frac{\mathcal{R}_2}{s\mathcal{T}\Phi} &= \frac{1-N\gamma_0(1+2\gamma_0)+n(1+N\gamma_0)^2}{1+2\gamma_0+n(1-B\gamma_0)}, \\ \mathcal{R} \frac{w^2}{s\mathcal{T}^2} &= -\frac{2N^2\gamma_0^2(1+\gamma_0)^2}{(1-B\gamma_0)(n+1+pB\gamma_0)}.\end{aligned}\quad (\text{D.18})$$

References

- [1] J. Armas, T. Harmark, N. A. Obers, M. Orselli, and A. V. Pedersen, “Thermal Giant Gravitons,” *JHEP* **1211** (2012) 123, [arXiv:1207.2789 \[hep-th\]](#).
- [2] J. Armas, N. A. Obers, and A. V. Pedersen, “Null-Wave Giant Gravitons from Thermal Spinning Brane Probes,” *JHEP* **1310** (2013) 109, [arXiv:1306.2633 \[hep-th\]](#).
- [3] J. Gath and A. V. Pedersen, “Viscous Asymptotically Flat Reissner-Nordström Black Branes,” *Accepted for publication in JHEP* (2013) , [arXiv:1302.5480 \[hep-th\]](#).
- [4] R. Narayan and J. E. McClintock, “Observational Evidence for Black Holes,” [arXiv:1312.6698 \[astro-ph.HE\]](#).
- [5] W. Israel, “Event horizons in static vacuum space-times,” *Phys. Rev.* **164** (Dec, 1967) 1776–1779.
B. Carter, “Axisymmetric black hole has only two degrees of freedom,” *Phys. Rev. Lett.* **26** (Feb, 1971) 331–333.
S. Hawking, “Black holes in general relativity,” *Communications in Mathematical Physics* **25** (1972) no. 2, 152–166.
D. C. Robinson, “Uniqueness of the kerr black hole,” *Phys. Rev. Lett.* **34** (Apr, 1975) 905–906.
- [6] J. D. Bekenstein, “Black holes and entropy,” *Phys. Rev. D* **7** (Apr, 1973) 2333–2346.
- [7] J. M. Bardeen, B. Carter, and S. W. Hawking, “The four laws of black hole mechanics,” *Communications in Mathematical Physics* **31** (1973) no. 2, 161–170.
- [8] J. Polchinski, “What is string theory?,” [arXiv:hep-th/9411028 \[hep-th\]](#).
- [9] G. T. Horowitz and A. Strominger, “Black strings and p-branes,” *Nuclear Physics B* **360** (1991) no. 1, 197 – 209.
<http://www.sciencedirect.com/science/article/pii/0550321391904409>.
- [10] J. Polchinski, “Dirichlet Branes and Ramond-Ramond charges,” *Phys.Rev.Lett.* **75** (1995) 4724–4727, [arXiv:hep-th/9510017 \[hep-th\]](#).

-
- [11] A. Strominger and C. Vafa, “Microscopic origin of the Bekenstein-Hawking entropy,” *Phys.Lett.* **B379** (1996) 99–104, [arXiv:hep-th/9601029](#) [[hep-th](#)].
- [12] J. M. Maldacena, “The large N limit of superconformal field theories and supergravity,” *Adv. Theor. Math. Phys.* **2** (1998) 231–252, [arXiv:hep-th/9711200](#).
- [13] S. S. Gubser, I. R. Klebanov, and A. M. Polyakov, “Gauge theory correlators from non-critical string theory,” *Phys. Lett.* **B428** (1998) 105–114, [arXiv:hep-th/9802109](#).
- [14] E. Witten, “Anti-de Sitter space and holography,” *Adv. Theor. Math. Phys.* **2** (1998) 253–291, [arXiv:hep-th/9802150](#).
- [15] O. Aharony, S. S. Gubser, J. M. Maldacena, H. Ooguri, and Y. Oz, “Large N field theories, string theory and gravity,” *Phys.Rept.* **323** (2000) 183–386, [arXiv:hep-th/9905111](#) [[hep-th](#)].
- [16] J. Erlich, “Recent Results in AdS/QCD,” *PoS CONFINEMENT8* (2008) 032, [arXiv:0812.4976](#) [[hep-ph](#)].
- [17] S. A. Hartnoll, “Lectures on holographic methods for condensed matter physics,” *Class.Quant.Grav.* **26** (2009) 224002, [arXiv:0903.3246](#) [[hep-th](#)].
- [18] C. P. Herzog, “Lectures on Holographic Superfluidity and Superconductivity,” *J.Phys.* **A42** (2009) 343001, [arXiv:0904.1975](#) [[hep-th](#)].
- [19] S. Bhattacharyya, V. E. Hubeny, S. Minwalla, and M. Rangamani, “Nonlinear Fluid Dynamics from Gravity,” *JHEP* **0802** (2008) 045, [arXiv:0712.2456](#) [[hep-th](#)].
- [20] S. Bhattacharyya, R. Loganayagam, I. Mandal, S. Minwalla, and A. Sharma, “Conformal Nonlinear Fluid Dynamics from Gravity in Arbitrary Dimensions,” *JHEP* **0812** (2008) 116, [arXiv:0809.4272](#) [[hep-th](#)].
- [21] P. Kovtun, D. Son, and A. Starinets, “Viscosity in strongly interacting quantum field theories from black hole physics,” *Phys.Rev.Lett.* **94** (2005) 111601, [arXiv:hep-th/0405231](#) [[hep-th](#)].
- [22] G. Policastro, D. Son, and A. Starinets, “The Shear viscosity of strongly coupled N=4 supersymmetric Yang-Mills plasma,” *Phys.Rev.Lett.* **87** (2001) 081601, [arXiv:hep-th/0104066](#) [[hep-th](#)].
- [23] C. G. Callan and J. M. Maldacena, “Brane dynamics from the Born-Infeld action,” *Nucl. Phys.* **B513** (1998) 198–212, [arXiv:hep-th/9708147](#).
- [24] R. C. Myers, “Dielectric branes,” *JHEP* **9912** (1999) 022, [arXiv:hep-th/9910053](#) [[hep-th](#)].
- [25] J. McGreevy, L. Susskind, and N. Toumbas, “Invasion of the giant gravitons from Anti-de Sitter space,” *JHEP* **0006** (2000) 008, [arXiv:hep-th/0003075](#) [[hep-th](#)].

-
- [26] M. T. Grisaru, R. C. Myers, and O. Tafjord, “SUSY and goliath,” *JHEP* **0008** (2000) 040, [arXiv:hep-th/0008015 \[hep-th\]](#).
- [27] A. Hashimoto, S. Hirano, and N. Itzhaki, “Large branes in AdS and their field theory dual,” *JHEP* **08** (2000) 051, [arXiv:hep-th/0008016](#).
- [28] N. Drukker and B. Fiol, “All-genus calculation of Wilson loops using D-branes,” *JHEP* **02** (2005) 010, [arXiv:hep-th/0501109](#).
S. Yamaguchi, “Wilson loops of anti-symmetric representation and D5- branes,” *JHEP* **05** (2006) 037, [arXiv:hep-th/0603208](#).
- [29] S. Kobayashi, D. Mateos, S. Matsuura, R. C. Myers, and R. M. Thomson, “Holographic phase transitions at finite baryon density,” *JHEP* **02** (2007) 016, [arXiv:hep-th/0611099](#).
- [30] M. Kruczenski, D. Mateos, R. C. Myers, and D. J. Winters, “Towards a holographic dual of large $N(c)$ QCD,” *JHEP* **0405** (2004) 041, [arXiv:hep-th/0311270 \[hep-th\]](#).
- [31] R. Emparan, T. Harmark, V. Niarchos, N. A. Obers, and M. J. Rodriguez, “The Phase Structure of Higher-Dimensional Black Rings and Black Holes,” *JHEP* **0710** (2007) 110, [arXiv:0708.2181 \[hep-th\]](#).
- [32] M. M. Caldarelli, R. Emparan, and M. J. Rodriguez, “Black Rings in (Anti)-deSitter space,” *JHEP* **11** (2008) 011, [arXiv:0806.1954 \[hep-th\]](#).
- [33] J. Armas and N. A. Obers, “Blackfolds in (Anti)-de Sitter Backgrounds,” *Phys.Rev.* **D83** (2011) 084039, [arXiv:1012.5081 \[hep-th\]](#).
- [34] J. Camps, R. Emparan, P. Figueras, S. Giusto, and A. Saxena, “Black Rings in Taub-NUT and D0-D6 interactions,” *JHEP* **0902** (2009) 021, [arXiv:0811.2088 \[hep-th\]](#).
- [35] R. Emparan, T. Harmark, V. Niarchos, and N. A. Obers, “New Horizons for Black Holes and Branes,” *JHEP* **04** (2010) 046, [arXiv:0912.2352 \[hep-th\]](#).
- [36] M. M. Caldarelli, R. Emparan, and B. Van Pol, “Higher-dimensional Rotating Charged Black Holes,” *JHEP* **1104** (2011) 013, [arXiv:1012.4517 \[hep-th\]](#).
- [37] R. Emparan, T. Harmark, V. Niarchos, and N. A. Obers, “Blackfolds in Supergravity and String Theory,” *JHEP* **1108** (2011) 154, [arXiv:1106.4428 \[hep-th\]](#).
- [38] J. Camps, R. Emparan, and N. Haddad, “Black Brane Viscosity and the Gregory-Laflamme Instability,” *JHEP* **1005** (2010) 042, [arXiv:1003.3636 \[hep-th\]](#).

-
- [39] M. M. Caldarelli, J. Camps, B. Gouteraux, and K. Skenderis, “AdS/Ricci-flat correspondence and the Gregory-Laflamme instability,” *Phys. Rev. D* **87**, **061502** (R) (2013), [arXiv:1211.2815 \[hep-th\]](#).
- [40] J. Armas, J. Camps, T. Harmark, and N. A. Obers, “The Young Modulus of Black Strings and the Fine Structure of Blackfolds,” *JHEP* **1202** (2012) 110, [arXiv:1110.4835 \[hep-th\]](#).
- [41] J. Armas and N. A. Obers, “Relativistic Elasticity of Stationary Fluid Branes,” *Phys.Rev.* **D87** (2013) 044058, [arXiv:1210.5197 \[hep-th\]](#).
- [42] J. Armas, “How Fluids Bend: the Elastic Expansion for Higher-Dimensional Black Holes,” [arXiv:1304.7773 \[hep-th\]](#).
- [43] J. Armas, “(Non)-Dissipative Hydrodynamics on Embedded Surfaces,” [arXiv:1312.0597 \[hep-th\]](#).
- [44] J. Camps and R. Emparan, “Derivation of the blackfold effective theory,” *JHEP* **1203** (2012) 038, [arXiv:1201.3506 \[hep-th\]](#).
- [45] J. Armas and T. Harmark, “Black Holes and Biophysical (Mem)-branes,” [arXiv:1402.6330 \[hep-th\]](#).
- [46] J. Armas, J. Gath, and N. A. Obers, “Black Branes as Piezoelectrics,” *Phys. Rev. Lett.* **109** (2012) 241101, [arXiv:1209.2127 \[hep-th\]](#).
- [47] J. Armas, J. Gath, and N. A. Obers, “Electroelasticity of Charged Black Branes,” *JHEP* **1310** (2013) 035, [arXiv:1307.0504 \[hep-th\]](#).
- [48] G. Grignani, T. Harmark, A. Marini, N. A. Obers, and M. Orselli, “Heating up the BIon,” *JHEP* **1106** (2011) 058, [arXiv:1012.1494 \[hep-th\]](#).
- [49] G. Grignani, T. Harmark, A. Marini, N. A. Obers, and M. Orselli, “Thermodynamics of the hot BIon,” *Nucl.Phys.* **B851** (2011) 462–480, [arXiv:1101.1297 \[hep-th\]](#).
- [50] V. Niarchos and K. Siampos, “M2-M5 blackfold funnels,” *JHEP* **1206** (2012) 175, [arXiv:1205.1535 \[hep-th\]](#).
- [51] V. Niarchos and K. Siampos, “Entropy of the self-dual string soliton,” *JHEP* **1207** (2012) 134, [arXiv:1206.2935 \[hep-th\]](#).
- [52] V. Niarchos and K. Siampos, “The black M2-M5 ring intersection spins,” [arXiv:1302.0854 \[hep-th\]](#).
- [53] V. Niarchos, “Supersymmetric Perturbations of the M5 brane,” [arXiv:1402.4132 \[hep-th\]](#).

-
- [54] G. Grignani, T. Harmark, A. Marini, N. A. Obers, and M. Orselli, “Thermal string probes in AdS and finite temperature Wilson loops,” *JHEP* **1206** (2012) 144, [arXiv:1201.4862 \[hep-th\]](#).
- [55] E. Poisson, A. Pound, and I. Vega, “The Motion of point particles in curved spacetime,” *Living Rev.Rel.* **14** (2011) 7, [arXiv:1102.0529 \[gr-qc\]](#).
- [56] R. Emparan, T. Harmark, V. Niarchos, and N. A. Obers, “World-Volume Effective Theory for Higher-Dimensional Black Holes,” *Phys.Rev.Lett.* **102** (2009) 191301, [arXiv:0902.0427 \[hep-th\]](#).
- [57] R. Emparan, T. Harmark, V. Niarchos, and N. A. Obers, “Essentials of Blackfold Dynamics,” *JHEP* **1003** (2010) 063, [arXiv:0910.1601 \[hep-th\]](#).
- [58] J. Armas, J. Gath, V. Niarchos, N. A. Obers, and A. Vigand Pedersen, “To appear,”.
- [59] R. Myers and M. Perry, “Black holes in higher dimensional space-times,” *Annals of Physics* **172** (1986) no. 2, 304 – 347. <http://www.sciencedirect.com/science/article/pii/0003491686901867>.
- [60] R. Emparan and H. S. Reall, “A Rotating black ring solution in five-dimensions,” *Phys.Rev.Lett.* **88** (2002) 101101, [arXiv:hep-th/0110260 \[hep-th\]](#).
- [61] R. Emparan, “Rotating circular strings, and infinite nonuniqueness of black rings,” *JHEP* **0403** (2004) 064, [arXiv:hep-th/0402149 \[hep-th\]](#).
- [62] T. Harmark, “Domain Structure of Black Hole Space-Times,” *Phys.Rev.* **D80** (2009) 024019, [arXiv:0904.4246 \[hep-th\]](#).
- [63] R. Emparan and R. C. Myers, “Instability of ultra-spinning black holes,” *JHEP* **0309** (2003) 025, [arXiv:hep-th/0308056 \[hep-th\]](#).
- [64] H. B. Nielsen and P. Olesen, “Vortex Line Models for Dual Strings,” *Nucl.Phys.* **B61** (1973) 45–61.
- [65] R. Leigh, “Dirac-born-infeld action from dirichlet σ -model,” *Modern Physics Letters A* **04** (1989) no. 28, 2767–2772.
J. Dai, R. Leigh, and J. Polchinski, “New connections between string theories,” *Modern Physics Letters A* **04** (1989) no. 21, 2073–2083.
- [66] B. Carter, “Essentials of classical brane dynamics,” *Int. J. Theor. Phys.* **40** (2001) 2099–2130, [gr-qc/0012036](#).
- [67] T. Ortín, *Gravity and strings*. Cambridge Univ. Press, Cambridge, 2004.
- [68] J. D. Brown and J. York, James W., “Quasilocal energy and conserved charges derived from the gravitational action,” *Phys.Rev.* **D47** (1993) 1407–1419, [arXiv:gr-qc/9209012 \[gr-qc\]](#).

-
- [69] V. Balasubramanian and P. Kraus, “A Stress tensor for Anti-de Sitter gravity,” *Commun.Math.Phys.* **208** (1999) 413–428, [arXiv:hep-th/9902121 \[hep-th\]](#).
- [70] R. Emparan, V. E. Hubeny, and M. Rangamani, “Effective hydrodynamics of black D3-branes,” [arXiv:1303.3563 \[hep-th\]](#).
- [71] R. C. Myers, “Stress tensors and Casimir energies in the AdS / CFT correspondence,” *Phys.Rev.* **D60** (1999) 046002, [arXiv:hep-th/9903203 \[hep-th\]](#).
- [72] R. M. Wald, *General Relativity*. University Of Chicago Press, first edition ed., 1984.
- [73] L. D. Landau, E. M. Lifshitz, J. B. Sykes, and W. H. Reid, *Fluid Mechanics*. Pergamon Press Oxford, England, 1959.
- [74] P. Romatschke, “New Developments in Relativistic Viscous Hydrodynamics,” *Int.J.Mod.Phys.* **E19** (2010) 1–53, [arXiv:0902.3663 \[hep-ph\]](#).
- [75] S. Bhattacharyya, “Constraints on the second order transport coefficients of an uncharged fluid,” *JHEP* **1207** (2012) 104, [arXiv:1201.4654 \[hep-th\]](#).
- [76] R. Gregory and R. Laflamme, “The Instability of charged black strings and p-branes,” *Nucl.Phys.* **B428** (1994) 399–434, [arXiv:hep-th/9404071 \[hep-th\]](#).
- [77] M. M. Caldarelli, O. J. C. Dias, R. Emparan, and D. Klemm, “Black Holes as Lumps of Fluid,” *JHEP* **04** (2009) 024, [arXiv:0811.2381 \[hep-th\]](#).
- [78] N. Andersson and G. Comer, “Relativistic fluid dynamics: Physics for many different scales,” *Living Rev.Rel.* **10** (2007) 1, [arXiv:gr-qc/0605010 \[gr-qc\]](#).
- [79] M. Vasilic and M. Vojinovic, “Classical spinning branes in curved backgrounds,” *JHEP* **0707** (2007) 028, [arXiv:0707.3395 \[gr-qc\]](#).
- [80] T. Harmark and N. A. Obers, “New phase diagram for black holes and strings on cylinders,” *Class.Quant.Grav.* **21** (2004) 1709, [arXiv:hep-th/0309116 \[hep-th\]](#).
- [81] A. W. Peet, “TASI lectures on black holes in string theory,” [arXiv:hep-th/0008241 \[hep-th\]](#).
- [82] I. A. Bandos, A. Nurmagambetov, and D. P. Sorokin, “The Type IIA NS5-brane,” *Nucl.Phys.* **B586** (2000) 315–330, [arXiv:hep-th/0003169 \[hep-th\]](#).
- [83] P. Pasti, D. P. Sorokin, and M. Tonin, “Covariant action for a D = 11 five-brane with the chiral field,” *Phys.Lett.* **B398** (1997) 41–46, [arXiv:hep-th/9701037 \[hep-th\]](#).
- [84] M. Costa and G. Papadopoulos, “Superstring dualities and p-brane bound states,” *Nucl.Phys.* **B510** (1998) 217–231, [arXiv:hep-th/9612204 \[hep-th\]](#).

-
- [85] J. Breckenridge, G. Michaud, and R. C. Myers, “More D-brane bound states,” *Phys.Rev.* **D55** (1997) 6438–6446, [arXiv:hep-th/9611174](#) [hep-th].
- [86] J. Izquierdo, N. Lambert, G. Papadopoulos, and P. Townsend, “Dyonic membranes,” *Nucl.Phys.* **B460** (1996) 560–578, [arXiv:hep-th/9508177](#) [hep-th].
M. S. Costa, “Black composite M-branes,” *Nucl.Phys.* **B495** (1997) 195–205, [arXiv:hep-th/9610138](#) [hep-th].
J. Russo and A. A. Tseytlin, “Waves, boosted branes and BPS states in m theory,” *Nucl.Phys.* **B490** (1997) 121–144, [arXiv:hep-th/9611047](#) [hep-th].
T. Harmark and N. Obers, “Phase structure of noncommutative field theories and spinning brane bound states,” *JHEP* **0003** (2000) 024, [arXiv:hep-th/9911169](#) [hep-th].
T. Harmark, “Open branes in space-time noncommutative little string theory,” *Nucl.Phys.* **B593** (2001) 76–98, [arXiv:hep-th/0007147](#) [hep-th].
- [87] S. S. Gubser, “Curvature singularities: The Good, the bad, and the naked,” *Adv.Theor.Math.Phys.* **4** (2000) 679–745, [arXiv:hep-th/0002160](#) [hep-th].
- [88] R. Argurio, F. Englert, and L. Houart, “Intersection rules for p-branes,” *Phys.Lett.* **B398** (1997) 61–68, [arXiv:hep-th/9701042](#) [hep-th].
R. Argurio, “Intersection rules and open branes,” [arXiv:hep-th/9712170](#) [hep-th].
- [89] M. Huq and M. A. Namazie, “Kaluza-klein supergravity in ten dimensions,” *Classical and Quantum Gravity* **2** (1985) no. 3, 293.
F. Giani and M. Pernici, “ $n = 2$ supergravity in ten dimensions,” *Phys. Rev. D* **30** (Jul, 1984) 325–333.
I. Campbell and P. West, “ $N = 2, d = 10$ non-chiral supergravity and its spontaneous compactification,” *Nuclear Physics B* **243** (1984) no. 1, 112 – 124.
- [90] E. Cremmer, B. Julia, and J. Scherk, “Supergravity in theory in 11 dimensions,” *Physics Letters B* **76** (1978) no. 4, 409 – 412.
- [91] A. A. Tseytlin, “Composite black holes in string theory,” [arXiv:gr-qc/9608044](#) [gr-qc].
- [92] R. Gregory and R. Laflamme, “Evidence for stability of extremal black p-branes,” *Phys.Rev.* **D51** (1995) 305–309, [arXiv:hep-th/9410050](#) [hep-th].
- [93] S. E. Gralla, A. I. Harte, and R. M. Wald, “A Rigorous Derivation of Electromagnetic Self-force,” *Phys.Rev.* **D80** (2009) 024031, [arXiv:0905.2391](#) [gr-qc].
- [94] T. Shiromizu, “Dilatonic probe, force balance and gyromagnetic ratio,” *Phys.Lett.* **B460** (1999) 141–147, [arXiv:hep-th/9906177](#) [hep-th].
- [95] H. Lin, O. Lunin, and J. M. Maldacena, “Bubbling AdS space and 1/2 BPS geometries,” *JHEP* **10** (2004) 025, [hep-th/0409174](#).

-
- [96] O. Lunin, “Strings ending on branes from supergravity,” *JHEP* **09** (2007) 093, [arXiv:0706.3396 \[hep-th\]](#).
G. W. Gibbons, “Born-Infeld particles and Dirichlet p -branes,” *Nucl. Phys.* **B514** (1998) 603–639, [arXiv:hep-th/9709027](#).
- [97] S. W. Hawking and D. N. Page, “Thermodynamics of black holes in Anti-De Sitter space,” *Commun. Math. Phys.* **87** (1983) 577.
- [98] I. R. Klebanov and A. A. Tseytlin, “Entropy of near extremal black p-branes,” *Nucl.Phys.* **B475** (1996) 164–178, [arXiv:hep-th/9604089 \[hep-th\]](#).
- [99] G. Arcioni and E. Lozano-Tellechea, “Stability and critical phenomena of black holes and black rings,” *Phys.Rev.* **D72** (2005) 104021, [arXiv:hep-th/0412118 \[hep-th\]](#).
- [100] R. Gregory and R. Laflamme, “Black strings and p-branes are unstable,” *Phys.Rev.Lett.* **70** (1993) 2837–2840, [arXiv:hep-th/9301052 \[hep-th\]](#).
- [101] T. Harmark, V. Niarchos, and N. A. Obers, “Instabilities of black strings and branes,” *Class.Quant.Grav.* **24** (2007) R1–R90, [arXiv:hep-th/0701022 \[hep-th\]](#).
- [102] R. Emparan, R. Suzuki, and K. Tanabe, “The large D limit of General Relativity,” *JHEP* **1306** (2013) 009, [arXiv:1302.6382 \[hep-th\]](#).
- [103] R. Emparan, D. Grumiller, and K. Tanabe, “Large D gravity and low D strings,” *Phys.Rev.Lett.* **110** (2013) 251102, [arXiv:1303.1995 \[hep-th\]](#).
- [104] T. Harmark, V. Niarchos, and N. A. Obers, “Instabilities of near-extremal smeared branes and the correlated stability conjecture,” *JHEP* **0510** (2005) 045, [arXiv:hep-th/0509011 \[hep-th\]](#).
- [105] J. Erdmenger, M. Haack, M. Kaminski, and A. Yarom, “Fluid dynamics of R-charged black holes,” *JHEP* **0901** (2009) 055, [arXiv:0809.2488 \[hep-th\]](#).
- [106] N. Banerjee, J. Bhattacharya, S. Bhattacharyya, S. Dutta, R. Loganayagam, *et al.*, “Hydrodynamics from charged black branes,” *JHEP* **1101** (2011) 094, [arXiv:0809.2596 \[hep-th\]](#).
- [107] D. T. Son and A. O. Starinets, “Hydrodynamics of r-charged black holes,” *JHEP* **0603** (2006) 052, [arXiv:hep-th/0601157 \[hep-th\]](#).
- [108] K. Maeda, M. Natsuume, and T. Okamura, “Viscosity of gauge theory plasma with a chemical potential from AdS/CFT,” *Phys.Rev.* **D73** (2006) 066013, [arXiv:hep-th/0602010 \[hep-th\]](#).
- [109] M. Caldarelli, J. Camps, B. Goutéraux, and K. Skenderis, “AdS/Ricci-flat correspondence,” [arXiv:1312.7874 \[hep-th\]](#).

-
- [110] G. Gibbons and K.-i. Maeda, “Black Holes and Membranes in Higher Dimensional Theories with Dilaton Fields,” *Nucl.Phys.* **B298** (1988) 741.
- [111] L. D. Landau and E. M. Lifshitz, *Fluid mechanics*. Course of Theoretical Physics, Vol. 6. Pergamon Press, London, 2nd ed., 1987. Translated from the Russian by J. B. Sykes and W. H. Reid.
- [112] A. Buchel and J. T. Liu, “Universality of the shear viscosity in supergravity,” *Phys.Rev.Lett.* **93** (2004) 090602, [arXiv:hep-th/0311175](#) [hep-th].
- [113] A. Buchel, “Bulk viscosity of gauge theory plasma at strong coupling,” *Phys.Lett.* **B663** (2008) 286–289, [arXiv:0708.3459](#) [hep-th].
- [114] B. Gouteraux, J. Smolic, M. Smolic, K. Skenderis, and M. Taylor, “Holography for Einstein-Maxwell-dilaton theories from generalized dimensional reduction,” *JHEP* **1201** (2012) 089, [arXiv:1110.2320](#) [hep-th].
- [115] M. Smolic, “Holography and hydrodynamics for EMD theory with two Maxwell fields,” *JHEP* **1303** (2013) 124, [arXiv:1301.6020](#) [hep-th].
- [116] S. Bhattacharyya, V. E. Hubeny, R. Loganayagam, G. Mandal, S. Minwalla, *et al.*, “Local Fluid Dynamical Entropy from Gravity,” *JHEP* **0806** (2008) 055, [arXiv:0803.2526](#) [hep-th].
- [117] A. Di Dato, J. Gath, and A. Vigand Pedersen, “Work in progress,”.
- [118] R. C. Myers and O. Tafjord, “Superstars and giant gravitons,” *JHEP* **0111** (2001) 009, [arXiv:hep-th/0109127](#) [hep-th].
- [119] J. T. Liu, H. Lu, C. Pope, and J. F. Vazquez-Poritz, “Bubbling AdS black holes,” *JHEP* **0710** (2007) 030, [arXiv:hep-th/0703184](#) [hep-th].
- [120] E. Gava, G. Milanese, K. Narain, and M. O’Loughlin, “1/8 BPS states in AdS/CFT,” *JHEP* **0705** (2007) 030, [arXiv:hep-th/0611065](#) [hep-th].
- [121] J. P. Gauntlett, N. Kim, and D. Waldram, “Supersymmetric AdS(3), AdS(2) and Bubble Solutions,” *JHEP* **0704** (2007) 005, [arXiv:hep-th/0612253](#) [hep-th].
- [122] B. Chen, S. Cremonini, A. Donos, F.-L. Lin, H. Lin, *et al.*, “Bubbling AdS and droplet descriptions of BPS geometries in IIB supergravity,” *JHEP* **0710** (2007) 003, [arXiv:0704.2233](#) [hep-th].
- [123] H. Lin, “Studies on 1/4 BPS and 1/8 BPS geometries,” [arXiv:1008.5307](#) [hep-th].
- [124] A. Mikhailov, “Giant gravitons from holomorphic surfaces,” *JHEP* **0011** (2000) 027, [arXiv:hep-th/0010206](#) [hep-th].
- [125] G. Grignani, T. Harmark, A. Marini, and M. Orselli, “Thermal DBI action for the D3-brane at weak and strong coupling,” [arXiv:1311.3834](#) [hep-th].

-
- [126] T. Harmark, “Supergravity and space-time non-commutative open string theory,” *JHEP* **07** (2000) 043, [arXiv:hep-th/0006023](#).
- [127] V. Balasubramanian, M. Berkooz, A. Naqvi, and M. J. Strassler, “Giant gravitons in conformal field theory,” *JHEP* **0204** (2002) 034, [arXiv:hep-th/0107119](#) [[hep-th](#)].
- [128] R. A. Janik, P. Surowka, and A. Wereszczynski, “On correlation functions of operators dual to classical spinning string states,” *JHEP* **1005** (2010) 030, [arXiv:1002.4613](#) [[hep-th](#)].
- [129] M. M. Caldarelli and P. J. Silva, “Multi-giant graviton systems, SUSY breaking and CFT,” *JHEP* **0402** (2004) 052, [arXiv:hep-th/0401213](#) [[hep-th](#)].
- [130] D. Bak, B. Chen, and J.-B. Wu, “Holographic Correlation Functions for Open Strings and Branes,” *JHEP* **1106** (2011) 014, [arXiv:1103.2024](#) [[hep-th](#)].
- [131] A. Bissi, C. Kristjansen, D. Young, and K. Zoubos, “Holographic three-point functions of giant gravitons,” *JHEP* **1106** (2011) 085, [arXiv:1103.4079](#) [[hep-th](#)].